

TECHNISCHE UNIVERSITÄT MÜNCHEN

Institut für Photogrammetrie und Kartographie

Lehrstuhl für Kartographie

Dynamics of spatially extended phenomena

Visual analytical approach to movements of lightning clusters

Dipl.-Ing. Stefan Peters

Vollständiger Abdruck der von der Ingenieurfacultät Bau Geo Umwelt der Technischen Universität München zur Erlangung des akademischen Grades eines

Doktor-Ingenieurs (Dr.-Ing.)

genehmigten Dissertation.

Vorsitzender: Univ.-Prof. Dr. phil. nat. Urs Hugentobler

Prüfer der Dissertation:

1. Univ.- Prof. Dr.-Ing. Liqiu Meng
2. Prof. Dr. rer. nat. Gennady Andrienko
City University London, United Kingdom
3. Univ.- Prof. Dr. rer. nat. Hans-Dieter Betz (em.)
Ludwig-Maximilians-Universität München

Die Dissertation wurde am 30.09.2014 bei der Technischen Universität München eingereicht und durch die Ingenieurfacultät Bau Geo Umwelt am 10.12.2014 angenommen.

Abstract

The world we live in is highly dynamic. The understanding of dynamic processes is crucial in all the fields that have to deal with moving objects or phenomena. It can be strongly supported by visual explorative methods and interactive tools. Investigating temporal changes of spatial patterns counts as one of the most challenging research tasks for geoscientists because it demands the capabilities of extracting the reliable temporal changes from large datasets, aggregating the extracted information and visualize it in an easily comprehensible way for the target users.

This thesis is dedicated to the visual exploration of a specific type of geographic data, namely the spatially extended moving objects or phenomena. Visual analytical approaches are developed and implemented to study the dynamics of the spatio-temporally evolving polygons. The lightning data are chosen as a real-world case.

The visual exploration of dynamic phenomena can be methodologically unfolded into three parts: (a) the data representation which typically requires data pre-processing, clustering and trajectory modeling; (b) the visual analysis empowered by user interactions; and (c) the visual analytics which is essentially an emerging discipline incorporating user interactions with multidimensional and multivariate visualization tools such as maps, diagrams and graphs. Different kinds of dynamic objects and events are comprehensively discussed with an emphasis on the specification of their semantic and geometrical attributes. The existing visualization technologies for the visual movement analysis of spatially extended objects (SEOs) are introduced and compared. While the visual analytical approaches for moving point objects have been extensively investigated in the recent years, the available methods for dynamic SEOs and phenomena remain rather limited. Even fewer works have been reported on the spatio-temporal changes of SEOs in form of trajectory lanes and their dynamic patterns.

The author proposes a generic concept for visual analysis of dynamic SEOs according to which appropriate visual explorative tools can be selected, depending on the data of SEOs and their expected applications. The concept is basically shaped by two components of dynamic SEOs. The first component is the momentary situation of the moving cluster which is defined either through a moment of time or by a specific time interval. The other component is the entire trajectory or "lane" of the moving SEO, representing the continuous cluster movement during the entire lifetime period. Both components contain certain movement aspects and behaviors. Furthermore, specific movement analysis tasks and their possible visual analytical solutions are presented in this work. A particular focus is on the internal structure change of SEOs represented by grouped point events. The existing approaches mainly apply to datasets with two different moments of time and thus do not provide adequate solutions for density mapping of dynamic points belonging to the same moving phenomena. The proposed approach termed as STDmapping intends to fill this research gap by incorporating and visualizing the temporal change of a point cluster in a 2D density map. The density surface is temporally segmented into layered tints. Moreover, the use of non-cartographical visual analytical approaches provides a further insight into temporally changing semantics and geometry of dynamic geoobjects, such as lightning data. Two of these existing methods, the radar plot and the parallel coordinate plot, do not adequately address the temporal aspect and are therefore extended to overcome their drawback. Thereby the author came across the idea of addressing temporal changes towards the third dimension. Further non-cartographical visual analytical approaches are introduced to investigate the similarity and complexity of trajectories of dynamic lightning data. In addition, a multivariate visual analytical prototype tool is implemented. It allows the combination and synchronization of different visualization methods, thus can provide an interactive visual insight into the dynamics of lightning data.

Zusammenfassung

Wir leben in einer hochdynamischen Welt. Das Verstehen von dynamischen Prozessen ist essenziell, besonders in Bereichen, die sich mit bewegten Objekten oder Phänomenen auseinandersetzen. Dabei können visuelle explorative Methoden und interaktive Tools einen wesentlichen Beitrag leisten. Die Erforschung von zeitlichen Veränderungen räumlicher Patterns zählt zu den anspruchsvollsten Aufgaben für Geowissenschaftler. Dies verlangt die Fähigkeit signifikante zeitliche Veränderungen in großen Datensätzen zu ermitteln, die extrahierten Informationen zu aggregieren und für bestimmte Zielgruppen auf einfache, verständliche und anschauliche Weise darzustellen.

Diese Arbeit beschäftigt sich mit der visuellen Untersuchung einer bestimmten Art von sich bewegenden Geoobjekten, und zwar räumlich ausgedehnte Objekte (SEO) beziehungsweise Phänomene. Visuell-analytische Methoden werden entwickelt und implementiert, um die Dynamik von bewegten und räumlich ausgedehnten Polygonen zu untersuchen. Als Anwendungsfall dienen Blitzdaten beziehungsweise dynamische Blitz-Cluster.

Die visuelle Exploration von dynamischen Phänomenen kann in drei methodische Teile gegliedert werden: (a) Daten-Repräsentation, welche üblicherweise Daten Aufbereitung, Klassifizierung und Trajektorien-Modellierung erfordert; (b) Interaktive visuelle Analyse; und (c) Visual Analytics - ein wachsendes Forschungsgebiet, in dem multidimensionale und multivariate graphische Tools interaktiv zum Einsatz kommen - darunter Karten, Diagramme und andere nicht-kartographische Darstellungen. Verschiedene Arten dynamischer Objekte und Ereignisse sowie deren semantische als auch geometrische Attribute werden ausführlich diskutiert. Ebenso werden vorhandene Visualisierungs-Techniken zur visuellen Bewegungsanalyse räumlich ausgedehnter Phänomene vorgestellt und miteinander verglichen. In der Fachliteratur gab es insbesondere in den vergangenen Jahren zahlreiche visuell analytische Ansätze zur Untersuchung von bewegten Punkt-Objekten. Methoden, die sich jedoch auf dynamische SEOs beziehen, blieben bisher eher begrenzt. Nur wenige vorhandene Arbeiten beschäftigten sich mit raum-zeitlichen Veränderungen von SEOs in Form von Trajektorien-Spuren und deren dynamische Muster.

Der Autor stellt ein allgemeines Konzept zur visuellen Analyse von dynamischen SEOs vor, mit dessen Einsatz visuelle explorative Tools ausgewählt werden können, abhängig von den zugrundeliegenden Daten und dem angestrebten Nutzungszweck. Das Konzept beruht auf zwei Komponenten von dynamischen SEOs. Dabei ist die erste Komponente die momentane Situation eines sich fortbewegenden Clusters zu einem bestimmten Zeitpunkt oder innerhalb eines spezifischen Zeitintervalles. Die zweite Komponente wird definiert durch die gesamte Trajektorie oder „Spur“ des dynamischen SEO, welche die zusammenhängende Clusterbewegung während der gesamten Lebensdauer des SEO darstellt. Beide Komponenten beinhalten gewisse Bewegungs-Aspekte sowie Informationen über das Bewegungsverhalten des SEO. Des Weiteren werden spezifische Aufgaben zur Bewegungs-Analyse von SEOs sowie deren visuell-analytischen Lösungen in dieser Arbeit vorgestellt. Ein besonderer Schwerpunkt wird auf die internen Strukturveränderungen von jenen SEOs gelegt, welche auf gruppierte punktbezogene Ereignisse beruhen. Bestehende Methoden sind hauptsächlich auf Datensätze für zwei verschiedene Zeitpunkte anwendbar und bieten keine adäquaten Lösungen für Dichtekarten von dynamischen Punkten welche bewegte Phänomene repräsentieren. Die vorgestellte Methode, bezeichnet als „STD-mapping“, versucht diese Forschungslücke zu füllen indem zeitliche Veränderungen von Punktclustern in der Erstellung von 2D Dichtekarten berücksichtigt und entsprechend visualisiert werden. Dabei werden die Dichte-Konturintervalle in zeitliche Segmente unterteilt und farblich angepasst.

Der Einsatz von nicht-kartographischen visuellen analytischen Ansätzen bietet zusätzliche Erkenntnisgewinnung über die sich zeitlich ändernde Semantik und Geometrie von dynamischen Geoobjekten, unter anderem auch von bewegten Blitzclustern. Zwei gebräuchliche Methoden, der „Radar plot“ und der „Parallele Koordinatenplot“, berücksichtigen zeitliche Aspekte nicht in der gewünschten Form und werden in dieser Arbeit dahingehend erweitert. Die Idee dabei ist die Ausdehnung dieser Methoden in die dritte Dimension. Außerdem werden weitere nicht-kartographische visuell analytische Ansätze vorgestellt, mit denen vor allem die Komplexität und die Ähnlichkeit von Blitz-Trajektorien untersucht werden können. Darüber hinaus wird eine multivariate visuell analytische graphische Benutzeroberfläche (Prototyp) implementiert, die es erlaubt, unterschiedliche Visualisierungsmethoden zu kombinieren als auch zu synchronisieren, um den Nutzer oder Analyst eine interaktive visuelle Einsicht in dynamische Blitzdaten zu ermöglichen.

Table of contents

| | |
|---|-----------|
| ABSTRACT | 2 |
| ZUSAMMENFASSUNG | 3 |
| TABLE OF CONTENTS | 5 |
| ABBREVIATIONS AND LIST OF TABLES | 7 |
| LIST OF FIGURES | 8 |
| 1. INTRODUCTION | 11 |
| 1.1. UBIQUITOUS MOVEMENTS AND MOVEMENT DATA | 11 |
| 1.2. MOTIVATION AND RELEVANCE OF THE WORK | 12 |
| 1.3. OBJECTIVES OF THE WORK | 13 |
| 1.4. THESIS STRUCTURE | 13 |
| 2. THEORETICAL BACKGROUND AND THE STATE OF THE ART | 15 |
| 2.1. TERMINOLOGIES AND NOTIONS | 15 |
| 2.1.1. <i>Geovisualization and geovisual analytics</i> | 15 |
| 2.1.2. <i>Geographic dynamics – a spatio-temporal process involving space, time, geographic entities and movement</i> | 19 |
| 2.2. SPATIO-TEMPORAL MODELING OF DYNAMIC PHENOMENA | 23 |
| 2.3. CARTOGRAPHIC REPRESENTATIONS OF DYNAMIC PHENOMENA | 25 |
| 2.4. MOVEMENT ANALYSIS AND VISUAL EXPLORATION OF DYNAMICS | 32 |
| 2.4.1. <i>Visual exploration of dynamic data in general</i> | 33 |
| 2.4.2. <i>Visual exploration of discrete dynamic objects (points)</i> | 35 |
| 2.4.3. <i>Visual exploration of dynamic fields</i> | 36 |
| 2.4.4. <i>Visual exploration of dynamic “polygons”</i> | 37 |
| 2.5. DENSITY MAPS FOR STATIC AND DYNAMIC POINTS | 37 |
| 2.6. TRAJECTORY SIMILARITY MEASUREMENT AND VISUALIZATION | 41 |
| 2.7. PREDICTION AND UNCERTAINTY VISUALIZATION OF MOVEMENT DATA | 45 |
| 2.8. CHAPTER CONCLUSION | 47 |
| 3. VISUAL ANALYSIS/ANALYTICS OF DYNAMIC SEOS/SEPS | 48 |
| 3.1. REFINING SEOS OR SEPS | 48 |
| 3.2. PRE-PROCESSING OF MOVING SEOS | 49 |
| 3.3. VISUAL EXPLORATION OF MOVING SEOS | 51 |
| 3.3.1. <i>Representation (mapping) and non-visual description of dynamic SEPs and their features</i> | 51 |
| 3.3.2. <i>Movement behavior/aspects of dynamic SEOs</i> | 54 |
| 3.3.3. <i>Investigating movement of SEOs through task specific visual analytical approaches</i> | 56 |
| 3.4. CHAPTER CONCLUSION | 62 |
| 4. A CASE STUDY OF LIGHTNING DATA | 63 |
| 4.1. LIGHTNING DATA - A DYNAMIC PHENOMENON | 63 |
| 4.1.1. <i>Detection and position accuracy of lightning data</i> | 64 |
| 4.1.2. <i>Identification, tracking and prediction of lightning clusters</i> | 64 |
| 4.1.3. <i>Test data/scenario description</i> | 65 |
| 4.1.4. <i>Test data pre-processing</i> | 67 |
| 4.1.5. <i>Comparison to similar scenarios</i> | 69 |

| | |
|---|------------|
| 4.2. REPRESENTATION OF LIGHTNING DATA | 69 |
| 4.2.1. <i>Lightning cluster visualization concept</i> | 72 |
| 4.2.2. <i>Lightning trajectory visualization concept</i> | 76 |
| 4.2.3. <i>STC concept</i> | 80 |
| 4.2.4. <i>Cluster and trajectory concepts applied to the test dataset</i> | 83 |
| 4.2.5. <i>Visualizing predicted lightning data</i> | 87 |
| 4.2.6. <i>Lightning nowcasting, uncertainty and visual presentation</i> | 87 |
| 4.2.7. <i>Interactive graphic user interface</i> | 91 |
| 4.3. DENSITY MAPS FOR DYNAMIC LIGHTNING DATA | 93 |
| 4.3.1. <i>STDmapping method</i> | 93 |
| 4.3.2. <i>Implemented STDmapping approach - results and discussion</i> | 99 |
| 4.4. INVESTIGATING MOVEMENT PATTERNS OF LIGHTNING CLUSTERS USING VISUAL ANALYTICAL APPROACHES | 103 |
| 4.4.1. <i>Trajectory complexity</i> | 104 |
| 4.4.2. <i>Trajectory similarity</i> | 111 |
| 4.4.3. <i>Temporal radar plots</i> | 113 |
| 4.4.4. <i>Temporal PCP</i> | 115 |
| 4.4.5. <i>Table lens</i> | 118 |
| 4.4.6. <i>Multivariate visual analytics of lightning data</i> | 119 |
| 4.5. DISCUSSION OF THE PROPOSED VISUAL EXPLORATIVE APPROACHES FOR LIGHTNING MOVEMENTS | 121 |
| 4.6. USERS AND USABILITY ISSUES | 124 |
| 4.7. CHAPTER CONCLUSION | 124 |
| 5. FINAL DISCUSSION | 125 |
| 5.1. APPROACHES AND RESULTS IN RELATION TO THE RESEARCH QUESTIONS | 125 |
| 5.2. LIMITATIONS OF THE PROPOSED METHODS AND COMPARISON WITH RELATED RESEARCH | 127 |
| 6. CONCLUSION AND OUTLOOK | 130 |
| 6.1. TERMINOLOGY REFINEMENT OF SEOs AND PRE-PROCESSING | 130 |
| 6.2. VISUAL EXPLORATION OF MOVING SEOs | 130 |
| 6.3. REPRESENTATION AND VISUAL ANALYSIS OF LIGHTNING DATA | 130 |
| 6.4. DENSITY MAPS FOR DYNAMIC LIGHTNING DATA | 131 |
| 6.5. VISUAL ANALYTICAL APPROACHES FOR LIGHTNING CLUSTERS | 131 |
| 6.6. OUTLOOK | 131 |
| 6.6.1. <i>General improvements</i> | 132 |
| 6.6.2. <i>Improvements of specific approaches</i> | 132 |
| 6.6.3. <i>Verifications of proposed approaches</i> | 132 |
| 7. REFERENCES | 134 |
| 8. ACKNOWLEDGMENTS | 144 |

Abbreviations

| | | | |
|----------|------------|---|------------------------------------|
| Abbr. 1 | GIS | – | Geographic information system |
| Abbr. 2 | GUI | – | Graphic user interface |
| Abbr. 3 | GC | – | Ground-cloud |
| Abbr. 4 | IC | – | Intra-cloud |
| Abbr. 5 | KDE | – | Kernel density estimation |
| Abbr. 6 | DKDE | – | Directed kernel density estimation |
| Abbr. 7 | PCP | – | Parallel coordinate plot |
| Abbr. 8 | SEO | – | Spatially extended object |
| Abbr. 9 | SEP | – | Spatially extended phenomenon |
| Abbr. 10 | STC | – | Space time cube |
| Abbr. 11 | STDmap | – | Spatio-temporal density map |
| Abbr. 12 | STDmapping | – | Spatio-temporal density mapping |
| Abbr. 13 | TCG | – | Trajectory complexity gain |

List of tables

| | |
|---|-----|
| Table 2-1: Methods for visualization of detailed (not aggregated) movement or event data, from (Andrienko et al. 2011a)..... | 34 |
| Table 2-2: Analysis tasks and respective supporting techniques, from (Andrienko et al. 2011a). | 34 |
| Table 2-3: Visual exploration approaches for dynamic point data (selected examples)..... | 36 |
| Table 3-1: Types of dynamic objects and examples..... | 49 |
| Table 3-2: Typical features of a dynamic SEO and their attributes. | 52 |
| Table 3-3: Visual variables for dynamic SEO..... | 54 |
| Table 3-4: Analysis of moving SEOs: tasks and visual analytical approaches..... | 58 |
| Table 3-5: An overview of the visual analytical tools for dynamic SEO | 61 |
| Table 4-1: Example of given stroke data..... | 66 |
| Table 4-2: Adjustable parameters within lightning cluster and tracking processing workflow. | 68 |
| Table 4-3: Lightning test dataset..... | 69 |
| Table 4-4: Visual presentation of past and predicted lightning information. | 70 |
| Table 4-5: Graphic variables of cluster and track representations. | 71 |
| Table 4-6: Attributes and statistical data of lightning clusters and tracks. | 72 |
| Table 4-7: Properties, pros and cons of 3D cluster visualization options. | 75 |
| Table 4-8: Properties, pros and cons of trajectory visualization options..... | 79 |
| Table 4-9: Properties, pros and cons of cluster and trajectory visualizations for STC. | 82 |
| Table 4-10: Important lightning track attributes..... | 86 |
| Table 4-11: Trajectory complexity based on attribute changes. | 106 |
| Table 4-12: Attributes of two different tracks..... | 111 |
| Table 4-13: The relative suitability of proposed visual analytical approaches for lightning cluster attributes and movement events..... | 121 |
| Table 4-14: Use of approaches for task specific movement analysis..... | 123 |
| Table 5-1: Approaches in the thesis and their innovations. | 125 |

List of figures

| | |
|---|----|
| Figure 1-1: Thesis organization..... | 14 |
| Figure 2-1: Map use cube according to MacEachren & Taylor (1994). | 16 |
| Figure 2-2: Different stages involved in the visual analytics, source: visual-analytics.eu..... | 18 |
| Figure 2-3: Schematic representation of the interplay of geovisual analytics, geovisualization and cartography, proposed by Schiewe (2013). | 18 |
| Figure 2-4: A triad framework based on Peuquet (1994b). | 20 |
| Figure 2-5: Dimensions of temporal variability in geographic objects (Goodchild et al. 2007). | 21 |
| Figure 2-6: Objects and their spatio-temporal structure and relations (Andrienko et al. 2011a). | 22 |
| Figure 2-7: A conceptual framework of the three-domain model, based on Yuan (1996). | 23 |
| Figure 2-8: Taxonomies of spatio-temporal change patterns, after (Yang et al. 2008). | 24 |
| Figure 2-9: Temporal topological relationships, based on Allen (1983). | 24 |
| Figure 2-10: Visual presentation of spatio-temporal relationships in a 2-dimensional space, based on Claramunt & Jiang (2000). | 25 |
| Figure 2-11: A historical map (extract) showing movement: Emigrant's Routes to North America, by Gotthelf Zimmermann (1853), source: http://www.wdl.org/ | 26 |
| Figure 2-12: A historical map. | 27 |
| Figure 2-13: A nutshell of different temporal map types for spatio-temporal data. | 28 |
| Figure 2-14: Piechart symbols for two different moments of time, source: www.gitta.info | 29 |
| Figure 2-15: Spreading of the plaque in Europe, 1347 – 1350, source: www.von-scheidt.de | 29 |
| Figure 2-16: Representations of aggregated movement data. (A, B) Time series associated with places (A) and links (B). (C, D) Spatial situations in terms of presence (C) and flows (D), source: Andrienko et al. (2012). | 30 |
| Figure 2-17: Bertin's visual variables, source: makingmaps.net | 31 |
| Figure 2-18: Geovisualization of dynamics - research topics based on Andrienko et al. (2008a). | 35 |
| Figure 2-19: Different point symbolizations for soil texture attributes, source: Mitas et al. (1997). | 36 |
| Figure 2-20: KDE principle. Source for a) and b): www.geography.hunter.cuny.edu | 38 |
| Figure 2-21: Linear kernel (left) and Directed linear kernel taking point speed and movement direction into account (right), source: Peters & Krisp (2010). | 40 |
| Figure 2-22: Airplane positions at two moments of time (left) and the resulting DKDE-map (right), source: Peters & Krisp (2010). | 40 |
| Figure 2-23: Density visualization of crime events in a STC, source: Nakaya and Yano (2013). | 40 |
| Figure 2-24: Aggregated vessel trajectories, left: Multi-scale density with continuous color mapping, right: Density with discrete color mapping; source: Willems et al. (2009). | 41 |
| Figure 2-25: Traffic data of Milan, Italy, a) clustered by color, b) aggregated to arrows, c) STC, source: http://www.rockpaperink.com/post/92434324658/designing-mobility | 43 |
| Figure 2-26: Trajectory density map of vessels, source: Scheepens et al. (2011b). | 44 |
| Figure 2-27: Trajectory wall with time lens of traffic jam along one main road in San Francisco (above) and corresponding time graph (below), source: (Tominski et al. 2012) | 44 |
| Figure 2-28: Uncertainty visualizations for point symbols with variations in saturation (left), crispness (center) and transparency applied to the smaller symbol (right), source: MacEachren et al. (2005). | 46 |
| Figure 2-29: Visualized Vessel prediction and uncertainties of three time intervals, source: (Scheepens et al. 2014). | 46 |
| Figure 3-1: Dynamic SEOs - data capturing and pre-processing..... | 50 |
| Figure 3-2: Some available visual analytical approaches relevant for the exploration of dynamic SEOs, source: https://github.com/mbostock/d3/wiki/Gallery | 61 |
| Figure 4-1: Lightning test dataset during April 2013 (black: IC lightning, grey: CG lightning, red: country borders). | 66 |
| Figure 4-2: The subset of lightning points (April 26th 2013) on a base map. | 67 |

| | |
|---|-----|
| Figure 4-3: The workflow from data detection to visual analysis..... | 67 |
| Figure 4-4: GC lightning density map for South-German districts 1999-2011, source: http://www.gdv.de/2013/06/blitz-und-ueberspannung-sorgen-fuer-viele-schaeden/ , © Blitz-Informations-Dienst von Siemens..... | 70 |
| Figure 4-5: Concept for lightning cluster visualization using plan view..... | 73 |
| Figure 4-6: Concept for lightning cluster visualization in a 3D space..... | 74 |
| Figure 4-7: Lightning cluster visualization - GC and IC data..... | 76 |
| Figure 4-8: Various ways of lightning track visualization in a 2D space..... | 77 |
| Figure 4-9: Various ways of lightning track visualization in a 3D space..... | 78 |
| Figure 4-10: Pseudo code for point selection with density based symbol size..... | 80 |
| Figure 4-11: Concept for lightning track visualization using STC..... | 81 |
| Figure 4-12: A plan view showing the track line of cluster centroids with point quantity-based symbol size and color..... | 83 |
| Figure 4-13: Track-lane presented in 2D and 3D (selected points)..... | 84 |
| Figure 4-14: Track lane derived from selected points with point quantity-based symbol size..... | 84 |
| Figure 4-15: Track-line together with cluster convex hull and points at one time interval (5:00- 5:10pm)..... | 85 |
| Figure 4-16: The STC with convex hulls and centroids of quantity-based symbol size and color..... | 85 |
| Figure 4-17: The STC with all lightning points..... | 86 |
| Figure 4-18: Nowcasted lightning data 26.4.2014, left: 2D view, middle: 3D view, right: STC..... | 87 |
| Figure 4-19: Cluster centroid nowcasting concept for 2D..... | 88 |
| Figure 4-20: Past-processed '10minutes nowcasted' and 'measuring-based updated' centroids..... | 89 |
| Figure 4-21: Centroid standard deviation after past-processed prediction of each time interval..... | 90 |
| Figure 4-22: A buffer representing the prediction uncertainty of nowcasted lightning cluster (left: last two lightning clusters; right: predicted clusters with uncertainty buffers; middle: past and predicted clusters)..... | 90 |
| Figure 4-23: The GUI for interactive data exploration of the lightning data dynamics..... | 92 |
| Figure 4-24: KDE map (left) and colored points based on temporal clusters (right)..... | 93 |
| Figure 4-25: Temporally clustered point data..... | 94 |
| Figure 4-26: The workflow of STDmapping of lightning data..... | 95 |
| Figure 4-27: Temporal clustered points and cluster centroids in black with straight tendency line and perpendicular temporal borders (left) and with curved tendency line and perpendicular temporal borders (right)..... | 96 |
| Figure 4-28: Suggested solution for intersecting temporal border lines (red)..... | 96 |
| Figure 4-29: Density contours with temporal borders based on a linear tendency line (left) and with temporal borders and thresholds for smooth color gradients based on a curved tendency line (right)..... | 97 |
| Figure 4-30: Rainbow color scheme..... | 98 |
| Figure 4-31: Different color scheme approaches..... | 99 |
| Figure 4-32: Segmented KDE in one map (a: no transparency, b: transparency of 50%)..... | 99 |
| Figure 4-33. STDmap with abrupt (left) or smooth (right) color gradient based on straight tendency lines and the temporal interval of one hour (above) or 30 minutes (below)..... | 100 |
| Figure 4-34. STDmap with abrupt (left) or smooth (right) color gradient based on curved tendency lines and the temporal interval of one hour (above) or 30 minutes (below)..... | 101 |
| Figure 4-35: Wrongly assigned points (in black), using abrupt (left) or smooth temporal borders (right)..... | 103 |
| Figure 4-36: Time plot of geometrical cluster attributes..... | 104 |
| Figure 4-37: The bar chart of the TCG..... | 106 |
| Figure 4-38: The curves of TCG..... | 107 |
| Figure 4-39: TCG - by travelled distance..... | 107 |
| Figure 4-40: TCG bar chart on top of 2D map..... | 108 |

| | |
|---|-----|
| Figure 4-41: TCG diagram on top of 2D map..... | 108 |
| Figure 4-42: Connected stacked normalized cluster attribute value (left) and bar chart (right) on top of 2D map with 2D track points in orange and cluster centroids in black. | 109 |
| Figure 4-43: Trajectory wall with stacked complexity attribute bands on top of 2D map. | 109 |
| Figure 4-44: STC with stacked attributes values (complexity) applied to one track..... | 110 |
| Figure 4-45: Similarity matrix and bar chart of two lightning tracks..... | 112 |
| Figure 4-46: Radar plot with interactive cluster selection..... | 113 |
| Figure 4-47: A “temporal radar plot”. | 113 |
| Figure 4-48: A temporal radar plot of the lightning data: from above (2D), 3D and side perspective. a-c) show 1 single track while attributes are drawn in different colors; d-f) display 11 tracks colored by track affiliation on April 26th; g-i) show 11 tracks on April 26th with a time-based rainbow color scheme; j-l) contain all tracks during April with rainbow-time-color scheme. | 114 |
| Figure 4-49: Parallel plot with the interactive highlighting of two clusters. | 116 |
| Figure 4-50: Clustered PCP lines (left), resulting 3D PCP (right), source: Streit et al. (2006)..... | 116 |
| Figure 4-51: 3D PCP, source: Rübél et al. (2006). | 117 |
| Figure 4-52: PCP (left) vs. temporal PCP (right) for lightning test dataset above: track-based polyline colors (April 26th 2013, 2-7pm) middle: time-based rainbow-colored polylines (April 26th 2013, 2-7pm) below: time-based rainbow-colored polylines (entire April 2013). | 117 |
| Figure 4-53: The table lens representing attributes and their values of six different lightning tracks..... | 119 |
| Figure 4-54: Multivariate visual analytics for lightning data (April 26th)..... | 120 |

1. Introduction

This chapter addresses the nature of movements and the categorization of movement data. The research field related to the *visualization* and analysis of movement data is outlined along with a narrative of its social relevance. In line with the motivation and the goal of the involved research work, the author defines the scope and structure of the dissertation.

1.1. Ubiquitous movements and movement data

We live in a dynamic world. Dynamics in a geographical context includes, on the one hand, *moving objects*, such as people, vehicles or animals and on the other hand, it deals with the spatio-temporal change of our environment including urban objects (e.g. houses, streets) as well as natural phenomena on the earth surface (e.g. water, forests) and those related to the atmosphere (e.g. clouds, wind) and belowground (e.g. soil composition). Furthermore, people interact on certain places at or during certain times with each other and with our environment. These spatio-temporal activities also lead to movements and changes, such as shifting of boundaries (e.g. political or cultural ones). Understanding of movements is an important mental process for the informed decisions in the modern society. An appropriate representation of geographic dynamics should tell us a story about the respective evolving process and thus facilitate the comprehension.

With the increasing availability of big data including large quantities of movement data acquired through sensory devices such as mobile phones, GPS and navigational facilities, the exploration of dynamic geographic data and thus movement pattern detection have become an important research focus (Dykes & Mountain 2003). Thus movement data are ubiquitous – technically available everywhere to any time. Consequently appropriate visual analytical methods and tools are needed to analyze movement data, to derive an insight into them and to make decisions based on visualizations and the interactive use of visual tools.

The visual analytical investigations presented in this thesis support the approaches of *visual analytics* – a brand new research discipline that emerged from a number of scientific works. In 2004, the National Visualization and Analytics Center (NVAC) was founded in USA (NVAC 2012). NVAC gathered experts from different disciplines and proposed a research agenda for visual analytics. Its European counterpart VisMaster is dedicated to the coordination of research activities of visual analytics (VisMaster 2012). Moreover, a working group of the MOVE project is dedicated on visual analytics for movement and cognitive issues (MOVE). The main goal of MOVE (COST Action IC0903) is to develop improved methods for knowledge extraction from large amounts of data about moving objects.

Different research groups have been engaged in the studies of movement data with each having a different scientific focus, for instance:

- Social Movement
- Movement in ecology
- Movement in spatio-temporal data bases
- Movement in spatio-temporal data mining
- Movement in Information-and-communication-technology
- Representation/visual analytics of movement (VisMaster, NVAC, MOVE)

Obviously, the movement research is either targeted on a specific application domain or is driven by technology. The last listed focus (representation/visual analytics of movement) has an interdisciplinary nature. The related working groups are engaged in developing general methods and

tools as well as data/application-specific concepts and solutions. This thesis addresses the visual analytical approaches for a specific type of geographic movement data – spatially extended dynamic objects or phenomena, taking the movements of lightning clusters as a case study.

1.2. Motivation and relevance of the work

In general, tools in cartography, *geographic information systems* (GIS) tools as well as other visual tools are used to represent and explore geodata. Many existing approaches are conceptualized for static two-dimensional data. Taking into account also the third dimension in space, the dynamics of data (change in time) and the possibility of user interaction, many visual tools need to be adapted and extended in order to handle the additional constraints. MacEachren & Kraak (2001) appealed the cartographic research community to take full advantage of technological advances that make it possible to personalize representation, generate complex multidimensional and dynamically linked views, merge representation with reality and take advantage of non-visual perceptual channels. According to the research agenda of the International Cartographic Association, an important issue in *geovisualization* and visual analytics is that “geovisualization techniques have extended the map medium to embrace dynamic, three- and four-dimensional data representation” (Virrantaus et al. 2009).

Efficient visual exploration may enable the analysis of large datasets. But current methods are not effective enough for a *visual analysis*. Considerable visual disorder and overplotting might cause illegible data representation. Furthermore, it is not always straightforward to identify, track and understand abundant simultaneously changing visual components (Andrienko et al. 2008a). In (Cook et al. 2012), the challenges in extreme-scale visual analytics are explained. Two of them are addressed in this work: the analytics of temporally evolved features; data summarization and triage for interactive query. Both require a meaningful representation and modeling of complex spatiotemporal phenomena and the representation of other non-spatial attributes that may exist in space-time (Goodchild 2010). The visualization, visual analysis and visual analytics of dynamic geographical data and phenomena are regarded as a crucial research field (Andrienko & Andrienko 2013) which is expected to deliver some useful solutions. The foundations, in particular in geo-spatial and temporal visual analytics of dynamic geodata, have been already laid. Application domains where the analysis including the visual analysis of dynamic geographic data is relevant include those dealing with the mobility of people, animals, goods, such as transportation, tourism, urban and rural planning, resource management, crisis management, ecology etc.; or those focusing on the dynamics of environmental phenomena, such as meteorology, wildfire analysis, water management, landslide analysis etc. Further possible application domain could be microbiology and medicine.

Notably, numerous frameworks, strategies, methods and tools for the visual analysis of moving discrete point data such as cars, airplanes, vessels etc. have been proposed and implemented, but only few approaches have touched the dynamics of *spatially extended objects* (SEOs) or *spatially extended phenomena* (SEPs) such as clouds, swarms and herds which change their sizes, shapes and other attributes in time. The individual instances for a SEO or SEP may demand customized visual analysis solutions. The dynamic lightning clusters which represent the most dangerous part of a thunderstorm, for example, cannot yet be thoroughly studied due to inadequate approaches of visual analysis/analytics and missing interactive visual exploration tools for target groups such as weather researchers and decision makers (e.g. at airports). With this thesis, the author attempts to fill some research gaps based on the preliminary work on the visual analysis for lightning data as reported in (Peters & Meng 2013).

1.3. Objectives of the work

The thesis aims to construct a framework for the visual exploration of dynamic SEPs in which different types of phenomena are addressed and visual exploration methods and tools are accommodated. Furthermore, the thesis will provide an overview of visual analysis approaches, report the implementation of existing visual analytical approaches and introduce the development of new ones for general dynamic SEP and the moving lightning clusters as a special instance. In more details, the thesis aims to make methodological contributions in three categories of innovations:

(I) Novel methods

Density maps, illustrated for example through contour intervals, support the visual exploration of spatio-temporal phenomena represented by point data. Nonetheless, the temporal information is not yet adequately addressed in existing approaches. A novel approach for the creation of two-dimensional density surfaces for dynamic (spatially and temporally changing) points or phenomena will be developed and implemented on lightning data. Moreover, moving lightning clusters – a specific type of SEPs, partly require individual solutions for their visual exploration. Two novel visual analytical approaches for the trajectory complexity and trajectory similarity investigation are introduced and applied to a test dataset.

(II) Extension or elaboration of existing approaches:

Existing *geovisual analysis* and *geovisual analytics* approaches may help provide an insight into spatial data and derive general patterns. Some of these approaches, in particular, visual analytical approaches, will be extended to deal with spatio-temporal data. These include two elaborated methods *radar plot* and *parallel coordinate plot* (PCP).

(III) Verification (implementation and adaptation) of existing approaches:

Existing approaches for visually exploring the complex and information-rich type of moving lightning clusters will be implemented and verified. They include *space time cube* (STC) and *table lens* plot. Moreover, an interactive web-based *graphic user interface* (GUI) will be implemented for a comprehensive visual exploration of dynamic lightning data.

The following research questions are involved in order to reach the above objectives:

- 1) How can we describe and visually present dynamic SEOs/SEPs – in particular dynamic lightning clusters?
- 2) How can we visually analyze the movement of dynamic SEOs, in particular lightning clusters, using maps and other displays?
- 3) How can we incorporate temporal information in two-dimensional density contour maps for dynamic SEPs that are characterized by moving points or events?
- 4) How can existing geovisual-analytics approaches for spatial data be refined to address the visual exploration of dynamic data, in particular dynamic SEOs/SEPs?
- 5) Which information can be derived using geovisual analysis and geovisual analytics methods for dynamic SEOs?

1.4. Thesis structure

The thesis is divided in six chapters. Figure 1-1 provides an overview about the organization of the thesis. Following the introductory chapter (Chapter 1), Chapter 2 consists of a theoretical background including terminologies related to the dynamics of geographic objects and phenomena as well as the evolution from visual analysis to visual analytics. The state of the art is summarized along with a literature review on visual analysis approaches for dynamic geobjects, in

particular of SEOs/SEPs. A framework for the visual analysis of dynamic SEOs/SEPs is generated in Chapter 3. In Chapter 4 the framework is tailored to the application case of moving lightning data, which involves elaboration and specialization of the visual representation and visual analysis/analytics for the spatio-temporal nature of lightning data. Several approaches are implemented for a lightning test dataset and evaluated. They are either elaborations of the existing methods or novel approaches. Some of them are specifically developed for lightning data, others are generally appropriate for dynamic SEOs/SEPs. The novel technique - Spatio-temporal-Density mapping (*STDmapping*) is described in detail, providing a solution to incorporate temporal information in two-dimensional density contour maps for dynamic SEOs/SEPs. Existing visual analytical approaches such as radar plot and PCP are extended as three-dimensional tools – using the third dimension to integrate the movement information. For the case study with lightning data two novel visual analytical approaches are suggested, providing an insight into trajectory complexity and similarity. The advantages as well as the drawbacks of all suggested approaches are summarized in the final chapter, followed by an outlook about further research issues.

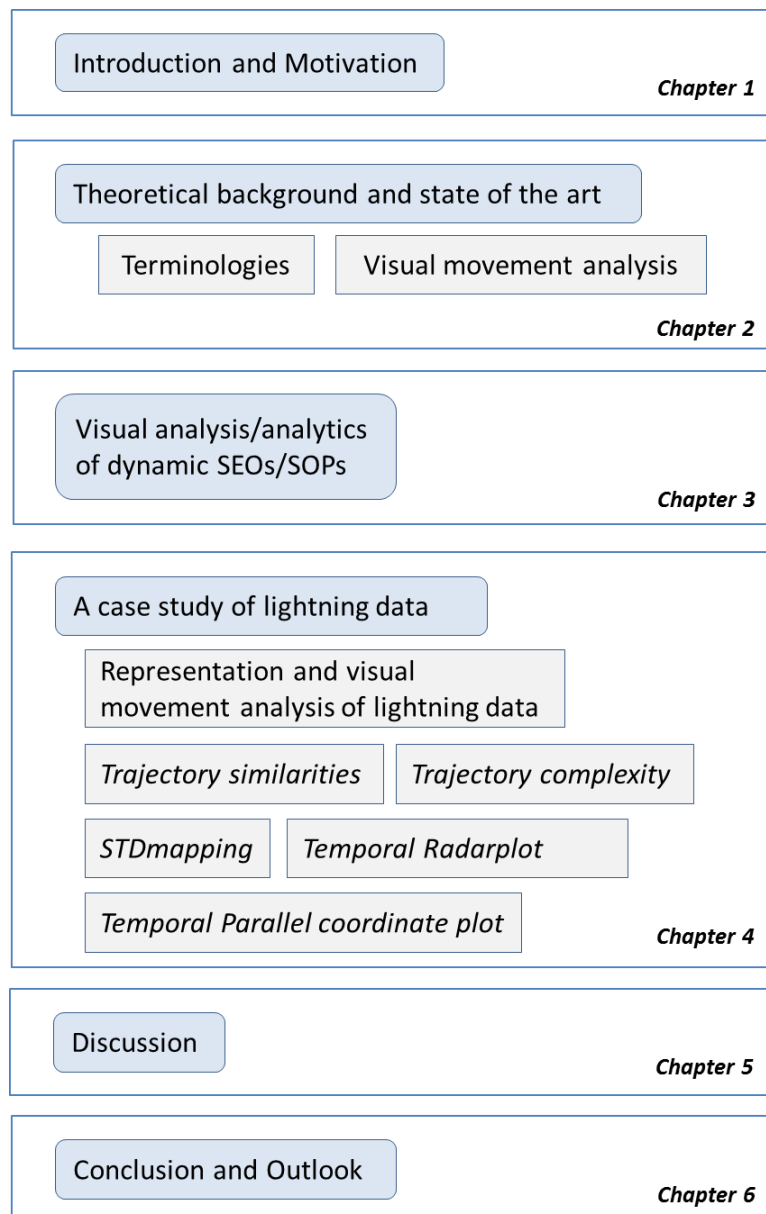


Figure 1-1: Thesis organization.

2. Theoretical background and the state of the art

This chapter aims to provide the fundamentals needed to understand the approaches in subsequent chapters. In Section 2.1, the terms visualization, geovisualization, geovisual analysis and geovisual analytics as well as their position and importance in *cartography* are introduced. It is followed by dedicated discussions on the geographic dynamics – a spatio-temporal process involving space, time, geographic entities and movement. Different kinds of *dynamic objects* and *events* as well as their semantic and geometrical attributes are specified. Section 2.2 is dedicated to spatio-temporal modeling of dynamic phenomena. Object- as well as event-oriented modeling approaches are presented along with an introduction of taxonomies of spatio-temporal change patterns and spatio-temporal relationships of moving objects, in particular, those of dynamic polygons. Section 2.3 is dedicated to existing cartographic representation techniques for dynamic phenomena. By means of map examples showing temporal information and movement information, different temporal map types are identified. Furthermore, various strategies for representing dynamic data (e.g. trajectories and aggregated trajectories) on static as well on dynamic maps are discussed. Section 2.4 deals with visual analysis methods for movement data which can be discrete points, fields and dynamic polygons. Dynamic phenomena extended in space and based on moving points or events also change their internal structure including their point density. Usually, they can be visualized in density maps. The state of the art of density mapping techniques is summarized and evaluated in Section 2.5, which brings about the associated research question. The similarity measurement of trajectories is discussed in Section 2.5. Section 2.6 introduces theories for uncertainty visualization of predicted dynamic data.

2.1. Terminologies and notions

2.1.1. Geovisualization and geovisual analytics

The term visualization has its roots in *scientific visualization* and was developed to investigate large multivariate datasets (Slocum et al. 2009). McCormick et al. (1987) stated that scientific visualization aims to leverage existing scientific methods by providing an insight into the observed data through visual methods. More recently, the term and the field of *information visualization*, closely related to scientific visualization have been introduced, focusing on the visual representation and analysis of numeric and nonnumeric information with the purpose to construct a visual mind image. Today, the visualization can be also understood as a graphic representation of data or concepts (Ware 2012). The concept of visualization exists in cartography at least since 1950 (MacEachren & Taylor 1994) when cartographers manage to define the visualization of geographic information. One basic definition given by MacEachren & Monmonier (1992) encompasses both paper and computer-displayed maps: “The use of concrete visual representations – whether on paper or through computer displays or other media – to make spatial contexts and problems visible, so as to engage the most powerful human information-processing abilities, those associated with vision”. Thus a broader term for geographic visualization was introduced, taking all types of geographical data and non-spatial data as input and maps, areal images, diagrams, graphs and many other visual forms as output.

Visualization as a process of making things visible is an enabling mechanism that helps to understand and explore complex relationships in a spatial context. It does not necessarily advance information communication, but it aims to increase the probability of doing so (Peters & Meng 2013). On the one hand, visualization complements and expands our capability of perception. On the other hand, visualization aims to steer our perception in a certain direction in order to enable innovation.

Maps are among the most favored visualization techniques. They are traditionally used to represent geographic information in an abstract form, support the identification of spatial patterns at different abstraction levels and highlight characteristic features of spatial phenomena. In today's society, the amount of shared information and data is constantly increasing. Therefore, there is an increasing demand for data abstraction (Mackaness et al. 2007). A direct projection of digital geodata on a display surface does not make sense from the cartographic perspective. Instead, maps are elaborately designed to reveal patterns that may not be immediately recognized in the real world (Andrienko et al. 2008a). Maps are often treated as a subset of visualizations, in particular, geographic visualizations or geovisualizations (MacEachren et al. 1999). Geovisualization as a research domain addresses and integrates approaches from multiple disciplines, such as visual exploration, analysis, synthesis and presentation of geographic data, information and knowledge (Dykes et al. 2005). Thereby, the ease of use is the key to effective visual data analysis.

Figure 2-1 illustrates a map use cube introduced by MacEachren & Taylor (1994). Depending on the type of user, the form of interaction and on the pre-knowledge about the visualized information, the cube embraces different functions of map usage ranging from presentation (communication of mostly general messages in a pre-assembled way) and all the way through analysis and synthesis to the exploration of structures and processes.

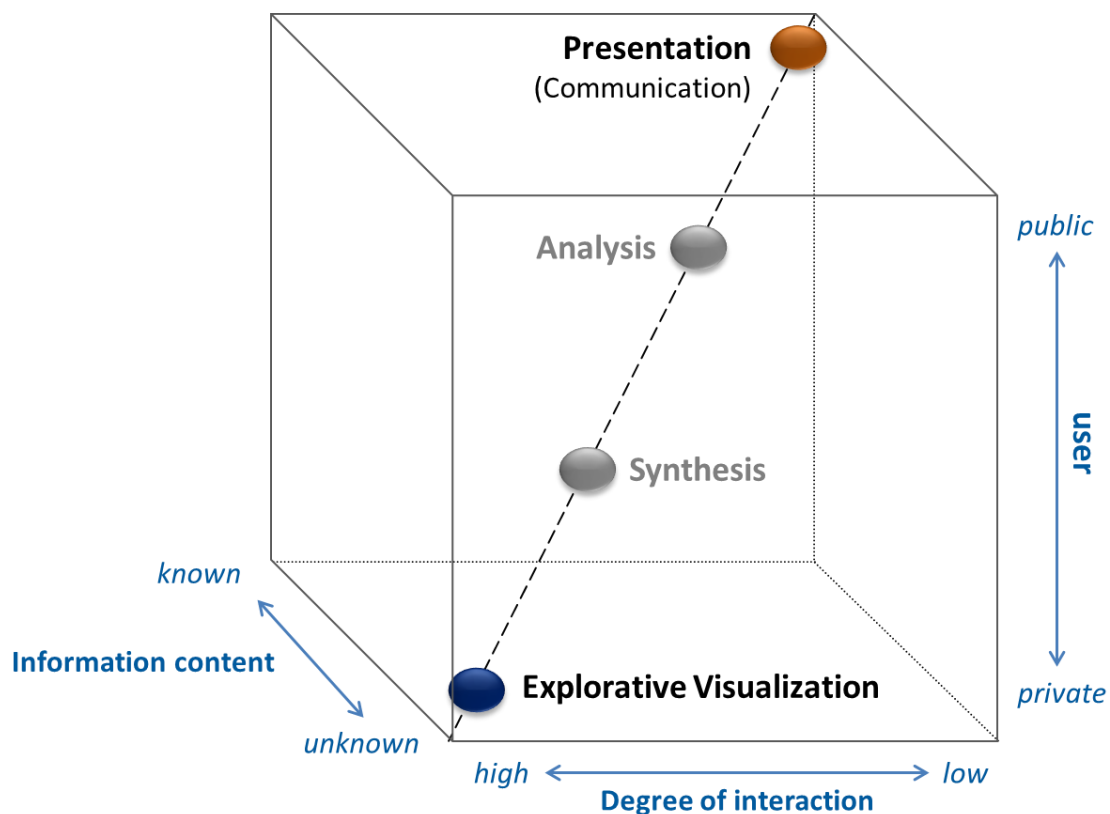


Figure 2-1: Map use cube according to MacEachren & Taylor (1994).

Geovisualization aims to facilitate data exploration, cognition and interpretation of geographic information by the use of appropriate visual representations. Thus the use of geovisualization can be understood as visual analysis of geographic data or geovisual analysis. The rapidly increasing amount of data and its complexity that now demands both visual representation and analysis has given rise to the new scientific field of visual analytics (Keim et al. 2008). Conventional maps have been obviously extended and elaborated to involve further graphic presentations. According to Thomas & Cook (2005), the term visual analytics stands for the science of analytical reasoning

supported by interactive visual interfaces. The basic idea behind any visual analytical process is to combine human cognitive capabilities with computer advance graphics representations of a natural phenomenon. This aims to provide better reasoning and understanding of the natural phenomenon characteristics. Furthermore, interactive visual exploration facilitates the revealing of hidden information with a high quality, thus enable the analyst to draw correct conclusions and make right decisions (Andrienko et al. 2010). Visual analytics is an interdisciplinary field, including among others mathematics, statistics, information visualization, scientific visualization, data mining, geospatial and cognitive sciences. Starting from the visualized data, it supports pattern recognition, imagination, association and analytical reasoning (Andrienko et al. 2003).

Geovisual analytics focuses on visual analytical approaches for geographic information, in particular for multidimensional data with complex structures and features. Schiewe (2013) extended the definition of geovisual analytics as “a linkage of visual and computational methods and tools for extracting hypotheses and information from spatial data”. He understands “analytics” as an umbrella for different map use functions comprising synthesis and exploration. Since the integrated visual and automated analysis is focused on the reasoning function, geovisual analytics goes beyond the scope of geovisual analysis.

Certain differences between visualization, geovisualization (geovisual analysis) and geovisual analytics are perceivable in their definitions. In general, the graphic representation of geographic information is mainly used for demonstration and illustration purpose. The uses of static graphic representations for multidimensional data, however, have drawbacks, such as inevitable occlusion and overlapping, which may cause information loss. Furthermore, spatio-temporal data can only be displayed for a certain moment of time or time interval. To visually gain an insight into the complex and large spatial or spatio-temporal data and their behavior, explorative tools are needed. Geovisual analysis includes interactions enabled by explorative tools such as panning, zooming, rotating and further analytical operations etc. These tools may help partly overcome the disadvantages of simple data representation. However, current techniques may not be sufficient to deal with very complex and large datasets. Displays may become illegible due to visual clutter and massive overplotting and users may have difficulties to perceive, track and understand the changing visual elements (Andrienko et al. 2008a).

Geovisual analytics goes a step further. It deals not only the visual exploration of the geographic locations of data items, but also the understanding of the semantic attributes of the georeferenced data, their relationships among each other and their interactions with the geographic locations. Besides standard cartographic map displays, graphics, diagrams, charts and further innovative solutions can also be used to visualize the large amount of data. By means of methods of geovisual analytics we can derive intermediate results, which themselves, can be visualized in an appropriate way. Thus visual analytics enables a systematic - and if needed iterative - visual insight-discovery of large datasets including the semantic attributes. To distinguish geovisual analysis from geovisual analytics we have to differentiate the terms analysis and analytics from each other. An analysis can be described as a process of decomposing a complex entity into simpler components in order to facilitate the comprehension of it. Analytics is focused on the entire methodology rather than the individual steps (as analysis). As a discipline it uses different tools and techniques from several fields (e.g. mathematics, statistics) to gain knowledge from data and to provide a comprehensive insight into the data and data characteristics.

Geovisual analytics has far more theories, methods than just visual analysis tools; and it consists of not only a value-adding chain of geovisualization, but also the studies of user behavior and usability. Figure 2-2 illustrates the realm of visual analytics. It combines visual analysis and automatic methods. Thereby, human interaction is essential to gain knowledge from data. Four differ-

ent stages are shown: Data, Models, Visualization and Knowledge. Relations/transitions between these stages are iterative and illustrated via arrows.

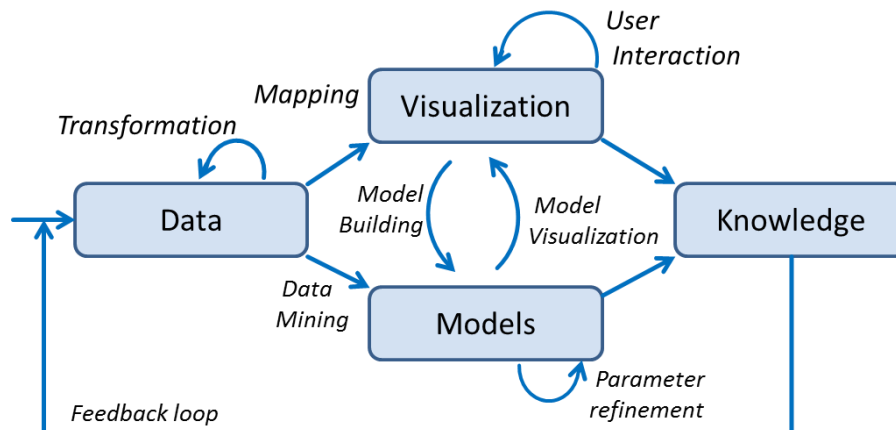


Figure 2-2: Different stages involved in the visual analytics, source: *visual-analytics.eu*.

Nevertheless, existing research in visual analytics was devoted mainly to elaborating tools to visualize data and their features rather than capturing and analyzing the insight. Schiewe (2013) proposed a schematic representation of the interplay of geovisual analytics, geovisualization and cartography as illustrated in Figure 2-3. Schiewe's scheme clearly shows that geovisualization, geovisual analytics, cartography and related fields interplay and are therefore not isolated fields.

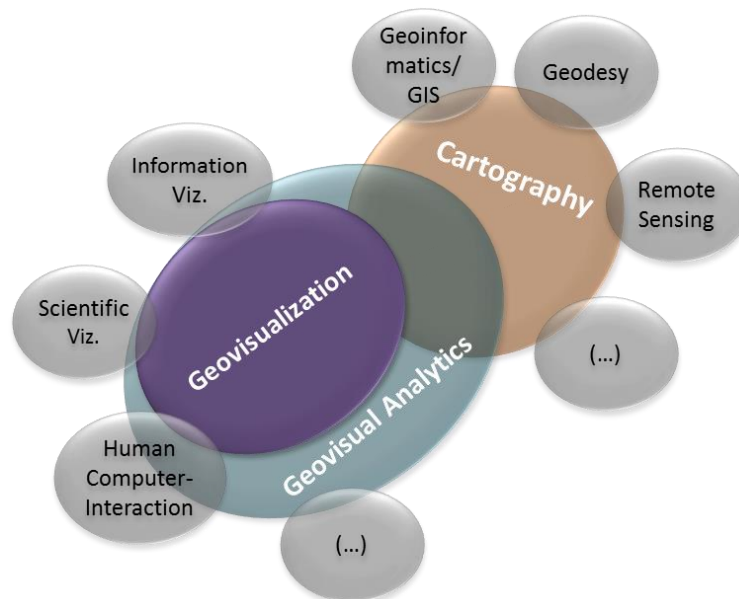


Figure 2-3: Schematic representation of the interplay of geovisual analytics, geovisualization and cartography, proposed by Schiewe (2013).

Schiewe (2013) argued that a key problem with the term geovisualization is caused by its “visualization” component which generally includes how spatial information is made visible but not its purpose. On the other hand, geovisualization was defined with a focus on usage (as explained before and illustrated in Figure 2-1). Consequently, the focus of geovisualization is on the purpose of the visual product rather than the product generation as such. These different views (generation and usage) may lead to some confusion with the term geovisualization. Researches in cartography nowadays are focused on ubiquitous and interactive exploration of real-time accessible geodata using the Internet technology, distributed databases, multiple data integration systems etc. This trend confirms Schiewe's view that cartography and geovisual analytics tend to

interplay more and more. Since this thesis deals with geographical data the terms “geovisual analysis” and “geovisual analytics” are - for the sake of simplicity – reduced to “visual analysis” and “visual analytics” and we will use the term “visual exploration” when we speak about both, visual analysis and visual analytics. The concepts and approaches presented in this thesis refer to the visual analysis and visual analytics of movement data. In particular, the process of object movement is emphasized.

2.1.2. Geographic dynamics – a spatio-temporal process involving space, time, geographic entities and movement

Traditionally, GIS data modeling emphasizes the spatial representation of the real world (Peuquet 1984). In this section we attempt to scrutinize the dynamics of geodata that typically involves the term ‘moving’ or ‘evolving’. Dynamic geographic phenomena can be conceptually represented as spatio-temporal patterns, space-time processes or events (Shiple et al. 2013). Geographic dynamics describes all time-dependent aspects of the Earth surface and near-surface, including results of processes that transform and modify it (Goodchild & Glennon 2008). It involves both physical and social phenomena. Tools and models in GISscience may enable the analysis of dynamic phenomena. Goodchild and Glennon divide the identification of dynamic processes in object-based and field-based.

The adjective geographic refers first and foremost to the Earth surface and near-surface. For many applications and purposes the 2D surface is sufficient, but in fields such as atmospheric sciences, the full 3D knowledge about the domain is needed. Dynamics refers to changes caused by time and their characteristics. Changes in the geographic world may result from natural processes, such as erosion or caused by human activities, such as global warming. In general we relate ‘dynamics’ to the change of something. Dynamics of geographical phenomena can refer to a change of object position (e.g. movement) and/or object attributes (e.g. deformation, erosion). This thesis mainly addresses the movement of SEOs. With the movement of such objects, some of their attributes may change as well.

About 25 years ago, Goodchild (1988) stated, that dynamic phenomena have not been adequately addressed in GIS-science and cartography due to difficulties of their acquisition and storage. Instead, the emphasis is so far laid on the static aspects of the surface. In recent years, a wide range of tools and methods for the dynamic phenomena domain have been developed, including visualization and interactive visual analytical approaches. Nevertheless, many of these approaches are data specific, raster-based and developed for 2D scenario. Some examples are given in Burrough et al. (2005). Peuquet (1994b) described the relation between What, Where and When. This triad framework fits the geographic movement: If a geographic object or event (“What”) changes its spatial location (“Where”) in time (“When”) it can be called Spatio-temporal object/phenomena (see Figure 2-4).

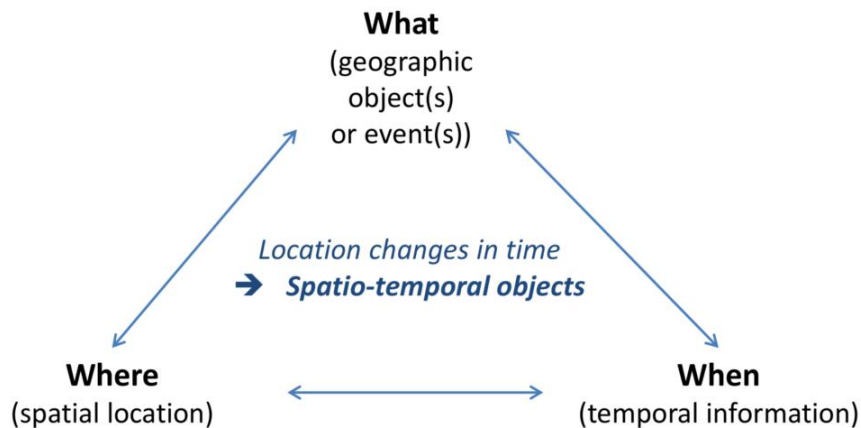


Figure 2-4: A triad framework based on Peuquet (1994b).

In traditional mapmaking, the dynamic behavior of spatial objects is considered in a limited way. In static maps, the time is mostly treated as an attribute of spatial objects, describing for example the time stamp of data acquisition (date and time during a day) or occurrence time/time interval. In the last decade, in digital maps, in particular with the use of animations, ‘time’ became more central in map-making process and easier to represent (e.g. within a STC). Isard (1970) described four types of time in geography: ‘universe time’ which is linear and absolute, ‘cyclic time’ such as diurnal patterns, ‘ordinal time’ which records the relative ordering of events and ‘time as distance’ in which the spatial dimension is used to represent time. Besides, Haggett (1990) characterized four types of temporal changes: constants, trends, cycles and shifts. An event can be understood as a significant change of a spatial object or phenomena. This change happens within a specific time period or at a certain moment of time. Whereas a spatio-temporal process is a sequence of dynamically related states showing how something evolves in space and time. Yuan & Hornsby (2007) defined an ‘event’ within geographic dynamics as “an occurrence of something with significance that drives noteworthy change at locations over time. The decision on significance and noteworthy is situational and problem-dependent”.

How can spatio-temporal objects/phenomena been described and distinguished? Galton (2003, 2004) provided a theoretical framework and stated that phenomena - changing in time and space – appear in different forms: as *objects* and *events* (or *processes*). Galton specified these phenomena and introduced the terms ‘*dual-aspect phenomena*’ and ‘*multi-aspect phenomena*’. Regarding dual-aspect phenomena, he draws attention to their object-event duality. Examples of the dual aspect are hurricanes, floods, wildfires, epidemics, processions, flocks, swarms and plagues. Each of them have in common that at some point of time they come into existence, move along a *trajectory* (*track*), perhaps changing in character and then ceases to exist. In case of multi-aspect phenomena, they come into existence more than once. One example of this would be a certain epidemics which could be temporally curbed, but for some reason the same plague breaks out again. Moreover, Galton ‘philosophically’ distinguished between *continuants* and *occurents*, which are extended in time. Objects are traditionally classed as continuants and events as occurents. Besides, geographical objects are defined by Mennis et al. (2000) as “geographic conceptual entities that have a unique and cohesive identity and are related to a specific combination of observational data stored in the location, time and theme perspective”. A theme can be understood as a spatiotemporal field of measurement (e.g. temperature).

Many dual-aspect-phenomena contain large numbers of similar units acting in a more or less coordinated way. The phenomena’s dynamic aspect and the collective behavior of its individuals are essential components. Thus Galton calls these discrete dual-aspect phenomena ‘*dynamic collectives*’ while for instance swarms, crowds and traffic events are naturally conceptualized as

dynamic collectives; whereas storms, floods, etc., which arise from the action of large numbers of water- or air-molecules, are for many purposes more naturally thought of as continuous fluid masses (Galton 2004). Bearing in mind the importance of these dual-aspect phenomena to GIS-science, we need a set of conceptual tools which will enable justification to their distinctive characters. Galton believed that visualization and visual analysis are approaches to answer the question how higher-level phenomena emerge from their lower-level constituents. Goodchild et al. (2007) introduced three essential dimensions of describing the dynamic behavior of geographic objects: the geometry, the movement and the internal structure. Each dimension can change in time to a certain extent as illustrated in Figure 2-5.

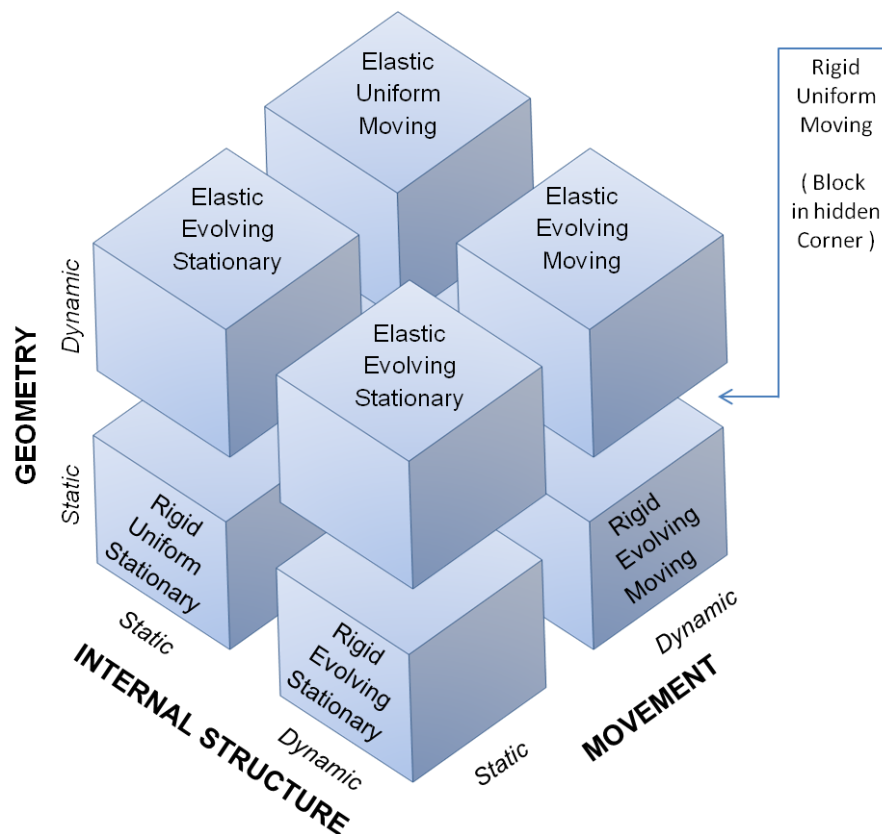


Figure 2-5: Dimensions of temporal variability in geographic objects (Goodchild et al. 2007).

The concept of *discrete objects* (or entities) and *continuous fields* proposed by (Longley 2005) provides a convenient framework for the discussion of geographic dynamics. Discrete objects (geographic individuals with well-defined boundaries) are subdivided into points, lines and polygons. Considering the movement of discrete geographic objects, dynamic points (e.g. cars, vessels) and dynamic SEOs (2D/3D-polygon, e.g. floods, swarms, thunderstorms) bear a special interest while changing their spatial locations/extensions as well as their properties in time. Moving line objects rarely exist in reality. However, changing borders could be one example. “Spatio-temporal data, in particular, movement data, involve geographical space, time, various objects existing and occurring in space and multidimensional attributes changing over time” (Andrienko et al. 2011a). In their conceptual framework for movement analysis the authors classified objects according their spatial and temporal properties as illustrated in Figure 2-6.

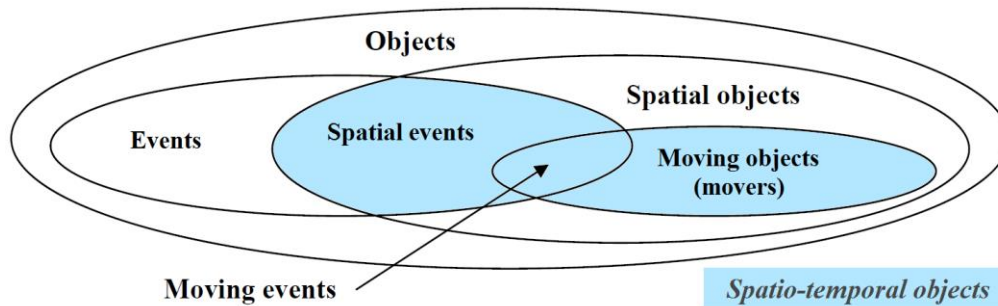


Figure 2-6: Objects and their spatio-temporal structure and relations (Andrienko et al. 2011a).

Spatial objects have a specific position in space and in any moment of time of their existences. Events (temporal events) are mental units and have a limited time of existence, or, in other words, a particular position in time (e.g. New Year's Eve). *Spatial events* have a particular position in time and in space (e.g. lightning strike). Moving objects (*movers*) are spatial objects that change their spatial position over time (e.g. vehicles). *Moving events* are events that change their spatial positions over time (e.g. a lynx chasing a deer). Longley (2005) called such spatial or moving events as 'geographical phenomena' respectively space-time processes. Spatial events and moving objects can be together referred to as spatio-temporal objects (Andrienko et al. 2011a).

In several prior publications 'events' are defined as discrete changes over time (e.g. earthquakes or Olympic games) respectively as something that happen somewhere and occur when spatial objects change or interact (Casati & Varzi 2008; Shipley 2008; Tversky et al. 2008). In (Andrienko & Andrienko 2013) a distinction is made between three different kinds of movement data: 1) discrete objects whose spatial positions can be represented by points; 2) fields, such as ocean currents and 3) SEOs changing their sizes and shapes, such as clouds. The focus within this thesis lies on spatio-temporal objects and in particular on the moving events consisting of a changing spatial expansion at each moment of time (SEOs).

Investigating dynamic phenomena aims to detect location-based events that appear over time and detect temporal and spatial information as well as reasons of events. Spatio-temporal events and their pattern behavior represent a higher level of knowledge in comparison to changes. Thus, events are very valuable for decision making. Additionally, pattern behaviors can be irregular and very complex. However, visualization and visual analysis supports further investigations of events (Krisp et al. 2012). In space-time crime analysis the term *near-repeats* is used, defining events that are close in both space and time. Near-repeats had been a topic of much research (Bowers & Johnson 2004; Johnson et al. 2007; Short et al. 2009). Besides, Andrienko et al. (2011a) introduced the term *situation* to describe the composition of object configuration, spatial distribution of attribute values and values of time-specific thematic attributes in a given time interval. Usually the semantic information (or semantic attributes) in movement data are rather poor. These attributes can be obtained by calculating means of exploratory analysis while using background knowledge and common senses (Andrienko et al. 2011b).

In literature there exist various terms for the semantic and geometrical object description such as attributes, features or properties. In this thesis the terms semantic attributes and geometrical attributes are used. The movement of objects implicate multiple aspects, such as the resulting trajectory, movement characteristics itself, such as speed and direction and their dynamics over time (Andrienko et al. 2008b). A trajectory is defined as the path that a moving object follows through space as a function of time. In case of dynamic SEOs the geometrical form of the path is a lane instead of a line. We can also distinguish so-called 'Quasi-continuous movement trajectory-

ries' which can be described as movement data with fine temporal resolutions allowing an estimation of the continuous paths by means of interpolation and/or map matching. Trajectories of moving objects are complex spatio-temporal constructs and the investigation of multiple and multidimensional trajectories is a challenging task (Rinzivillo et al. 2008).

A spatio-temporal phenomenon consists of one or more changing objects. The object changes geometrically or semantically during the course of time. In a formal modeling of movements, space and time are treated as mathematical abstractions. In reality, however, analysts are confronted with physical space and time. Andrienko et al. (2011a) underline the heterogeneity of the physical space and time as the main difference from their mathematical abstractions. As an example for such a heterogeneity the authors mentioned the variation of properties from position to position or in other words that every physical or geographical location has some degree of uniqueness relative to others. Furthermore, the movement analysis may be impeded by very complex dynamic data or data properties, for instance, a very large amount of data; multiple nested and overlapping temporal cycles; inaccurate and imperfect data values or irregular data samplings.

2.2. Spatio-temporal modeling of dynamic phenomena

The geographic dynamics modeling is driven by the requirements for visualization and analysis. Its fundamentals in spatio-temporal modeling were set in the late 80ties and 90ties. A conceptual framework of the three-domain model as illustrated in Figure 2-7 was introduced by Yuan (1996). It combines the relationships between semantic, spatial and temporal domains.

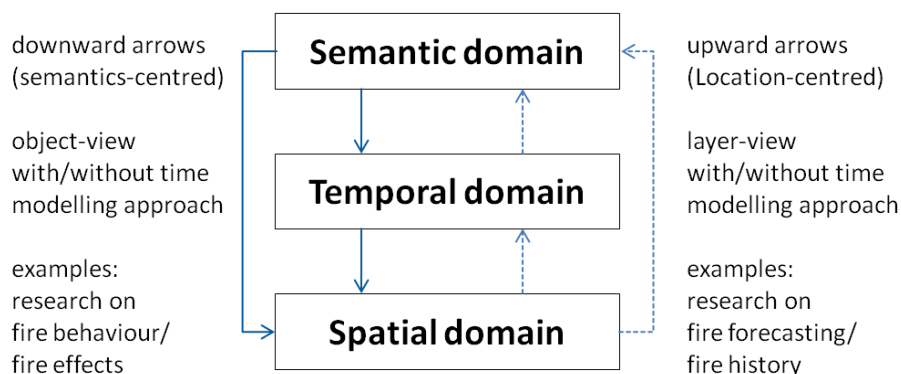


Figure 2-7: A conceptual framework of the three-domain model, based on Yuan (1996).

The dynamics of moving geographic entities, such as moving discrete point objects (e.g. persons, vehicles) or SEPs (e.g. storms) can be described and represented by something commonly called events. However, an *object-oriented modeling* of dynamic geographical entities only considers relations between entities. In order to consider the impacts of event on dynamic entities, an *event-oriented modeling* approach is needed to consider semantic relations of dynamic aspects (e.g. changes of geographic entities, of their properties and relations caused by events). However, while event-based models are conceptualized to analyze distinct changes in discrete or continuous spatial data, Wilcox et al. (2000) introduced a spatio-temporal graph model to support the analysis of continuous changes in discrete spatial data, in particular for modeling dynamic and interacting polygon objects.

In literature several event-oriented modeling approaches, such as an ontology relation approach introduced by Martinez & Levachkine (2009) or a causal relation approach published by Huang et al. (2007), were reported. Yuan & Hornsby (2007) provided an overview of the existing modeling approaches for geographic dynamics. The authors distinguished between the following modeling

approaches: time stamped-based, change-based, event-based, movement-based, activity-based and process-based.

Yang et al. (2008) proposed a process taxonomy for spatio-temporal change patterns of dynamic phenomena, as illustrated in Figure 2-8. These patterns are divided in thematic and geometrical changes. The latter include the situation when a spatio-temporal object comes into existence, changes in position and extension during its lifetime (e.g. expanding, contracting, merging, splitting, moving and transforming) and the state the object ceases to exist.

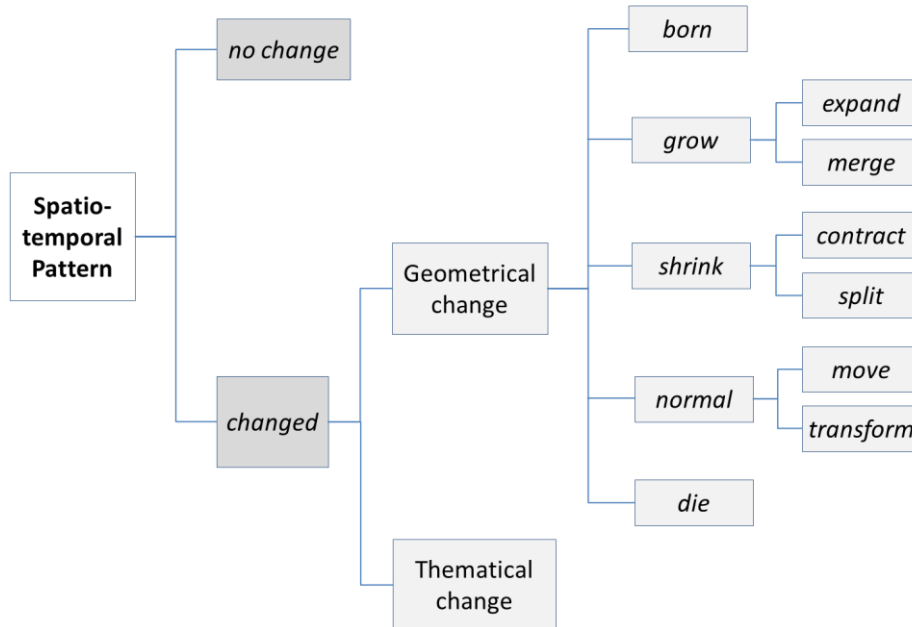


Figure 2-8: Taxonomies of spatio-temporal change patterns, after (Yang et al. 2008).

When presenting geographical objects in maps, the topological relationship of two objects can be described by their proximity, connectivity, adjacency, membership and orientation. Dealing with dynamic geographical data, in particular with events, we have to consider also the temporal aspect in topological relationships. Allen (1983) introduced different temporal topological relationships as illustrated in Figure 2-9. Considering also the inverse option for “before”, “meets”, “overlap”, “during”, “starts” and “end”, altogether 13 different temporal topological relationships are possible.

| RELATION | SYMBOL | Inverse | X | Y |
|--------------|--------|---------|---|---|
| X equal Y | = | = | | |
| X before r | < | > | | |
| X meets Y | m | mi | | |
| X overlaps Y | o | oi | | |
| X during Y | d | di | | |
| X starts Y | s | si | | |
| X ends Y | e | ei | | |

Figure 2-9: Temporal topological relationships, based on Allen (1983).

Claramunt & Jiang (2000) combined spatial relationships (SR) and temporal relationships (TR) as illustrated in Figure 2-10.

| SR | TR | equals | before/ after | meets/ met | overlaps/ overlapped | during/ contains | starts/ started | finishes/ finished |
|----------|----|--------|------------------|---------------|-------------------------|---------------------|--------------------|-----------------------|
| equals | | | | | | | | |
| touch | | | | | | | | |
| in | | | | | | | | |
| contain | | | | | | | | |
| cover | | | | | | | | |
| covered | | | | | | | | |
| overlap | | | | | | | | |
| disjoint | | | | | | | | |

Figure 2-10: Visual presentation of spatio-temporal relationships in a 2-dimensional space, based on Claramunt & Jiang (2000).

The spatio-temporal aggregation is necessary for an efficient visual investigation of the movements of dynamic objects in a large number and can be conducted in a database (Andrienko & Andrienko 2010). Visual analysis approaches and queries based on a database system of moving objects was introduced by Güting et al. (2000) and Sakr et al. (2011).

2.3. Cartographic representations of dynamic phenomena

The mapping of dynamic phenomena in cartography exists for a long time. Temporal information as well as movement information can be found in many static maps. The “Emigrant's Map and Guide for Routes to North America”, created by Gotthelf Zimmermann in 1853 is just one of the examples. This map reflects the importance of German immigration to North America in the mid-19th century (see Figure 2-11). Emigration origins and destinations are shown via red dots. Emigration trajectories over the Atlantic Ocean are drawn in dotted brown lines, the main overland emigration trajectories are presented through red lines, except people travelled along shipping routes. In fact, the overland trajectories are derived from the aggregated routes of all emigrants. This generalization happened in the cartographer’s mind. Nowadays modern technology enables automatic data collection of such routes, which then can be aggregated using digital cartographic methods.

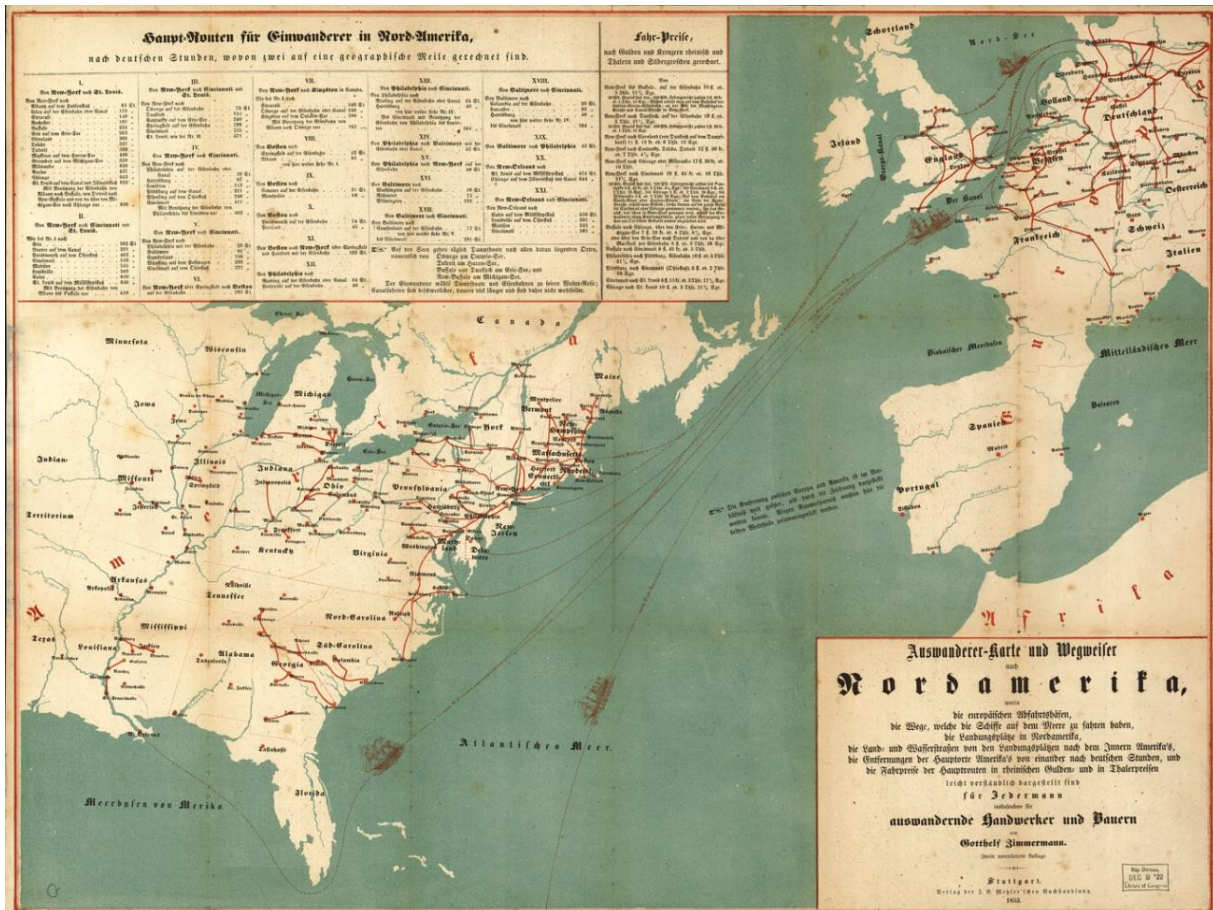


Figure 2-11: A historical map (extract) showing movement: Emigrant's Routes to North America, by Gotthelf Zimmermann (1853), source: <http://www.wdl.org/>.

An even more explicit representation of dynamics is shown in an historical map (Figure 2-12) with a flow map about Napoleon's Invasion of Russia 1812-1813 published in 1869 by Charles Minard, a French civil engineer and one of the pioneers in the field of information graphics. This map demonstrates the geodata aggregation and the use of visualization as catalyst for knowledge management. It contains, in addition to geographic information about the invasion area, spatio-temporal information about Napoleon's troops including their locations, movement direction, successive losses in men and important events such as river crossings and major battles. The width of the troop flow represents the army size. The flow lane shown in fawn illustrates the offensive toward Moscow and the one in black the retreat. Furthermore, on certain locations text labels provide explicit information about the troop size as well as the respective date (days) and the local temperature. This enables the map reader to extract spatio-temporal information and at the same time to reason for sudden changes, such as the strong decrease of the troop (ca. 50%) during the crossing of the Berezina river on the retreat at a temperature of 20 degrees below zero.

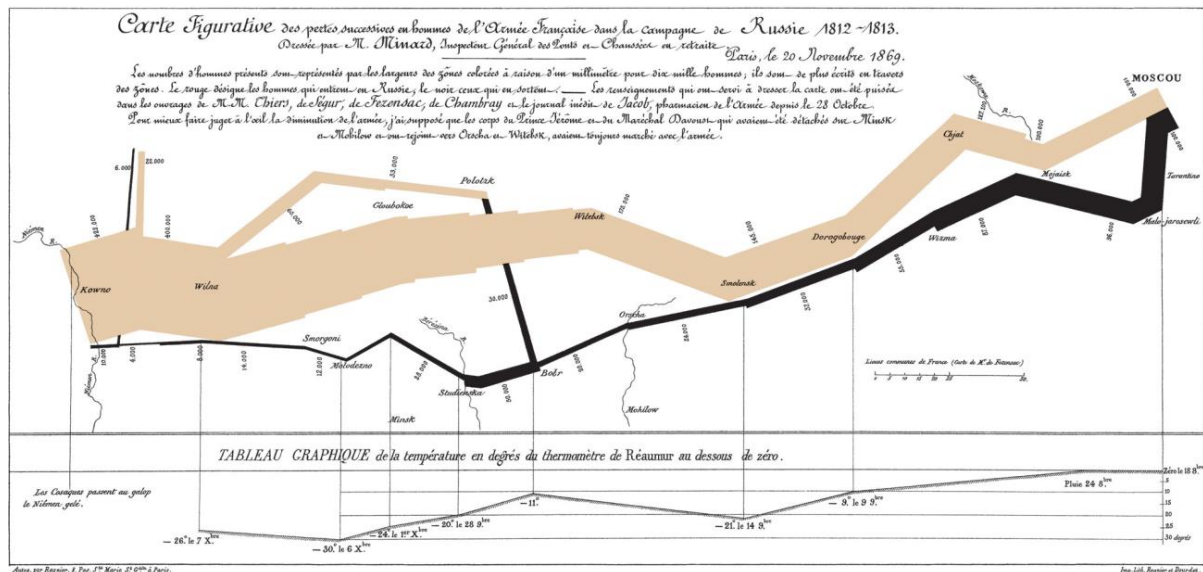


Figure 2-12: A historical map.

Visualizing spatio-temporal data is a complex process, wherein the following aspects have to be considered: Temporal information implicates the fourth dimension of spatial data. Temporal aspects are crucial for the modeling of dynamic processes, including planning or future prediction. We distinguish between a certain moment of time and a time period. Time information is associated with the change of spatial data components, such as geometry, attributes or relations (Čerba & Brašnová). Furthermore, time information holds certain accuracy, depending on the time measurement method and on the needed temporal scale (century/year, month, day, minute, second, millisecond/weekday/season, etc.). Thus, time information can be abstracted or generalized (e.g. “Spring 2013” rather than “2013-April-12th-10:51:59.5126pm”). The integration of time in cartographic representations depends on the map purpose as well as the source data and application. Important questions this work tries to answer are what kind of temporal information of dynamic SEOs is needed to be visualized and how to represent it. Wood & Keller (1996) identified five different groups of time information on maps and distinguished cartographic solutions for point-, line- and polygon symbols:

1. Moments: dates of events (text, e.g. “2007”)
2. Duration: continuance of an occurrence in space (text, e.g. “15 – 29 Dec”)
3. Order/Structured time: space is organized by time, representing sequence and frequency of events (e.g. space division in different time zones)
4. Time as distance: spatial distance between two objects represents their temporal difference
5. Space as clock: spatial information is related to time information (e.g. visualized snow-covered areas indicates winter time)

In the following, we try to classify maps and visualization methods of dynamic phenomena. Concerning time information in spatial data, Kraak & MacEachren (1994) differentiated ‘non-temporal maps’ and ‘temporal maps’ (also called ‘spatio-temporal’ maps). The authors argued that non-temporal maps describe states or evidences and thus treat time implicitly and provide no information about change. Whereas temporal maps explicitly portray temporal aspects of geographic phenomena while visually describing events or episodes. Moreover, they defined a temporal map as “a representation or abstraction of changes in geographical reality: a tool (that is visual, digital or tactile) for presenting geographical information whose locational and/or attribute components change over time”. Furthermore, Kraak & MacEachren (1994) discussed the terms ‘dynamic

maps', which refer to dynamic actions/effects on digital maps (e.g. symbols will blink, flash, bubble, sparkle, throb, erupt, sink, explode, rotate or shake on screen) whereas the contrary is termed as '*static map*'. Animations can be linked to spatio-temporal changes. Their main purpose is to attract the map reader's attention. The terms 'animation' and 'dynamic actions' occurred frequently in cartography-related literature about 10 to 15 years ago. Nowadays these terms can be seen as an integral part of interactive dynamic maps. Both static and dynamic maps might occur as a single map or in map series (multiple map) as explained in (Monmonier 1990). '*Animated maps*' refer to a series of static maps which are displayed one after another on screen at a rate of more than 24 frames a second (Kraak & Ormeling 2011).

The afore-mentioned actions on dynamic maps are also called animations in some references. Whereas the notation 'dynamic maps' refers sometimes to '*interactive maps*' which imply the interactive operations, such as pan, zoom and rotate. In this thesis the term 'animation' refers to spatio-temporal symbol changes and is different from dynamic effects. Figure 2-13 illustrates a prevailing nutshell of the temporal map types suitable for movement data. Moreover, Monmonier (1990) proposed three different strategies for representing spatio-temporal data on static maps: *dance maps*, *change maps* and *chess maps*. Dance maps illustrate multiple time states on a single static map and are easy to read. Change maps show the change of an attribute between two time periods on a single static map. Chess maps display multiple time states. However, chess maps require a large mental work of the map reader while visually switching between multiple map parts in order to reveal the changes (e.g. geographic changes in position, extension or existence).

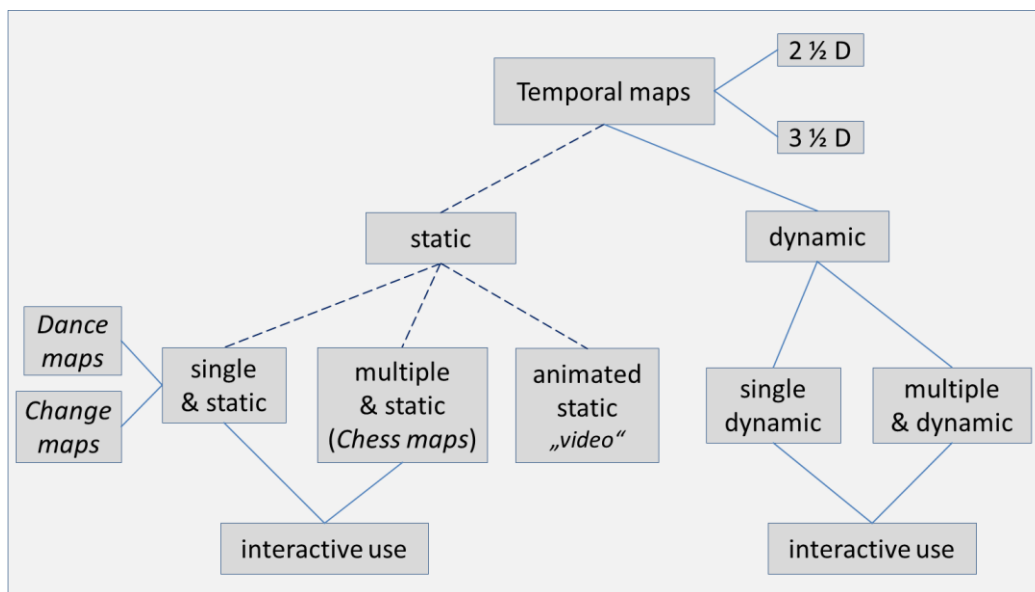


Figure 2-13: A nutshell of different temporal map types for spatio-temporal data.

Not only cartographical displays, but also maplike or non-cartographic displays (e.g. PCPs, e.g. cartograms) may be used to visually describe movement information. Now, let's have a closer look at cartographic methods for single and static temporal maps (in 2D) emphasizing temporal information in spatial data. Movement information and thus temporal aspects can be visualized through a single value (e.g. speed change) represented through map symbols or labels (Čerba & Brašnová 2012). Two (or more) diagram symbols enable comparison of the different temporal stages as shown in Figure 2-14. Furthermore, point symbols, polygon areas or line widths can be distorted based on their associated temporal values – this technique is called temporal cartogram. The polygon sizes change with the temporal values.

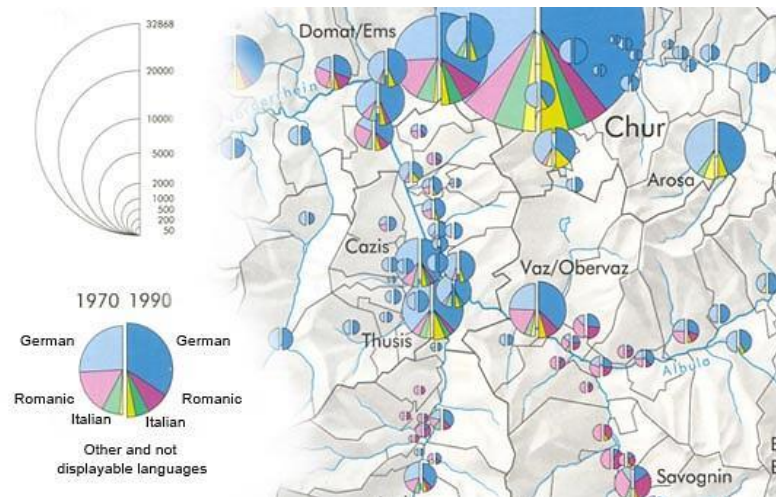


Figure 2-14: Piechart symbols for two different moments of time, source: www.gitte.info.

Other techniques include the use of arrows or *flow maps* as well as contour lines/intervals which can indicate the position- or extension change of a dynamic phenomenon at a specific time or during a certain time interval. An example is illustrated in Figure 2-15, wherein brown arrows indicate the movement of the plaque while contour intervals indicate extension of the plaque during the time period from 1347 to 1350. Furthermore, at certain locations (cities) the year of the most terrible plaque events are shown. Instead of using a time stamp as variable for isosurfaces (as in the given example below), the travel time could be used as well, resulting in so-called isochronic maps. Thereby, physical space is held constant and time is transformed (Vasiliev 1997).

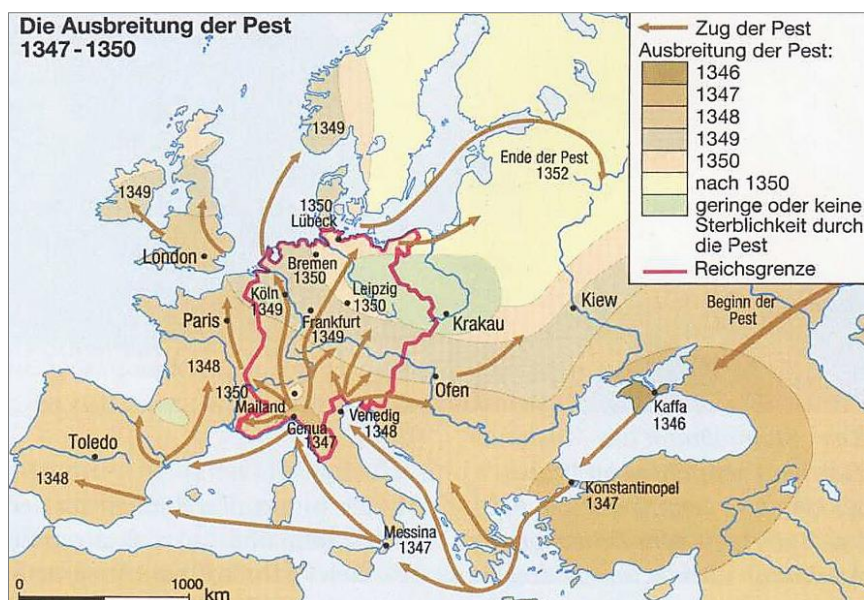


Figure 2-15: Spreading of the plaque in Europe, 1347 – 1350, source: www.von-scheidt.de.

In addition to the moving direction arrow, movement can be represented also through a tail-like visualization: the tail is defined as the last small part of the trajectory which the moving object just passed through during the most recent past. Many existing research works on the visualization of dynamic data are concentrated on trajectories representing moving point objects on two or three-dimensional displays (Eccles et al. 2008). Some other approaches deal with the aggregation of trajectory lines. The aggregations can be based on spatial, temporal, spatio-temporal or semantic attributes. In Figure 2-16 four different examples for the representation of aggregated episodic

movement data are illustrated. In A and B time series are associated with places and in C and D spatial situations in terms of presence (C) and flows (D) are shown.

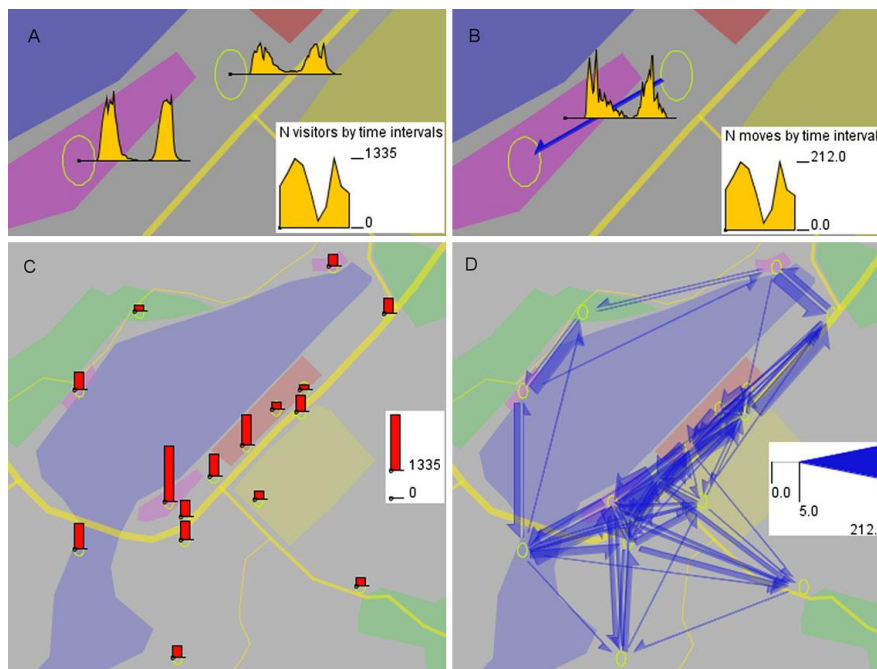


Figure 2-16: Representations of aggregated movement data. (A, B) Time series associated with places (A) and links (B). (C, D) Spatial situations in terms of presence (C) and flows (D), source: Andrienko et al. (2012).

The *kernel density estimation* (KDE) is one of the most common aggregation methods, for trajectory points (Dykes & Mountain 2003) or trajectory lines in 2D (Willems et al. 2009) or in 3D (Demšar & Virrantaus 2010). It can be noted that there is a manageable number of methods for single static maps dealing with movement. However, these methods can hardly handle location- and movement information over time. In the following, some key approaches beyond the single static maps are listed, which help to improve the visual insight into movement information of dynamic geographic objects:

- Dynamic map features (symbol actions, such as blinking or shaking)
- Map series or animations (e.g. by using a time slider)
- Interactive map use (e.g. pan, zoom, rotate, select and show attribute information)
- Interactive temporal legend (e.g. cyclical or bar legend)
- Tangible user interfaces: integration of physical and digital representation of reality with dynamic user interaction (Ratti et al. 2004)
- Temporal extrusion: time as z-axis (STC)
- Combination of maps with (synchronized) maplike or non-cartographic displays (tables, diagrams, etc.)
- Fly-throughs, e.g. along a trajectory with correlated sequence pace and movement speed)

When visually representing spatio-temporal phenomena, a static map might be the best choice for some tasks, whereas a dynamic map could be more appropriate for other tasks. A combination of a static map with superimposed dynamic symbol actions would be a third option and relevant for certain tasks. A static map representation is often chosen in order to provide a holistic view of the entire time period at once, whereas dynamic maps (symbol actions) are used to focus

the map user's attention on a specific moving or changing object. Further important aspects for the use of dynamic maps can be temporal legend, temporal scale/granularity and pace. Representations of dynamic phenomena in maps (points, trajectories, SEOs) have certain graphic/visual variables which were first introduced by Bertin (1983) and consist of form, color, texture, luminance, size, orientation, sharpness, transparency and saturation as illustrated in Figure 2-17 with their use for emphasizing qualitative and/or quantitative differences.

| | <i>Points</i> | <i>Lines</i> | <i>Areas</i> | <i>Best to show</i> |
|------------------------|---------------|--|------------------|---|
| <i>Shape</i> | | <i>possible, but too weird to show</i> | <i>cartogram</i> | <i>qualitative differences</i> |
| <i>Size</i> | | | <i>cartogram</i> | <i>quantitative differences</i> |
| <i>Color Hue</i> | | | | <i>qualitative differences</i> |
| <i>Color Value</i> | | | | <i>quantitative differences</i> |
| <i>Color Intensity</i> | | | | <i>qualitative differences</i> |
| <i>Texture</i> | | | | <i>qualitative & quantitative differences</i> |

Figure 2-17: Bertin's visual variables, source: *makingmaps.net*.

Furthermore, point objects can be represented through certain symbols (e.g. a symbol showing a post horn represents a post office). Considering the dynamics in animated maps, Köbben & Yaman (1996) defined six visual variables, introduced by (MacEachren 1995) as "dynamic visual variables":

- Display date (moment of display): the time at which some display change
- Order: the sequence of frames or scenes (a scene is a number of sequential frames with no changes)
- Duration: the length of time between two identifiable states
- Frequency: the number of identifiable states per time interval
- Rate of change: the difference in magnitude of change per time interval for each of a sequence of frames or scenes
- Synchronization: the temporal correspondence of two or more time series

MacEachren (1995) indicated a capability (good, marginal, poor) of each visual variable (static and dynamic ones) for different data levels (nominal, ordinal or interval/ratio data). Moreover, he assigned the appropriateness of the visual variables to distinguish visual levels and to isolate data visually. Certain visual variables of an object (e.g. color, size) could be linked to movement information, such as speed. Dukaczewski (2007) investigated the combination of static and dynamic visual variables and their usage for points, lines and areas.

In the following section we will shift our focus from 'simple' representation methods towards visual analysis of movement data.

2.4. Movement analysis and visual exploration of dynamics

Movement analysis aims to understand the spatio-temporal dynamics of events and processes, to identify movement patterns and investigate behaviors of moving objects. Both the visual analysis and non-visual analysis are involved. The visual analysis is conducted in different, partly overlapping research fields such as geographic information science, cartography and visual analytics. The latter field also includes information visualization, whereas the non-visual analysis necessitates methods and techniques from mobility analysis, spatio-temporal data mining, spatio-temporal database technologies, knowledge discovery, spatial statistics and time geography. Visual and non-visual analyses benefit from each other because they serve each other as a supporting means. Results of non-visual analyses can be visually presented and explored. Visual analyses help users to focus on specific parts of dataset. Some fundamental approaches for the representation and visual analysis of temporal dynamics of geographic information were reported in Andrienko et al. (2011a); Andrienko & Andrienko (2013); Andrienko et al. (2003); Blok (2000); Peuquet (1994a, 2002).

Movement analysis approaches differ from each other, depending on the type of movement, on the type of moving objects and on the analysis purpose. Andrienko & Andrienko (2007) identified four factors influencing *movement behavior* of dynamic entities: space, time, object activity and the context with further spatio-temporal phenomena such as traffic or weather). The focus of the movement analysis can be laid on one of the three questions: what (a given object, a set of objects), where (a location, a set of locations occupied by a given object or a set of objects) or when (times that a given object or a set of objects occupy). Thereby, 'what' depends on 'when' and 'where'; 'what' and 'when' will define where; and 'when' will result from 'when' and 'where' (Peuquet 1994b).

Movement analysis tasks can also deal with a certain question (analysis task) related to a single moving object, a set of dynamic objects or the entire phenomenon. Furthermore, analysis tasks for dynamic data can rely on the types of changes occurring over time, such as existential changes as appearance and disappearance or changes in certain spatial or temporal properties (Blok 2000). Moving objects show various behaviors during their moving phase. Determining, analyzing and representing such movement behavior are important aspects within this work. In general movement behavior refers to changes of movement attributes (e.g. speed, movement direction) or to changes of other object attributes during or due to its movement. Andrienko & Andrienko (2007) distinguished between *momentary collective behavior* (behavior of a collective of entities at a certain moment of time) and *dynamic collective behavior* (for a certain time period). The movement behavior can be observed for an individual moving object, a group of objects or all objects at a certain moment of time or at a certain time interval (also during the entire lifetime of an moving object).

Peuquet's model could be extended to accommodate 'what'. Instead of only considering dynamic objects, the following could be added: object properties; the behavior of objects; the behavior of dynamic phenomena; the context such as interactions/relations between objects or with other objects and the environment. Many existing approaches for movement analysis address specific tasks such as spatio-temporal land use change detections. Robertson et al. (2007) suggested to categorize existing approaches based on their respective lineages and put forward some more general approaches suitable for a wider range of applications within spatio-temporal polygon change analyses. The authors introduced various ideas summarized as "STAMP" (spatial-temporal analysis of moving polygons): These include five new movement events suitable for defining spatial processes: displacement, convergence, divergence, fragmentation and concen-

tration. Furthermore, they introduced spatial–temporal measures of events for size and direction for two or more time periods.

2.4.1. Visual exploration of dynamic data in general

The starting point for any kind of visual analysis of movement data is provided by the existing graphic representations such as static maps, animations, multiple displays etc. The visual analysis is essentially triggered by human organs for visual perception and cognition with or without an interactive interface. One of the pioneers for visualization of geographic spatial-temporal data is Mark Monmonier who introduced a conceptual framework for time-series maps and graphs (Monmonier 1990). He divided principal tools into (1) multiple views, (2) time and space scaling, (3) interaction with the data and display and (4) integration of maps and time-series graphics. Furthermore, Monmonier distinguished between single and multiple, static and dynamic maps and graphs with or without user interactions. He provided an overview about existing solutions such as time series graphs, data arrays, cartographic cross-classification arrays (Small multiple maps), temporal glyphs/symbols, quadratic polynomial trend surfaces, flow-linkage diagrams and change maps.

Foundations in geo-spatial and temporal visual analytics were discussed in (Andrienko et al. 2010; Andrienko et al. 2008a; Andrienko et al. 2007a; Andrienko et al. 2011c; Andrienko & Andrienko 2006, 2012) and (Keim et al. 2008). The principal task for visual analysis of dynamic data is to provide interactive multidimensional multivariate visual exploration tools. Such tasks or visual solutions include among others:

- Time-dependent visualization:
 - o Draw objects which occur at a selected moment of time
 - o Draw objects which occur during a selected time interval
- Space-dependent visualization:
 - o Draw objects which occur within a selected region
- Spatio-temporal visualization:
 - o Draw objects which occur within a selected region at/during a certain time
 - o Visualize objects at different scales and for 3D-displays: from different perspectives
- Determine, visualize and visually analyze trajectories
- Aggregate moving objects, trajectories, segments of trajectories or attributes of objects/trajectories:
 - o Spatial aggregation, temporal aggregation, spatio-temporal aggregation (first spatial then temporal aggregation or vice versa)
- Visualize object attributes (speed, moving direction, etc.)
- Highlight unique movement situations, for example location where trajectories merge/split

Visual analysis tasks, methods and solutions differ for different types of movement data. Mostly movement data are tracked point objects, but dynamic geographic objects include also moving fields and spatio-temporal evolving polygons. Table 2-1 demonstrates four visualization techniques for non-aggregated movement or event data (point data). It shows a part of the original table suggested by Andrienko et al. (2011a). The table provides information about the respective visualization methods (e.g. map, time graph, temporal bar chart) schematized by a pictograph respectively and information to be visualized (e.g. spatial position, temporal position, semantic attributes).

Table 2-1: Methods for visualization of detailed (not aggregated) movement or event data, from (Andrienko et al. 2011a).




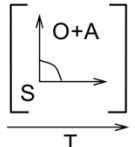
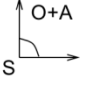
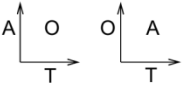
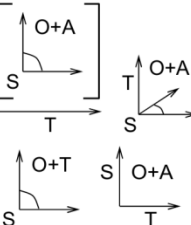
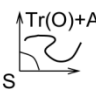
| What is portrayed | Visualization technique description | Pictograph |
|---|---|---|
| Spatial positions of objects (+ thematic attributes) | <u>Map</u> : spatial positions (S) → positions on the map; objects (O) → geometries on the map; thematic attributes (A) → retinal properties |  |
| Temporal positions of objects (+ thematic attributes) | <u>Time graph</u> : temporal positions (T) → positions on the time axis; thematic attributes (A) → positions on the attribute axis; objects (O) → points or lines |  |
| Temporal positions of objects (+ thematic attributes) | <u>Temporal bar chart</u> : objects (O) → positions on the object axis; temporal positions (T) → positions on the time axis; thematic attributes (A) → retinal properties |  |
| Spatial and temporal positions of objects (+ thematic attributes) | <u>Map sequence</u> : temporal positions (T) → positions in the sequence; spatial positions (S) → positions on the map; objects (O) → geometries on the map; thematic attributes (A) → retinal properties |  |

Table 2-2 demonstrates another part of Andrienko’s work (2011a) with a number of visualization methods for aggregated movement and event data as well as an overview about movement analysis tasks together with the respective supporting visualization technique.

Table 2-2: Analysis tasks and respective supporting techniques, from (Andrienko et al. 2011a).

| Analysis focus | Target characteristics or relations | Visualization | Aggregation | Computation |
|-------------------------|--|---|---------------------|-----------------------------------|
| Spatial objects | Spatial positions; thematic attributes; spatial relations |  | S→A | C(O S); C(O S×A) R(O×O) |
| Temporal objects | Temporal positions; thematic attributes; temporal relations |  | T→A | C(O T); C(O T×A) R(O×O) |
| Spatio-temporal objects | Spatio-temporal positions; thematic attributes; spatio-temporal relations |  | S→(T→A); T→(S→A) | C(O S×T); C(O S×T×A) R(O×O) |
| Movers | Spatial aspect of the trajectories; thematic attributes; spatial relations |  | | C(Tr S); C(Tr S×A) R(O×O) |

Current research in geovisualization of dynamics includes theories, computational approaches as well as visual and interactive methods. Andrienko et al. (2008a) provided an overview about the respective research activities as illustrated in Figure 2-18. The approaches cover one or several

of the four parts (theory, computing, visualization, interaction) while focusing on data, summaries, patterns and/or knowledge.

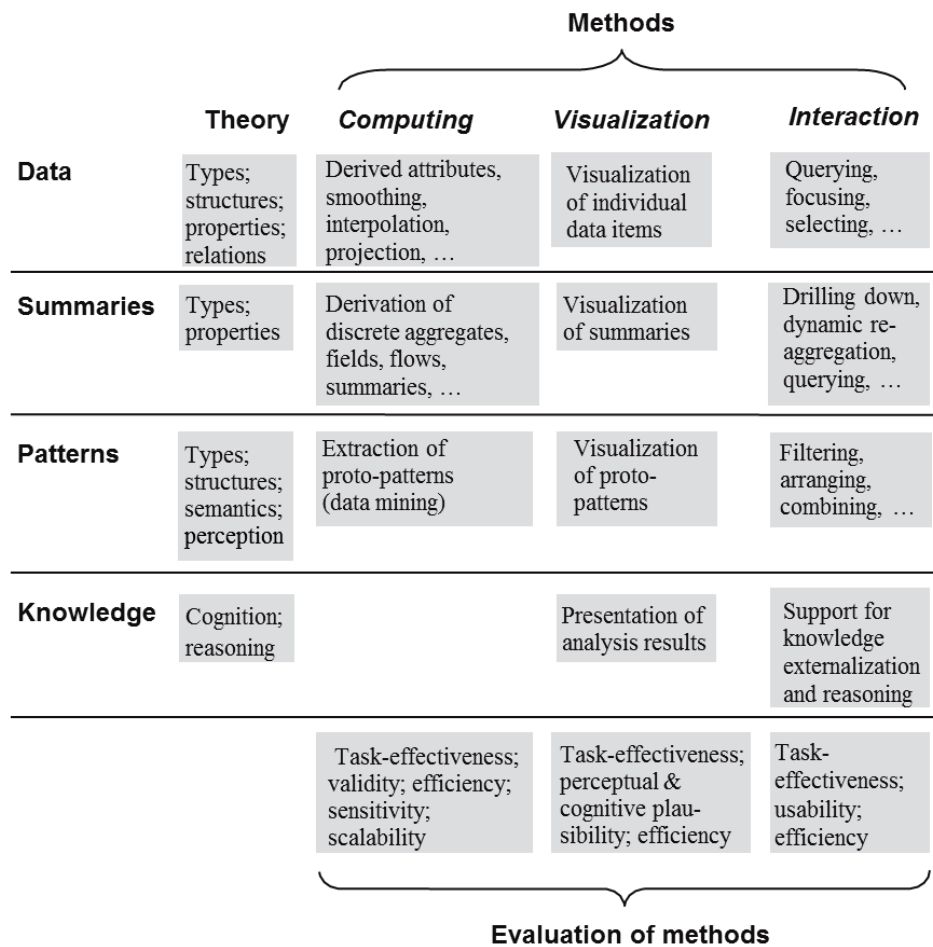


Figure 2-18: Geovisualization of dynamics - research topics based on Andrienko et al. (2008a).

2.4.2. Visual exploration of discrete dynamic objects (points)

In recent years numerous approaches for the visual analysis/analytics of dynamic point objects were published. Discrete dynamic points can be distinguished between points that change their spatial position in time and events (points with a certain spatial position which occur at a specific moment of time/during a particular time interval). Moreira et al. (1999) also distinguished between objects that have a completely free trajectory (e.g. flying bird) and objects that have a constrained trajectory (e.g. trains moving on railway network). Moreover, points whose attributes change in time sometimes are called dynamic objects as well. (Andrienko & Andrienko 2013) provided a structured survey of the state of the art in visual analytics concerning the analysis of moving point objects. The authors divided relevant works into four categories: a) Looking at whole trajectories; b) Looking inside trajectories; c) Bird's-eye view on movement; and d) Investigating movement in context. Table 2-3 lists only some examples for visual exploration approaches for dynamic point data.

Table 2-3: Visual exploration approaches for dynamic point data (selected examples).

| Visualization technique | Reference |
|---------------------------------|------------------------------|
| STC | Gatalsky et al. (2004) |
| Trajectory wall display | (Tominski et al. 2012) |
| Aggregated trajectories | Liu et al. (2011) |
| Multiple Origin-Destination map | Wood et al. (2010) |
| Trajectory Contingency Table | Willems et al. (2009) |
| Treemaps | Johnson & Shneiderman (1991) |
| Flowstrates | Boyandin et al. (2011) |
| Variable Binned Scatter Plots | Hao et al. (2010) |
| Small multiple maps | Guo et al. (2006) |
| PCP | Guo et al. (2006) |
| Self-organized maps | Guo et al. (2006) |

Furthermore, Andrienko et al. (2011a) suggested a taxonomy of generic techniques and a systematic classification of existing approaches for visually analyzing movement. Thereby, the authors considered mainly events and spatial objects.

2.4.3. Visual exploration of dynamic fields

Dynamic fields, characterized by changing attributes (e.g. temperature, wind speed) on a static polygon, haven't been yet addressed much in visual analysis research. Existing approaches are mostly application-specific. Holtt et al. (2014), for example, introduced an interactive visual analysis tool of sea surface height simulations, commonly used in ocean forecasting. Thereby, the sea surface heights are visualized either in 2d or 3d in differently colored contour intervals on top of a base map. Additional graphs, diagrams and a 3D volumetric cursor provide further statistical information. Mitas et al. (1997) suggested to use cartographic animations for the static representation and simulation of landscape processes (e.g. erosion, deposition). Interactive, dynamic and animated 2D and 3D maps with adapted symbolizations were suggested for various phenomena, such as precipitation, soil horizon, soil texture as well as chemical concentrations below ground and in water. An example is illustrated in Figure 2-19. Mitas et al. concluded that visualization plays a crucial role in understanding landscape processes.

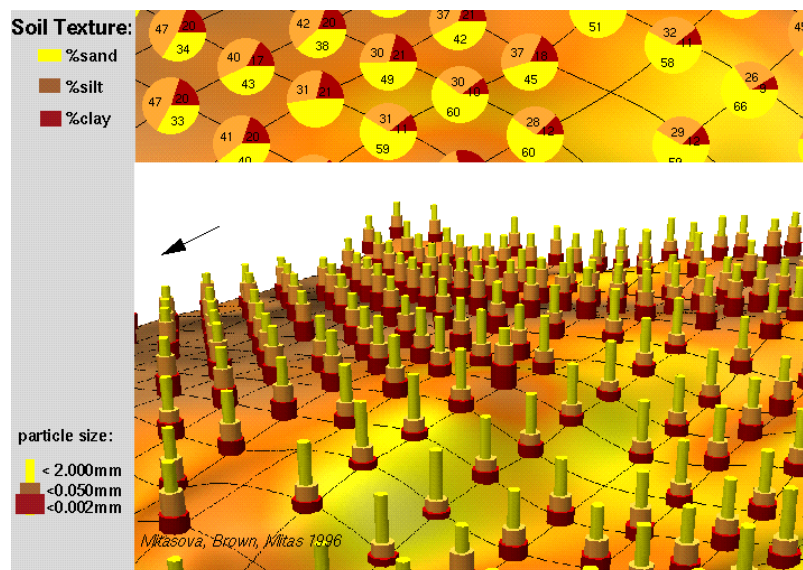


Figure 2-19: Different point symbolizations for soil texture attributes, source: Mitas et al. (1997).

2.4.4. Visual exploration of dynamic “polygons”

SEOs are regarded in this work as dynamic phenomena delimited by a certain spatial extension which changes in time. In geometrical terms, each of these objects covers a certain area in 2D space, a certain volume in 3D space, in a specific moment of time/during a certain time interval. The object's area (volume) increases or decreases with time. Dynamic collectives, such as crowds, herds and swarms can also be analyzed as dynamic polygons. In that case, the focus is not on the trajectory of each individual point, but the dynamics of the group as an entity. Some general theories for movement pattern analysis of dynamic collectives were provided by Galton (2005) and Huang et al. (2008). Thereby Galton (2005) introduced a formal theory of dynamic collectives; and Huang et al. (2008) investigated quantitative and qualitative changes of herds during their evolvments.

Clouds or lightning clusters are typical examples for SEOs with movement. Existing approaches for visual analysis of dynamic SEOs are rare and mostly application-driven. Turdukulov et al. (2007), for instance, reported a solution for interactive visual exploration of spatio-temporal cloud cell data using a STC. They considered clouds as being composed of points. Different from their approach, this thesis aims to provide generic concepts and solutions for the visual analysis of dynamic SEOs and to justify the general solutions for a tangible application scenario of moving lightning clusters. Some previous publications of the author dedicated to the visual analysis of lightning clusters have laid down the foundation for this thesis (Peters et al. 2014; Peters & Meng 2013). In case a dynamic SEO is based on moving points or events, changes of the internal structure within the spatial extension are of particular interest. During movement of the SEO, point distribution and density might change. As spatio-temporal density mapping (STDmapping) forms an important component of this thesis, in the following section we will introduce the existing density map approaches for static and dynamic point data.

2.5. Density maps for static and dynamic points

This section is based on (Peters & Meng 2014a, b), summarizing existing density mapping approaches for static and dynamic points.

In today's society, the need for data abstraction along with the growing amount of available digital geodata is rapidly increasing. One reasonable way of abstracting data is provided by density maps (Mackanness et al. 2007). Visualizing density and distribution information is a key support for understanding spatio-temporal phenomena represented by point data. However, the temporal information is not yet adequately handled in existing density map approaches. Density maps can be applied for point data in various fields, for instance, in physical or human geography, geology, medicine, economy or biology (Romanenko et al. 2012; Stoilova-McPhie et al. 2002). How to present the density for dynamic data/phenomena is, however, not yet adequately addressed.

One of the most straight forward ways to visualize point density is a scatter plot or a dot map. Graphic variables for point symbols, such as size, shape, color and transparency, can be applied in relation with the attribute value. In order to discern the density distribution, these graphic variables can be iteratively adapted to the given map scale, but still the occlusion of neighboring points cannot be always desirably avoided. The density value of each point can be obtained by counting all points within a buffer around the point or within a grid cell the point is located in. In the following, the density estimation and map principles are shortly presented and the state of the art of density maps with static or dynamic data is given.

A. Kernel Density Estimation (KDE)

The KDE is a classic method widely used to determine densities of individual points that represent a continuous surface (Tukey 1977). The KDE approach is described in detail in (Cressie

1992; Silverman 1986; Tukey 1977). The standard KDE, a normal distribution function, uses a Gaussian kernel. A certain bandwidth (search radius) is defined for the kernels, located around each point. For each cell of an underlying grid (defined by a certain resolution) a density value is calculated as shown in Equation 1 and hence a smooth surface is provided (Scott 2009).

Equation 1:

$$\hat{f}_h(x) = \frac{1}{N \cdot h} \sum_{i=1}^N K(u) \quad \text{whereby} \quad u = \frac{X - X_i}{h} \quad \text{and} \quad K_G(u) = \frac{1}{\sqrt{2\pi}} \cdot \exp\left(-\frac{1}{2}u^2\right)$$

with: $\hat{f}_h(x)$ = general Kernel density function
 K = Kernel function
 K_G = standard Gaussian function
 h = smoothing parameter (bandwidth)
 X = point (x,y) for which the density will be estimated
 X_1, X_2, \dots, X_N = sample points, placed within the kernel radius h

The resulting density surface is strongly influenced by the bandwidth value (O'Sullivan & Unwin 2003). A formula for an optimal bandwidth is offered by Silverman (1986) as shown in the following equation.

Equation 2:

$$bw_optimal = 1.06 * \min\left(\sqrt{\text{var}(P)}, \frac{\text{IQR}(P)}{1.34}\right) * n^{-\frac{1}{5}}$$

with: $bw_optimal$ = optimal bandwidth
 P = point dataset (coordinates)
 $\text{IQR}(P)$ = interquartile range (distance 1st - 3rd quartile)
 $\text{var}(P)$ = variance of P
 n = number of points

The KDE principle is illustrated in Figure 2-20-a,b,c with a sample dataset and the resulting KDE contour map with two different bandwidths in Figure 2-20-d,e,f. Beside a Gaussian kernel, also other kernel types can be applied, such as Triangular, Biweight, Epanechnikov or Uniform kernel (Silverman 1986).

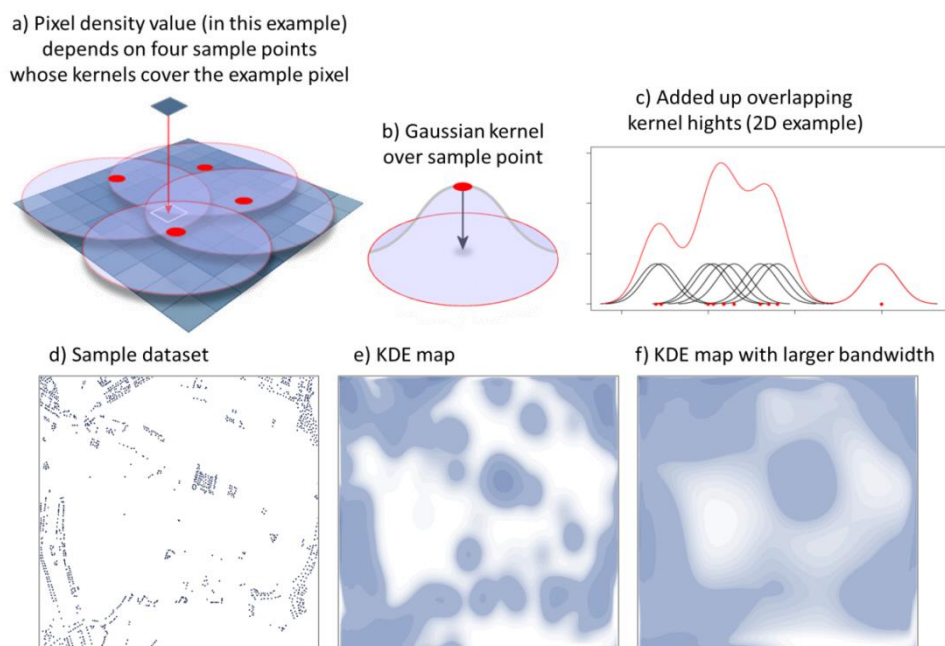


Figure 2-20: KDE principle. Source for a) and b): www.geography.hunter.cuny.edu.

Kernel density estimates have been used for cluster detection in various fields, such as crime and population analysis. Kwan (2003) uses geovisualization of activity patterns in space–time and displays the results as a continuous density surface. She applies the density estimation as a method of geovisualization to find patterns in human activities related to other social attributes. Assent et al. (2007), Krisp & Špatenková (2010) and Maciejewski et al. (2010) investigate the classic KDE and define it as a visual clustering method. In these works, KDE maps were created in order to visually provide a better overview and insight into the given data.

B. Contour lines and intervals

A common technique to map point densities calculated using KDE are isopleth maps with filled contour intervals. The term “isopleth map” refers to one of two types of isoline maps (also called isarithmic or contour maps). In the first type of isoline maps each contour line indicates a constant rate or ratio derived from the values of a buffer zone or kernel area. In this sense, the continuous density surface is derived from an originally discrete surface. In the other type of isoline maps (commonly referred to “isometric map”), contour lines (isometers) are drawn through points with directly measurable equal value or intensity such as terrain height or temperature (Schmid & MacCannell 1955). It is assumed that the data collected for enumeration units are part of a smooth, inherently continuous phenomenon (Slocum et al. 2009). In our context, we only use contour lines to delimit the intervals (the areas between contour lines) as exemplary shown in Figure 2-20-b,c. Furthermore, Langford & Unwin (1994) provided a good overview of density surfaces used in Geographic Information Systems (GIS) as choropleth population density maps, population density on grids, population density surfaces and pseudo-3D population density surfaces. In several works as (Romanenko et al. 2012; Stoilova-McPhie et al. 2002), the KDE concept is adapted for the 3D space density mapping of static 3D data.

C. Dynamic data and density information

In the following sections, an overview is given about existing works related to density maps of dynamic points.

1) KDE for dynamic points: sequence of density surfaces

A straightforward way of visualizing the density of dynamic points would be a sequence of density surfaces (one per time interval). The change of the density in time could be better discernable by means of an animation of these density maps. We could also arrange the local density contours of each time interval on the same map. Transparency and a unique color scheme for each time interval could be applied in order to distinguish different density contours. However, the tinted intervals may spatially overlap and make the map reading a difficult endeavor.

2) Dual KDE

Jansenberger & Stauer-Steinnocher (2004) analyzed two different point datasets recorded within the same area, but at two different moments of time. The authors suggest a Dual-KDE approach, which results in a map illustrating the spatiotemporal density difference of the two datasets. The absolute difference is used, that is, the absolute density of the second point dataset subtracted from that of the first one.

3) DKDE

The approach called directed kernel density estimation (DKDE) that takes the dynamics of moving points inside density maps into account was suggested in previous works (Krisp & Peters 2011; Krisp et al. 2013; Krisp et al. 2009; Krisp et al. 2011; Peters & Krisp 2010). The DKDE is applicable for discrete moving points and it considers two moments of time. Instead of an upright kernel as in the KDE method, a tilted kernel is used, as illustrated in Figure 2-21. The tilt depends on the movement direction vector of the respective point. The resulting DKDE-map shows the so-

called “ripples”, which can be interpreted as an indicator for the movement direction and density change of points that are located closely to each other with very similar movement speeds and directions. These ripples are visible among overlapped contour lines. The tinted contour intervals do not contain the information about movement or density change. Peters & Krisp (2010), for instance, used 2D airplane positions in the area of Germany at two moments of time with a time lag of five minutes. The resulting DKDE-map is shown in Figure 2-22.

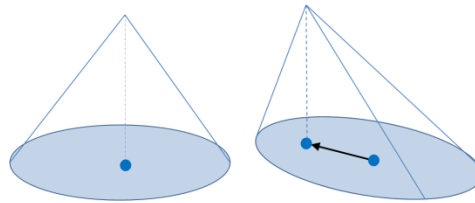


Figure 2-21: Linear kernel (left) and Directed linear kernel taking point speed and movement direction into account (right), source: Peters & Krisp (2010).

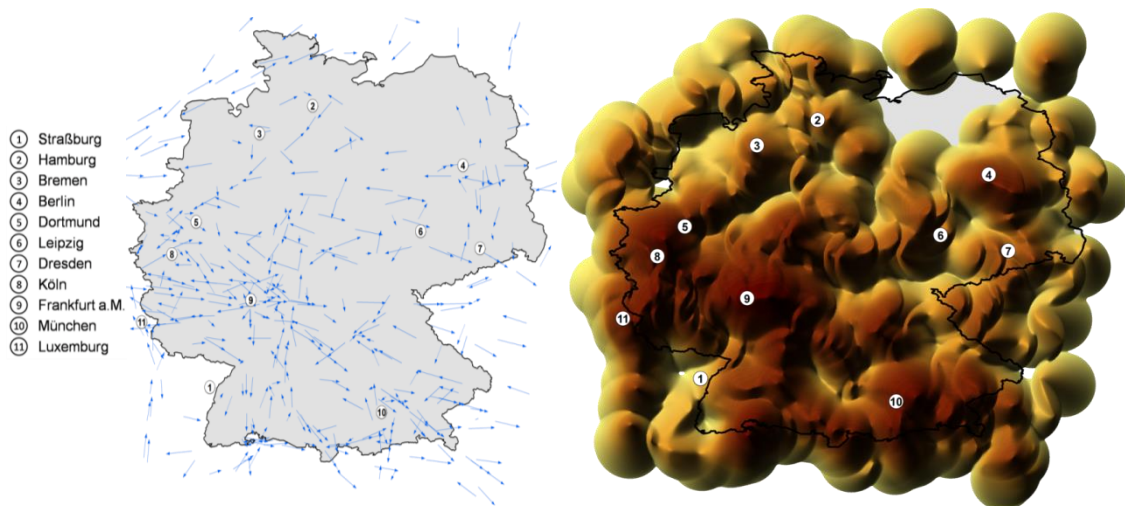


Figure 2-22: Airplane positions at two moments of time (left) and the resulting DKDE-map (right), source: Peters & Krisp (2010).

4) 3D density map using STC

Nakaya & Yano (2010) suggested a method using a STC to visually explore the spatio-temporal density distribution of crime data in an interactive 3D GIS. Thereby the author adapted the KDE by using space-time variants and scan statistics. In order to investigate the dynamics and density change, an interactive use within a 3D environment is essential.

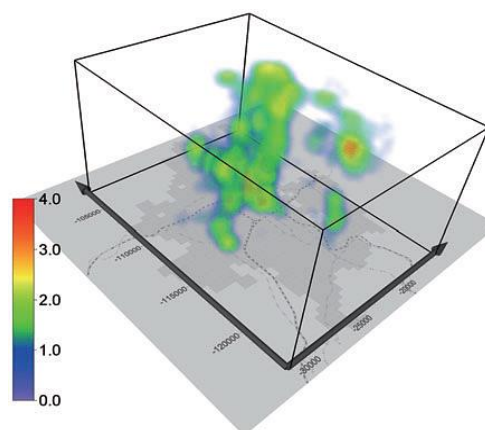


Figure 2-23: Density visualization of crime events in a STC, source: Nakaya and Yano (2013).

5) KDE for trajectories

In a comprehensive review of the existing visual analytical approaches (Andrienko & Andrienko 2013), methods, tools and concepts for moving objects were introduced. A section is dedicated to continuous density surfaces (fields) derived from trajectories or from point-related attributes. Density maps of moving objects were created on the basis of aggregated points of trajectories. A trajectory is understood as a function of time or a path left by a moving object in space. Moving objects can be confined within a network (such as cars along streets of a traffic network) or float freely over a region (boats) or in space (airplanes). Spatio-temporal density maps of trajectories were investigated in (Demšar & Virrantaus 2010; Lampe & Hauser 2011; Scheepens et al. 2011a; Willems et al. 2009). In these approaches, the KDE method is adapted to trajectories as a function of changing velocity and direction. Willems et al. (2009), for example, built his kernels assuming constant speeds. Other approaches assume constant acceleration. The resulting density maps can reveal simultaneously large-scope patterns and fine features of the trajectories. An example of aggregated vessel trajectories is given in Figure 2-24.

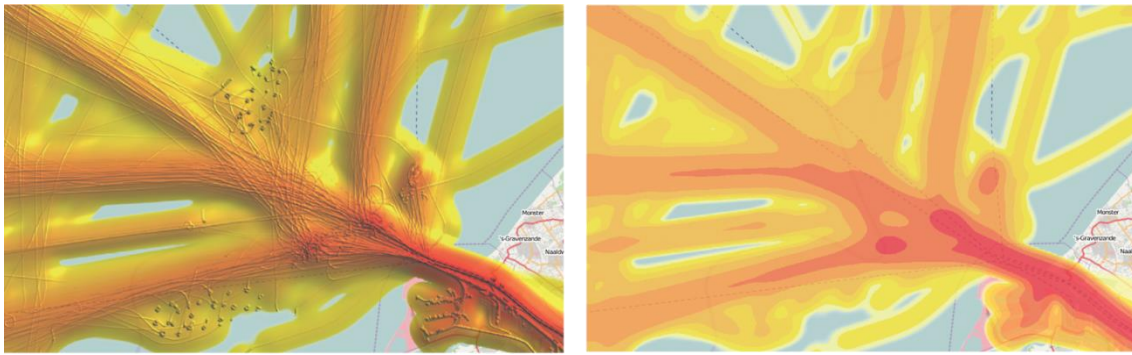


Figure 2-24: Aggregated vessel trajectories, left: Multi-scale density with continuous color mapping, right: Density with discrete color mapping; source: Willems et al. (2009).

This mapping idea was extended to the 3D space in (Demšar & Virrantaus 2010) where the trajectory densities are visualized inside a STC. Another possibility of displaying density information of trajectories is to use derived discrete grid cells, whereby each cell color refers to the amount of trajectories passing through the cell (Forer & Huisman 2000). In the existing 2D density maps based on KDE, the time is either frozen on a certain moment or confined within a certain time interval. Consequently, the resulting contour lines do not carry information of temporal changes. Although various approaches for density visualization of trajectories have been investigated, an appropriate method for 2D density maps of moving point clouds is still missing. Whether the dynamics of SEPs - represented by points – can be adequately expressed in a single contour map remains an open question. To tackle this question, we develop an approach termed as spatio-temporal density mapping which will be explained in Chapter 4. Beside internal structure changes of SEOs, another component of this thesis forms the exploration of similarities of different trajectories of SEOs. In the following section we will emphasize on the state of the art of similarity measurement and visualization for trajectories.

2.6. Trajectory similarity measurement and visualization

Similarity measure of trajectories is a crucial part for the investigation of object movements. Trajectories might be defined (to a certain degree) as similar if they:

- Fully or partly coincide in space or/and time
- Have similar average speed or movement direction
- Have similar spatial lengths

- Have similar shapes
- Have common starts and/or ends
- Have similar dynamic behaviors such as route motions (curve characteristics), speed changes or acceleration changes

“It depends on the application and goals of analysis which of these respects are relevant. Therefore, it is useful to have a clustering tool allowing the analyst to choose an appropriate similarity measure (also called distance function) from a number of alternatives” (Andrienko et al. 2007b). An example for an algorithm of such “route similarity” distance function is provided by Andrienko et al. (2007b) which repeatedly scans two trajectories, searching for the closest pair of positions. Trajectory similarities can be visually or statistically derived from clustering. In most cases, spatially and/or temporally close trajectories are clustered and cluster-wise visualized and analyzed (by applying a certain distance or time interval and defining a minimum number of trajectories per cluster, e.g. 5). In other words, moving objects can be clustered based on the similarity of the respective time series on the one hand, and, on the other hand, time intervals can be clustered based on the similarity of the spatial situations. Thus, similarities in trajectory dynamics can be already revealed, for instance through applying different symbols (e.g. color) to the resulting clusters. Thereby entire trajectories and/or parts/compartments of trajectories could be clustered. It may also be reasonable to group trajectories by spatial closeness of their starts and ends.

Trajectories or compartments could also be clustered by similarities of other attributes than spatial location or time, such as spatial length, shape, duration, average speed, average moving direction and route-behavior, their respective temporal variations could be then cluster-wise analyzed (Andrienko & Andrienko 2013). Most existing approaches for spatial clustering of trajectories include the use of the euclidean distance, which, however, is somewhat sensitive to noise. Vlachos et al. (2002) introduced a computational approach for similarity measures of trajectories in a two or three dimensional space. In their work, the authors developed a non-metric similarity functions based on the Longest Common Subsequence (LCSS), which are very robust to noise and can provide an intuitive notion of similarity between trajectories by giving more weight to similar trajectory compartments. Furthermore, the authors mentioned the problem of comparing trajectories of different lengths, which, however, was not considered in their computational approach.

A similar approach for distance function considering outliers and being robust against data imperfections - edit distance on real sequence (EDR) - was introduced in (Chen et al. 2005). Outliers could also be defined as trajectories that remain un-clustered. As mentioned before, it really depends on the given data, the application case, the similarity measure and the targeted trajectory similarity. Another common method for aggregating spatially close trajectories is density-based; an approach valid for 2D trajectory lines was introduced by Willems et al. (2009) and for lines in 3D space by Demšar & Virrantaus (2010). Similar density-based approaches using line bundling are introduced by Hurter et al. (2012) and with the extension of force-directed bundling by Holten & Van Wijk (2009). Solutions (partly graph-based) for similarity search of trajectories with restrictions on spatial networks (e.g. road networks) are provided, among others, in (Hwang et al. 2005); Tiakas et al. (2006).

Another important issue during trajectory comparison is to detect similar motions of trajectories in different space regions and at different scales (spatial or/and temporal). A trajectory, large in space and long in duration, could hold similar motions/dynamics as a much smaller one. For trajectory motion comparison rigid transformations such as shifting, scaling and rotation might be necessary. For instance, transformation of trajectory times for common start times would enable better comparison. Pelekis et al. (2007) offered a distance function approach based on primitive

(space and time) as well as derived motion parameters of trajectories (speed and direction). Considering space dimensions, similarities of trajectory in 3D can differ from those taking only projected data on the 2D surface into account. Each group of trajectories, derived from similarity-based clustering, could be aggregated and then again compared/analyzed for similarities/dissimilarities with other aggregated trajectory groups. It can be summarized, that existing approaches focus on similarity measures of line trajectories representing moving points.

How can we now visualize or visually analyze trajectory similarities?

Visual comparison of trajectory similarities (of two or more trajectories) can be done by overlaying one map display over the other one or placing two or more map displays next to one another – each visualizing a different trajectory. Some appropriate methods and tools used for visually explore trajectory similarities are density maps, STC, temporal displays, trajectory wall, time graph, etc. Most visual approaches for trajectory similarity visualization and analysis are based on summarizing trajectories (e.g. clustering and/or aggregating) based on similar properties. Multiple trajectories, which are clustered through spatial or spatial temporal proximity, can be represented by polylines of different colors (as in Figure 2-25-a). Large difference in colors indicates much dissimilarity between clusters. Thus, similar trajectories are summarized by color, but there is no information about trajectory quantity and thus an obvious demand for generalization in order to avoid overplotting. The generalization approach suggested by (Andrienko & Andrienko 2009) enables another visual summarization of trajectories as illustrated in Figure 2-25-b. Thereby, arrows or half-arrows (vectors) show the movement directions and the arrow widths are proportional to the number of trajectories. The approach has the added values of making trajectory data less overloaded so that the user/analyst is able to identify how many trajectories have common start and end points and thus able to distinguish frequent paths from less frequent and occasional ones. Figure 2-25-c illustrates a STC of the same traffic data as in Figure 2-25-a. In the STC details of grouped trajectories can be detected much more clearly as well as temporal information and movement behaviors such as moving speed changes and moving directions. The STC demands a high degree of user interactions in order to fully visually explore the data.

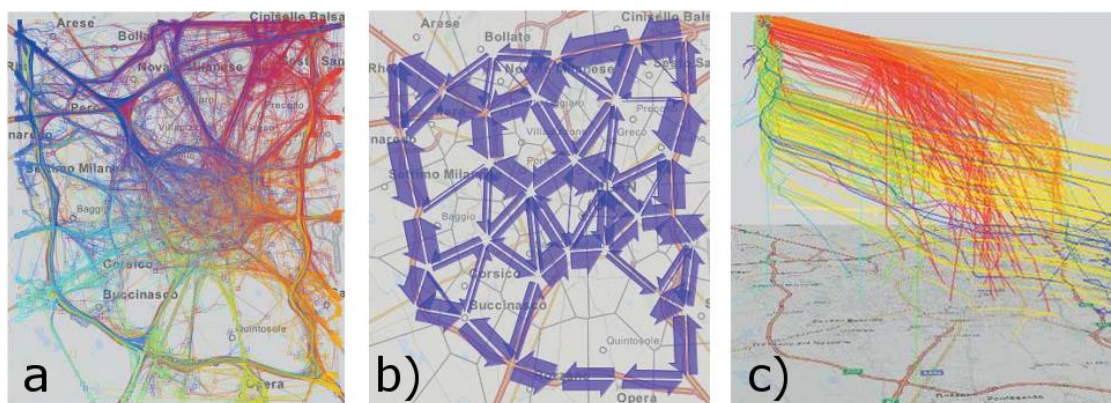


Figure 2-25: Traffic data of Milan, Italy, a) clustered by color, b) aggregated to arrows, c) STC, source: <http://www.rockpaperink.com/post/92434324658/designing-mobility>.

Figure 2-26 illustrates a vessel trajectory density map as solution for summarized trajectories introduced by (Scheepens et al. 2011b). The vessel traffic during one day in front of Rotterdam is shown, revealing four different density levels: night vessel traffic in dark blue, morning in bright yellow, afternoon in dark yellow and evening in bright blue.

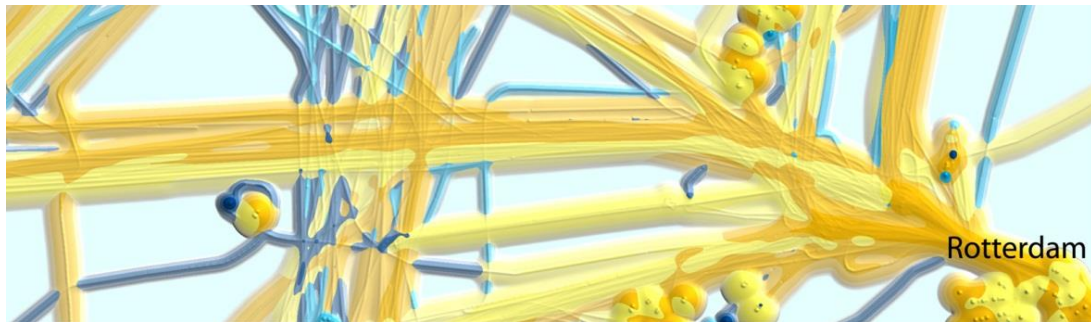


Figure 2-26: Trajectory density map of vessels, source: Scheepens et al. (2011b).

Another approach is called ‘trajectory wall’, as illustrated in Figure 2-27. The hybrid 2D/3D trajectory wall represents trajectory attribute data (e.g. speed) of one chosen trajectory group/cluster by stacking 3D color-coded bands on a 2D map (Andrienko et al. 2014). Stacked trajectories can be ordered along the vertical axis according to their temporal order. It could also be reasonable to order them according to other criteria such as average speed which would support the comparison of fast and slow trajectories and the respective location for certain speeds. Additionally, a time lens - an interactively chosen circular area – can show the spatial positions of the trajectory points in its interior and temporal aspects on the lens rim. The 2D time graph complementarily provides detailed temporal information through assembled 2D trajectory bands. The bands indicate trajectories, which are divided into segments. Segments are colored according to attribute values (speed). While the trajectory wall enables summarization of attribute values with locations, the time graph enables summarization of attribute values associated with temporal intervals (Tominski et al. 2012).

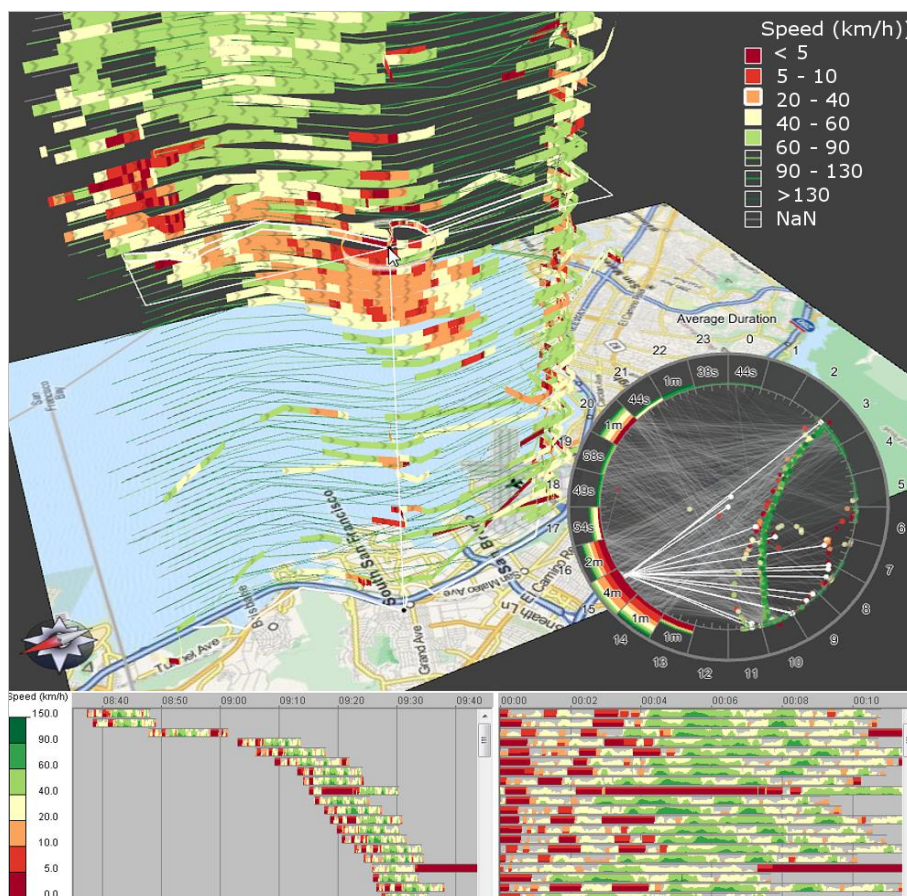


Figure 2-27: Trajectory wall with time lens of traffic jam along one main road in San Francisco (above) and corresponding time graph (below), source: (Tominski et al. 2012)

Further visual analytical tools for trajectory comparison include radar plots, PCPs or table lenses. The similarity computation and the extended visual analytical tools for lightning data will be introduced in this thesis (Section 4.4.2). They are based on trajectory lines. If trajectories are spatially extended, these approaches need to be adapted in order to analyze similarities of lanes and their attributes.

In the following section we will discuss representations of forecasted dynamic objects in particular the visualization of their uncertainties.

2.7. Prediction and uncertainty visualization of movement data

With regard to the visual analysis of dynamic geographical data, the near-time prediction and visualization of spatial and aspatial information is crucial for the understanding of data dynamics and for decision-making. The visualized predictions of traffic data, thunderstorms or forest fires are just a few examples. An important aspect of the prediction or forecasting, is its uncertainty. Uncertainty can be caused not only by the underlying detected data, but also by data processing and visualization. Definitions for ‘uncertainty’ in literature are not consistent. Pang (2001) stated, that “uncertainty is a multi-faceted characterization about data, whether from measurements and observations of some phenomenon and predictions made from them. It may include several concepts including error, accuracy, precision, validity, quality, variability, noise, completeness, confidence and reliability”. In cartographic literature, the terms “reliability” and “quality” are used as well (Slocum et al. 2009).

In our context, we focus on uncertainties of dynamic geodata, including information such as polygon location/extension and attributes. A particular attention in this work will be on the uncertainty visualization of predicted lightning clusters. Based on the background knowledge and a series of recorded spatio-temporal data, the probability/uncertainty of predicted movement data can be computationally determined and visualized. Thus three parts are important: I) data as well as their pre-processing, II) prediction including the determination of prediction uncertainty and III) visualization of the uncertainty. For dynamic geodata, uncertainty visualization of forecasted data principally depends on the prediction method. Possible prediction methods for moving objects are linear or nonlinear extrapolations (e.g. Spline), polynomial regressions or the use of statistical models (e.g. Bayesian network, Markov model). Besides, the prediction of the spatial location of a moving point object can also be computed using a simple velocity model and taking into account the current object velocity and moving direction.

Geographic objects, in particular their position, geographic extension and attributes, reveal certain accuracies, depending on the acquisition methods. These accuracies are crucial for forecasting methods. Systematic, random and gross errors have to be considered in order to determine the accuracy. It is expressed either in percentage or in the measurement unit of the object attribute (e.g. “cm”). For dynamic objects, location and movement uncertainty usually differs, depending on the respective moment of time or time interval. For predicted attributes, uncertainty increases with the growing distance to the future time. In our context, two basic prediction models are relevant: (a) History model which extrapolates into the future based on the attributes of the last two or more time steps and (b) Simulated or Learning model which takes the movement characteristic into account, learned from the entire given dataset. Both models were explained in more detail in (Scheepens et al. 2014).

In general the predicted objects can be illustrated in the same way as present and past objects. If several future steps are presented, temporal information should be provided. Visualized uncertainties of predicted information definitely bring an added value for decision making. In our context, we will focus on the visualization of uncertainty of location and attributes of geographic objects. Griethe & Schumann (2006), MacEachren et al. (2005), as well as (Slocum et al. 2009)

provided an overview about existing concepts and approaches for visualizing uncertainties of geographic data. Basically the values of visual variables of points/lines/polygons can be correlated with uncertainty information. Gershon (1998) distinguished intrinsic visual variables (e.g. size, color, saturation, transparency) and extrinsic visual variables (added objects, such as arrows, bars, charts, dials and objects of different shapes). Using intrinsic visual variables, we may change the size of a point, the size, color or texture of a line, the transparency or the saturation of colored tones on a choropleth map. Some examples for different uncertainty visualizations for point symbols using various intrinsic visual variables are shown in Figure 2-28.

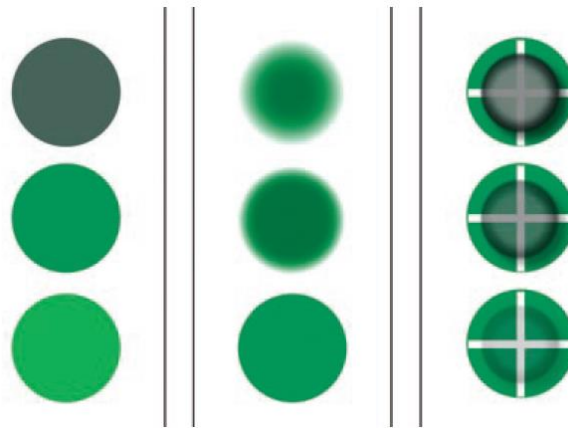


Figure 2-28: Uncertainty visualizations for point symbols with variations in saturation (left), crispness (center) and transparency applied to the smaller symbol (right), source: MacEachren et al. (2005)

Furthermore the resolution of raster data could reflect uncertainty. An appropriate legend is necessary for the user to understand the visualized uncertainty. Another common method is to use bounding buffers around geo-objects representing their uncertainties. The uncertainty information can be embedded in the visualization of the underlying data or rendered in an adjacent map so as to avoid overloading the map information. Animations and/or dynamic symbol actions can also be used to represent uncertainty information. Moreover, uncertainty can be presented as well via typology (e.g. “+/- 1 minute” for time error).

For the visualization of the uncertainty of predicted moving objects, many approaches use a buffer around the predicted spatial position/extension, illustrating the uncertainty of the forecasted spatial information. Another possibility is the use of temporally weighted kernel density approach introduced by Porter & Reich (2012) to predict and visualize locations and their uncertainties of event in a series. Scheepens et al. (2014) introduced a contour-based approach to visualize predicted moving objects including position uncertainty information as illustrated in Figure 2-29.

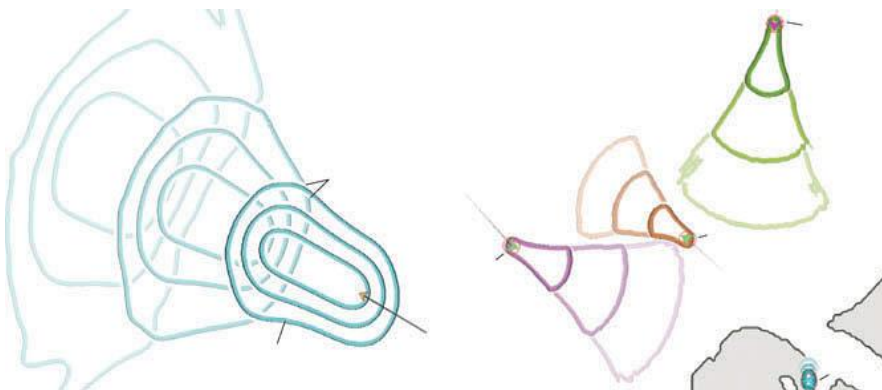


Figure 2-29: Visualized Vessel prediction and uncertainties of three time intervals, source: (Scheepens et al. 2014).

Different colors represent different vessels. For each time interval of the blue vessel on the left, three probability percentiles are drawn: 95% (outer contour line), 25% and 15% (inner contour line). The saturation and lightness of contour lines decrease with increasing time in order to differentiate between time intervals and to convey the notion of increasing uncertainty for vessel position predictions. Their approach includes the prediction of vessel positions, velocity and course. They defined a temporal probability distribution as a positional probability distribution that changes over time. Furthermore, the authors presented a contour-line-based interactive visual approach for the exploration of predicted vessel interactions and its probability. Another example for trajectory uncertainty visualization is provided by Álvarez & Gilberto (2013). An interactive explorative tool for the visual analysis of uncertainties of dynamic fields was introduced by Hollt et al. (2013) and applied for ocean forecasts in order to support the planning and operation of off-shore structures. Further existing approaches dealing with the determination and visualization of uncertainties of moving objects can be found in (Harrower 2003; Hengl 2003; Pfoser & Jensen 1999).

2.8. Chapter conclusion

The relevant terminologies as well as the evolution of visualization technologies in the context of visual movement analysis of SEOs were explained and compared. The issue of spatio-temporal modeling of dynamic geodata was introduced and the state of the art of cartographic representation and visual exploration of dynamic geodata analyzed. So far, the visual analysis has been extensively conducted for dynamic discrete point data, but much less was reported about the visual exploration of dynamic polygons (SEOs). With regard to the internal structure change of moving point groups, we have shown that existing approaches do not address adequate solutions for density mapping of dynamic points belonging to the same moving phenomena. Available solutions mainly apply to datasets with two different moments of time. Trajectory similarity measurement and visualization approaches exist for trajectory-lines and need to be adapted for similarity of track-lanes. Moreover, we shed some light on the concepts for uncertainty representation of predicted dynamic SEOs.

3. Visual analysis/analytics of dynamic SEOs/SEPs

This chapter is dedicated to a conceptual discourse about the visual exploration of dynamic SEOs with a focus of movement analysis. This includes a detailed inspection of the following questions.

- How can we describe and define different types of spatially extended moving objects or phenomena?
- Which pre-processing steps are needed for different types of dynamic SEOs in order to derive spatio-temporal polygons and thus the polygonal trajectory lane of a SEO?
- How to visually and non-visually describe and represent dynamic SEOs and their movement features/attributes?
- Which applicable visual variables apply to the visualization options for SEOs and their movement features/attributes?
- How to describe the movement behavior of dynamic SEPs?
- What are the specific tasks of movement analysis and their corresponding visual analytical approaches to accomplishing these tasks?

3.1. Refining SEOs or SEPs

Based on the definitions and differentiations for dynamic (spatio-temporal) data in the previous chapter, we divide the dynamic data into three main groups: (1) discrete point objects, (2) spatially continuous fields (or surfaces) and (3) SEOs. The term “dynamic objects” refers to the spatially moving objects on which this work is mainly focused.

Discrete objects such as moving persons, vehicles (cars, ships and airplanes), animals or goods have a spatial extension that can be represented by points. More precisely, there is a second type of dynamic discrete point objects which are moving events, whereby each event reappears at a certain location on/during a certain moment of time. For example, every year the National Garden Festival (event) takes place in a different location/city. Besides, events can also be related to discrete moving objects. For example a truck driver bringing goods from place A to B has to stop at certain locations to refill the empty tank with fuel. The second group ‘dynamic fields/surfaces’, such as oceans, represent phenomena where for each location on the surface a value of a dynamic phenomenon-attribute is allocated. SEOs change their sizes and shapes. SEOs can be divided into two sub-categories: (3a) SEOs defined by groups of moving discrete objects such as animal swarms/herds (e.g. bird swarms, insect swarms, bacterial colonies) or moving crowd of people (tribes, armies, explorers etc.) and (3b) SEOs formed throughout a SEP which cannot be described via a detected group of points. Examples are clouds, thunderstorms or land-use. Members of (3a) originate from natural arrangements (e.g. animal herds) or are constructed during data analysis (e.g. by clustering) as it is the case for lightning clusters, diseases or the spatio-temporal change of dialects. Furthermore, we can distinguish groups of (3a) by the traceability or non- traceability of group members: For instance birds within a bird swarm can be tracked via GPS. Thus a certain point-ID, belonging to a spatio-temporal cluster can stay in the cluster or change the cluster while moving in space and time (3a-I). Lightning for instance, on the contrary, appear only once. Consequently, lightning clusters are formed via spatio-temporal clustering, but lightning points cannot be tracked since they do not appear twice or more often (3a-II). In case of swarms, the focus within this thesis is not on swarm object analysis, but on the investigation of the entire swarm. Table 3-1 illustrates these different kinds of dynamic data.

A dynamic SEO usually consists of a series of polygons/clusters. Within that series successive polygons spatially overlap and each polygon is related to a certain time or time interval within which the polygon was detected.

Table 3-1: Types of dynamic objects and examples.

| | (1) Discrete point objects | (2) Continuous fields/ surfaces | (3) SEO | | |
|----------|---|--|---|--|---|
| | | | (a) polygons based on captured point groups | | (b) other polygons* (non-point-based) |
| | | | (I) moving point group | (II) clustered point events | |
| examples | humans, animals, vehicles, goods, planets | wind speed, temperature, oceans, currents, soil values | animal herds, bird swarm, moving crowds (tribes, explorers, armies) | lightning clusters, diseases, epidemics, dialect areas | clouds, thunderstorms, land-use change, floods, wildfires |

* no group membership, SEOs are formed throughout a SEP which cannot be described via a detected group of points.

In order to model the trajectories and perform spatio-temporal queries of moving SEOs, we define a “cluster” as a spatio-temporal interval of a SEO. Thus, it forms the smallest meaningful state of interest for a relevant application of the moving SEO. The polygon corresponding to a cluster can contain a group of points. An example is the spatial extension of a wildfire extracted from an aerial photo taken at a specific moment of time. The entire wildfire – from the moment it came into existence until the moment it disappears – defines the dynamic SEO. Another example is a moving lightning cluster, which is part of a thunderstorm and forms a three-dimensional lane (trajectory) during movement. Its associated SEO of lightning contains spatio-temporally grouped lightning points which are detected during a predefined temporal interval (e.g. from 3pm until 4pm on March 21st 2014) and spatially close to each other (e.g. nearest neighbor distance threshold of 6 km). All existing dynamic SEOs including their characteristics and behavior finally describe the SEP and its dynamics.

We can also take into account how objects are moving through the space, or in other words how we can describe the trajectories of dynamic objects. On the one hand the space can be two- or three-dimensional. On the other hand objects can move in either a non-confined space without fixed extension or a confined space such as along a road respectively within a 2D polygon or 3D polygon (polyhedron). Depending on the context, it is necessary to specify the type of dynamic data in order to get a better insight into what dynamic objects, phenomena, fields or SEOs really mean in the respective situation: Discrete entities can remain similar or identical shapes and sizes or change their sizes and/or shapes. A moving crowd could be composed of discrete entities with changing or with fixed identities. In case of changing entities, the change could be based on disappearing, merging or splitting.

3.2. Pre-processing of moving SEOs

Moving SEOs can be geographically described as polygons whereby each polygon exists at a certain moment of time of time interval. How to detect these dynamic polygons? As shown in Table 3-1, we suggest dividing SEOs into two main types: (a) groups of discrete point objects and (b) moving areas. Polygons of type (a) can be either a group of moving points, originated from natural arrangements (a-I) or they can be constructed based on processing/analysis of point events, for instance by clustering (a-II). Point coordinates are detected through GPS tracking (e.g.

animal swarms), via sensors (e.g. lightning detection sensor network, see Section 4.1.1), from raster images (e.g. people crowd movement), etc. The corresponding dynamic polygon is shaped via spatio-temporal clustering of detected points (e.g. tracking of bird locations and subsequent spatio-temporal clustering of bird swarms). The second type (b) could be formed by anything but moving point groups. One example is polygon extraction from raster images (e.g. floods, clouds).

Furthermore, the detection or creation time of initial points or/and polygons is crucial for a spatio-temporal analysis and initial data can be available in a two- or three-dimensional space, depending on the application case. Moreover, points may have additional attributive information describing the point and the dynamics of the phenomenon. Attribute values as well might change in time (in case of moving points). Figure 3-1 illustrates the workflow of how different types of dynamic SEOs are created, including data capturing methods, derived initial vector data and – if needed – data pre-processing. Theoretically a point event could also occur more than once. In case of swarm points and point events, the spatio-temporal clustering of points into polygons as well as the allocation and aggregation of these clusters to trajectories counts as an important pre-processing of dynamic SEOs. Thereby, spatial and temporal intervals have to be defined in order to derive clusters. Furthermore, outliers and errors have to be detected and removed and data gaps filled (e.g. via data interpolations).

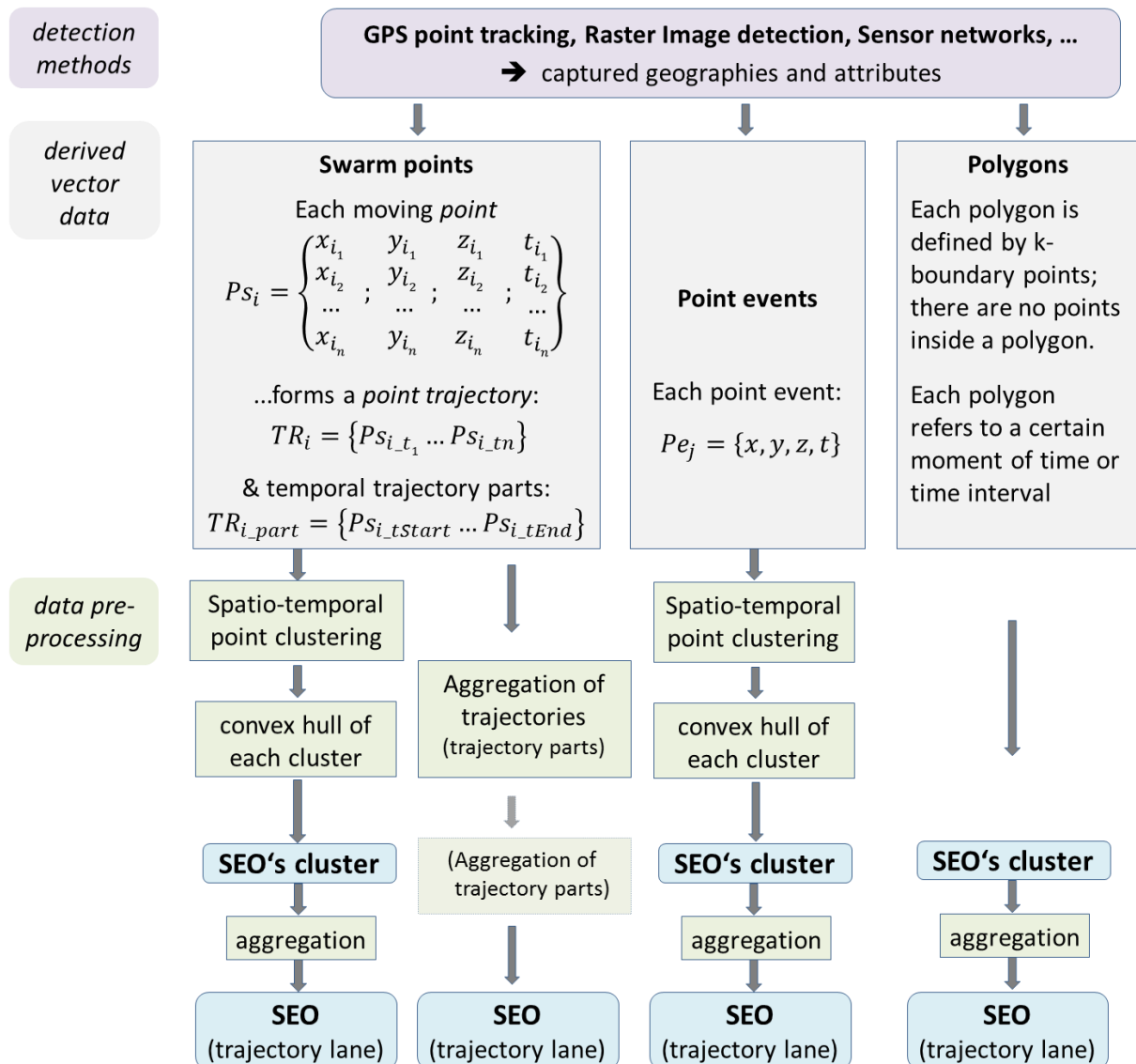


Figure 3-1: Dynamic SEOs - data capturing and pre-processing.

In the next section we will present a generic concept for visually analyzing dynamic SEOs. First, spatio-temporal relationships will be briefly discussed followed by an overview about representation methods including appropriate visual variables. Then we will develop adequate visual solutions for specific movement analysis tasks.

3.3. Visual exploration of moving SEOs

This chapter aims to answer the question of how dynamic SEOs and their features can be adequately visualized and analyzed. It addresses data pre-processing, cartographic techniques as well as tools and approaches from the fields of visual data mining, information visualization and visual analytics. The visual exploration of dynamic SEOs conceptually consists of the following parts: Map representation and non-visual description of SEOs and a task-specific visual analysis of the moving SEOs as well as the analysis of their movement behaviors. In the following, we discuss at first the spatio-temporal relationships of SEOs.

Modelling spatio-temporal relationships of moving SEOs is crucial for the visual analysis of the dynamics of SEOs. In Section 2.2 (Figure 2-10) we discussed spatio-temporal relationships for temporally evolving polygons, based on Claramunt & Jiang (2000). However, the authors assumed constant spatial polygon extension and treated the polygon as an event without taking the trajectory of a moving polygon into account. An adaptation of Claramunt and Jiang's model is therefore necessary which will consider the clusters (polygons), cluster centroids (points), trajectory lines (polylines formed by connected centroids) and trajectory lanes (polygons) of SEO in 2D and 3D space. Based on (Andrienko et al. 2011b), we can subdivide relations between moving SEO and context-elements in topological relations ('in', 'cross', 'touch', etc.) and metric relations (spatial and temporal distance, spatial direction).


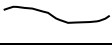




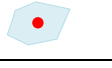



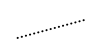
3.3.1. Representation (mapping) and non-visual description of dynamic SEPs and their features



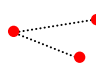


When describing or mapping dynamic SEOs, it is necessary to consider spatial, temporal, spatio-temporal and further attributive information. Table 3-2 gives an overview about components and attributes of dynamic SEOs, their non-visual description and their rudimental graphic expressions in a two-dimensional map display. All suggested representations support the exploration of SEOs and their characteristics. The table is divided into four main parts: dynamic SEOs in terms of the entire track lifetime (I); a cluster as the smallest spatio-temporal interval at any track location and time (II); a particular movement event or situation of a SEO (III) and uncertainty information of SEO's attributes (IV). In general a moving SEO comes into existence at some moment of time, it moves while location and/or spatial extension as well as attributes might change. A SEO can merge with other or split into several SEOs and it cease to exist at some moment of time. The geographical information of a cluster or an entire SEO includes spatial extension, form, cluster area and volume, centroid position and the trajectory (moving polygons can be allocated and aggregated to trajectories).

Trajectories can be represented either by a track line or a track lane. A track line can be determined by connecting successive centroids of dynamic clusters of SEO. A track lane is assigned through the convex hull of the whole spatial extension of a SEO. Track lines and track lanes can be simplified via smoothing. If a SEO cluster is shaped by a point group, further information such as point quantity, point distribution, spatio-temporal point dispersal and migration can be derived. Besides, a dynamic SEO cluster contains movement information, such as speed, acceleration and movement direction. Further statistical information of the entire SEO may include lifetime duration, cluster quantity, as well as distribution, averages, standard deviations and peaks (minima, maxima) of all values (e.g. of speed, area, number of points). The dynamics of a SEO is

reflected in the changes occurring to its spatial and non-spatial attributes. The extrapolation of the changes to the near future is called nowcasting. The cluster information can also be used to predict its future state. The uncertainties of geographical information are rooted in the measurement errors.

Table 3-2: Typical features of a dynamic SEO and their attributes.

| Features / attributes | | Descriptions | Legend | |
|---|--------------------------------------|---|--|--|
| (I) Trajectory of cluster lifetime | 1) Form / extension | Polygon area, spatial range (dX, dY, dZ) |  | Exact (convex hull) or simplified form; abrupt or fuzzy boundaries |
| | 2) Track-line | Length |  | Line connecting cluster centroids |
| | 3) Track-lane | Length, width |  | Lane formed by the moving SEO |
| | 4) Average moving direction | Direction angle or cardinal direction |  | Linear arrow |
| | 5) Moving tendency | E.g. from northeast to southwest |  | Curved arrow |
| | 6) Point quantity* | Total number of points | 350 | A number or a point quantity-based color |
| | 7) Further attributes | Lifetime (number of clusters) average/min/max of speed, altitude, number of splits/merges | | |
| (II) Spatio-temporal cluster | 1) Form / spatial extension | Polygon area, spatial range (dX, dY, dZ), form index |  | True or prototypical form |
| | 2) Cluster centroid | Coordinates $P_c = (x,y,z)$ |  | |
| | 3) Movement attributes | a) Movement direction arrow |  | Arrow |
| | | b) Movement direction tail |  | Symbol like a comet-tail |
| | | c) Direction text description (angle or cardinal direction) | NW | Northwestwards |
| | | d) Value of speed and acceleration | Text or adapted polygon color/comet-tail length | |
| | 4) Cluster point quantity* | Number of points |  | Point quantity-based centroid size, color/polygon color or text |
| | 5) Distance to previous/next cluster | Length |  | Line between successive cluster centroids |
| | 6) Further information | e.g. state/position within trajectory | 13/19 | Step no. 13 out of 19 |
| 7) Cluster prediction | Same as other cluster descriptions | | | |

| | | | |
|--|--|--|---|
| (III) Particular SEO's movement events/ situation | 1) Coming to birth, cease to exist | Time and spatial location |  Polygon/centroid of first/last cluster |
| | 2) Merging | Time, cluster information of involved SEOs |  Overlapping polygons, connected cluster centroids |
| | 3) Splitting | Time, cluster information of involved SEOs |  Overlapping polygons, connected cluster centroids |
| | 4) Peaks | a) Maximum/minimum altitude | 10,2 km |
| b) Maximum cluster point quantity* | | |  Point quantity-based size or color/polygon color |
| (IV) Uncertainty | 1) Uncertainty of spatial position/extension | Relative or absolute |  Buffer around polygon (with abrupt or smooth color gradient) |
| | 2) Uncertainty of semantic attributes | Relative or absolute | +/- 5% |

* *only valid for SEO formed through moving point groups/ point events*

The legend (last column of Table 3-2) can be visualized in different ways, using the seven visual variables - form, color, size, sharpness, transparency, orientation and texture including pattern arrangement and orientation. Table 3-3 gives an overview of how these basic visual variables are used to visualize text information, points, lines and polygons representing moving SEOs.

In addition, appropriate dynamic actions are inserted to reflect movement and movement changes. Such dynamic symbol actions include blinking, flashing, erupting, sinking, shacking, frequent flash impulses, smooth directional color ("flying in") or desaturation. Appropriate visual variables are marked with filled circles. Possible but not suitable visual variables are shown with unfilled circles. Different map styles and variables for dynamic SEOs can be drawn simultaneously. The resulted multivariate visualization of clusters and their attributes may lead to an improved insight into the dynamic phenomena. In order to avoid information loss caused by overlapping, some visual variables (e.g. transparency) need to be adapted. In addition, user interactions can be embedded to the visualization to support the visual analysis. The basic visual analytical tools are panning, zooming, rotating, enabling and disabling map objects or different object symbolizations, fetching textual attribute information via click, using a time slider to explore temporal changes. Moreover, various graphic types other than maps can also support the visual exploration of dynamic SEOs. In the following sections, the 'movement behavior' of SEOs will be discussed, the specific tasks of movement analysis identified and the necessary visual analytical approaches introduced.

Table 3-3: Visual variables for dynamic SEO.

| Text information Points Lines Polygons | | Numbering is based on Table 3-2 | | | | | | | |
|---|--|---------------------------------|---------------------------------------|---------|----------------|-----------------|----------------------|------------|---------------------------|
| | | A) Form/Shape (symbol style) | B) Color (saturation, luminance, hue) | C) Size | D) Orientation | E) Transparency | F) Pattern crispness | G) Texture | H) Dynamic symbol actions |
| I-6) | Cluster point quantity | | | | | | | | |
| I-7) | Further track attributes (e.g. lifetime) | | | | | | | | |
| II-4) | Cluster point quantity** | | ● | ● | ● | ● | | ○ | ○ |
| II-6) | Further track information | | | | | | | | |
| II-7) | Further cluster information | | | | | | | | |
| IV-2) | Uncertainty of attributes | | | | | | | | |
| III-4a) | Peaks (altitude, etc.) | | | | | | | | |
| III-4b) | Maximum cluster point quantity | | ● | ● | ● | ● | | ○ | ● |
| II-3c) | Direction (angle or cardinal) | | | | | | | | |
| II-3d) | Speed, acceleration* | | | | | | | | |
| II-2) | Position (cluster centroid) | | | | | | | | |
| I-1) | Trajectory by point clouds ** | ○ | ● | ● | ● | ● | ● | ● | ○ |
| II-1) | Cluster by point clouds ** | | | | | | | | |
| III-1) | Coming to birth, cease to exist | ● | ● | ● | ● | ● | ● | ● | ● |
| I-2) | Trajectory (track-) line | | | | | | | | |
| I-4) | Average moving direction | | ● | ● | | ● | | ● | ○ |
| I-5) | moving tendency | | | | | | | | |
| II-3a) | Cluster direction arrow | | | | | | | | |
| II-5) | Distance to previous/next cluster | | ● | ● | | ● | | ● | ● |
| III-2) | Cluster merging via lines | | | | | | | | |
| III-3) | Cluster splitting via lines | | | | | | | | |
| I-1) | Trajectory form/extension | | | | | | | | |
| I-3) | Trajectory (track-) lane | | ● | | | ● | ● | ● | ○ |
| IV-1) | Uncertainty buffer | | | | | | | | |
| II-1) | Cluster form/spatial extension | | | | | | | | |
| II-3b) | Cluster direction tail | | ● | | | ● | ● | ● | ● |
| III-2) | Cluster merging via polygons | | | | | | | | |
| III-3) | Cluster splitting via polygons | | | | | | | | |

* in particular significant changes

** only valid for SEO formed through moving point groups

3.3.2. Movement behavior/aspects of dynamic SEOs

As mentioned before, space properties, time, the object’s movement activities and various context characteristics influence the dynamics of a moving object. As explained before, a cluster is defined as the smallest spatio-temporal interval of a moving SEO and the lifetime evolvement of such cluster forms the SEO’s trajectory and its complexity.

The behavior of a single cluster can be described by

- Momentary movement situation (instant movement characteristics): moving or stopping
 - o In case of movement:
 - Movement direction
 - Speed
- Cluster shape and spatial extension
- Internal cluster properties: point distribution and point quantity (in case the SEO is based on moving points or point events)
- Status change at the current time (t) in comparison with the previous time (t-1):
 - o Change of movement: direction (turn), speed (acceleration)
 - o Change of further cluster properties (shape: expand/shrink/deform, spatial extension, internal cluster changes)
- Specific cluster situation:
 - o Moment of appearance (cluster birth or re-appearance)
 - o Moment of last appearance (extinction)
 - o Splitting into two or more clusters
 - o Merging of two or more clusters into one
 - o Interactions with another (static or moving) point object or area of interest: touching/covering/being covered/overlapping
 - o Spatial return to certain points
 - To a previously passed location (e.g. place of first appearance)
 - To a location of special interest

Next, we will look at movement characteristics of the trajectory of an SEO during its entire (past) lifetime respectively during a certain period of time of interest.

This trajectory behavior contains information about:

- Average movement direction (exact or cardinal direction)
- Cluster movement statistics:
 - o Speed information: average speed, maximum speed, number of accelerations and decelerations
 - o Altitude information: average altitude, maximum altitude, number of climbs and falls, fastest/steepest climb/fall
 - o Trajectory occurrence time and lifetime (if it is the case consideration of re-appearances)
 - o Traveled distance and displacement (in 2D or 3D)
 - o Statistics of the instant/momentary cluster characteristics
 - o Trajectory sinuosity and tortuosity
 - o Trajectory events (movement events):
 - Stops: number of stops, analysis of stops at certain locations of interest, temporal patterns (average stop time, total time of all stops)
 - Returns: number of trajectory intersections respectively number of returns to a specific location, temporal patterns
 - Maximum altitude, birth, death, merging, splitting, significant movement change (direction, speed), temporal patterns
 - o Movement complexity (see Section 4.4.1)
- Course description (linear, curved, unregularly, constrained/unconstrained, smooth/abrupt direction/speed changes, sinus-shaped, etc.)
- Interactions of different trajectories:

- Looking at trajectory line:
 - Splitting, merging, touching, intersecting
- Looking at trajectory lane:
 - Splitting, merging, touching, overlapping
- Interaction with context-elements:
 - Topological relations ('in', 'cross', 'touch', etc.)
 - Metric: spatial and temporal distance, spatial direction

From different clusters or trajectories the following information can be derived:

- Similarities of attributes (e.g. movement direction, speed, cluster size, trajectory length)
- Correlations of changes (e.g. temporal synchronization, temporal dependence)
- Group formation, change of shape, outliers
- Spatio-temporal point distribution and point quantity
- Behavior of an entire phenomenon with all clusters and all trajectories

Most of the above-mentioned information can be strongly reinforced if temporal information (when) and spatial information (where) are visualized in a user-friendly way and explored at different temporal scales and cycles (daily, yearly, etc.).

Andrienko et al. (2011b) introduced a topology of relevant derived trajectory attributes of moving discrete objects. We can also apply this typology for moving SEOs: Relevant attributes can be distinguished in a) attributes originally available from the initial data the moving SEO is based on, b) attributes derived from the analysis of the moving SEO with context data and c) those attributes computed from the derived clusters and trajectories – which again can be separated in instant, interval and cumulative movement characteristics (attributes). Instant attributes describe a moving cluster at a certain moment of time. Interval attributes specify the cluster movement during a certain time interval. Cumulative attributes comprise all interval measures for the entire trajectory. Furthermore attributes of movement events include spatial and temporal position as well as duration, spatial extent, average speed and direction of the movement, and statistical aggregates (average, minimum, maximum, median, etc.) of user-selected dynamic attributes. Dynamic attributes refer to time-varying are also called (Andrienko et al. 2011b).

Another point to discuss is the relationship between change and movement. Can we really differentiate them? In general, movement happens because our world is dynamic or in other words, because our world is changing. For instance, due to seasonal meteorological and environmental conditions a bird swarm is moving to a warmer region. In movement analysis of dynamic SEOs, swarm-cluster attributes are changing in time due to movement. However, the change of some attributes takes place during the movement rather than being caused by the movement.

3.3.3. Investigating movement of SEOs through task specific visual analytical approaches

Generally visual exploration and analysis can be performed in a 2D or/and 3D digital or analog space. Thereby, static, dynamic or animated map representations can be used. A graphic user interface with interactive functions supports the exploration. Furthermore, synchronized non-cartographical displays (e.g. graphs, diagrams) can enhance the insight into data characteristics. Visual exploration of dynamic SEOs can be based on a selection of SEOs of interest out of the entire dataset. Selection methods include spatial selection (all objects in a defined area), temporal selection (all objects within the temporal interval of interest), spatio-temporal selection (first spatial and then temporal selection or vice versa) and object selection (which actually relates to a

spatio-temporal selection). Thus, the focus within visual analysis of dynamic SEOs can be on the entire phenomenon, but also on selected (individual/a pair of/a group of) clusters or trajectories.

Besides an emphasis on “What”, the focus within visual exploration can be also on “Where” or on “When”. “Where” can be analyzed with different spatial resolutions or map scales. Likewise, “When” can be investigated for the recent or the long term past as well as the near respectively the far future. The present situation is explorative in particular with help of a real-time monitoring/visualization. Table 3-4 provides an overview about specific analytical tasks for the exploration of dynamic SEOs as well as suggested visual analytical approaches which support to solve the defined tasks. All tasks help to understand movement behavior and to identify tendencies and patterns. Suggested visual methods/tools are necessary to accomplish the identified tasks. Our goal is to extract patterns from dynamic SEOs with the help of visual tools. Most of the visual tools are coupled with necessary computing tasks. We assume that clusters and trajectories are already calculated via clustering and aggregation as described in Section 3.1.

Aggregation is a key issue for the visual analysis of moving points and their trajectory. As mentioned in Section 3.1 and Figure 3-1, spatial and temporal aggregation is needed to derive spatio-temporal clusters from point data/events – in case of moving swarms of point events belonging to a moving SEP. The detected clusters have to be aggregated again in order to derive trajectories (spatially extended lanes). Generally, SEOs’ trajectories can be temporally, spatially or spatio-temporally aggregated in order to reduce information overload (and thus to ease information communication) to detect and display common movement patterns and behavior (e.g. SEOs with similar dynamics). The spatial and temporal thresholds describing the similarity of clusters/trajectories depend on the purpose of aggregation as well as the application case of the data. Furthermore, the thresholds can depend on the temporal and spatial scale. Nearly all of the visual tasks listed in Table 3-4 are based on aggregated clusters and trajectories resulted from aggregation.

The derived trajectories can be aggregated as well. The SEOs’ trajectory lines and lanes (polygons) need to be treated differently. However, they share certain aspects. One aspect is the aggregation of trajectory parts: Imagine two SEOs move spatio-temporally close enough to each other only during a part of their lifetime. Consequently, solutions are needed for merging and splitting of aggregated trajectories. Furthermore, SEOs moving in 3D can be aggregated in either 2D or 3D space. The resulted aggregations may differ. Moreover, the polygon form (borderline) of aggregated trajectories may be simplified or schematized if needed (e.g. with arrow symbol of certain length and direction). Instead of aggregating SEOs’ trajectory lines, alternatively, the median (linear tendency line) or average trajectory (curved tendency line) could be determined via a polynomial approximation (e.g. cubic spline) through cluster centroids. The resulted line could be cartographically symbolized in order to represent the aggregation of the initial trajectory lines. This can be done by increasing the line width, changing its color or adding a polygon-buffer (with a certain color) up to the spatial extension of all aggregated lines.

The aggregation of SEOs’ clusters or trajectories can be based on their spatio-temporal geometry (e.g. trajectories involve the same/similar start time and location) and/or on their semantic attributes (e.g. bird species). Table 3-4 includes the most important tasks involved in the movement analysis of SEOs. Every task can be performed for the entire or a selected part of the study area, for the whole or part of the time period in which SEOs occurred. Moreover, each task could be applied only for certain SEOs of interest. The focus is on 2D data, but the investigation of moving SEOs with changing altitude in time is considered as well. The table consists of two main parts: Analyzing momentary movement of clusters and investigating the dynamics of SEOs’ trajectories during a certain time period.

Table 3-4: Analysis of moving SEOs: tasks and visual analytical approaches.

| Tasks of movement analysis | Visual analytical approaches |
|--|--|
| Cluster movement at a specific moment of time | |
| 1) Identify moving objects | <ul style="list-style-type: none"> - Symbol adaption¹ of moving objects - Dynamic effects - Animations |
| 2) Retrieve cluster movement attributes: <ul style="list-style-type: none"> - Speed - Acceleration - Moving direction angle | <p>Speed and acceleration:</p> <ul style="list-style-type: none"> - Classified cluster symbol (e.g. color) based on Speed/acceleration values - Extrude cluster fill or/and cluster border while extrusion height is based on speed/acceleration values - Text <p>Moving direction:</p> <ul style="list-style-type: none"> - Arrow in the moving direction - "Comet-tail" like visualization towards where the cluster moved from - Text (exact angle or cardinal direction) |
| 3) Analyze special cluster events: <ul style="list-style-type: none"> - Birth, splitting, merging, disappearance, returns, stops | Identify and highlight special cluster event and their attributes of interest through symbol adaption ¹ |
| 4) Analyze special cluster hot spots: <ul style="list-style-type: none"> - Location and time of maximum velocity, maximum/minimum altitude etc. | Identify and highlight special cluster situation and their attributes of interest through symbol adaption ¹ |
| 5) Retrieve momentary cluster attribute changes (in comparison to previous time interval): <ul style="list-style-type: none"> - Change of location, velocity, cluster shape (expand, shrink, deform), size, point/event quantity/distribution etc. - Detect significant changes | <ul style="list-style-type: none"> - Symbol adaptation¹ - Display text information (e.g. velocity change value) - Bar chart/pie chart of cluster attribute changes |
| 6) Investigate cluster interaction with other clusters or other objects of interest: <ul style="list-style-type: none"> - Touching, overlapping, covering | Symbol adaptation ¹ (entire cluster respectively cluster part which is covered/overlapped) |
| 7) Compare (two or more) clusters: <ul style="list-style-type: none"> - Detect similarities and dissimilarities of geometrical and semantic cluster attributes | <ul style="list-style-type: none"> - Symbol adaptation¹ of similar clusters - Interactive similarity matrix (of two selected clusters) |
| 8) Predict near future situation of clusters and cluster attributes | - Same visual approaches as for past clusters |
| 9) Analyze internal cluster structure (in case of moving points or event data) <ul style="list-style-type: none"> - Cluster point quantity - Cluster point distribution | <ul style="list-style-type: none"> - Contour interval map based on KDE - Nearby points aggregated to polygons with point quantity based fill color - Point size depending on local density |
| Time period dynamics (SEO trajectory analysis) | |
| 10) Retrieve trajectory movement attributes: <ol style="list-style-type: none"> a) Average movement direction/tendency b) Trajectory movement range: <ul style="list-style-type: none"> - Spatial length - Lifetime c) Number of accelerations/decelerations d) Number of climbs and falls (increasing/decreasing altitude) e) Maximum/average velocity f) Maximum/average altitude g) Maximum/average width h) Fastest/steepest climb/fall | <ol style="list-style-type: none"> a) Arrow (linear or curved), text (exact angle or cardinal direction) b-d) Text, symbol adaptation¹ e-h) - Display text <ul style="list-style-type: none"> - Highlight map location via symbol adaption¹ - Emphasize location in additional displays (STC, graphs/tables²) |

| | |
|---|--|
| 11) Detect and analyze specific movement events along the trajectory: - Stops, Returns - Birth, death, merging, splitting - Cluster attribute of significance/ of interest (e.g. slow speed) - Significant movement change (direction, speed) | - Interactive clustering - Display text - Highlight map location via symbol adaptation ¹ - Emphasize location in additional displays (STC, event graph, attribute graph, further graphs/tables ²) |
| 12) Describe trajectory course: - Linear, curved, unregularly, constrained/unconstrained, smooth/abrupt direction/speed changes, sinus-shaped, etc.) | Displayed trajectory line or lane (if needed) Smooth/simplified line or lane-polygon - linear: arrow or straight direction line - curved: smooth curve via polynomial approximation (e.g. cubic spline) through cluster centroids |
| 13) Analyze interactions and topological relations of different trajectories (merge, split, touch, move parallel) | - Interactive tool to select two trajectories - Symbol adaptation ¹ |
| 14) Compare (two or more) trajectories: - Detect similarities and dissimilarities | - Interactive tool to select, display and highlight specific trajectories and their attributes of interest - Enable further displays in order to compare attributes of the selected trajectories (STC, similarity matrix, etc.) |
| 15) Analyze trajectory attribute data (e.g. coordinates, object time stamp, land use) | - Plotting of text information - Attribute based adaption of graphic variable (e.g. color/size) - Symbolization (proportional point symbol/bar chart/pie chart) |
| 16) Investigate temporal dependence of spatial, temporal or attribute data in respect to both linear and cyclic time models | - Time slider tool, temporal glyph, STC, graphs/tables ² |
| 17) Analyze uncertainty of movement path (past and predicted) | - Uncertainty buffer and respective legend, text |
| 18) Analyze movement anomalies: - SEO at surprising locations (outliers) - SEO at unusual time in usual locations - SEO moves with unusual speed | - Highlight "unusual" part of SEO via symbol adaption ¹ |
| 19) Investigate significant trajectory changes along its course | - Define how significant changes are defined - Detect significant changes - Highlight locations and emphasize attribute change via symbol adaption ¹ or text - Enable further displays (graphs/tables ²) |
| 20) Predict future situation of current moving a) Short time predictions b) Medium time predictions c) Long time predictions | - Same visual approaches as for past clusters (a) - Same visual approaches as for past trajectory (b,c) |
| 21) Analyze cluster changes along its trajectory | - Display cluster attribute variations via symbol adaption ¹ - Analyze spatio temporal cluster attributes via further non-cartographic displays (e.g. STC, attribute graphs) - Temporal density maps (see Section 4.3) |
| 22) Investigate movement complexity | - TCG diagram (see Section 4.4.1) |

¹ Highlighting via adaptation of visual variables defining the cluster symbol:
 Polygon fill: color*, transparency, pattern crispness, texture, animated effect
 Polygon border line: size, color*, transparency, texture, animated effect
 * hue, luminance, saturation

² Other non-cartographic displays, such as graphs/tables: see Table 3-5 (3)

Symbol adaptation includes static and dynamic visual variables (see 2.3) of displayed points/events, clusters (polygons), trajectory lines and lanes (polygons). A combination of suggested visual solutions is also possible (e.g. momentary speed information via text or adapted object symbol). It only makes sense if the readability and information communication would profit rather than suffer from such combination. Combination of momentary cluster movement visualization together with past/entire trajectory representation can provide cluster movement information for a specific moment of time and at the same time global trajectory information for the entire past (and future) movement course of the cluster. To evaluate if the task-specific information can be visually understood by the user, a comprehensive user test is necessary to find out which method is best for each task regarding its usefulness and effectiveness.

The visual exploration of dynamic data (including dynamic SEOs) in particular the exploration of trajectories can be enhanced by the use of common interaction techniques (Andrienko & Andrienko 2013):

1. Manipulations of the view (pan, zoom, rotate, change visibility and rendering order of different layers, changing opacity levels, etc.)
2. Manipulations of the data representation (selection of objects/attributes to be shown, adaptation of visual variables defining the object symbol, e.g. color, line thickness)
3. Manipulations of the content (e.g. selection/filtering of the objects to be shown)
4. Interactions with display elements (highlighting, provide detailed information by mouse clicking/pointing, selection of objects to explore in other views, etc.)

Moreover, it is important to investigate visual analysis of “SEOs in context”, in other words with underlying geographical data, such as infrastructural data, further environmental data, depending on the purpose of analysis. Context information may allow to visualize base data for a better orientation; highlight context-related correlations of SEOs; detect context-related behavior of dynamic SEO; emphasize effects of the SEO’s events to other geodata (e.g. in case of dynamic lightning clusters: mapping burnt land area after a wildfire caused by lightning; or in case of a moving bird swarm: temperature- or wind related movements).

Existing visual analytical tools – an overview

Table 3-5 gives an overview about the most representative visual analytical tools for SEOs. Some of the tools are relevant for both spatio-temporal data and ‘non-dynamic’ spatial datasets. Most of them have been applied to dynamic datasets which are mainly moving discrete points (see Section 2.4.2).

In Table 3-5 the visual analysis is divided into three categories: (1) traditional plan view mapping, (2) 3D-displays with geographic altitude or time information projected onto the z-axis and (3) non-cartographical displays, such as graphs and tables. The rendering of the maps/graphics can be described through different characteristics: They can take various forms: as single elements, as a unified combination of two or more elements (e.g. a plan view proportional symbol map with rectangle calendar graph used as temporal glyphs) or as multiple small displays. Moreover, the displays can be used interactively or non-interactively. Interactive multiple displays are often synchronized, thus changes appear in one display and are simultaneously reflected in other displays. Maps and graphics can be illustrated as static displays with or without dynamic effects. Geographic and non-geographic information of dynamic SEOs can be illustrated and analyzed at certain temporal and spatial scales (resolutions/granularity) and dimensions. Examples for a temporal scale are time intervals: year-month-week-day-hour-minute-second, seasons or week-days. Spatial scales are for instance 1:100, 1:1000 and 1:10.000. Some visual analytical approaches relevant for the exploration of dynamic SEOs are demonstrated in Figure 3-2.

Table 3-5: An overview of the visual analytical tools for dynamic SEO

| | |
|--|--|
| <p>Visual analysis tools</p> <p><u>Visualization properties:</u></p> <ul style="list-style-type: none"> - Single/ combined/ multiple (synchronized) - Interactive/ non-interactive - Static/animated # Temporal scale # Spatial scale # Temporal dimension # Spatial dimension # Spatio-temporal dimension # Semantic domain | <p>1) “traditional” map view (2D):</p> <ul style="list-style-type: none"> - Flow map (flow-linkage diagram) - Change maps: use of traditional thematic map techniques (choropleth/isopleth/dot map/proportional symbol map) - Quadratic polynomial trend surface (isochronic lines) - Temporal glyphs (e.g. clock face, rectangle graph, framed time-line) |
| | <p>2) 3D displays (XYZ or STC)</p> <ul style="list-style-type: none"> - Statistic surface, block diagram, perspective projection - Trajectory wall display for STC (Stacking-based visualization of trajectory attribute data) |
| | <p>3) Other (non-cartographical) displays such as graphs and tables</p> <p>Appropriate for visualizing dynamic geographic data</p> |
| | <ul style="list-style-type: none"> - Time series graphs, time-nets - Variable binned scatter plots - Treemaps, flowstrates - Visualizing of object group changes - Chord diagram - Sunburst partition, Reingold-Tilford tree - Hierarchical edge bundling - Sankey diagram - Parallel sets and Icicle plot - PCP - Self organized maps - Table lens - Data arrays - ThemeRivers |
| | <p><u>Combinations of map and graphics:</u></p> <ul style="list-style-type: none"> - Small multiple maps - Multiple origin-destination map - Trajectory contingency table - Arrays of graphics <p><u>Further common graphics:</u></p> <ul style="list-style-type: none"> - Bar chart, time bar chart - Stacked value bar graph - Stacked dot plot, dot plot - Variable binned scatter plots - Scatter plot, scatter-plot-matrix - Histogram, frequency table - Box plot, hat plot |

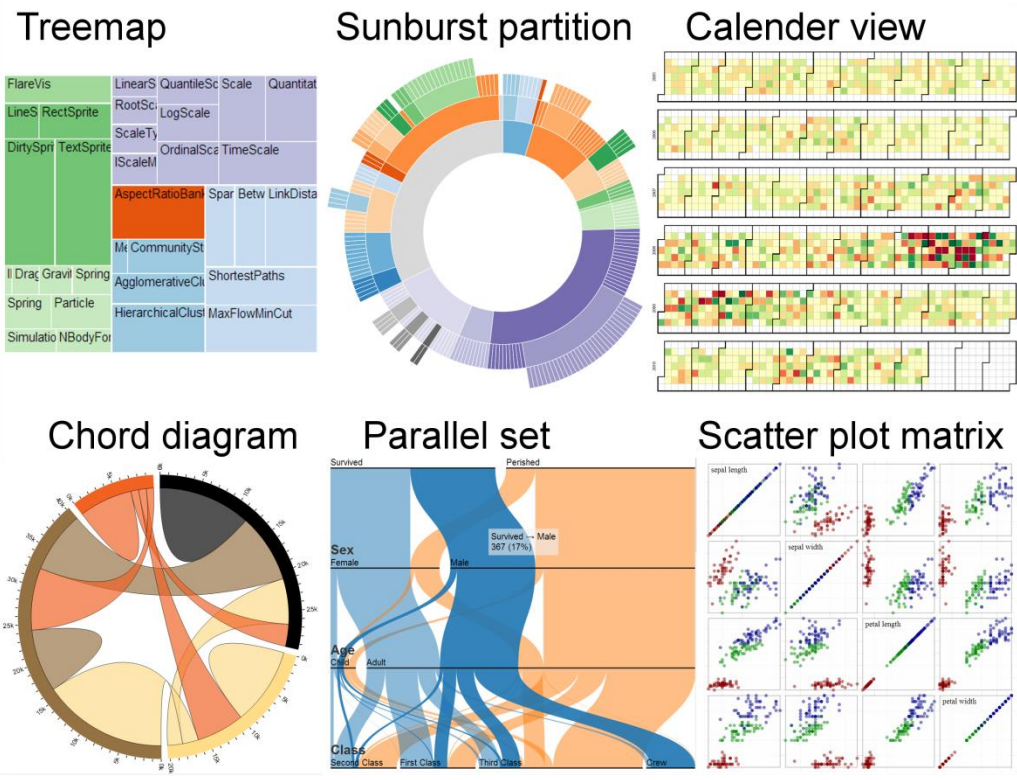


Figure 3-2: Some available visual analytical approaches relevant for the exploration of dynamic SEOs, source: <https://github.com/mbostock/d3/wiki/Gallery>

Spatial dimensions are 2D and 3D whereby temporal dimensions are past, present and future. Instead of treating semantic and temporal information as attributes of spatial objects, we could treat them as individual domains as the spatial domain.

3.4. Chapter conclusion

This chapter provided a generic concept for visual exploration of SEOs and an overview of the existing visual analytical tools and tasks. The usage of the individual tools is strongly dependent on the data of SEOs and expected applications. For instance, with regard to the swarm analysis, it would be relevant to distinguish between absolute movements - which are moving swarm objects - and relevant movements – which are non-moving swarm objects located on other moving objects. First we refined SEOs which change in time and space. We divided them into polygons based on captured point groups (e.g. bird swarm), clustered point events (lightning clusters) and natural polygons (e.g. landslides). Then, we analyzed the spatio-temporal relationships of SEOs. The visual exploration of moving SEOs was addressed, involving a conceptual demonstration of representation methods for dynamic SEPs as well as their features. Furthermore, an overview about applicable static as well as dynamic visual variables for the previously defined cluster- and trajectory representations of moving SEOs was provided. Based on the movement aspects of SEOs, different movement behaviors of dynamic SEOs were outlined. Finally we pointed out specific movement tasks and their possible visual analytical solutions. The existing visual analytical approaches were elicited. They include “traditional” 2D map views, 3D displays and other graphic or tabular displays.

4. A case study of lightning data

“Globally seen, most weather-related damages are caused by thunderstorms. Besides floods, strong wind and hail, one of the major thunderstorm ground effects is lightning. Therefore, lightning investigations, including detection, cluster identification, tracking and nowcasting are essential. To enable reliable decisions, the current and predicted lightning clusters and trajectories as well as analysis results have to be represented in the most appropriate way” (Peters & Meng 2013). Moreover, adequate interactive visual exploration methods are needed to enable analysts a comprehensive insight into the lightning data dynamics.

This chapter aims to introduce specific representations and visual analytical approaches for investigating the dynamic phenomena of lightning clusters. We will discuss and answer the following questions:

- Which pre-processing steps are required to derive spatio-temporal lightning clusters as well as lightning trajectory lanes from detected lightning points?
- What are similar scenarios to moving lightning clusters?
- How can we adequately visualize and visually analyze past, present and predicted lightning clusters and their trajectories - conceptually and applied to the case of a provided test dataset?
- How can we visually present the uncertainty of nowcasted lightning data?
- Can we incorporate temporal information in KDE-based density maps in order to create a static density map for dynamic points?
- How can the dynamics of lightning data be explored by using non-cartographic visual analytical approaches? The following inquiries are involved:
 - How can the similarity of two lightning trajectory lanes be visually compared?
 - Which components of a lightning trajectory describe its moving complexity and how can we visually explore that complexity?
 - How far can we apply commonly used approaches to address spatio-temporal change of lightning clusters and their attributes?
- What is important for a comprehensive interactive visual exploration of dynamic lightning data and of how could such exploration prototype be designed?
- Who are relevant user groups and which usability issues have to be considered for the suggested visual approaches?

4.1. Lightning data - a dynamic phenomenon

The following subsections (including 4.1.1 and 4.1.2) are based – with slight refinements – on (Peters & Meng 2013), wherein an overview about the state of the art of lightning data identification, tracking and prediction was published.

Lightning is a very complex event. A flash is a lightning discharge in its totality; the average duration of a flash is 0.5 s. A stroke is a partial discharge consisting of a downward-moving leader streamer of low luminous intensity followed by an upward-moving return streamer of high luminous intensity. One flash may consist of one single stroke or a series of strokes in the same or adjacent channels (Kitagawa et al. 1962). In this work we only use the term lightning. The test data used are detected lightning points, whereby every lightning point corresponds to an individual discharge (single stroke). Within this study, ‘event’ refers to the occurrence and prediction of

thunderstorms represented by tracked and nowcasted lightning clusters. A concept for visual analytics of dynamic lightning clusters in 3D will be investigated. We briefly describe how to detect lightning data and how to track and nowcast lightning clusters. The term lightning cluster is used to define lightning detections clustered in time and space to represent a part of a thunderstorm with lightning activities. The term 'nowcasting' refers to lightning cluster predictions for time periods of less than a few hours. We focus on the visualization of experimental dynamic lightning position data and we do not intend to provide any analysis of the meteorological implications of thunderstorms. Furthermore, we do not consider the degree of applicability of the presented visualization to different types of storms. Our aim is to provide a computational framework for 3D lightning stroke visualization of given historical data in the form of a graphic user interface (GUI) tool, including its geometrical extrapolation in space and time to the extent allowed by the data. Rather than developing a perfect tracking and nowcasting solution, we instead aim to enable users to accomplish visual analysis of tracked and nowcasted lightning cluster and their attributes in an integrated system (Peters & Meng 2013).

4.1.1. Detection and position accuracy of lightning data

The 3D lightning test data are provided by the lightning detection network (LINET) in Europe (Betz et al. 2009). LINET was established at the University of Munich (Department of Physics) and put into permanent operation by nowcast GmbH in 2006. The network currently contains 130 sensors distributed over 30 European countries. The acquisition of the emission altitude in-cloud (IC) lightning is unique. As stated in Betz et al. (2008) the 2D-location accuracy amounts to about 150 m. The accuracy of in-cloud lightning point altitudes is about 10%; for example, an IC lightning at 10 km height has its accuracy of ± 1 km (Peters & Meng 2013).

4.1.2. Identification, tracking and prediction of lightning clusters

A main part of thunderstorm investigation is to detect, track and nowcast lightning cells. Thunderstorm nowcasting algorithms consist of three procedures: cell identification, cell tracking and cell prediction. The nowcasting comprises the detailed description of the current weather along with forecasts obtained by extrapolation for a period of up to six hours in advance (WMO 2013). Theories of crowd or herd movement analysis are only of limited utility for lightning cells. Based on Galton (2005), lightning points are neither dynamic collectives, nor discrete dual-aspect phenomena as crowd events. However, lightning points can be described as events within the same moving thunderstorm cell.

The existing methods are conducted on satellite data, radar data, lightning data, microwave-based temperatures or a combination of them. Meyer (2010) comprehensively reported about existing thunderstorm nowcasting methods. In (Johnson et al. 1998; Li et al. 1995; Rinehart & Garvey 1978; Zinner et al. 2008) methods applied to satellite image data were described. In (Dixon & Wiener 1993; Handwerker 2002; Hering et al. 2004) solutions for on radar data are introduced. Steinacker et al. (2000) and Bonelli & Marcacci (2008) provided a solution for both radar data and lightning data. In (Betz et al. 2008), a cell identification and tracking approach for the lightning data derived from the LINET network was introduced. Cell tracking techniques can be divided into overlapping techniques as reported in Zinner et al. (2008) and Hering et al. (2004), pattern-oriented correlation techniques as in Bolliger et al. (2002), and cost functions techniques as in Bonelli & Marcacci (2008) and Dixon & Wiener (1993). Some of the tracking approaches consider the cell splitting and merging behavior. To track lightning data, cells first have to be identified by means of spatial-temporal clustering of the detected lightning point data. Usually, time intervals of 10–15 minutes are applied to divide lightning point datasets into temporal frames. Spatial point clustering methods can take three major types: point quantity-based, hierarchical and partitioning methods. An overview of existing point clustering methods is

provided by (Jain & Dubes 1988). The spatial clustering of lightning data usually relies on a simple partitioning method based on distances between lightning clusters. Thereby, the basic idea is to expand the given cluster as long as the distance towards a neighborhood point does not exceed some threshold. Such a method can lead to arbitrarily shaped clusters and can also be used to filter out noise or outliers (Han & Kamber 2006). If lightning clusters are identified within each time interval, connected clusters can be allocated to enable cell tracking. Thus appearance, changes in size/shape/location/density, merging, splitting and disappearing of each cell can be investigated (Peters et al. 2014).

Most nowcasting or extrapolation methods are applied on radar or satellite data. Some of them can be applied on the cells derived from lightning point data. Basically, two principal extrapolation techniques can be distinguished: area and cell trackers. Area trackers such as Tracking Radar Echoes by Correlation (TREC) (Rinehart & Garvey 1978) and continuity of TREC vectors (CO-TREC) (Li et al. 1995) use cross-correlations between temporally separated consecutive pattern maps to find motion fields. It is common for cell trackers to extrapolate the cell centroid into the future based on the centroids of the past cells. The simplest method for cell trackers to generate a forecast is to predict future cells from past cell positions. Here it is common to extrapolate cell centroid positions. A ‘persistent nowcast’ does not assume any route tendency, whereas a ‘trend nowcast’ uses trend models in order to capture cell trends from the latest cell history; for example TITAN (thunderstorm identification, tracking, analysis and nowcasting) (Dixon & Wiener 1993). GANDOLF (Generating Advanced Nowcasts for Deployment in Operational Land-based Flood forecasts) (Soul et al. 2002) and SWIRLII (Short-range Warning of Intense Rainstorms in Localized Systems) (Yeung et al. 2007) employ a conceptual model to consider nowcast trends of lightning cell objects. Thereby, physical knowledge about cell evolution is taken into account. With regard to cell tracking with lightning data, simple extrapolation based on three or four consecutive time intervals of five or ten minute intervals often produces useful results, especially when cells are not too short-lived (Betz et al. 2008).

In this work, we do not use the term “lightning cell”, because identified spatio-temporal clusters differ from the “lightning cells” which refer to thunderstorm clouds in meteorology. Several cells in a storm track can appear and disappear during intensive interactions within a limited space. Thus, the cluster itself cannot always be seen as a group of lightning produced from the same cell due to the temporal sampling in the determination of a cluster (Peters & Meng 2013).

4.1.3. Test data/scenario description

According to Galton’s theory (see 2.1.2) the lightning data forms the spatio-temporal phenomena and can be viewed with a dual-aspect. The phenomenon behind the occurring lightning is the moving thunderstorm. Thereby, the moving lightning clusters can be understood as objects or continuants, while the lightning (lightning points) themselves can be viewed as events or occurrences. The dynamic collective in our case is the lightning track; it consists of a lightning cluster, which comes into existence, moves, merges with other lightning clusters or splits into several ones and finally disappears.

As test data we used lightning points recorded by LINET, a lightning detection network (Betz et al. 2009). The test dataset is typical for storms that occur in central Europe. It contains altogether 70007 detected lightning in the region of Central Europe as shown in Figure 4-1 (41,2°N–51,5°N Latitude and 1,9°E–18,8°E Longitude) and covers the period from 1st until 30th of April 2013. Each point is encoded with its geographic coordinates (longitude, latitude) as well as the exact lightning occurrence time.

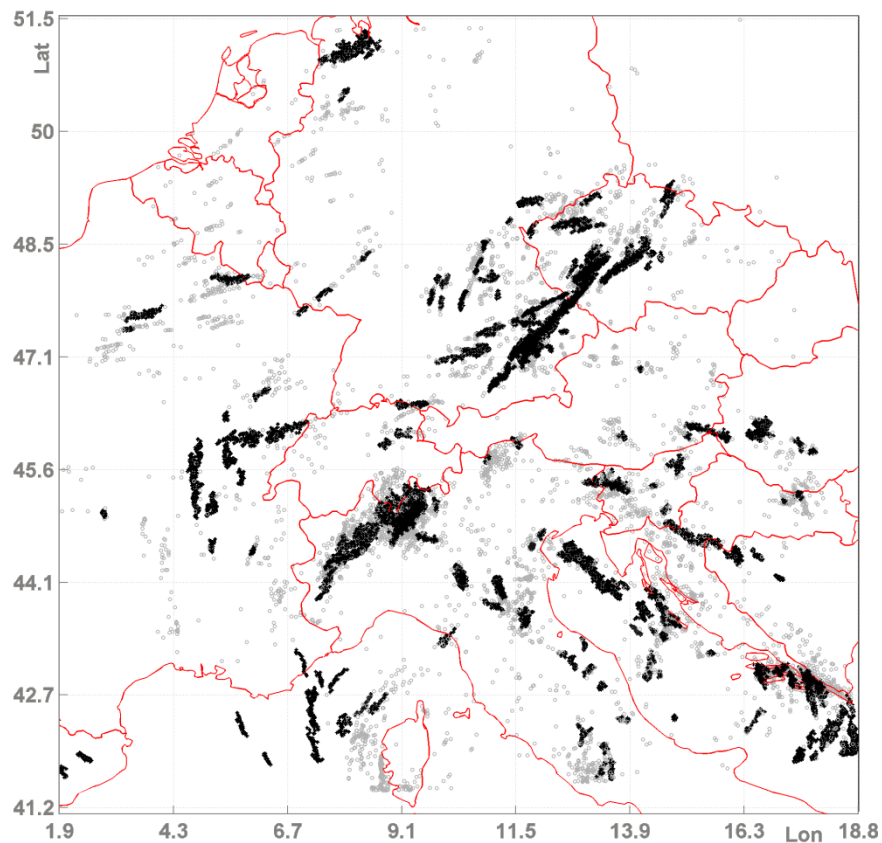


Figure 4-1: Lightning test dataset during April 2013
(black: IC lightning, grey: CG lightning, red: country borders).

Furthermore, each lightning point comprises the information about whether the point is an intra-cloud lightning (IC) or a ground-cloud lightning (GC). In Figure 4-1 altogether 21005 IC lightning points (black dots) and 49002 GC lightning points (grey dots) are displayed. Table 4-1 provides two examples of recorded point data.

Table 4-1: Example of given stroke data.

| Date | Time (hh:mm:ss) | Latitude (°) | Longitude (°) | Altitude (km) |
|----------|-----------------|--------------|---------------|---------------|
| 20130102 | 10:02:56.747247 | 41.6565 | 10.9017 | 0 |
| 20130102 | 18:11:57.669808 | 43.8164 | 14.2545 | 6.6 |

For most of the presented approaches in this thesis a subset of the provided data was used. The subset, as shown in Figure 4-2, contains altogether 8184 detected lightning points (5565 CG and 2919 IC) in the region between Munich, Germany and Prag, Czech Republic (47°N–49°N Latitude and 10°E–12,5°E Longitude) on April 26th 2013 between 2pm and 7pm.

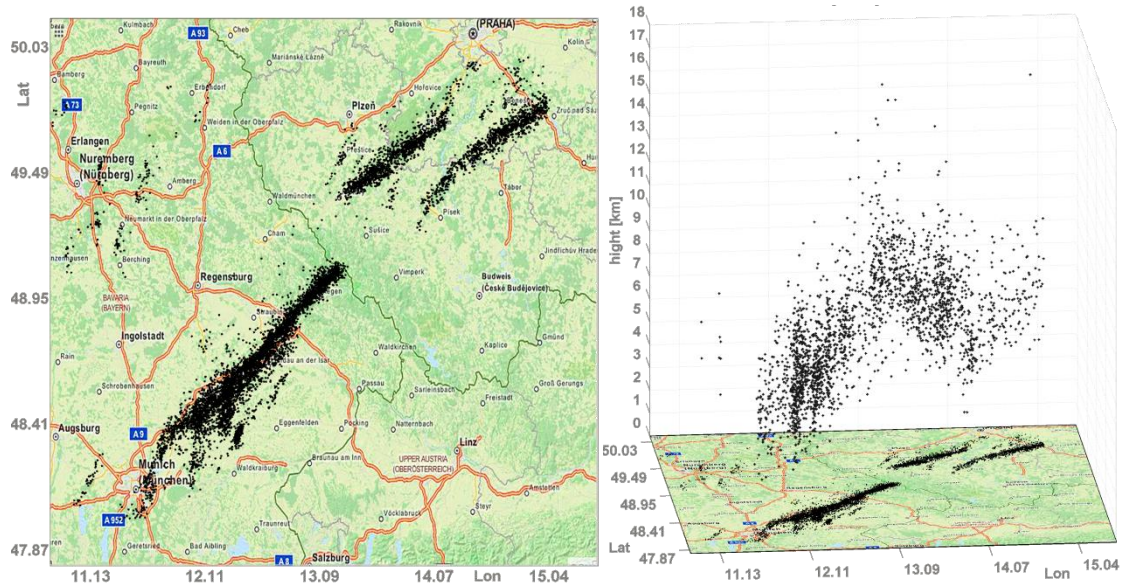


Figure 4-2: The subset of lightning points (April 26th 2013) on a base map.

The use of a static plot of lightning data as illustrated in Figure 4-1 and Figure 4-2 is limited for the investigation of the dynamics in lightning data. In order to solve this problem and to visually explore the past and predicted lightning cluster- and track attributes, we developed interactive visual explorative tools.

4.1.4. Test data pre-processing

In general, data pre-processing consists of cluster identification, tracking and nowcasting. Then, processed lightning clusters can be statistically and visually analyzed using a lightning GUI. Figure 4-3 illustrates the entire workflow including (1) Data acquisition and pre-processing; (2) Spatial and temporal clustering; (3) Cluster tracking; (4) Prediction of lightning clusters and cluster attributes; and (5) Visual analysis and visual analytics. Referring to the general pre-processing workflow presented in Section 3.2, the implemented pre-processing steps for lightning data (1-3) relate to the 'point events option' in Figure 3-1. Thus consistency and continuity of this research is ensured.

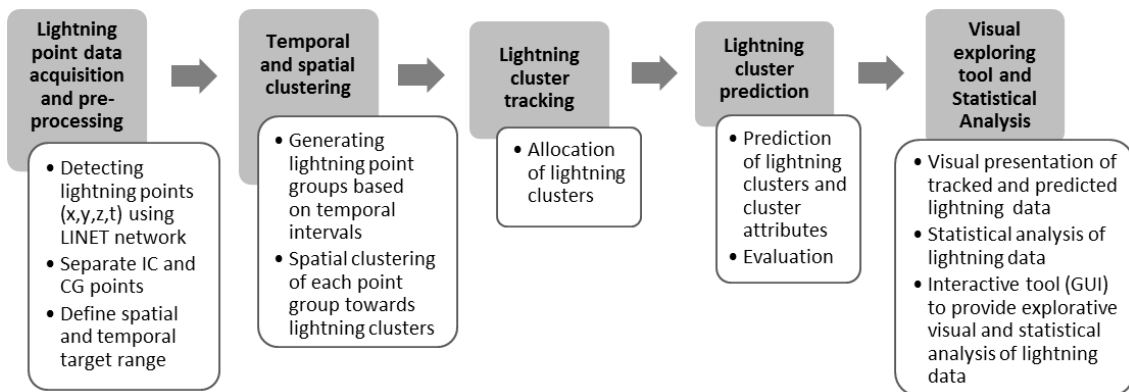


Figure 4-3: The workflow from data detection to visual analysis.

Firstly, detected lightning point data, were divided into in-cloud-lightning data (IC) and cloud-to-ground lightning (CG). Thunderstorms and thus lightning usually occur in the lower stratosphere in an area between 6500 and 60000 feet above the Earth's surface. Consequently, we used only IC data with an altitude between 2 and 18 km in order to eliminate outliers. If demanded, temporal or spatial intervals of interest can be applied to the lightning point dataset. Next, lightning point data were divided into 10 minutes time intervals. This commonly used temporal aggregation

threshold of 10-15 minutes is suitable to identify movement directions of a weather front. Each time interval (constant sample rate) had to contain at least 10 points. Based on a 2D distance-based clustering method (Jain & Dubes 1988) lightning points of each temporal interval were grouped into lightning clusters by using a threshold of 6 km. Thereby, only x- and y-coordinates of all points (IC and GC points) were used. The common distance thresholds from the lightning cell and thunderstorm tracking domain are between 4 and 10 km (Betz et al. 2009; Hering et al. 2004; Zinner et al. 2008). For the spatial clustering, altitude of IC points was set to zero. In our case, a 2D buffer with a radius of 6 km was applied to each lightning point. All points within overlapping buffers were agglomerated towards the same group. The resulting groups represent lightning clusters within the respective time interval. Point groups with less than 10 points were not considered. Increasing this threshold will eliminate further smaller clusters. In the third step, identified spatio-temporal clusters were tracked. Clusters were allocated if their 2D convex hulls spatially overlap within two time sequences. This tracking method was based on (Dixon & Wiener 1993; Zinner & Betz 2009). A larger buffer threshold would result in fewer but longer tracks – a smaller threshold in more but shorter tracks. Furthermore, cluster splitting and merging were taken into account. In the fourth step, clusters as well as cluster attributes were predicted for the near future. Finally, a concept for visual analysis and visual analytics of past and nowcasted clusters and cluster attributes is established. It should be mentioned that we did not aim to establish a perfect tracking and nowcasting solution. Our focus is on enabling users to conduct visual and statistical exploration of tracked and nowcasted lightning cluster in an integrated system. Table 4-2 gives an overview of all adjustable parameters within spatio-temporal clustering, cluster tracking and nowcasting. The parameter values for the test dataset used in this thesis are shown in bold (Peters & Meng 2013).

Table 4-2: Adjustable parameters within lightning cluster and tracking processing workflow.

| | |
|---|--|
| Temporal and spatial clustering | <ul style="list-style-type: none"> • Time interval: 10 minutes • Points per time cluster: ≥10 distance-based spatial clustering, distance threshold: 6 km |
| Lightning cluster tracking | <ul style="list-style-type: none"> • Points per cluster: ≥10 • Determine convex hull of each lightning cluster • Allocate if convex hull border lines of 2 consecutive time intervals overlap |
| Nowcasting of clusters and cluster attributes | Define the future time intervals: +10/20/30/...+60 minutes <u>Nowcasting of cluster centroid:</u> <ul style="list-style-type: none"> - Based on last 2 or 3 track centers - Direction change threshold: $\Delta\alpha \geq 30^\circ$ <u>Nowcasting of geometrical cluster attributes:</u> (density, area, extension) Decide method: <ul style="list-style-type: none"> a) Based on polynomial regression 2nd order b) Based on values of last 2 or 3 track steps |

We applied to our test dataset the proposed pre-processing, temporal and spatial clustering as well as cluster allocation and aggregation towards trajectories. Table 4-3 provides an overview about the total amount of initial test data, the quantity of its components (IC and GC points) and the extracted number of lightning clusters and tracks for the entire month April in 2013 and for the subset of April 26th.

Table 4-3: Lightning test dataset.

| | April 2013 | April 26, 2013 |
|----------------------------------|------------|----------------|
| Total number of lightning points | 70007 | 8184 |
| No. of CG lightning | 49002 | 5565 |
| No. of IC lightning | 21005 | 2619 |
| No. of tracks | 183 | 11 |
| No. of clusters | 948 | 102 |

4.1.5. Comparison to similar scenarios

Andrienko et al. (2011c) stated that one of the challenges for researchers within geovisualization and visual analytics is to deal with different types of spatio-temporal data (e.g. spatial time series, events, movement data, sequences of satellite images) and find appropriate solutions for the respective data. In our context we face the challenge of handling lightning points, lightning clusters and derived trajectories. It is important to compare with some similar scenarios. Turdukulov et al. (2007) focused on precipitating clouds with a set of satellite images (2D) as initial data whereas in our work 3D lightning point coordinates are used as initial data. Furthermore, the authors developed a STC with icons, whose radius is proportional to the size of the precipitating cloud region. Thus they treated clouds as points while in our work lightning clusters are treated as 2D/3D polygons. Moreover, we intend to provide not only a STC, but also a 3D view with help of an interactive tool which may offer different lightning cluster/track presentations to the user (see Section 4.2.5). While the concept of cloud cell tracking in (Turdukulov et al. 2007) is similar to our lightning cluster tracking approach, we want to introduce a variety of visual and statistical representations of lightning clusters and tracks. Furthermore, we aim to provide a lightning cluster prediction approach including visualization of future clusters and their uncertainties.

In the following section, concepts for the visual representation of lightning clusters and trajectories for 2D, 3D, and STC displays are introduced.

4.2. Representation of lightning data

With the recent improvements in lightning data detection and accuracy, there is a growing demand for multidimensional and interactive visualization of such data. Traditional visual investigations on lightning data are mainly focused on source data representation on a 2D cell-grid. Thereby, lightning points were temporally aggregated for each grid cell in order to derive local lightning density information for a certain time interval. A recent example is provided by Neuwirth et al. (2012). Figure 4-4 illustrates GC lightning data aggregated for South-German administrative districts which are colored according the district's lightning density per square kilometer during 2012.

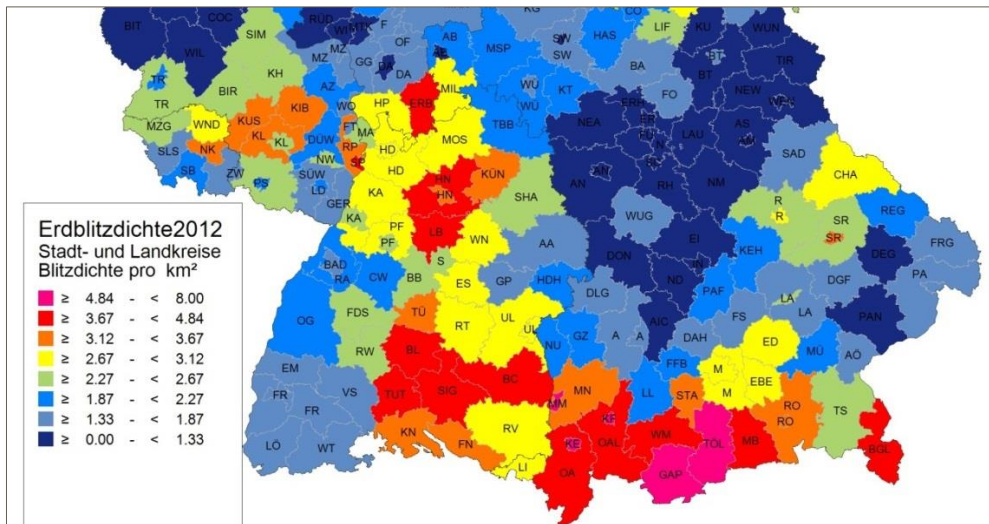


Figure 4-4: GC lightning density map for South-German districts 1999-2011, source: <http://www.gdv.de/2013/06/blitz-und-ueberspannung-sorgen-fuer-viele-schaeden/>, © Blitz-Informationen-Dienst von Siemens

Lakshmanan et al. (2004) extended the traditional grid-based point aggregation towards 3D space and integrated a temporal map series into a decision-support system of the lightning warning. Thereby, lightning points were temporally averaged and spatially smoothed in order to represent local lightning densities. Furthermore, Resch et al. (2013) suggested a pseudo photo-realistic visualization of lightning points in 3D. The authors implemented a time slider tool for a temporal selective visualization of CG lightning points extruded to 3D flash-like pseudo photo-realistic illustrations.

A lightning or thunderstorm expert needs to have visual and statistical information about each moving lightning cluster and its geometrical attributes within a temporal and spatial range of interest. Relevant visual cluster and track information is listed in Table 4-4 together with information about their 2D/3D/STC appearance.

Table 4-4: Visual presentation of past and predicted lightning information.

| | | 2D | 3D | STC | |
|--|----------------------------------|-------------|----|-----|---|
| Visual presentation of lightning cluster | Point cloud | ● | ● | ● | |
| | Centroid point | ● | ● | ● | |
| | Extension | Convex hull | ● | ● | ● |
| | | Ellipse | ● | | ● |
| | | Ellipsoid | | ● | |
| | | Rectangle | ● | | ● |
| | | Cuboid | | ● | |
| | Direction indicator (e.g. arrow) | ● | ● | ● | |
| *Uncertainty buffer | ● | ● | ● | | |
| Visual presentation of lightning track | Track line | ● | ● | ● | |
| | Track lane | ● | ● | ● | |
| | *Uncertainty buffer | ● | ● | ● | |

* only of nowcasted cluster/track

As already introduced in chapter 3.3, we basically distinguish between clusters and tracks. Visual cluster presentations include point cloud (all points inside a cluster), cluster centroid, derived extension visualizations (convex hull, rectangle/cuboid, ellipse/ellipsoid) and direction indicator (arrow). The lightning cluster centroid is defined as the geometrical center of k cluster points. Visual track presentations include track line and track lane (polygon).

Table 4-5 lists graphic variables that are applicable and adaptable for different representations of lightning clusters and lightning tracks.

Table 4-5: Graphic variables of cluster and track representations.

| | Cluster representation | | | | | | | | Track representation | | | | |
|---|------------------------|--|---------------------|-------------------|----------------------------|-------------------------|---------------------------|------------------------|----------------------|------------|------------------|---------------------|---------------------|
| | Point cloud | Centroid (including point density information) | Convex hull surface | Convex hull edges | Ellipse/ellipsoid interior | Ellipse/ellipsoid edges | Rectangle/cuboid interior | Rectangle/cuboid edges | *Uncertainty buffer | Track line | Track lane edges | Track lane interior | *Uncertainty buffer |
| Form/Shape (symbol style) | • | • | | | | | | | | | | | |
| Color (hue, luminance, saturation) | • | | • | • | • | • | • | • | • | • | • | • | • |
| Size | • | • | | • | | • | | • | | • | • | | |
| Sharpness/Crispness | | • | | • | | • | | • | | • | • | | |
| Transparency | | | • | | • | | • | | • | | | • | • |
| Texture (including Pattern orientation and arrangement) | | | • | • | • | • | • | • | • | • | • | • | • |

* only for nowcasted clusters/tracks

In addition, statistical data of geometrical cluster- and track attributes derived from the processed cluster tracking and nowcasting play an essential role for the analysis of lightning cluster.

Table 4-6 lists all important attributes and statistical data about lightning clusters and tracks. They could be included in the lightning GUI, thus, currently highlighted/selected clusters or tracks could be illustrated and analyzed with the help of additional visual tools (e.g. by using diagrams).

Table 4-6: Attributes and statistical data of lightning clusters and tracks.

| | | |
|----------------------------------|--|---|
| Lightning cluster | Spatial extension | Spatial range (dX, dY, dZ) |
| | | Area, volume |
| | Cluster location | Point coordinates |
| | | Centroid coordinates or medoid coordinates in case of skewed clusters |
| | Maximum and minimum altitude (coordinates) | |
| | Internal structure | Point quantity/density |
| | | Point spatial distribution* |
| | Movement information | Velocity, acceleration |
| | | Movement direction |
| | | Distance to last cluster centroid |
| Special cluster situation | Birth, splitting, merging, disappearance, returns, stops | |
| | Location/moment of maximum velocity, maximum/minimum altitude, etc. | |
| Uncertainty of nowcasted cluster | | |
| Lightning track | Lifetime | |
| | Length (distance) | |
| | Hot spots/extremes of cluster attributes (maximum, minimum) | |
| | Track size | Sum of clusters |
| | | Sum of points |
| | | Sum of area/volume |
| | Movement information | - Average movement direction (direction tendency represented by a linear regression line using all track centroid points) - Average velocity |
| Course description | - Course description (linear / curved, etc.) - Number of stops, returns, splits, merges, etc. | |

*point spatial distribution will not be further discussed, since each cluster is already a result of a spatial clustering. It can be assumed, that lightning points within a cluster are irregularly distributed.

In summary, we defined 'what' to visualize in order to visually explore lightning data. In the following, we will demonstrate 'how' to visualize the defined representations for lightning clusters and tracks in 2D, 3D and within a STC.

4.2.1. Lightning cluster visualization concept

A lightning cluster consists of k spatially clustered lightning points, occurring during a certain time (in our case within 10 minutes). It forms the smallest spatio-temporal interval of interest. Figure 4-5 illustrates 8 different lightning cluster visualizations using plan view: a) point cloud, b) cluster centroid, c) cluster centroid with quantity-based point size, d) cluster centroid with quantity-based point color, e) convex hull with grey border line and semitransparent color filling, f) rectangle with grey border line – defined by the spatial extension of the convex hull, g) ellipse which fits into the rectangle and h) a combination of convex hull, point cloud and cluster centroid with quantity-based point size (a,c,e). The figure parts f) and g) are simplifications of the convex hull e). For option d) the centroid point symbol needs a certain size constant for all clusters in order to recognize and distinguish different quantity-based color fillings.

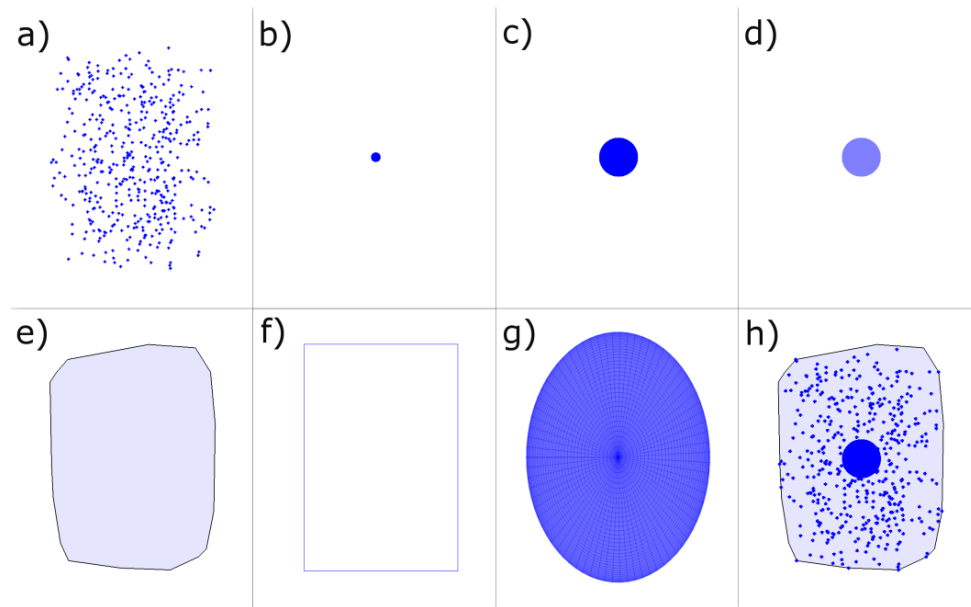


Figure 4-5: Concept for lightning cluster visualization using plan view.

The cluster visualizations (a-h) in Figure 4-5 for the 2D space contain different momentary geometrical information, such as centroid position (b-d), spatial extension (a, e-g) and internal structure (a, c, d). To get all the information at once, different visualizations can be combined, such as in h) where the point cloud presents point distribution and density, the centroid circle provides location and quantity information and the convex hull presents the cluster extension. In addition to f) and g) the cluster convex hull could also be simplified by smoothing the outer convex hull borderline. Beside generalization, the convex hull could also be slightly extended up to, for instance, 1km, since the probability of cluster lightning events in the extended buffer area is quite high. Depending on the data explorer's needs, all above introduced plan view visualization options could be applied to CG lightning data, IC lightning data or both of them at the same time. If a plan view and the altitude information are demanded at the same time, the average altitude of each cluster could be calculated as the mean altitude of all cluster points and related to cluster symbol color or centroid symbol size.

Figure 4-6 illustrates 10 different lightning cluster visualizations in a 3D space: a) point cloud, b) cluster centroid, c) cluster centroid with quantity-based size, d) cluster centroid with quantity-based color, e) cuboid, f) ellipsoid with illumination effect, g) convex hull with semitransparent color filling, h) convex hull in blue and border lines dark blue, i) the same as 'g' including illumination effect, j) a combination of convex hull, point cloud, cuboid and cluster centroid with quantity-based cluster centroid size (a,c,e,i). The 3D convex hulls could be smoothed as well. Thereby, angular edges would be replaced by a smooth geometrical gradient.

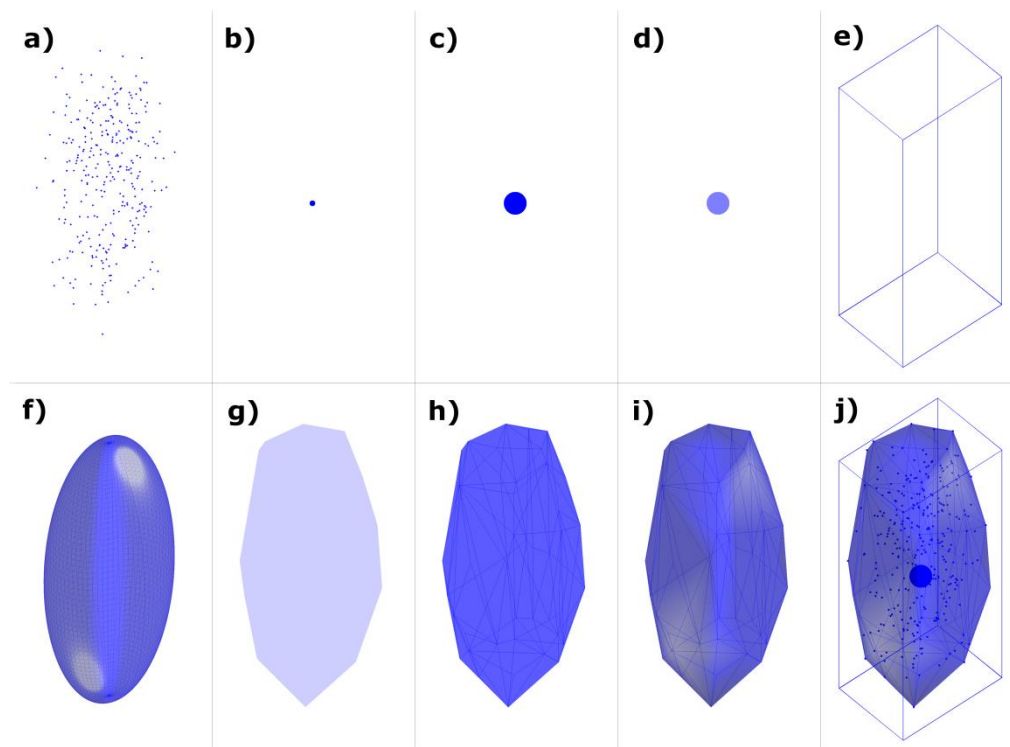




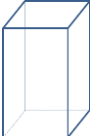
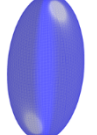


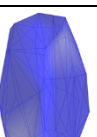
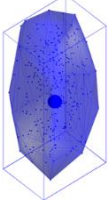


Figure 4-6: Concept for lightning cluster visualization in a 3D space.

These 10 suggested cluster visualizations for the 3D space also contain different momentary geometrical information, such as centroid position (b-d), spatial extension (in a, e-i) and internal structure (a, c, d). In Figure 4-6-j) various kinds of geometrical information is combined. The details about properties, pros and cons of each cluster visualization option are provided in Table 4-7. Although the table is based on 3D options shown in Figure 4-6, it is also valid for their 2D counterparts in Figure 4-5. In Table 4-7 the corresponding 2D sub-figures are noted below each 3D sub-figure reference. Basically, point cloud visualization contains internal structure information but may lead to overplotting and makes the recognition of cluster centroid and point quantity difficult. To represent the cluster only through its centroid can be seen as an oversimplification that misses information about internal structure and cluster extension. However, point quantity can be provided by adapting the centroid symbol size. The cluster extension can be represented via convex hull or its simplified options including rectangle or ellipse. The options (Figure 4-6-e,f,g,h,i) miss centroid, point quantity and information about the internal cluster structure. To provide comprehensive insight into lightning clusters without overplotting or oversimplification we suggest a combination of convex hull with 3D effect (i) and centroid with quantity-based size (c). In case the amount of lightning points is reasonably small, thus no overplotting would occur and points could be additionally plotted to provide internal structure information. Another option is to simplify the point cloud through a representative point selection. An approach focusing on that task will be presented in the following section (4.2.2).

Table 4-7: Properties, pros and cons of 3D cluster visualization options.

| Cluster visualization | | Properties/advantages | Disadvantages |
|---|---|---|--|
| a) Point cloud (2D-a) |  | <ul style="list-style-type: none"> - Detailed internal structure - Cluster extension | <ul style="list-style-type: none"> - Overplotting - Cluster center and point quantity are difficult to read |
| b) Cluster centroid (2D-b) |  | <ul style="list-style-type: none"> - Only cluster centroid position (x,y,z) | <ul style="list-style-type: none"> - Oversimplification - No information about internal structure and point quantity |
| c) Cluster quantity-based centroid size (2D-c) |  | <ul style="list-style-type: none"> - Cluster centroid position - Point quantity | <ul style="list-style-type: none"> - Oversimplification - No information about internal structure |
| d) Cluster quantity-based centroid color (2D-d) |  | <ul style="list-style-type: none"> - Cluster centroid position - Point quantity | <ul style="list-style-type: none"> - Oversimplification - No information about internal structure |
| e) Cuboid (2D-f: rectangle) |  | <ul style="list-style-type: none"> - Cluster extension (simplified) | <ul style="list-style-type: none"> - No information about internal structure, centroid position and point quantity |
| f) Ellipsoid (2D-g: ellipse) |  | <ul style="list-style-type: none"> - Cluster extension (simplified) | <ul style="list-style-type: none"> - No information about internal structure, centroid position and point quantity (illumination may obstruct the patterns) |
| g) Convex hull without 3D effect (2D-e) |  | <ul style="list-style-type: none"> - Basic cluster extension | <ul style="list-style-type: none"> - No information about internal structure, centroid position and point quantity |
| h) Convex hull with convex hull edges |  | <ul style="list-style-type: none"> - Cluster extension | <ul style="list-style-type: none"> - No information about internal structure, centroid position and point quantity |
| i) Convex hull with 3D effect |  | <ul style="list-style-type: none"> - Cluster extension | <ul style="list-style-type: none"> - No information about internal structure, centroid position and point quantity |
| j) Combination of a, c, e and i (2D-h: combination of a, c and e) |  | <ul style="list-style-type: none"> - Detailed internal structure - Realistic cluster extension - Cluster centroid position - Point quantity | <ul style="list-style-type: none"> - Overplotting (in case of large amount of lightning points) |

One crucial advantage of 3D visualization is its capability of providing altitude information. However, user interactions such as rotate, pan and zoom are required to adequately explore altitude and thus 3D cluster information. Illumination effects that strengthen the 3D impression are demonstrated with ellipsoid (f) and convex hull (j).

Figure 4-7 illustrates four examples for combined visualizations of 2D and 3D lightning clusters: a) the point cloud shown in both 2D and 3D space, b) ellipsoid and cuboid in 3D space and convex hull in 2D space, c) convex hull in 2D and 3D space and d) convex hull with illumination effect as well as point cloud and cluster centroid with quantity-based centroid size in 3D and convex hull together with point cloud in 2D space.

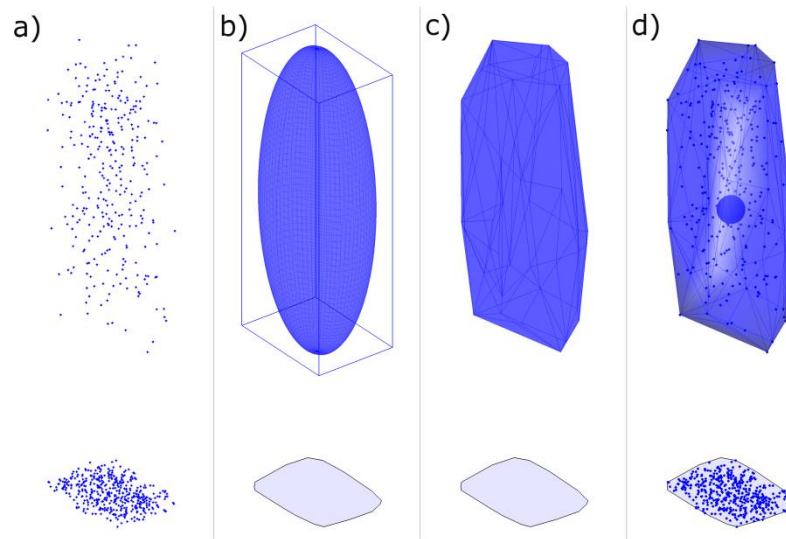


Figure 4-7: Lightning cluster visualization - GC and IC data.

The 3D-impression of cluster convex hull visualization can be enhanced by adding and adapting shadow-effect, transparency and user interactions.

The number of lightning points could be also a value for the potential danger of the particular lightning cell. Thus, visualizing such a risk via quantity-based symbol size or color would be an added value for decision makers and risk analysts. Another possibility would be to adapt the color filling of the convex hull based on the number of cluster points. Furthermore, cluster movement information such as velocity, movement direction and the distance to the last cluster centroid can be included in the proposed visualizations as described in Section 3.3.3. For instance, an arrow indicates the movement direction and the velocity can be communicated via texting the speed value or adapting the cluster symbol (e.g. color filling refers to the speed value). Further momentary cluster movement information such as speed and movement direction were not considered at this point, but presented and discussed in Section 3.3.3. In the following section lightning trajectory visualization options will be presented and discussed. Our focus is not on the momentary cluster situations. On a longer time period, a lightning cluster is evolving and forming a certain trajectory.

4.2.2. Lightning trajectory visualization concept

To visually describe the trajectory of moving lightning cluster, from the moment it comes into existence until its lifetime ends, we suggest two options: As a strongly generalized solution the trajectory can be displayed in form of the 'track-line', either in 2D or in 3D. The track-line is defined by the chronologically connected cluster centroids belonging to the same track. The line segment between the neighboring centroids can be a straight or smooth line, passing either exactly or approximately through the centroids. Basically the track-line contains dynamic infor-

mation about which entire length the track-line covered, where the cluster arose, where it moved to, where it split or merged with other clusters, where it reached its maximum altitude (for 3D visualization) and where it dissolved etc. Furthermore, the length of each track-line segment (between two centroids) provides information about the cluster speed for that respective time interval since centroids are calculated for 10 minute intervals. Moreover, track-line symbol (color, line width) could refer to the respective track ID in order to make it distinguishable among different tracks in terms of time interval or cluster density.

The second suggested solution is called '*track-lane*'. In contrast to the track-lines, whose visualization concept for 2D and 3D space can be viewed as more or less identical, the representation of track-lanes have to be regarded differently for 2D and 3D space. While the track-line contains no information about spatial extension of the track, the track-lane as a 2D or 3D polygon overcomes this drawback. Figure 4-8 and Figure 4-9 illustrate the examples of lightning track visualization in 2D and 3D space. Besides track-line and track-lane, all track clusters can be visualized using methods mentioned in section 4.2.1, e.g. by means of cluster points, cluster rectangle/cuboid, cluster ellipse/ellipsoid cluster centroids (optional with point quantity-based symbol size or/and color) or cluster convex/concave hull.

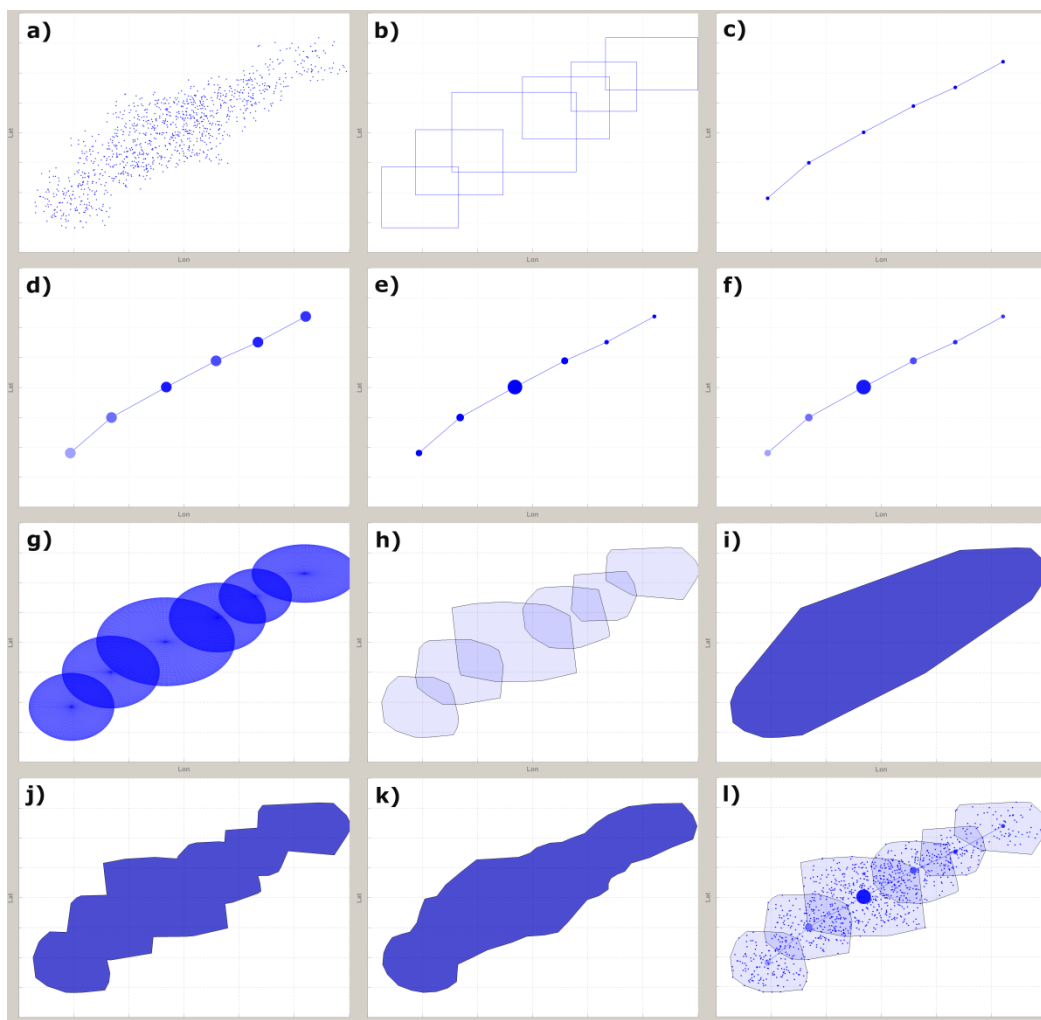


Figure 4-8: Various ways of lightning track visualization in a 2D space.

Let's have a more detailed look at the track-lane visualization. The simplest track-lane approach would be to apply a constant buffer around the track-line. The buffer ratio could be for instance the mean of all semi-minor axes of the cluster ellipses. A local buffer ratio could also be adapted to the local cluster extension. An alternative possibility is to use a convex hull based on all track

points as illustrated in Figure 4-8-i (and in Figure 4-9-i for 3D). A convex hull, however, has the disadvantage that it may contain large areas without points in case of very low density and uneven distribution. This drawback can be overcome by a concave hull (non-convex hull) as shown in Figure 4-8 j, which is nothing else than the agglomeration of all convex hulls from each time step (h). In addition, it makes sense to simplify the concave hull outline in order to avoid sharp polygon edges and improve readability of the track-lane (see Figure 4-8-k). Therefore, a 'simple moving average' (SMA) (Kreiß & Neuhaus 2006) could be used whereby both x- and y-coordinate of each new concave hull point are determined as the unweighted mean of k (e.g. $k=2$) previous and k following neighboring points of the original concave hull polygon.

Figure 4-9 illustrates the counterparts to all trajectory visualization options in Figure 4-8. Only option k) differs for 2D and 3D. Table 4-8 lists each trajectory visualization option, its properties, pro and cons – valid for 2D and 3D. Option k) is separately treated. Not mentioned in Table 4-8 is that 2D options do not contain altitude information.

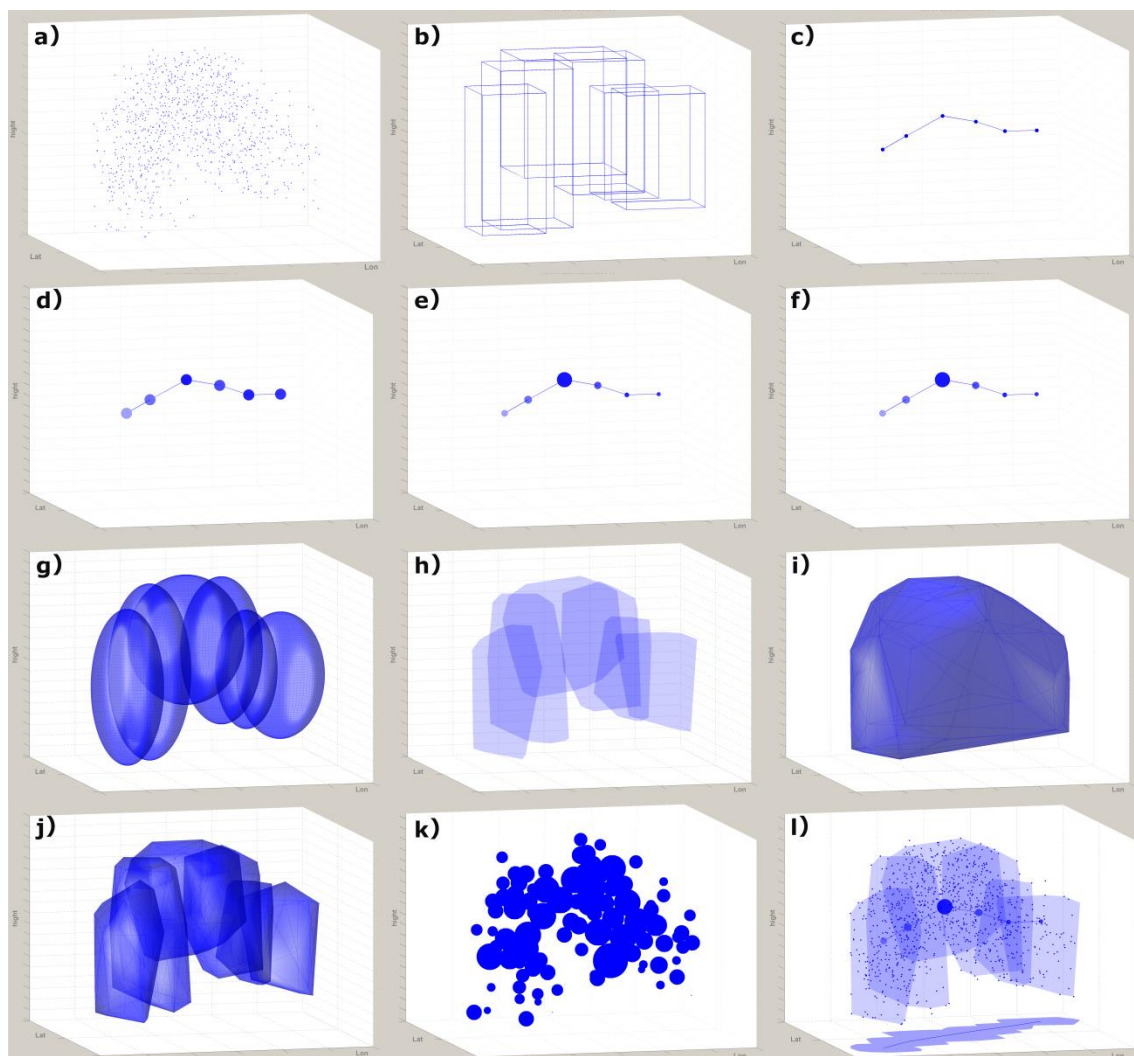


Figure 4-9: Various ways of lightning track visualization in a 3D space.

The smoothed concave hull (Figure 4-8-k), the track-line display containing cluster centroids with quantity-based symbol size (Figure 4-8-e) along with the moving direction could provide essential track-lane information for a bird perspective. With regard to the 3D space we may calculate on the one hand the 3D convex and concave hull (Figure 4-9h,i,j). On the other hand, light and shadow effects can be used to improve the 3D impression (see Figure 4-9-i,j).

Table 4-8: Properties, pros and cons of trajectory visualization options.

| Track visualization | Properties/advantages | Disadvantages (for all: no altitude information) |
|---|--|--|
| a) Point cloud | <ul style="list-style-type: none"> - Detailed internal structure - Track extension | <ul style="list-style-type: none"> - Overplotting - Cluster centroids and point quantity are difficult to read - No information about cluster steps |
| b) Cluster cuboids | <ul style="list-style-type: none"> - Cluster extensions - track extension | <ul style="list-style-type: none"> - No information about internal structure, centroid position and point quantity |
| c) Track-line (connected cluster centroids) | <ul style="list-style-type: none"> - Cluster centroid positions | <ul style="list-style-type: none"> - Oversimplification - No information about track extension and internal structure |
| d) Track-line and centroids with quantity-based centroid color | <ul style="list-style-type: none"> - Cluster centroid position - Point quantity | <ul style="list-style-type: none"> - Oversimplification - No information about cluster extension and internal structure |
| e) Track-line and centroids with quantity-based centroid size | <ul style="list-style-type: none"> - Cluster centroid position - Point quantity | <ul style="list-style-type: none"> - Oversimplification - No information about cluster extension and internal structure |
| f) Track-line and centroids with quantity-based centroid size and color | <ul style="list-style-type: none"> - Cluster centroid position - Point quantity | <ul style="list-style-type: none"> - Oversimplification - No information about cluster extension and internal structure |
| g) Cluster ellipses | <ul style="list-style-type: none"> - Cluster extension (simplified) | <ul style="list-style-type: none"> - No information about internal structure, centroid position and point quantity |
| h) Cluster convex hulls | <ul style="list-style-type: none"> - Realistic cluster extensions - Track extension | <ul style="list-style-type: none"> - No information about internal structure, centroid position and point quantity |
| i) Track convex hull | <ul style="list-style-type: none"> - Basic track extension | <ul style="list-style-type: none"> - No information about internal structure, centroid position and point quantity |
| i) Merged cluster convex hulls | <ul style="list-style-type: none"> - Realistic track extension | <ul style="list-style-type: none"> - No information about internal structure, centroid position and point quantity |
| k) for 2D: Simplified convex hull | <ul style="list-style-type: none"> - Simplified track extension | <ul style="list-style-type: none"> - No information about internal structure, centroid position and point quantity |
| k) for 3D: Simplified point cloud | <ul style="list-style-type: none"> - Simplified track extension - Point quantity - Internal structure | <ul style="list-style-type: none"> - No information about cluster steps (centroid positions, moving direction etc.) |
| l) Combination of a, e and h | <ul style="list-style-type: none"> - Detailed internal structure - Realistic extension of track and clusters - Cluster centroid positions - Track point quantity | <ul style="list-style-type: none"> - Overplotting (in case of large amount of lightning points) |

In order to keep point density and distribution information inside the 3D track-lane visualization we may select only a representative number from all lightning track points – in a way that point density and distribution are kept. The symbol size of selected points should correlate with local point density and symbols should partly overlap in order to get track-lane impression/information. In a previous publication the author introduced point selection methods for the 3D space: one based on quadtrees (Peters 2013) and the other based on polarization transformation (Peters 2011). We propose an iterative workflow for 3D point selection with symbol size adaption based on local point densities:

```

PROGRAM point_selection_with_density_based_symbol_size
REQUIRE  $P \{x,y\}$  // point coordinates
READ  $per$  // percentage of selected points (e.g.  $p = 10 \%$ )
READ  $k$  // number of points to be removed in each iteration
 $sel\_pts = P$  // initially selected points (all track points)
REPEAT
  for  $i = 1 : \text{COUNT}(sel\_pts)$  // for each of the selected points
    [ $d(i), ID\_NN(i)$ ]=density_fct( $i,P$ ) // determine nearest neighbor point and the distance to it
  end
   $d\_sort = \text{SORT}(d, ID\_NN)$  // sort nearest points (ascending) by computed distances
  if  $i == 1$ 
    READ  $thresh$  // threshold for nearest neighbor distance (e.g. 5 km)
    DELETE( $thresh, d\_sort$ ) // remove points with distances below the threshold
  end
   $sel\_pts = \text{DELETE}(d\_sort,k)$  // eliminate  $k$  points having the  $k$  largest distances
UNTIL  $\text{COUNT}(sel\_pts) > \text{COUNT}(P) / p$ 

```

Figure 4-10: Pseudo code for point selection with density based symbol size.

The method is computationally fast and works in 2D and 3D space. The percentage of selected representative points can be adapted as required. The results are shown in Figure 4-9-k in the way, the single remote points will be eliminated, but if there is a remote group with two or more points, the group will be preserved. Thus local and global point density as well as local and global point distribution is considered. These selected and symbolized points can also represent the track-lane for the bird perspective.

Looking at visualized clusters and trajectories in a 3D space from a certain static viewpoint may lead to overlapping and thus hidden information. An advanced solution would be an automatic displacement of foreground or/and background objects in order to minimize/avoid hidden information. Another option is to increase transparency of foreground objects to enable visibility of hidden background objects. As described before, track-line and track-lane visualization contain various movement information. Additionally, the symbol of each cluster step could be adapted in order to address the cluster movement information. For instance the color filling of the cluster convex hull could be based on the cluster speed. In summary, Figure 4-8 and Figure 4-9 provide different combinational visualizations for lightning trajectories. Depending on the users need, the visualization can reflect trajectory location, extension, internal structure, movement information and spatio-temporal cluster changes such as varying speed, movement direction, point density and cluster size.

4.2.3. STC concept

The STC is an appropriate tool for the investigation of the dynamics or a temporal insight into a lightning trajectory. Figure 4-11 illustrates five different lightning trajectory visualizations using STC. For each one, three different viewpoints are applied: a) side view from east, b) side view

from south and c) 3D view/bird view. The first visualization contains all lightning points. Thereby, the exact occurrence time can be extracted. In a2) cluster centroids are displayed, in b2) cluster centroids have quantity-based color fillings and in c2) cluster centroids have quantity-based sizes. In 3) centroids are connected to track-lines, in 4) the convex hull are shown and in 5) a combination of convex hull, track-line and cluster centroids with quantity-based point size is provided. Convex hulls comprise semi-transparent colors in order to allow visibility of centroids and track-lines.

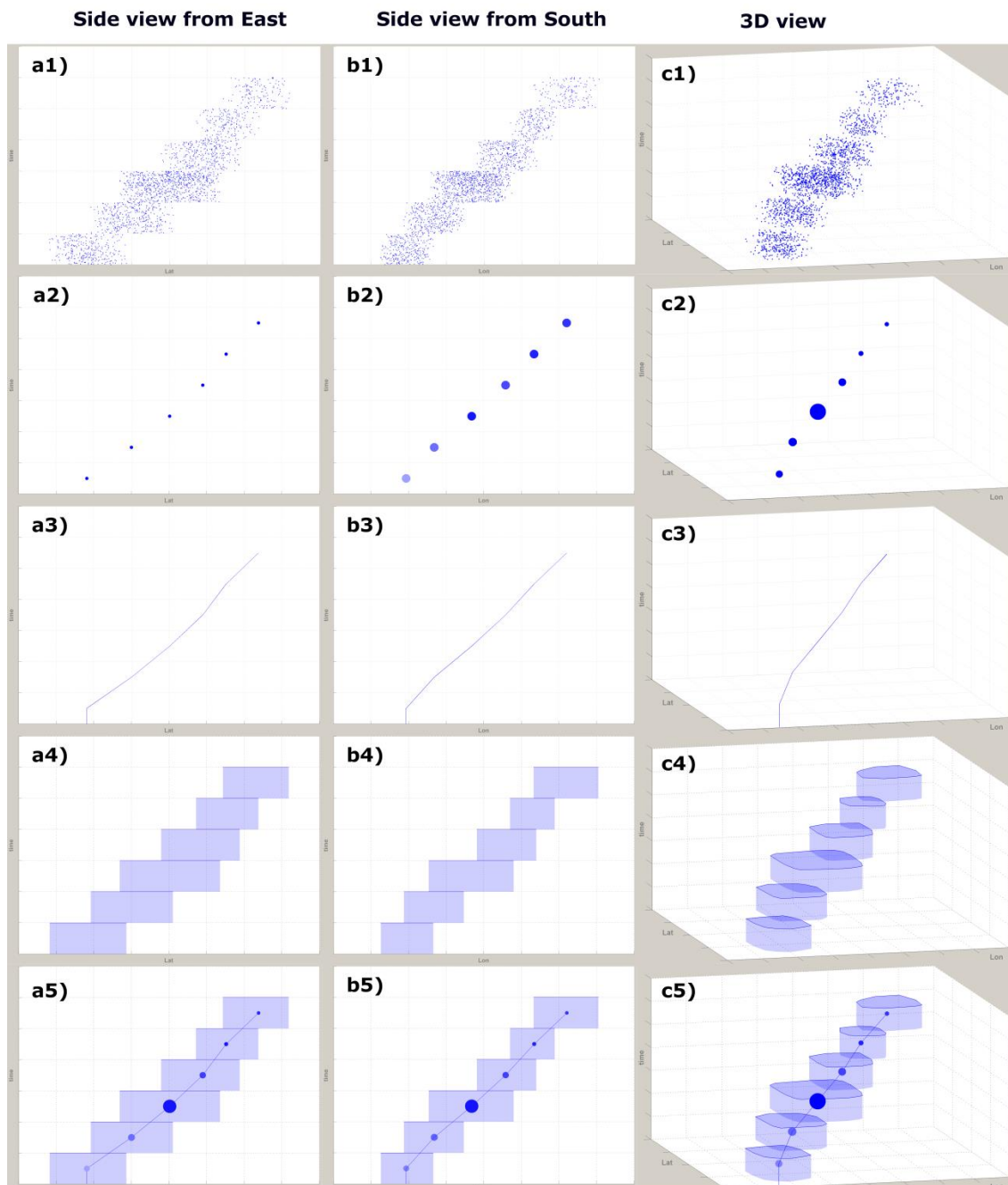


Figure 4-11: Concept for lightning track visualization using STC.

Using STC provides information about lightning dynamics. In particular changes of cluster position, extension and movement direction can be revealed. It would also be conceivable to use an adaptive cluster convex color based on cluster speed or cluster point quantity. Table 4-9 summarizes properties, pro and cons of lightning cluster and trajectory visualizations for STC. Point cloud visualization option contains information about internal structure of clusters/trajectory.

However, in case of large amount of points, overplotting might occur. Visualized centroids and/or connected centroids miss information about point quantity, internal structure and spatial extension and are thus seen as oversimplification. Centroid symbol size can be adapted related to point quantity. Extruded convex hulls contain 2D cluster extension information but miss information about centroids, point quantity and internal cluster structure. For an appropriate visualization with minimum information loss, we suggest as shown in Figure 4-11-c5) a combination of extruded 2D cluster convex hulls, point quantity based centroid symbol sizes and track-line option. As suggested in Section 4.2.2, a point cloud can be simplified via a representative selection and density-based symbol size in order to keep distribution and local point density information.

Table 4-9: Properties, pros and cons of cluster and trajectory visualizations for STC.

| Track visualization | Properties/advantages | Disadvantages (for all: no altitude information) |
|---|---|---|
| 1) Point cloud | - Detailed internal structure - 2D cluster extensions - 2D track extension | - Overplotting - 2D cluster centroids and point quantity are difficult to read - No information about cluster steps |
| 2) Cluster centroids, quantity-based color (b2) or quantity-based size (c2) | - Cluster centroid position - Point quantity (b2,c2) | - Oversimplification - No information about cluster extension and internal structure - no quantity information (a2) |
| 3) Connected centroids | - Spatio-temporal track-line | - Oversimplification - No information about cluster extension, point quantity and internal structure |
| 4) Extruded cluster convex hulls | - 2D cluster extensions - 2D track extension | - No information about point quantity and internal structure |
| 5) Combination of 2, 3 and 4 | - Spatio-temporal track-line - Point quantity - 2D cluster extensions - 2D track extension | - No information about internal structure |

Although the STC misses any altitude and 3D information, it provide a clear overview about the cluster evovement while each time interval and thus each cluster as well as the entire trajectory can be visually explored.

The previous subsections provided a visualization concept for lightning clusters and trajectories displayed in 2D plot, 3D plot and STC. Common user interaction tools were discussed in Section 3.3.3. Interactive variants of representations that allow dynamic highlighting and filtering according to attributes of interests (temporal, spatial, spatio-temporal, or other dynamic thematic attributes) are crucial for explorative analysis of lightning data. For example, one may want to see all lightning clusters characterized by high velocity or low altitude during a certain time interval, etc. Selected objects (clusters/trajectory part) can be displayed without the unselected ones or highlighted while showing also the unselected objects. Highlighting of the respective cluster or trajectory symbol is possible via adaptation of visual variables defining the cluster symbol:

- Cluster/Trajectory polygon fill: color, transparency, pattern crispness, texture, animated effect
- Trajectory line and cluster centroid point: size, color, transparency, texture, animated effect

An interactive tool for adaption of visual symbol variables would allow user-specific highlighting. Visualizing only selected lightning properties, might result in a change of the pros and cons mentioned in Table 4-7 - Table 4-9. For example, displaying only selected points instead of the entire point cloud will reduce or avoid oversimplification, but detailed information about internal structure and cluster extension will not be provided anymore.

4.2.4. Cluster and trajectory concepts applied to the test dataset

We applied the suggested visualization concepts for lightning clusters and trajectories to our test dataset. In the following, the derived visualization results will be presented and discussed. Figure 4-12 illustrates all lightning data of April 26th 2013 detected in our test area. Lightning trajectories can be distinguished via track-lines (connected cluster centroids) in different colors. Beside track lines, cluster centroids are drawn with a spherical radius indicating the varying cluster point quantity. This static 2D plot reveals the information of where certain lightning events took place, but we are not able to temporally distinguish them.

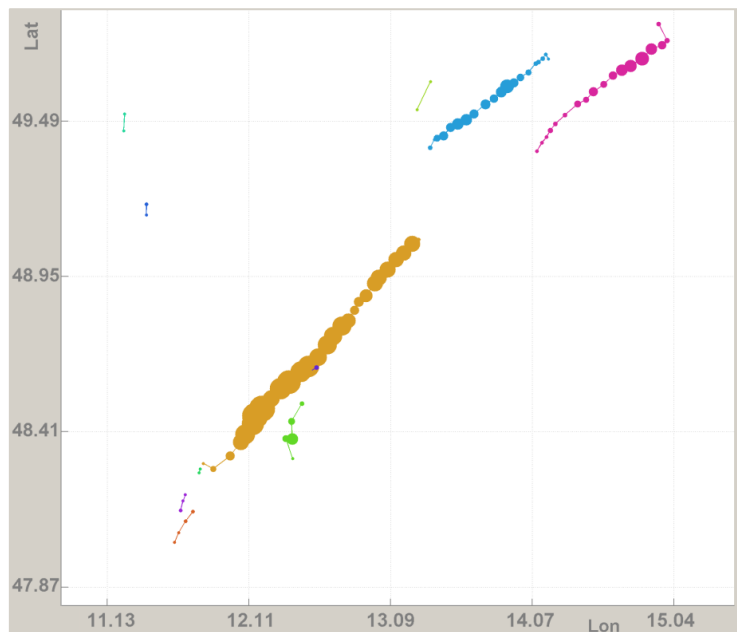


Figure 4-12: A plan view showing the track line of cluster centroids with point quantity-based symbol size and color.

Figure 4-13 focused on track-lane information of the test data. The 2D track-lane visualization (concave hull of all track points) provides a quick overview about where the lightning clusters occurred and moved to. The track-lane visualization approach in 3D add more detailed information about lightning point densities and distribution, while at the same time it also contains the general information about the entire track location and extension. The 2D and 3D approach are complementary when they are displayed side by side.

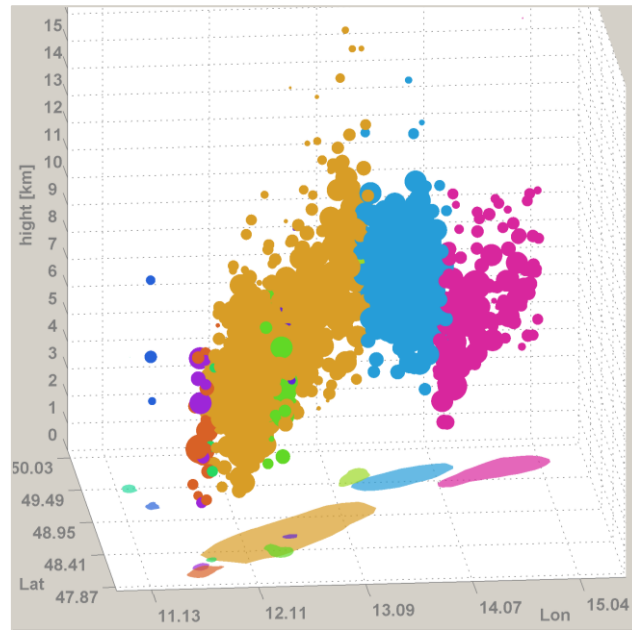


Figure 4-13: Track-lane presented in 2D and 3D (selected points).

Furthermore, Figure 4-14 presents more details about point selection and symbol adaption in 2D and 3D. Two alternatives with the selection of 33% and 10% are demonstrated where the red dots indicate the selected points from the original ones in black. Figure 4-14 b,c,g,h deals with 873 points from 2619 while Figure 4-14 d,e,i,j with 261 selected points. The selected points represent the track-lanes with symbol size and color indicating the relative point quantity and the corresponding track.

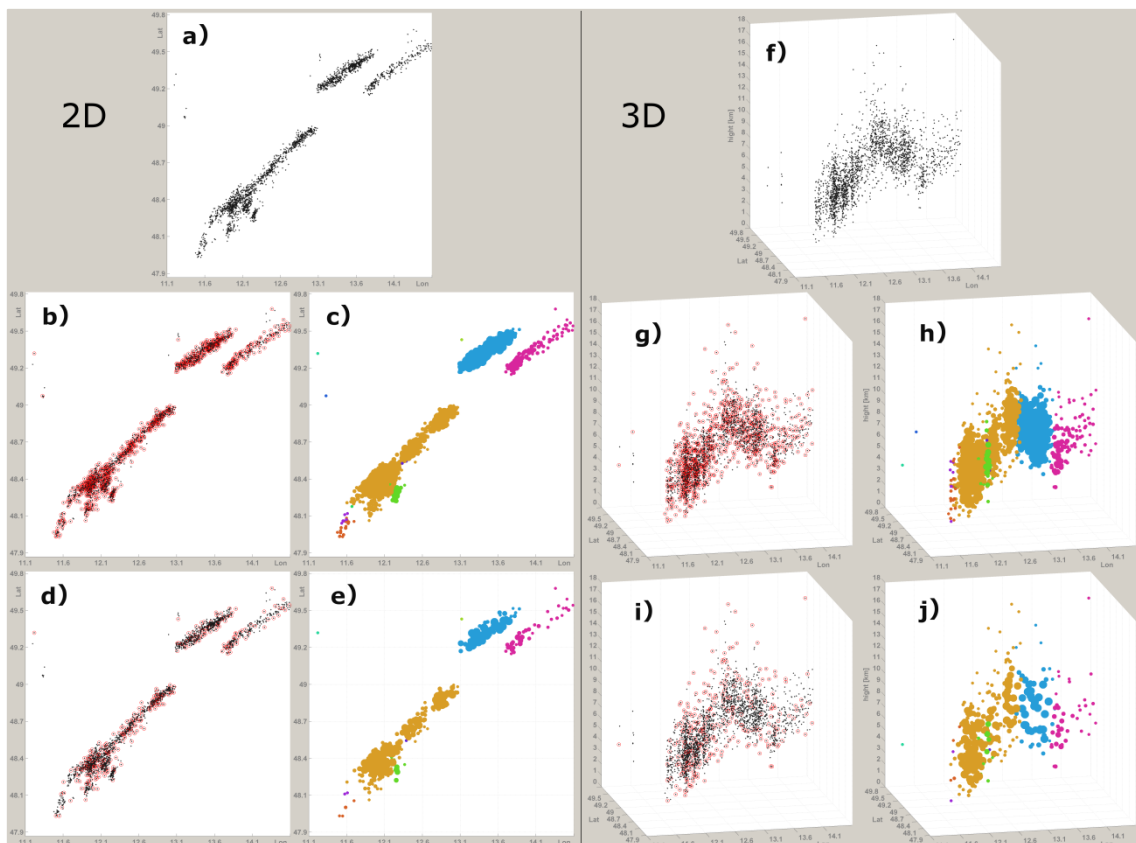


Figure 4-14: Track lane derived from selected points with point quantity-based symbol size.

The 3D view in Figure 4-15 involves 2D and 3D track-line together with cluster convex hull and points at one time interval.

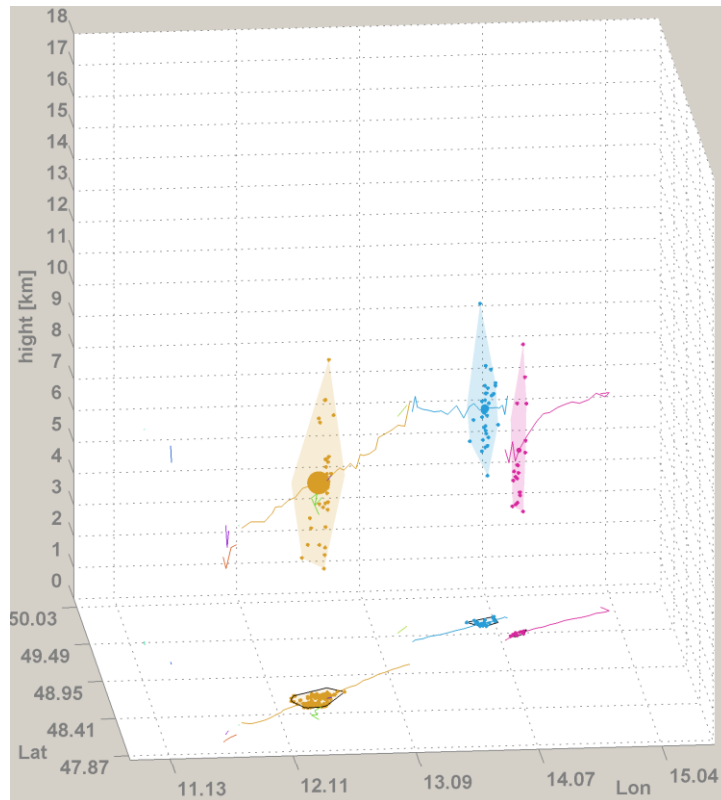


Figure 4-15: Track-line together with cluster convex hull and points at one time interval (5:00-5:10pm).

Figure 4-16 illustrates a STC including cluster scopes with semi-transparent 3D convex hulls. Moreover, trajectory lines and lightning cluster centroids are shown with a changing spherical radius indicating the point quantity. Another way to represent cluster point densities would be the use of changing luminance of the cluster polygon.

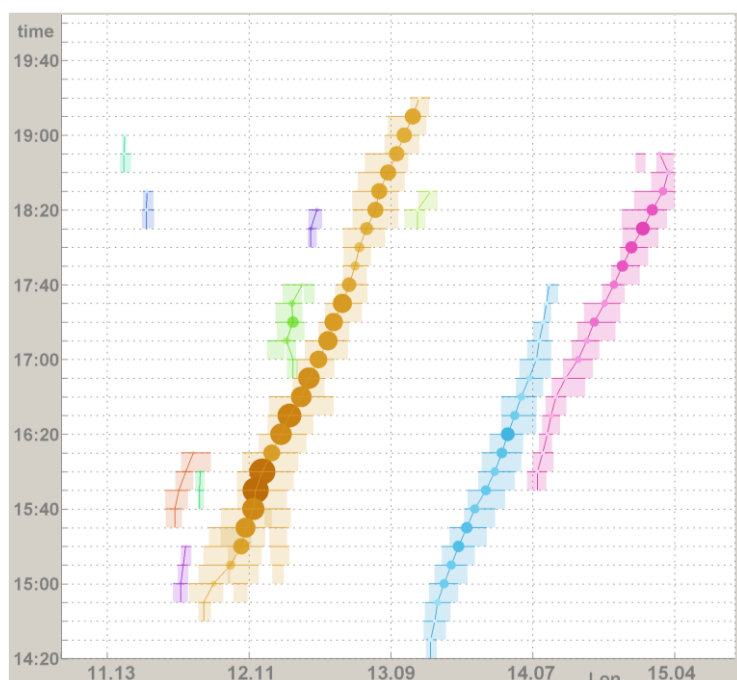


Figure 4-16: The STC with convex hulls and centroids of quantity-based symbol size and color.

In Figure 4-17, the 3D view includes 3D lightning points colored in accordance with the associated trajectory.

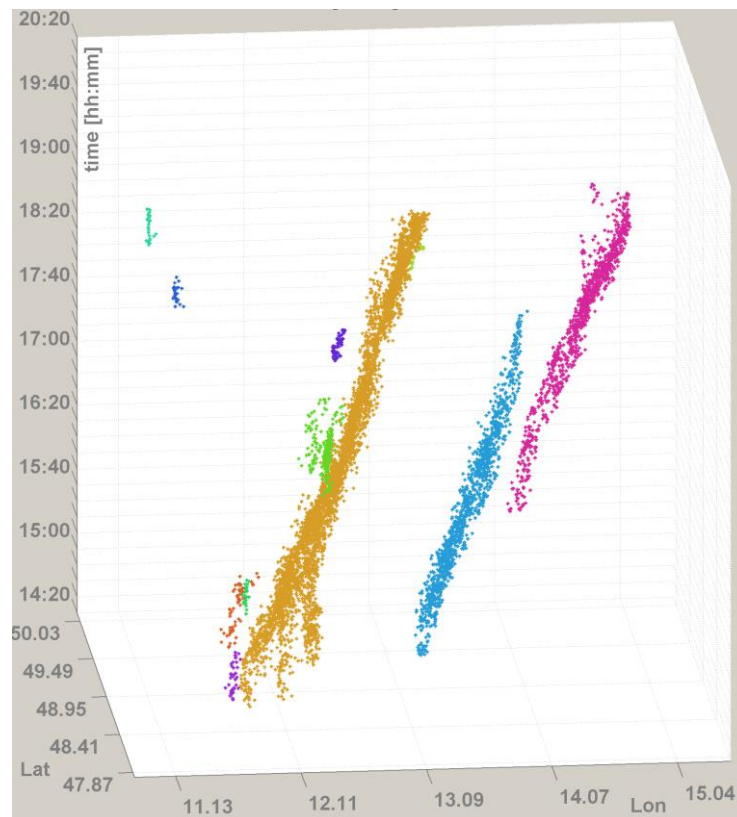


Figure 4-17: The STC with all lightning points.

Besides, we calculated various statistical information of each lightning cluster and track. Table 4-10 lists the derived information about the largest track occurred during April 26th 2013 and its largest cluster.

Table 4-10: Important lightning track attributes.

| Largest track (occurred during April 26th 2013): | | Largest cluster (occurred inside the largest track): | |
|--|-------|---|-------|
| Track lifetime (h) | 4,5 | No. of lightning points | 281 |
| No. of lightning points | 5588 | No. of CG lightning | 134 |
| No. of CG lightning | 3919 | No. of IC lightning | 147 |
| No. of IC lightning | 1669 | Longitude-extension (km) | 33,17 |
| No. of clusters | 65 | Latitude-extension (km) | 36,63 |
| No. of time intervals | 39 | Altitude-extension (km) | 6,8 |
| Track line distance (km) | 260 | Altitude-minimum (km) | 2,9 |
| Mean Track altitude, above ground (km) | 7,24 | Altitude-maximum (km) | 9,7 |
| Track lane area (km ²) | 7740 | Cluster area (km ²) | 655 |
| Track lane volume (km ³) | 71011 | Cluster volume (km ³) | 2210 |

4.2.5. Visualizing predicted lightning data

When visually analyzing dynamic phenomena such as lightning data, the interactive visual exploration plays a crucial role for the decision-making process. Our GUI (see 4.2.5) includes the same visual lightning cluster information (see Table 4-4) for predicted/future situation as for past time intervals. Figure 4-18 shows examples of predicted lightning data (26.4.2014, 5:30-6:20pm). The current time (“now”) for the nowcast analysis was set to 5:30pm on April 26th 2013 when altogether four cluster tracks were present. The cluster locations, extensions and densities for the near future (next +10, +20, +30, +60 minutes) were predicted. The four nowcasted time intervals of geometrical cluster attributes are based on attribute tendency of the last three time intervals.

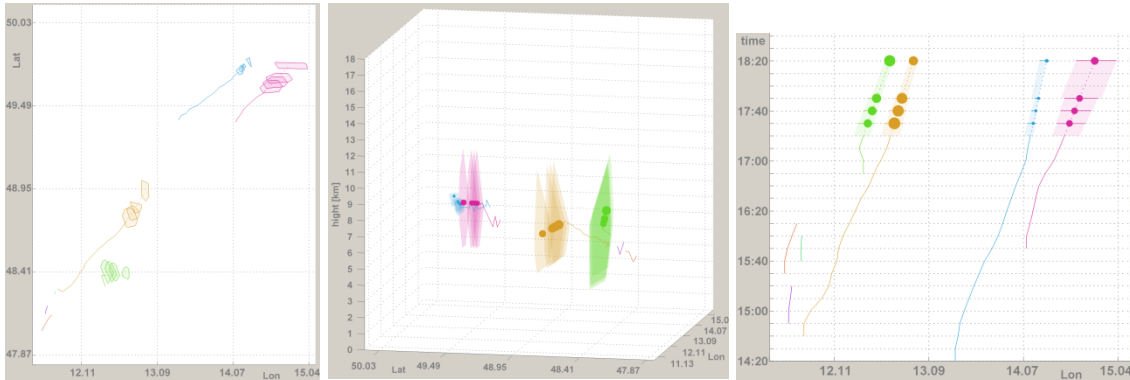


Figure 4-18: Nowcasted lightning data 26.4.2014, left: 2D view, middle: 3D view, right: STC.

On the left side of Figure 34, cluster 2D convex hulls are presented in a plan view. In the middle 3D convex hulls and cluster centroids with quantity-based symbol sizes are illustrated in 3D. On the right side a STC plot represents cluster extensions and nowcasted cluster centroids surrounded by spheres which reflect the possible spatial range for the predicted centroids. In all three illustrations the past track-lines are illustrated, thus provide the cluster history relating predicted, present and past information/situations. Figure 4-18 clearly illustrates a change of cluster extensions (convex hulls) and cluster intensity (the centroid size is based on predicted number of lightning points). An alternative to visualize the cluster intensity would be assigning a point quantity-based size or color to each cluster centroid. Likewise, further statistical and attributive cluster and track data are nowcasted considering the attribute tendency. Through an interactive use of the GUI, 2D view, 3D view and STC can be visually explored in more detail (via pan, zoom, rotate etc.).

4.2.6. Lightning nowcasting, uncertainty and visual presentation

Lightning cluster nowcasting is a complex process and up to date research topic, involving not only detected lightning, but also various further atmospheric data and modeled processes. In our work, the focus is on the visualization of predicted lightning clusters and their attributes. Thus, our approach is rather simple, purely geometric for the demonstration purpose and has been already published in (Peters & Meng 2013). We decided to project the future lightning cluster situation in 10, 20, 30 and 60 minutes (Δt). Nowcasted cluster locations are based on the extrapolated cluster centroid as shown in Figure 4-19 and Equation 3.

Equation 3:

$$\bar{P}_{t+1} = \bar{P}_{t0} + \frac{\bar{v}_{t-1} + \bar{v}_{t-2}}{2} \cdot \Delta t \quad \text{whereby } \bar{v}_t = \frac{\bar{d}_{P_t P_{t-1}}}{\Delta t}$$

With our ‘simple’ nowcasting method we can predict the near future position by taking cluster speed and direction changes of the last three temporal intervals into account. The velocity vector

of the last two cluster centroids is determined based on their positions (P_{t-k}). We assume a momentary cluster velocity as the mean of the velocity (v) of the previous two cluster centroids. Moreover, direction changes (α) were considered. In order to avoid the tight curves of the now-casted cluster trajectory, we suggest configuring a threshold for the value of α . Besides, α^* correlates with the prediction moment in the future (Δt) (see Figure 4-19). In other words, the longer the prediction time the larger the α^* . In case a cluster trajectory only contains two centroids, α^* will be given a value of 180° . The method has been implemented for 3D scenarios (Peters et al. 2014).

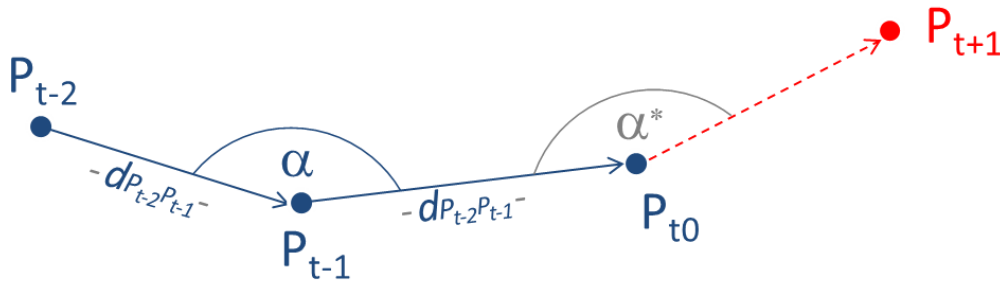


Figure 4-19: Cluster centroid nowcasting concept for 2D.

Furthermore, cluster attributes, such as cluster area or point quantity, can be predicted based on the attribute values (p) of the previous two, three or four temporal intervals. One considerable extrapolation method for lightning cluster attributes is the polynomial regression (of the second order), according to which the cluster centroid coordinates are described in Equation 4:

Equation 4:

$$p(x) = p_1x_n + p_2x_{n-1} + \dots + p_nx + p_{n+1}$$

The coefficients of a polynomial function $p(x)$ of degree n in Equation 4 are determined following the least square principle. The outcome p is a vector of the length $n + 1$ containing the polynomial coefficients in descending powers. The polynomial function has the disadvantage of having values which are unrealistically high or below zero.

To circumvent the drawback, we developed a *rule-based cluster prediction method* for lightning cluster nowcasting, which is based on cluster attribute values of the last three time intervals. Thus, only the tendency of value change (increasing/decreasing of ca. 10/20/...%) is reflected in the predicted cluster attribute values.

The accuracy of the extrapolated cluster centroids can be evaluated and improved with a learning model which allows the comparison of the predicted centroid locations and attribute values with updated ones. After each update the nowcast parameters are adapted until a threshold for α^* is reached. The mean differences between predicted and updated values indicate the degree of prediction uncertainty. Furthermore, measurement errors can be incorporated in the certainty model. Assume that the measurement accuracy for cluster centroids is the same as for detected lightning ($acc = 150$ m), a positional uncertainty (u) for nowcasted centroids (P_{t+k}) can be calculated by considering the future time interval (k) and the maximum inaccuracy between the last two cluster centroids according to Equation 5:

Equation 5:

$$u(P_{t+k}) = acc \times (k + 2)$$

Thus, the 2D uncertainty for predicted lightning cluster centroids results in an estimated value of 450m for a 10 minutes nowcasting ($k = 1$), 600m for 20 minutes ($k = 2$) and so on. The positional inaccuracy in 2D and in altitude may accumulate and propagate from the previous time intervals to the proceeding ones. Consequently a cluster centroid uncertainty average of about 10 km leads to an altitude accuracy of 1 km (acc). Our elementary lightning cluster prediction approach was applied to our test dataset. It is possible to perform cluster prediction at any time within the temporal range defined as “now”. To verify nowcasting results a past analysis was conducted. Test data were separated into 10 minute steps and predicted centroids were calculated. Successively, predicted geometrical cluster attributes such as centroid locations were compared with the updated ones.

One way to proof our rule-based cluster prediction method is to extrapolate geometrical cluster attributes (e.g. cluster centroid coordinates) - based on the last three time intervals - for each past time interval and compare the ‘nowcasted’ results with the ‘updated’ information. Updated information is understood as the originally derived cluster attributes based on spatio-temporal clustering of lightning points as described in section 4.1.4. Figure 4-20 illustrates the accuracy by connecting the associated ‘nowcasted’ and ‘updated’ cluster centroids for plus 10 minutes future prediction via thinner lines. The thicker lines connecting the ‘updated’ cluster centroids represent the lightning track-line. The illustration shows that if lightning clusters are moving more or less in the same direction, the past-processed ‘nowcasted’ centroid locations match well with the ‘updated’ centroids.

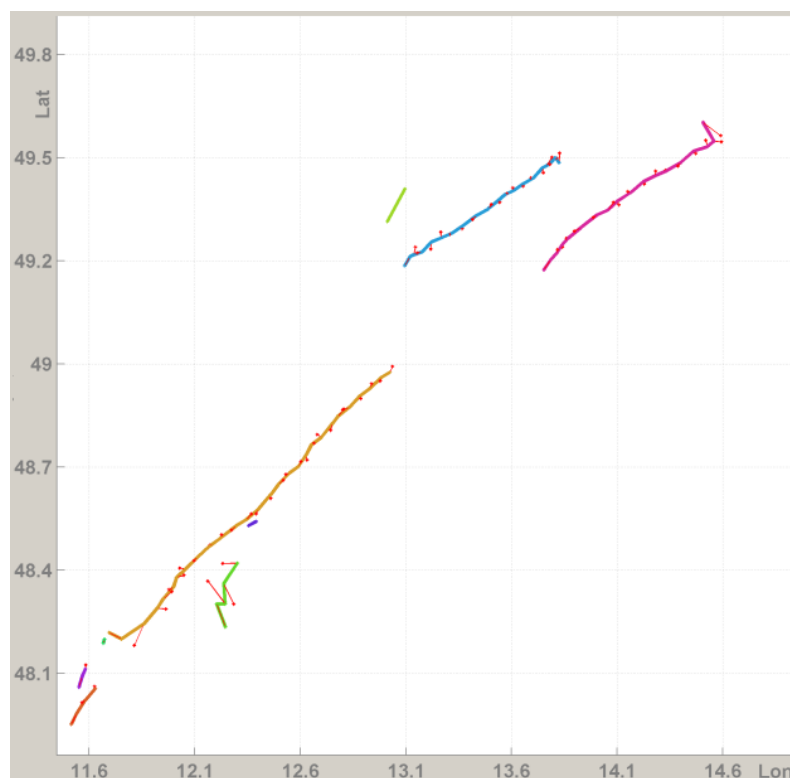


Figure 4-20: Past-processed ‘10minutes nowcasted’ and ‘measuring-based updated’ centroids.

Geometrical and semantic cluster attributes are nowcasted using our rule-based cluster prediction method. Figure 4-21 illustrates the centroid deviation histogram. The distance of predicted centroids to the updated ones defines the cluster position accuracy. Thereby, around 90% of the predicted cluster centroid locations could be detected with accuracy of less than 10km. Furthermore, nearly 10% of the predicted cluster centroid locations could be determined with accuracy between 10 and 20km. It can be added, that, since we only used aggregated data within our

nowcasting model, the prediction calculation is computationally performed much faster than if all initial points are included.

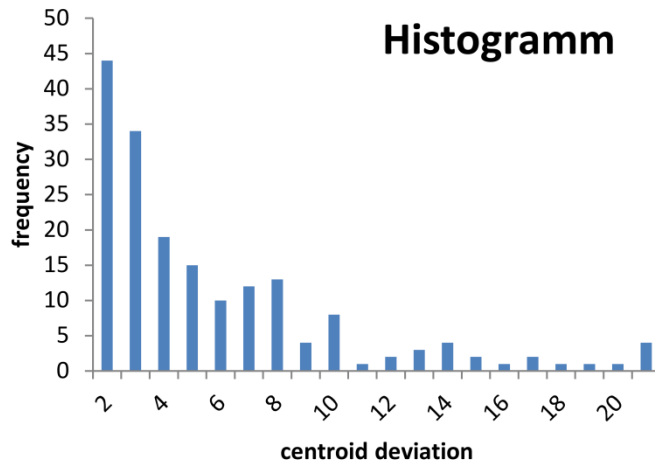


Figure 4-21: Centroid standard deviation after past-processed prediction of each time interval.

For the uncertainty visualization of predicted lightning data, adapted intrinsic visual variables or extrinsic visual variables (see Section 2.6) can be applied.

For the nowcasted lightning clusters, an *uncertainty buffer* - an extrinsic visual variable - can be illustrated demonstrating the accuracy of the predicted cluster location/extension. Figure 4-22 demonstrates the concept for certainty/probability visualization of nowcasted cluster extension (convex hulls). On the left, the lightning cluster centroid and convex hull of the last two time intervals ('now' and 'minus 10 minutes') together with the track-line are presented. On the right, the predicted lightning situation including track-line, cluster centroids and convex hull together with cluster extension uncertainty buffer are shown. A semi-transparent fawn color was used for the buffer. The ratio of the uncertainty buffer ratio is correlated with the future time interval ('now' +10, +20, +30 minutes). The buffer size was determined using our nowcasting uncertainty concept, which is purely geometric and only for the demonstration purpose – as described in Equation 5. The middle part of Figure 4-22 combines past and predicted visualizations.

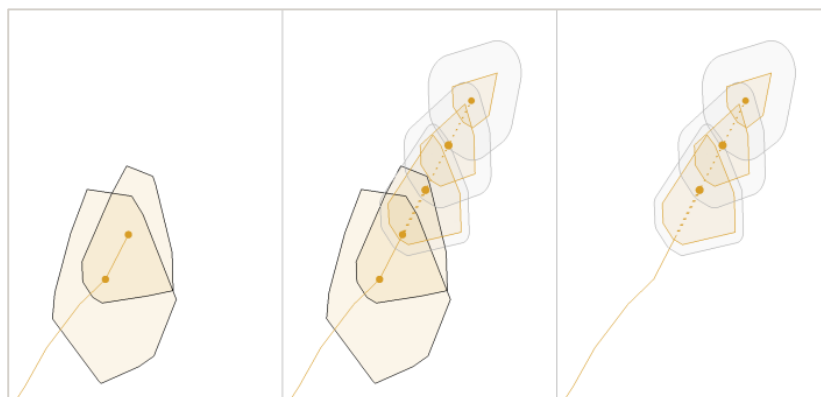


Figure 4-22: A buffer representing the prediction uncertainty of nowcasted lightning cluster (left: last two lightning clusters; right: predicted clusters with uncertainty buffers; middle: past and predicted clusters).

The buffer polygon symbol, including outer line type, width and color as well as polygon color and transparency (intrinsic visual variables), can be adapted depending on the map users need. Another option is to apply a smooth color gradient to the filled buffer, reflecting the uncertainty

decrease towards the outer buffer border line. Furthermore, a circular buffer could visually present the location certainty of a predicted lightning cluster centroid. In other words, the buffer would reflect the possible spatial range for the predicted centroid. The inclusion of additional visual tools (as the probability buffer) may support the analysis of potential dangers caused by lightning. The nowcasted centroid and cluster buffer apply as well for STC or 3D view in the form of 3D buffer using the similar buffer size as for 2D view. A further option is the use of an extruded cluster footprint along the positive z-axis instead of a 2D cluster buffer, whereby each extrusion height is equal to the respective buffer size of each cluster. The extrusion representing prediction uncertainty, can be applied as well to the nowcasted centroid in form of a bar or column. Furthermore, the contour line visualization (Scheepens et al. 2014) described in Section 2.6, would also be reasonable for representing uncertainty of predicted lightning centroids.

4.2.7. Interactive graphic user interface

Using an interactive graphic user interface (GUI) supports the movement analysis of lightning data. Peters et al. (2014) introduced the lightning-GUI including a 3D-view together with a STC approach. This GUI was enriched and extended for the investigation of nowcasted lightning data in (Peters & Meng 2013).

Using our interactive lightning-GUI, the user should be able to:

- Access lightning point coordinates (x,y,z,t)
- Change between 3D-view (x-y-z) and STC (x-y-t)
- Choose and/or combine various representations for lightning clusters and tracks
- Visually perform lightning cluster prediction for the next 10, 20, 30, ..., 60 min
- Adjust graphic variables for lightning clusters and trajectories
- Select lightning data for certain spatial and/or temporal intervals
- Visually explore lightning data via zoom, rotate, pan, animate etc.
- Add base map for better orientation
- Enable additional graphics for visual exploration of lightning cluster attributes

To provide the best performance, different visualizations of lightning clusters and tracks, such as cluster ellipsoid and convex hulls, should be pre-processed and downloaded during the interactive use of the GUI.

The outlook of our GUI is shown in Figure 4-23. It is possible to spatially and/or temporally limit lightning data in order to focus on specific time intervals or/and areas of interest. To the left, different representations of past and nowcasted clusters and tracks can be selected, enabled and combined. Nowcasting can be performed for the next 10, 20, 30 or 60 minutes. Moreover, interactive visual exploration of lightning data might be facilitated via zooming, rotating, panning and animation. For currently displayed data, either 3D view ("XYZ view") or the STC can be chosen. The time slider can be used to select a certain time interval. Thus, it is possible to adapt the current map display for a specific moment of time or, with the use of the 'hold on' button, for a time period of interest.

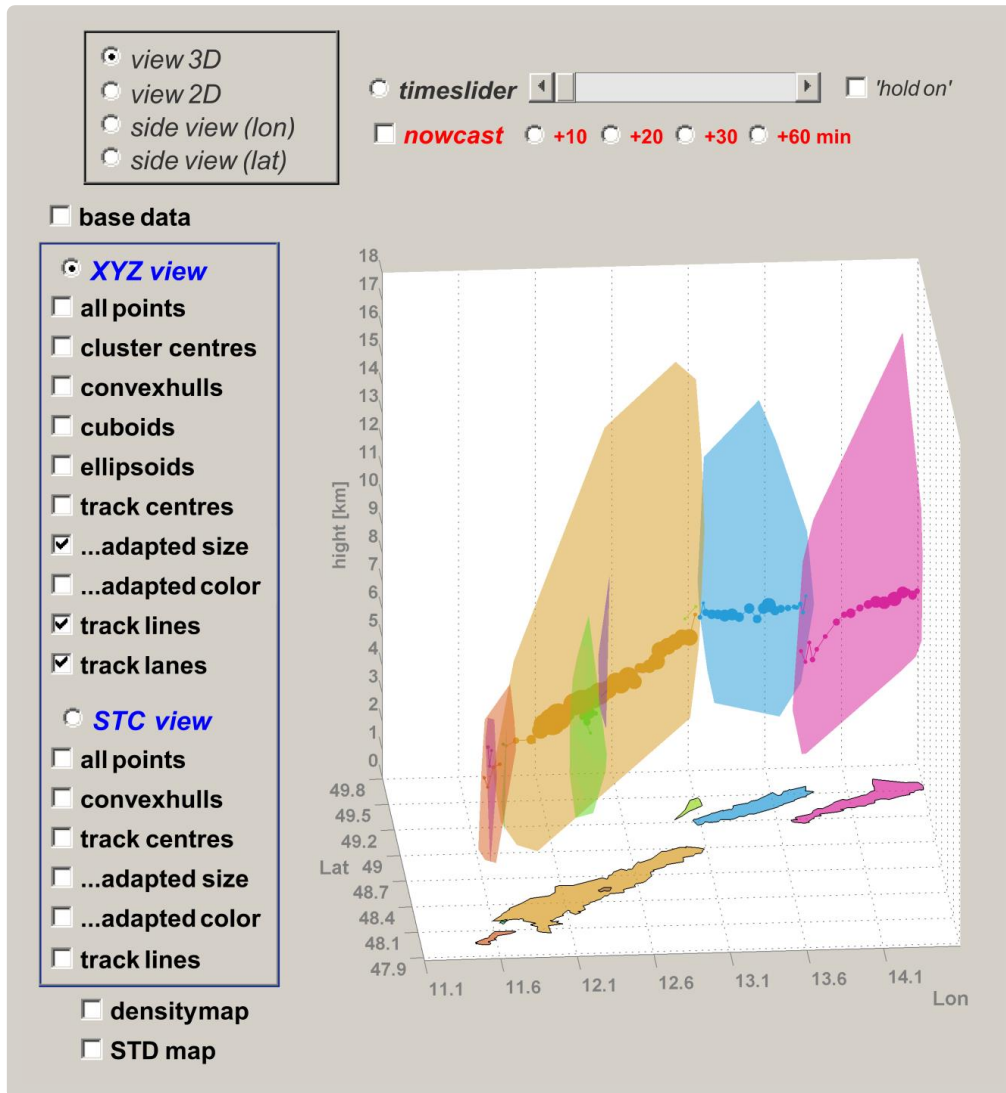


Figure 4-23: The GUI for interactive data exploration of the lightning data dynamics.

Two complementary visualization concepts are implemented: the 3D view and the STC. The 3D plot provides altitude information, whereas temporal information is missing. Within the 3D view, overlapping can arise when clusters occur to different moments at the same location area. The STC provides the temporal insight but misses the altitude information. The combination of both provides a variety of information about the lightning cluster dynamics. By changing the view perspective within the STC, an observation from above (top view) as the traditional 2D plot can be obtained. The GUI enables the user to combine or switch between different visualization options for lightning clusters, tracks and cluster-/track attributes. Furthermore, the GUI supports an interactive visual analysis of the currently displayed lightning data and their attributes. Statistical values of cluster- and track attributes (minimum, maximum, mean values etc.) could be displayed on demand using additional graphics with maximum values being highlighted in all current plots/graphics (Peters & Meng 2013).

As defined in Section 2.3, dynamic visual effects can be created by means of symbol blinking, flashing, bubbling, sparkling, throbbing, erupting, sinking, exploding, rotating or shaking on screen. These actions can be triggered to indicate lightning cluster movements on 2D or 3D maps as well as in a STC. Each action can be related to the spatio-temporal change of an object. Then, the action sequence should be set. Some fundamentals for dynamic visual effects in maps are provided by Buziek et al. (2000). These effects can be synchronized with their associated infor-

mation in non-cartographic displays (e.g. highlighting respective values in a time plot). Detected moving clusters could be highlighted via blinking effect. The important aspects of lightning cluster movements that can be emphasized by the dynamic effects include perceptual salience, thematic relevance, design and user characteristics. We prefer the use of animations with a time slider, showing symbol emerging and disappearing while changing the time settings. The user can either define a specific moment of time or time interval the data will be displayed. While operating the slider step by step, all cluster movements (birth, changes, existence ceasing) are visible. Thus, the occurrence of individual lightning events (points) containing exact time information as well as derived moving lightning clusters and trajectories can be explored through the use of the time slider. The slider can have fixed steps or elastic intervals. The elastic ones can be adapted when cluster states change. For our case it is also reasonable to change symbol transparency in order to create a fading effect of disappearing clusters, which on the other hand could provide information about the cluster moving direction.

4.3. Density maps for dynamic lightning data

Section 4.3 is based on (Peters & Meng 2014a, b), which proposed a novel approach for the creation of a 2D density surface – using contour intervals – for spatially and temporally changing points representing a SEP, applied to our lightning test dataset.

4.3.1. STDmapping method

First of all, density contour maps can be derived from point datasets using KDE while an optimal kernel bandwidth can be calculated according to Silverman's formula (Silverman 1986). In our work we deal with a lightning point dataset representing a dynamic phenomenon. Thus, instead of creating a single density contour map of the entire point dataset, we applied KDE in each case to all points belonging to the same lightning track. Thereby, lightning points are clustered, afterwards allocated and aggregated to trajectories. In doing so, a temporal clustering is applied to the initial point dataset using a time interval of one hour. Subsequently, all points within each temporal interval are spatially clustered using a buffer threshold of six kilometers.

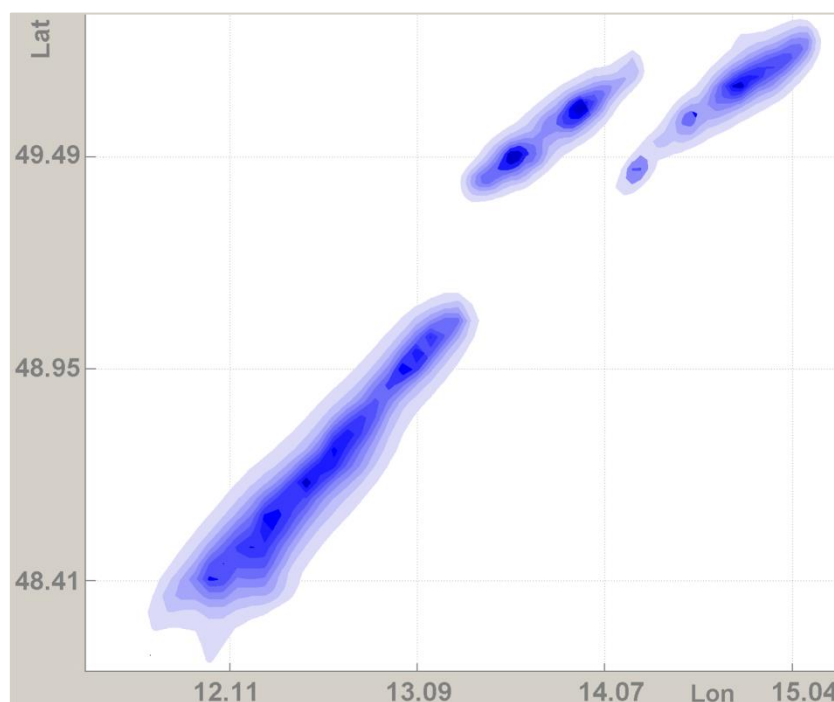


Figure 4-24: KDE map (left) and colored points based on temporal clusters (right).

In the resulting spatio-temporal clusters, the spatially overlapping parts within two time sequences are detected and afterwards allocated and aggregated to lightning trajectories. Further details of the temporal and spatial clustering of lightning data including explanations for thresholds can be found in (Peters et al. 2014; Peters & Meng 2013). The results of the density contour maps derived for the test dataset (lightning points during April 26th) are shown in Figure 4-24. Thereby all points, CG and IC points, projected onto the plane, of the three largest tracks were considered (see also Figure 4-2 and Figure 4-12). The importance of grouping dynamic points into tracks is discussed in the next section.

The resulting density contour layers in blue tones do not bear any temporal information. Nevertheless, the aforementioned temporal point clustering method provides time information for each lightning point. Figure 4-25 illustrates our initial point dataset whereby lightning points were segmented and colored according to the different time intervals, thus reveal the dynamic changes. In doing so, we used a time interval of 1 hour starting at 2pm for the temporal clustering. The overlapping convex hulls surrounding all spatially clustered points of the same temporal interval are allocated – as clearly visible in Figure 4-25 - to altogether three different trajectories.

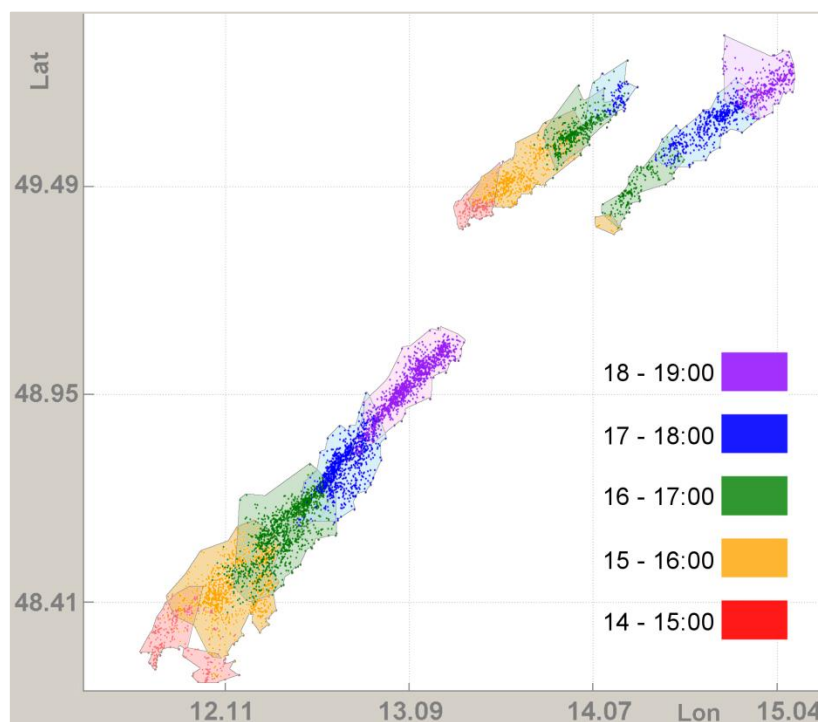


Figure 4-25: Temporally clustered point data.

Three main moving lightning clusters are perceivable within the test area. Their geo-graphic and temporal locations are apart from each other with one formed at lower left part and one upper left, both starting around 2pm and the third one upper right occurring around 4pm. All clusters are moving north-eastwards. The upper left cluster disappears around 5pm, whereas the lower left and the upper right last until 7pm. As mentioned before, traditional density mapping does not contain temporal information. Clustering and allocating dynamic point data (in our case lightning points) towards trajectories provides information about data movement (speed, direction, etc.). In the following we introduce a method which includes movement information, i.e. dynamics in KDE mapping. In other words, we suggest a solution to incorporate temporal information of moving points (as illustrated in Figure 4-25) inside the density contour intervals (as shown in Figure 4-24). An overview of our suggested method is illustrated through an overall workflow in Figure 4-26.

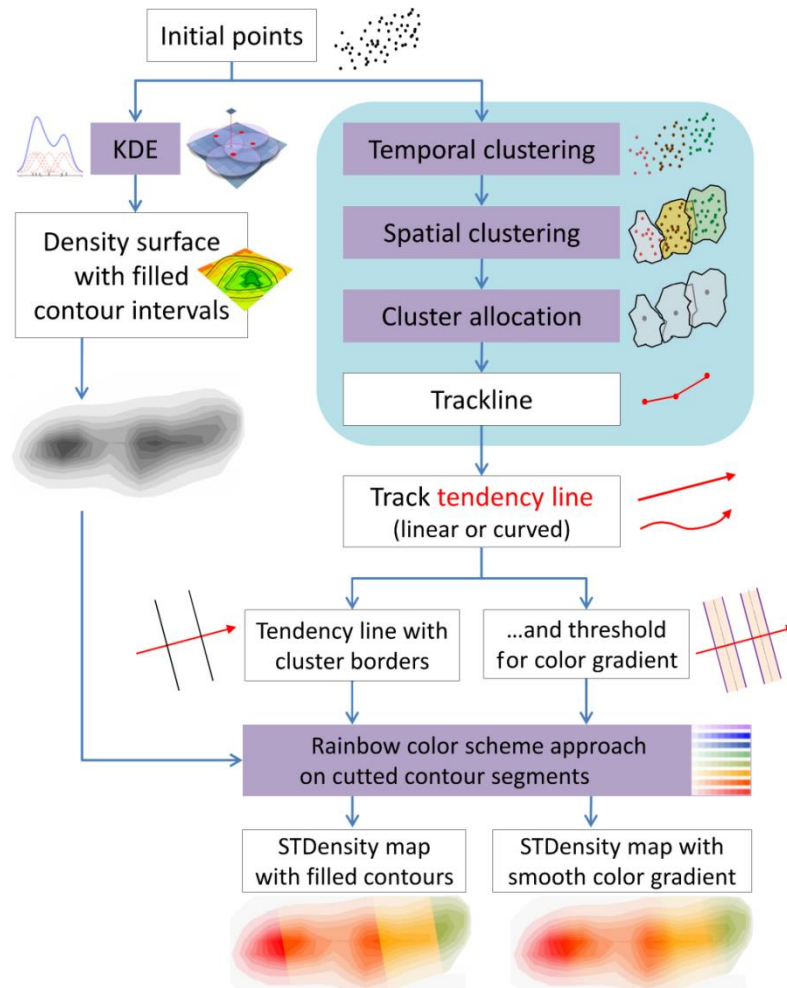


Figure 4-26: The workflow of STDmapping of lightning data.

First of all a density contour map using KDE is created. Additionally, the given point dataset (see Section 4.1.3) is temporally and spatially clustered. In the next step, the overlapping clusters (in case they are temporally successive) are detected and after that allocated and aggregated to independent tracks. Cluster centroids are embedded in the trajectories. A detailed description about these steps can be found in (Peters et al. 2014). A linear approximation of each track results in a straight tendency line, which represents the average moving direction of the point cluster. The linear approximation can be based either only on the cluster centroids or on the entire point datasets of a track. If the projected trajectory is curved rather than straight, the tendency line can be approximated by a polyline connecting the cluster centroids. In our case, a cubic spline interpolation function is used to fit a curve through the cluster centroids (De Boor 1978). Consequently, we have on the one hand the density surfaces represented by layered tints between neighboring contour lines and on the other hand the tendency line with either abrupt or smooth transition at borders of temporal clusters. This temporal border is a line perpendicular to the tendency line passing through the average locations of all points within a certain period (in our case 10 minutes) before and after a temporal border (e.g. full hour). If the phenomenon is moving, all points between two temporal borders (e.g. between “2pm line” and the “3pm line”) are grouped into the same temporal interval (period: “2pm - 3pm”). The next question is how we can incorporate the dynamics inside the density map. The idea is to divide the tendency line into temporal parts, which will in turn guide the segmentation of the density surface. Figure 4-27 illustrates two different ways of tendency line determination. In the left part, all points of an exemplary lightning track are colored according to the temporal cluster they respectively belong to. The

cluster centroids are presented as black dots. A straight tendency line representing the general movement direction of the lightning cluster is based on the coordinates of all cluster centroids. The temporal borders in red are detected and vertically aligned to the straight tendency line. The locations for temporal borders can be defined by the half distance between two temporally successive cluster centroids, or, by the centroid of the overlapping area of two sequential temporal point sets.

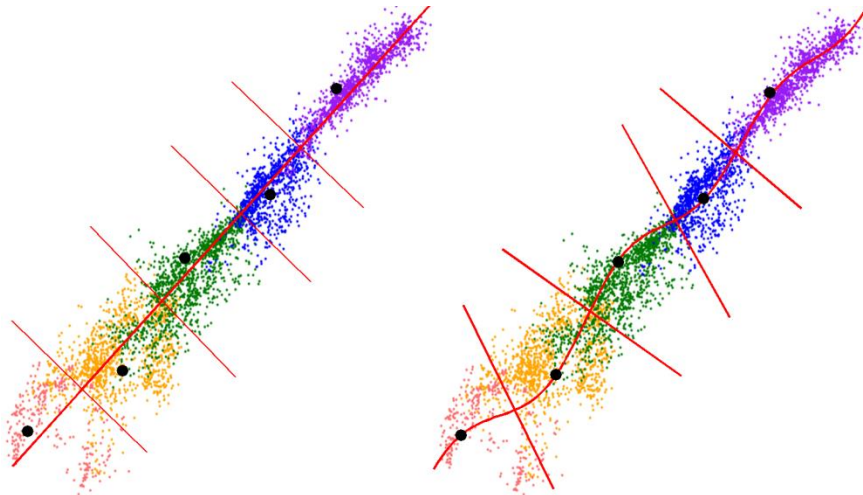


Figure 4-27: Temporal clustered points and cluster centroids in black with straight tendency line and perpendicular temporal borders (left) and with curved tendency line and perpendicular temporal borders (right).

In the right part of Figure 4-27, the tendency line is represented by a curve determined through cubic spline interpolation of all cluster centroids. The temporal borders in red are defined again as perpendicular lines of the curved tendency line. Thus, temporal border lines are not arranged parallel to each other as in the case for the straight tendency line. However, for very small temporal clusters (clusters of low velocity or very small temporal thresholds) temporal border lines are much closer to each other and thus – due to the curved tendency line route – they are almost parallel to each other. Nevertheless, it could be also possible that two sequential temporal borderlines intersect each other (in particular if the tendency line is strongly curved). In this case, the respective intersecting temporal borderlines need to be partly merged as shown in Figure 4-28. Thereby, different temporal segments are illustrated in different colors (beige, green, blue) and temporal borders in red. We suggest combining the two intersecting temporal border lines from the intersection point onwards towards the outer cluster extension in a way that each of both temporal border lines forms the same angle with the continuing merged border line part.

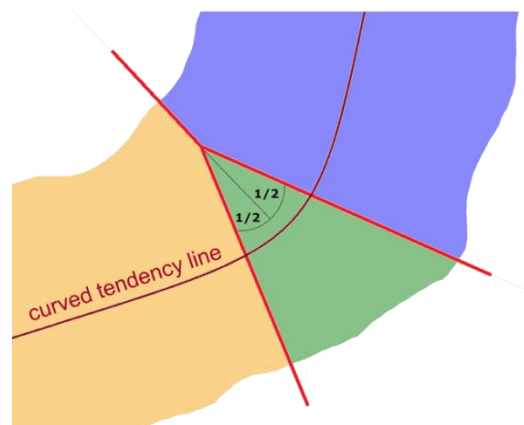


Figure 4-28: Suggested solution for intersecting temporal border lines (red).

In the next step density contours are separated through temporal borderlines into temporal surface segments as illustrated in Figure 4-29. As described before, temporal borders can be either parallel if they are based on a straight tendency line (see Figure 4-29 left) or temporal borders are perpendicular to the curved tendency line and thus non-parallel. Furthermore, thresholds for temporal borderlines can be applied for smooth color transitions. (see Figure 4-29 right)

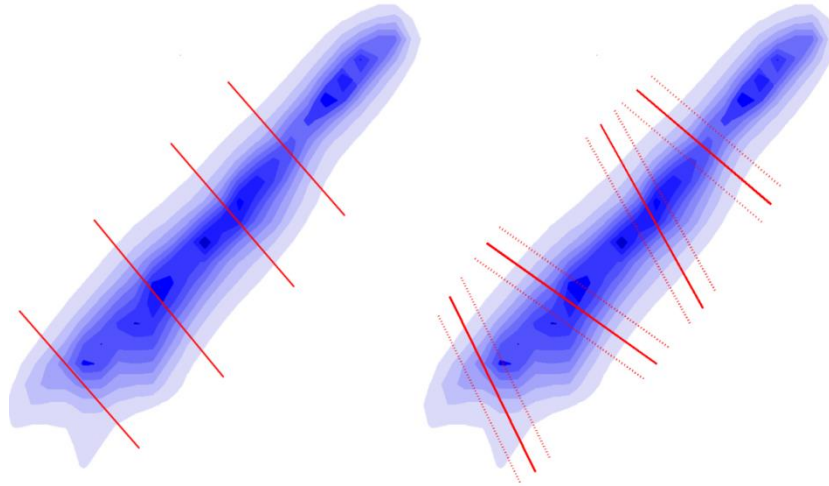


Figure 4-29: Density contours with temporal borders based on a linear tendency line (left) and with temporal borders and thresholds for smooth color gradients based on a curved tendency line (right).

Different temporal surface segments carry different color hues. Within the same surface segment, the color hue remains the same but its intensity varies with the change of density. In our approach, we adopted the “rainbow color scheme”, which is essentially the visible and continuous electromagnetic spectrum. Its main color hues transit from red, orange, yellow, green, blue to violet. The spectrum can be divided into an arbitrary number of intervals. Users may easily anticipate and comprehend the color transitions. In our approach, we assign each time interval to a certain color hue – the medium color of the rainbow subinterval. Figure 4-30 exemplary illustrates eight different rainbow color hues with each being displayed in up to six different color intensities from light to dark. For instance, the red color scheme refers to time period 1 and contains six different red tones, which are related to six different density values/value intervals. We split the entire time of our dynamic dataset into equal time intervals. The interval size can be determined based on the user’s interest. Hue represents time (e.g. discretized at 1 hour intervals) and color intensity corresponds to the density of observations (low intensity refers to low density and high intensity to high density). A continuous color scheme should not include more than three hues, otherwise the visual perception may suffer. An exception is the rainbow scheme. Most people know the differences in short and long wavelengths of visible light and are therefore familiar with the rainbow color gradation.

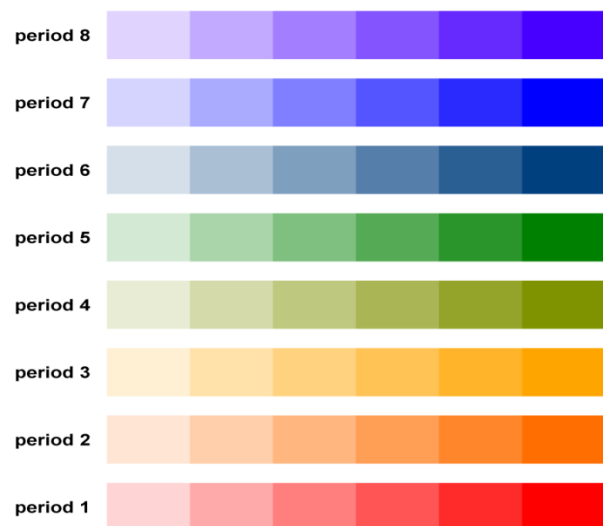


Figure 4-30: Rainbow color scheme.

We decided to use the rainbow color scheme in order to fulfill the following two criteria:

- (1) 'Clear differentiation': colors of adjacent segments should be clearly distinguishable from each other. In particular, the brightness spectrum from low to high intensity should be distinct for each color hue from those of the others.
- (2) 'Continuity': The color hues including their different intensities should represent the movement, thus, consists of a continuous color gradation. From the first hue allocated to the first temporal interval to the last one, the map user should be able to visually detect this continuity through a continuous color scheme. This color scheme has to be commonly known/familiar and intuitively understandable.

In literature, rainbow color maps are commonly used, but often are considered as harmful for continuous data (Borland & Taylor II 2007). The arguments against rainbow schemes include the inappropriateness for colorblind people, the appearing of divisions between hues which lead to visual "edges" in the map, the meaningless spectral order of the hues and difficulties to recognize details. In particular to differentiate qualitative and quantitative attributes through polygon hue, the use of the rainbow scheme is often criticized. Figure 4-31 illustrates five different color scheme approaches for the STDmap using the rainbow color scheme (a) and four alternatives involving a color gradient from blue to purple (b) as well as three color scheme from Colorbrewer.org (Brewer & Harrower 2014): sequential multiple hues (c), sequential single hue (d) and diverging (e).

To visualize continuous data, often bipolar color illustration is used. On the other hand, also the rainbow color scheme is frequently used, for example to visualize the earth gravitational field (geoid anomalies) or illustrate weather-related intensities, such as storm severity (Wicklin 2013). Although the rainbow color scheme with its color gradation is commonly known, the continuity information based on color gradation might be easier to identify in the options provided in Figure 4-31-b,c,d,e. In Figure 4-31-c,d,e individual contour segments are difficult to identify due to the use of/color transition to white or yellow. Although the movement of the SEO in time is clearly visible in Figure 4-31-b, individual neighboring temporal segments could be confusing – which is not the case in Figure 4-31-a. To fulfill/combine the two contradictory criteria of the continuity and the clear differentiation, we have to make a compromise. The rainbow scheme might be more appropriate for some cases while a continuous color scheme involving 2-3 hues might suit better for other applications. For our STDmapping approach, we preferred to use the rainbow scheme. However, a user test is needed to verify the proper use of rainbow color scheme for our STDmap.

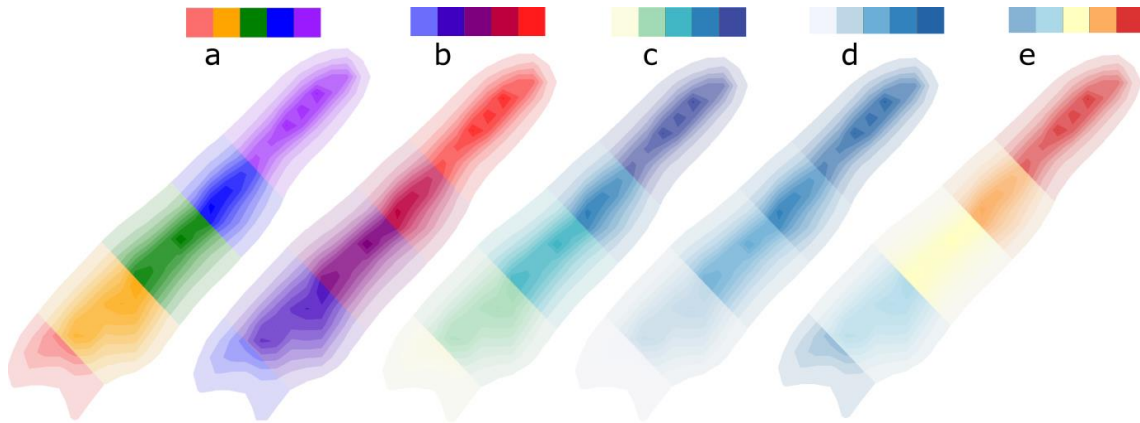


Figure 4-31: Different color scheme approaches.

With regard to the division of density surface by means of the temporal tendency lines (following either a straight or a curved route), we introduce the perpendicular lines to each tendency line as the temporal borders between the two neighboring time intervals of the underlying KDE map. The color transition between two temporal segments can be either abrupt or smooth. In case of smooth temporal borders, a defined threshold for the smooth color transition is set. The threshold refers to a certain time before and after the abrupt temporal borders. That leads to two parallel border lines – one to the left and one the other to the right of the abrupt border line. The distance (time) between each smooth border line and the respective abrupt border line can be constant and variable. Thus, our STDmapping (spatio-temporal density mapping) approach provides a solution for the visual incorporation of temporal information within density surfaces of layered tints.

4.3.2. Implemented STDmapping approach - results and discussion

The density visualization option ‘KDE for dynamic points’, as described in the previous section, was applied to our test dataset, containing lightning points during April 26th 2011. We applied both our proposed STDmapping approach and the commonly used KDE method. Applying the latter traditionally for each spatio-temporal cluster, a segment of density map with layered tints was produced as illustrated in Figure 4-32-a, which however is not satisfying due to parts of overlays and occlusion. It leads to a loss of certain local and of the overall density information.

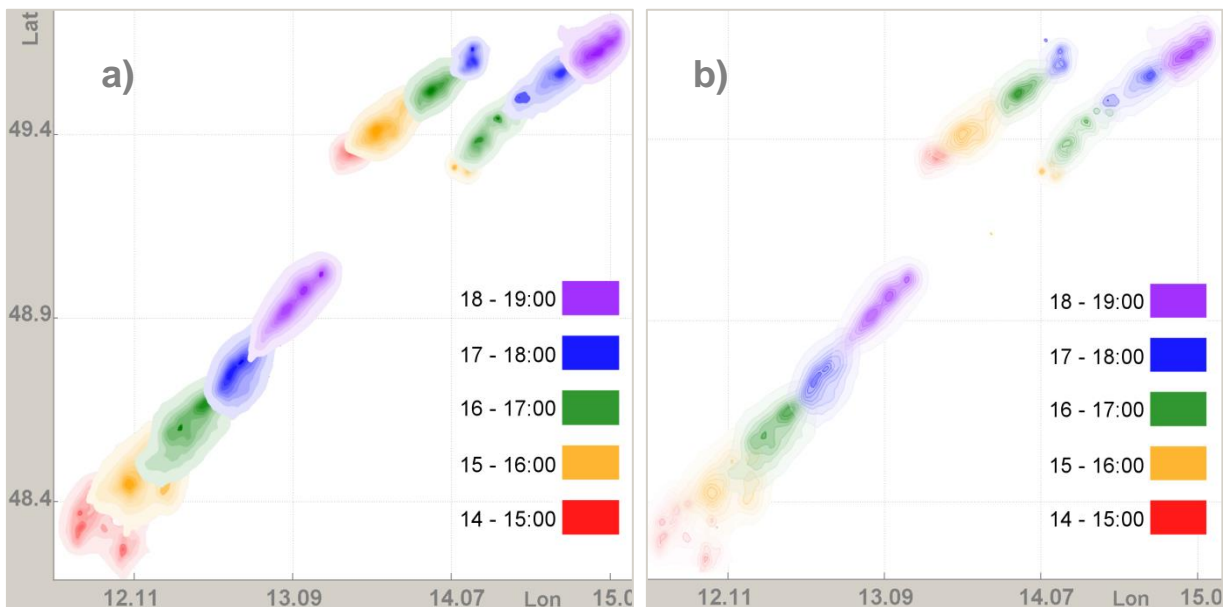


Figure 4-32: Segmented KDE in one map (a: no transparency, b: transparency of 50%).

Applying transparency does not solve this drawback adequately. Due to the fact, that the density contour intervals of each temporal interval have the same hue but differ in color intensities, a transparency changes the intervals with low intensities to almost invisible – even if a contour border with a slightly more intense color is added as shown in Figure 4-32-b. Moreover, hidden parts of overlapped contour intervals in Figure 4-32-a are not sufficiently recognizable in Figure 4-32-b in which all contour intervals have a transparency of 50%. Thus, using KDE maps for each spatio-temporal cluster provides only direct depiction of time for non-overlapping contour surfaces. Furthermore, visual exploration of density information in the overlapping parts is only possible for the surface on top; in case transparency is applied it is very difficult. Another disadvantage occurs when one is interested in density information including points detected shortly before and after the temporal interval border. By applying the new STDmapping approach to our test dataset and following the workflow in Figure 4-26, we created eight different output maps (Figure 4-33-a,b,c,d, Figure 4-34-a,b,c,d). The temporal borders were based on either the straight (A) or curved lightning cluster moving tendency lines (B). Furthermore, we used two different temporal thresholds: one hour respectively 30 minutes. Moreover, we applied the abrupt and the smooth concept for color gradients between temporal segments.

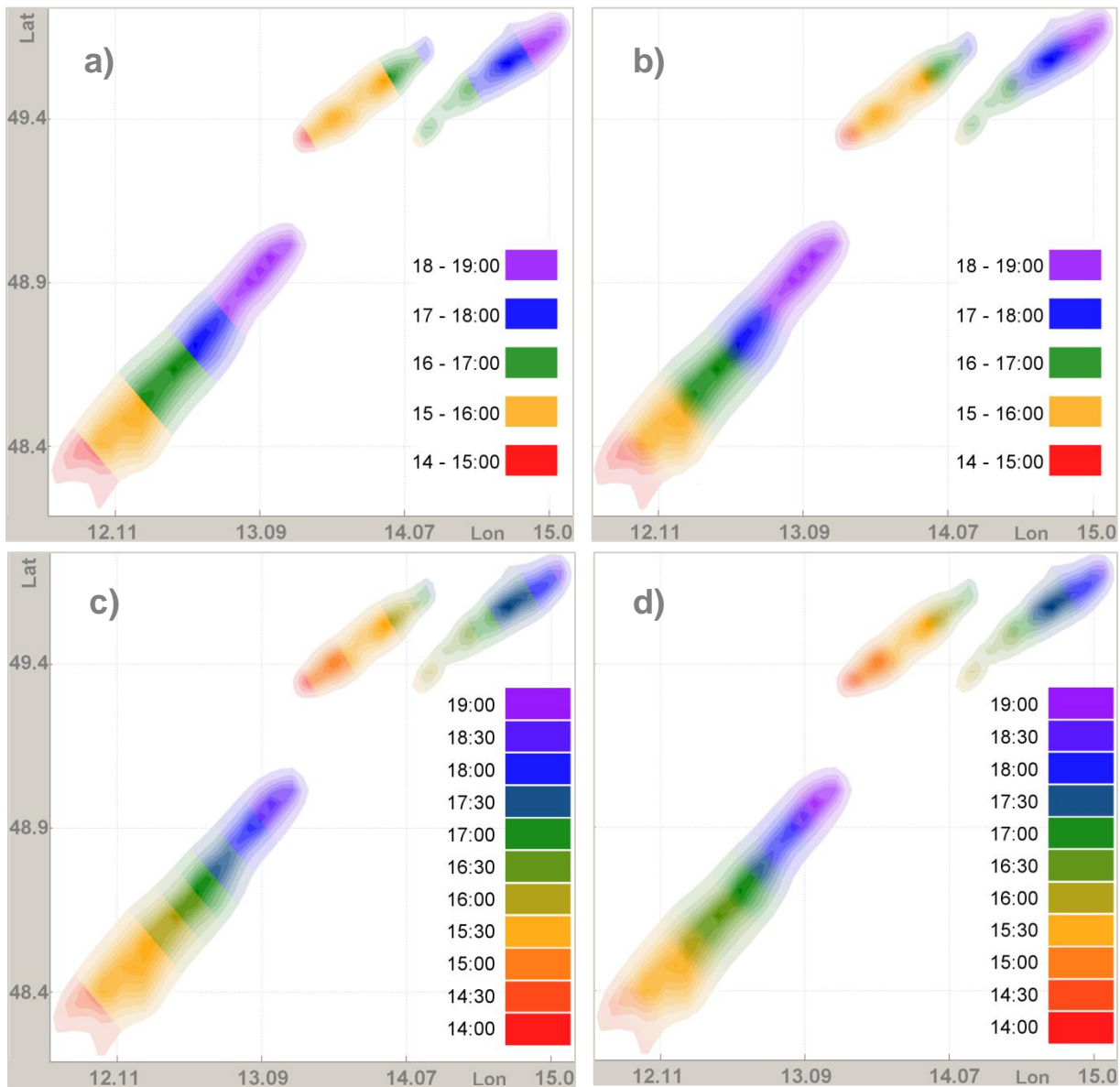


Figure 4-33. STDmap with abrupt (left) or smooth (right) color gradient based on straight tendency lines and the temporal interval of one hour (above) or 30 minutes (below).

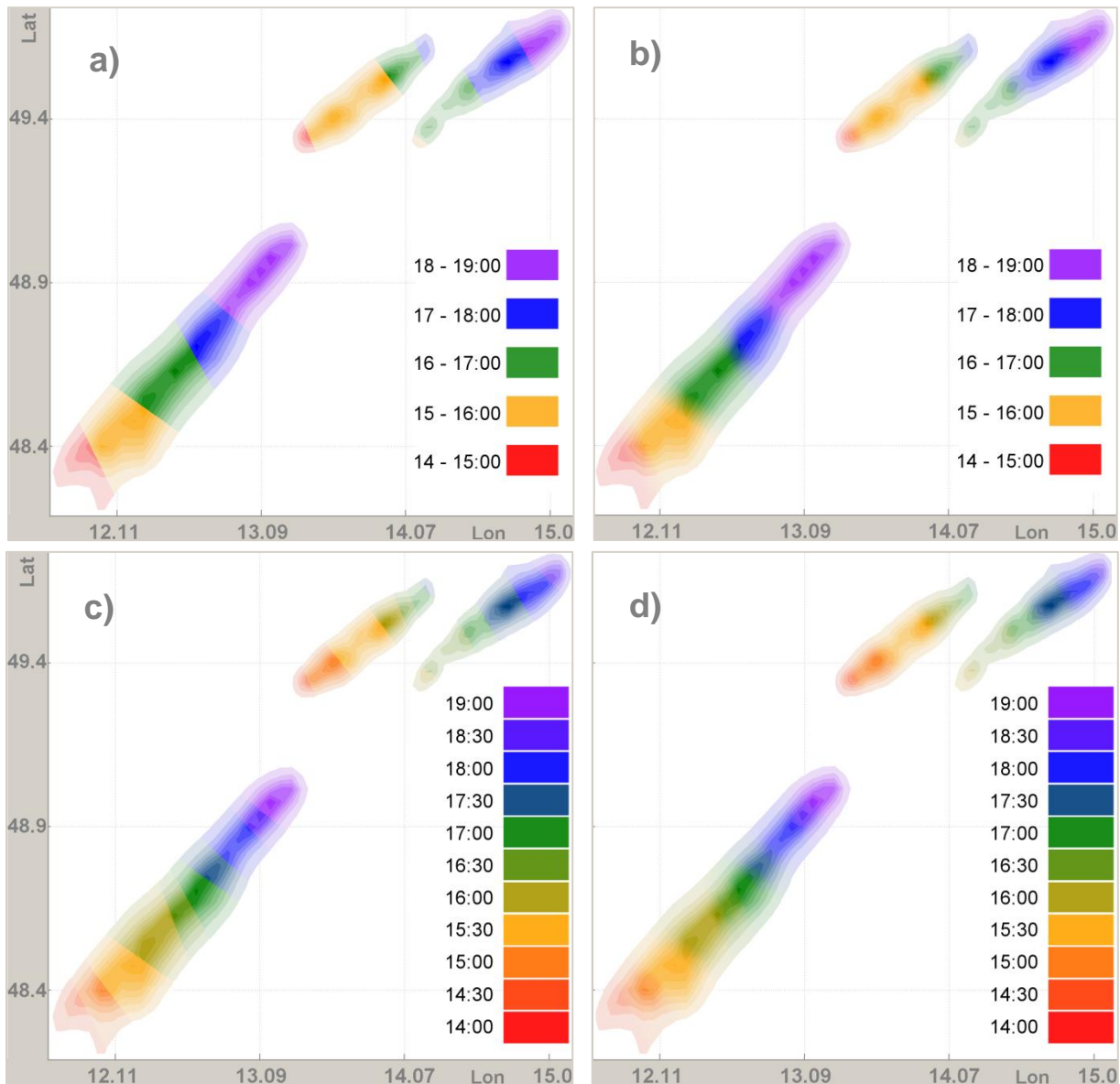


Figure 4-34. STDmap with abrupt (left) or smooth (right) color gradient based on curved tendency lines and the temporal interval of one hour (above) or 30 minutes (below).

Four figures illustrate results for spatio-temporal density maps (STDmaps) based on straight tendency lines with the interval of one hour in Figure 4-33-a and Figure 4-33-b and 30 minutes in Figure 4-33-c and Figure 4-33-d. The color gradients between temporal borders are abrupt in Figure 4-33-a and Figure 4-33-c and smooth in Figure 4-33-d and Figure 4-33-d. Using straight tendency lines, the temporal borders appear parallel to each other, in particular with abrupt color gradients. Larger distances between sequential temporal borders refer to a faster movement phase of the dynamic phenomenon, whereas the closer successive temporal borders indicate a slower movement of the lightning clusters. When fewer temporal segments are used (e.g. five segments in Figure 4-33-a), the map reader may fast and easily extract the distinctive temporal information. When a larger number of temporal segments are used (e.g. in Figure 4-33-c), the map reader has to distinguish between more different colors referring to temporal information. This explorative interpretation becomes more effortful. On the other hand, more temporal segments reveal more details and may thus enable a more comprehensive insight in the dynamics of the data (e.g. temporal change of local point density).

Four further figures illustrate the results for STDmaps based on curved tendency lines. The interval of one hour was used in Figure 4-34-a and Figure 4-34-b and 30 minutes for Figure 4-34-c and Figure 4-34-d. The color gradients between temporal borders are abrupt in Figure 4-34-a and Figure 4-34-c) and smooth Figure 4-34-b and Figure 4-34-d).

A comparison of the results from the straight tendency line with those from the curved tendency line (e.g. Figure 4-33-a with Figure 4-34-a using five temporal segments or Figure 4-33-d with Figure 4-34-d using 11 temporal intervals) clearly shows the visual similarity of STDmaps, particularly in case of a rather large threshold for temporal borders. It can be obviously perceived in all STDmaps that the entire density information is clearly visible while the temporal information about phenomena dynamics in terms of speed and moving direction provides the added value. All lightning clusters are moving northeastwards. The upper left cluster is moving faster around 3:30pm than at any other time and it had two density peaks around 3pm and 4pm.

The clear-cut temporal cluster borders reveal another advantage: Density information in layered tints within each specific time interval is clearly visible and separable from neighboring segments. The smooth color transitions between neighboring segments are closer to the reality and correspond better to the visual perception: lightning points occurring for instance some minutes after 3pm can be located inside the 2-3pm segment and points appearing some minutes before 3pm might be placed inside the 3-4pm segment. With the help of an adaptive slider, the smoothing effect can be set for a small time interval (e.g. 2:55pm – 3:05pm) or a large one (maximum smoothing interval: half of the time interval left and right of the temporal border, e.g. 2:30pm – 3:30pm). Moreover an elastic slider enables the use of different smoothing intervals adaptive to the cluster overlap and thus to the changing cluster speed. In our case we used a threshold of 10 minutes (five minutes before and after each abrupt border line). For an easy comprehension, we suggest to limit the number of colors (time intervals) to no more than about 15.

In case of very extensive temporal range, the brightness of the same tone within the same interval can be adopted. For instance, 24 hours can be cut into six by four hours intervals. Within each interval four different brightness of the same tone can be used.

In order to verify the proposed color mapping, an extensive user evaluation is necessary.

STDmapping approach is suitable for constantly moving SEOs. The approach creates a segmented contour interval for each track. However, the use of abrupt color gradients may lead to temporally wrongly assigned points. The tracking and in particular used clustering method (distance threshold) as well as the temporal segmentation (time intervals and tendency segmentation model) are decisive for the allocation of points to the temporal segments. These decisive steps (parameters) can be adapted to different moving situations along the trajectory. For example, in case a moving SEO changes its speed along the track, temporal intervals and smooth zones could be defined differently in order to reduce wrongly assigned points.

Figure 4-35 illustrates the temporally wrongly assigned points (in black) detected in the STDmap for our test dataset while using a temporal interval of one hour and a linear tendency line. On the left hand side abrupt temporal borders were used and on the right hand side smooth zones (for smooth color transitions) of +/- 10 minutes were applied (semi-transparent light red zones). We assume that the smooth zone visually refers to both adjacent temporal intervals. Out of altogether 6885 points for the 'abrupt' case 788 points (11,4 %) appeared to be assigned wrong and for the 'smooth' case 189 points (2,7 %) appeared to have the wrong temporal color code of the underlying STDmap. Thus, using the smooth STDmap fewer parts are visually allocated to the wrong real temporal interval.

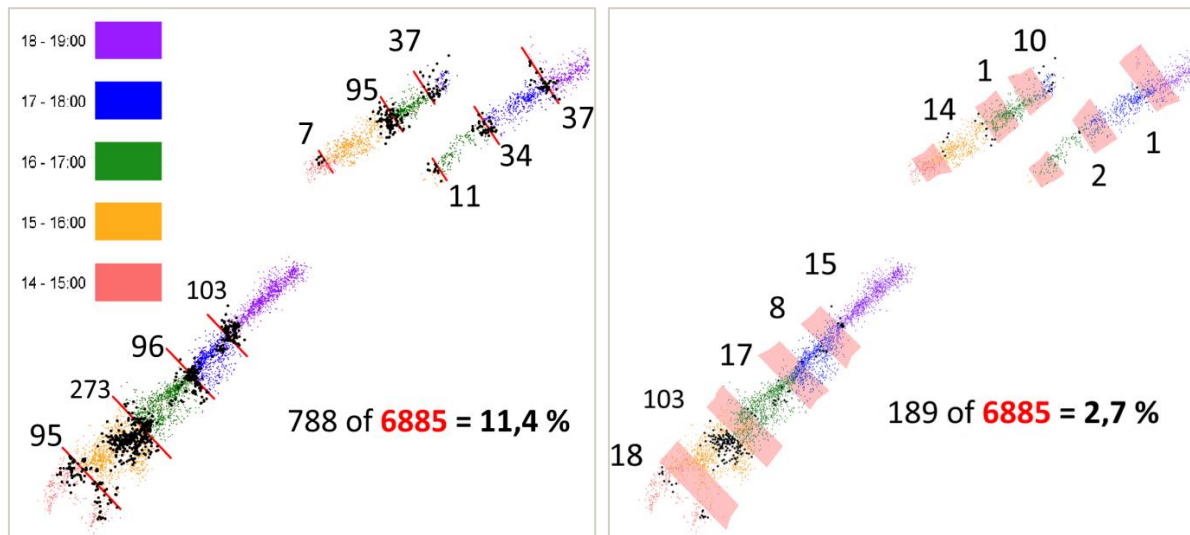


Figure 4-35: Wrongly assigned points (in black), using abrupt (left) or smooth temporal borders (right).

A lower distance threshold leads to fewer dis-allocated points. The smaller the number of temporal intervals, the more cutlines are defined and probably more temporally false allocated points occur. The wider the smooth area the fewer the number of wrongly assigned points. Basically as the tendency line and segmented cuts are more generalized, the more wrongly assigned points occur. Thus a spline tendency line should result in less wrongly assigned points than the use of a linear one. If a point is wrongly assigned, then it is mostly behind the segment border to the next temporal interval. A very slow movement consequently results in a higher number of wrongly assigned points. In case a SEO is moving for- and backwards or intersects a lot with itself, the produced contour intervals would overlap and thus map reading becomes more difficult, even if transparency is applied. A further future challenge is to automatically handle splits and merges of SEOs along the track. Between STDmapping and "KDE maps for each temporal interval" there are certain complementarities. We have shown that for both approaches have their pros and cons. Our proposed STDmap is an alternative procedure to the overlapping KDE maps. Surely, there might be applications for which the use of KDE maps is more appropriate and others for which the STDmapping approach is more suitable. For our application case of moving lightning data, we prefer the use of STDmap. Comprehensive user tests are necessary to verify the right choice for different applications.

4.4. Investigating movement patterns of lightning clusters using visual analytical approaches

Maps provide excellent information about spatial information (location, extension etc.). The dynamic data can be expressed using animated maps or map series. In order to have a closer look into dynamic geodata and their characteristics, we need to develop further visualization methods. This section is focused on the unconventional visualization (maplike and non-cartographic displays) of geographic information representing dynamic phenomena with the lightning dataset as an application case. In chapter 3 an overview of different visualization methods appropriate for the analysis of dynamic SEO was provided. In the following some of those useful methods were applied and adapted to the lightning dataset.

Figure 4-36 illustrates a simple solution for visualizing geometrical attributes of a dynamic lightning cluster using a temporal graph/time plot. The estimated geometrical cluster attributes such as cluster area, point quantity, extension, height and movement distance were determined for

every past time interval. The X-axis represent the cluster life time, starting from time = 0, when the cluster first arises until it disappears. The cluster attributes and their changes in time (x-axis) are displayed in four diagrams, arranged above each other. Thus comparison is possible and correlations can be visually detected. It is evident that cluster area and point quantity in this example correlates positively with each other.

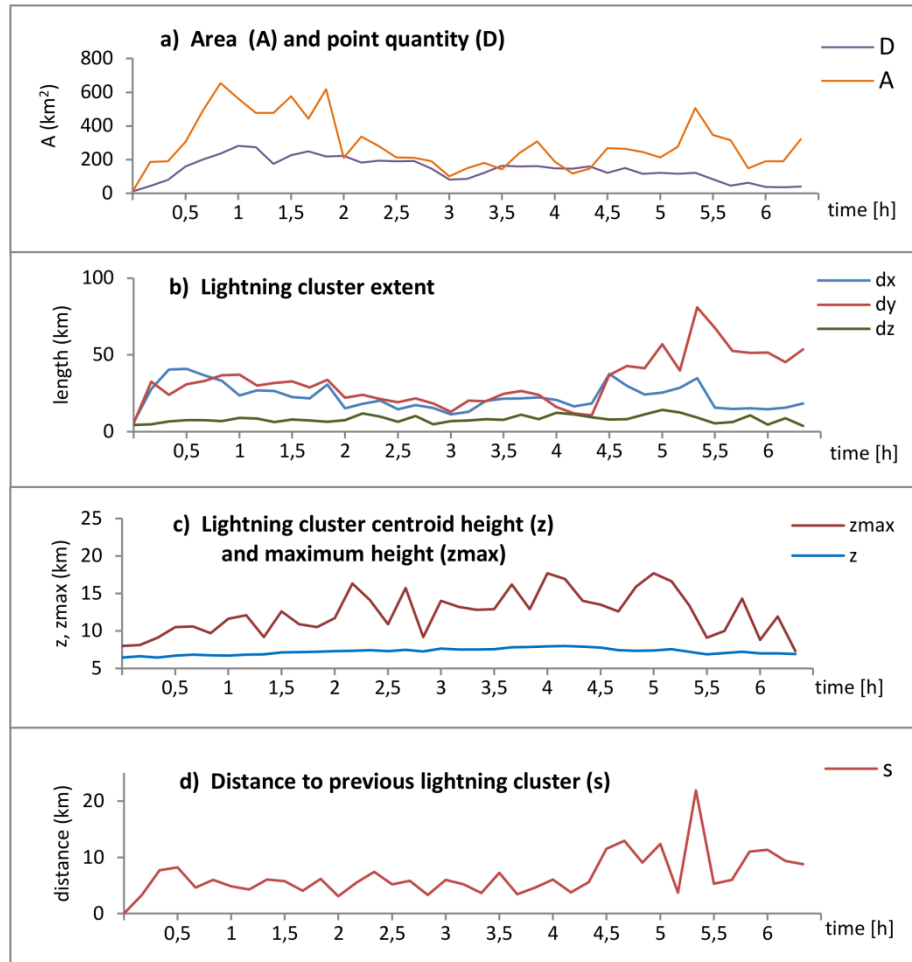


Figure 4-36: Time plot of geometrical cluster attributes.

4.4.1. Trajectory complexity

Moving objects create trajectories of quite complex spatio-temporal constructs (Andrienko & Andrienko 2013). The use of the 3rd dimension is a substantial added value for visual analysis of moving objects. On the one hand, objects moving in 3D space can be thoroughly investigated in 3D visualization (xyz). On the other hand, STCs support temporal exploration of object movements in 2D space. However, visualizing movements in 3D space, e.g. under water or in the air, is a much harder task than movement representation in 2D space (Andrienko & Andrienko 2013). (Hurter et al. 2009; Wiley et al. 2011) provided some examples of visualizing whales and airplanes in 3D space where the interactive tools, animations and multiple co-existing displays help to manipulate data representation and investigate object trajectories.

The complexity of a trajectory can be described using all semantic and geometrical attributes of the moving objects and in particular the degree of their changes, or in other words, by the behavior of object movement. Thus, we could determine complexity differences among trajectories by comparing the change of their movement behaviors in time. Such changes can be derived from database queries or through automatic data analysis. An object moving quite continuously without significant changes in speed, direction and shape reveals a trajectory with a low complexity.

According to Güting et al. (2000), it is possible to capture discrete changes such as sudden turns or high acceleration that happen to the continuously moving objects. If these changes exceed predefined threshold discontinuity occurs. We consider the change of the following geometrical cluster attributes as well as the occurrence of the succeeding situations/events as indicators for lightning trajectory complexity:

Change of geometrical attributes:

- Distance, velocity and acceleration
- Number of lightning points (IC and GC)
- Cluster centroid (latitude, longitude, altitude)
- Cluster extension (2D-area, 3D-volume)
- Movement direction
- Number of neighboring trajectories

Movement events:

- Returns or stops
- Cluster splitting or merging
- Dynamic attributes (time-varying attributes) of interest:
 - o Certain instant, interval, and cumulative attributes such as maximum speed, maximum altitude, maximum lightning point quantity
 - o Date/time components of the time references
 - o Certain attributes expressing relations to the spatio-temporal context
- Intersection with other context elements (locations, discrete objects, SEOs) of interest
- Speed up - slow down' shift
- Major course change (sinuosity, tortuosity)
- Cluster shape change (2D or 3D)

We define the change from speeding up to slowing down as a movement event indicating trajectory complexity. As soon as a lightning cluster changes during moving from speeding up to slowing down or vice versa, we describe this particular moment as significant speed change event. We consider a major course change as another movement event. Different predefined course descriptions such as continuous, episodic, irregular are combined with the current trajectory course taking for instance the last 3-5 time intervals into account. If the course template changes substantially with respect to the previous one, we declare the event of a major course change. Alternatively, a movement direction threshold could be used. For other geometrical attributes, predefined thresholds, also for various degrees of complexity, could be used.

Furthermore, we allocate cluster shapes to predefined templates, such as circle/sphere, ellipse/ellipsoid, 2D/3D irregular shape etc. Based on the coordinates dX, dY, dZ of cluster points describing the spatial extent, comparable shape templates could be automatically identified/allocated for each spatio-temporal lightning cluster. The change of the shape template will then indicate a movement event relevant for the trajectory complexity. Beside these cluster changes, the trajectory lifetime and its spatial length could also imply trajectory complexity as well as the entire shape of the trajectory path.

Our approach will be explained using the largest/longest track of our test dataset as an example. A part of this 'largest track' with its attributes is already documented in Table 4-10 and Figure 4-25. The entire track, its lightning points (IC and GC) in orange as well as its 39 cluster centroids in black are shown in Figure 4-40. For each time interval we compute the change of geometrical cluster attributes with respect to the previous time interval. We consider distance to previous cluster centroid, velocity, acceleration, lightning point quantity, cluster area and volume as well as

movement direction angle. Furthermore, we investigate if movement events are detected, namely, major course change and ‘speed up – slow down’ shift. Table 4-11 illustrates a part of these determined values. Attribute change values are normalized by scaling between 0 and 1 and movement change events are set to 1. In the last column all values of one time interval are added up and the sum reflects the momentary trajectory complexity during a certain time interval. The sum of all time interval change values results in the overall trajectory complexity measure value. Thus, Table 4-11 reflects the complexity gain of a lightning trajectory. We abbreviate that *trajectory complexity gain* with “TCG”. If needed, certain attributes/events in the TCG (e.g. velocity, acceleration) could be weighted with more importance (multiplied with a factor >1), thus, their influence within the complexity sum is stronger than other attributes/events.

Table 4-11: Trajectory complexity based on attribute changes.

| time interval | dis-tance | velocity | accel-eration | no.of light-ning | area | volume | alti-tude | direction angle | course direction | speed up/slow down | sum |
|---------------|-----------|----------|---------------|------------------|------|--------|-----------|-----------------|------------------|--------------------|------------|
| 2 | 0,2 | 0,4 | 0,0 | 0,3 | 0,4 | 0,3 | 0,5 | 0,0 | 0,0 | 0,0 | 2,1 |
| 3 | 0,2 | 0,3 | 0,6 | 0,4 | 0,0 | 0,2 | 0,4 | 0,5 | 0,0 | 0,0 | 2,7 |
| 4 | 0,0 | 0,1 | 0,4 | 0,8 | 0,3 | 0,4 | 0,6 | 0,1 | 0,0 | 1,0 | 3,9 |
| ... | ... | ... | ... | ... | ... | ... | ... | ... | ... | ... | ... |
| 38 | 0,1 | 0,2 | 1,0 | 0,0 | 0,0 | 0,0 | 0,0 | 0,2 | 1,0 | 1,0 | 3,6 |
| 39 | 0,1 | 0,0 | 0,2 | 0,0 | 0,3 | 0,0 | 0,2 | 0,2 | 0,0 | 1,0 | 2,0 |

sum: **118,6**

Based on Table 4-11, the following three figures present multivariate visualizations for the investigation of the TCG. In Figure 4-37 all attribute change and movement event values are stacked for each time interval on a bar chart (TCG bar chart). Not implemented but worth to be mentioned is the use of a pie chart as alternative to a bar chart. In the TCG diagram in Figure 4-38 and Figure 4-39, the change of individual attributes can be easily compared through the connected curve lines. While successive time intervals define the x-axis of Figure 4-37 and Figure 4-38, in Figure 4-39 the travelled distance of the cluster from its birth defines the x-values. Thereby stacked multivariate complexity attributes at different time intervals are drawn and connected where the time intervals are represented through vertical grey lines. Different colors are used to distinguish different attributes, or more precisely, different attribute changes.

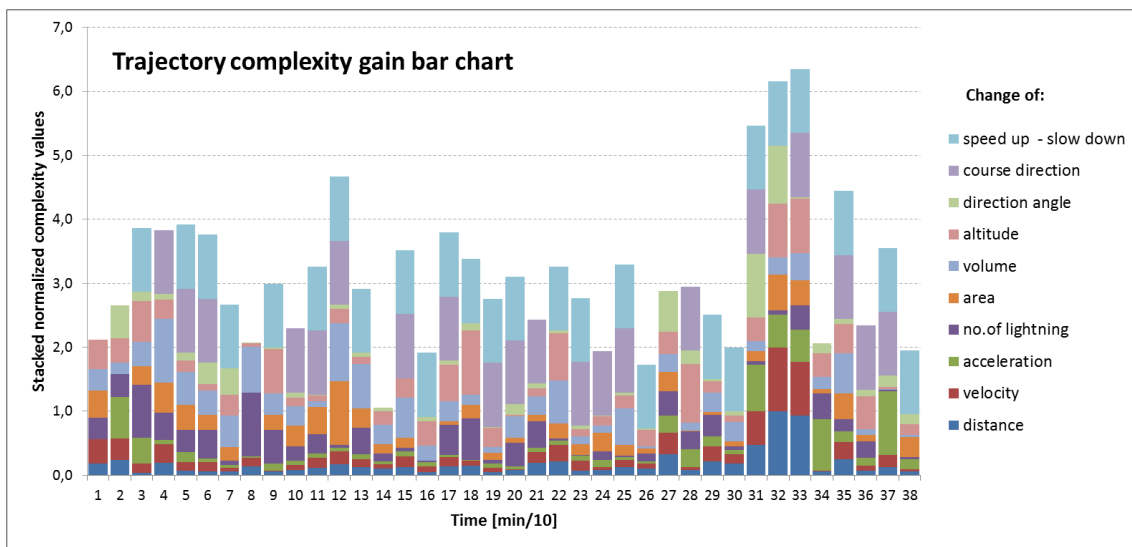


Figure 4-37: The bar chart of the TCG.

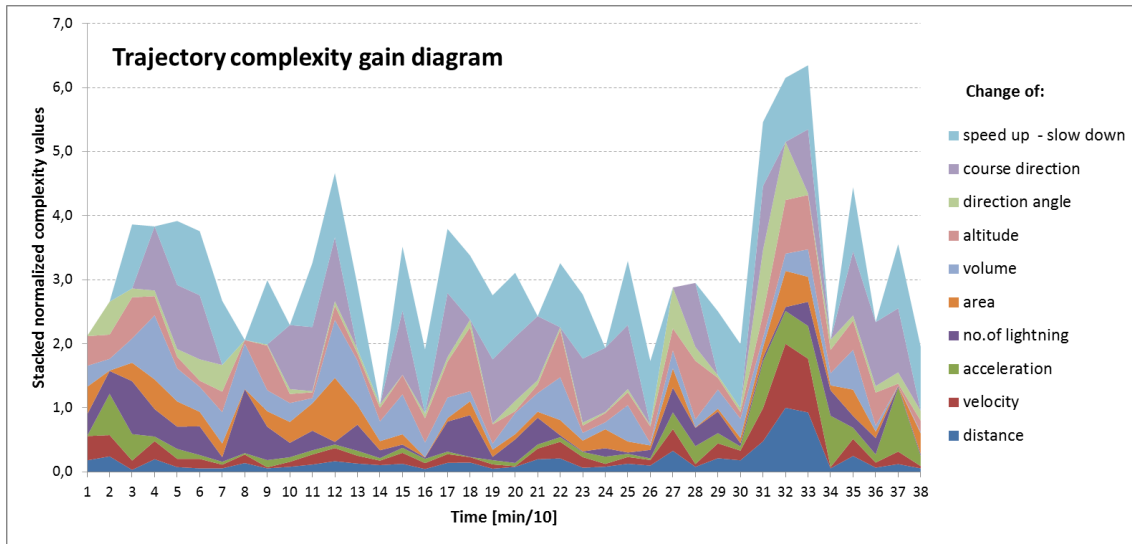


Figure 4-38: The curves of TCG.

A drawback of the complexity curves based on travelled distance is that the changes (complexity values) are difficult to see for very small distances between two successive time intervals/steps. However, this option has the advantage to show precise information of travelled distances and the associated attribute changes and movement events. In our example, it can be seen that a shift from speed up to slow down happens almost during the entire trajectory lifetime. The highest complexity is at the time '33' (330 minutes after start). At this point, distance, velocity and cluster altitude changed dramatically.

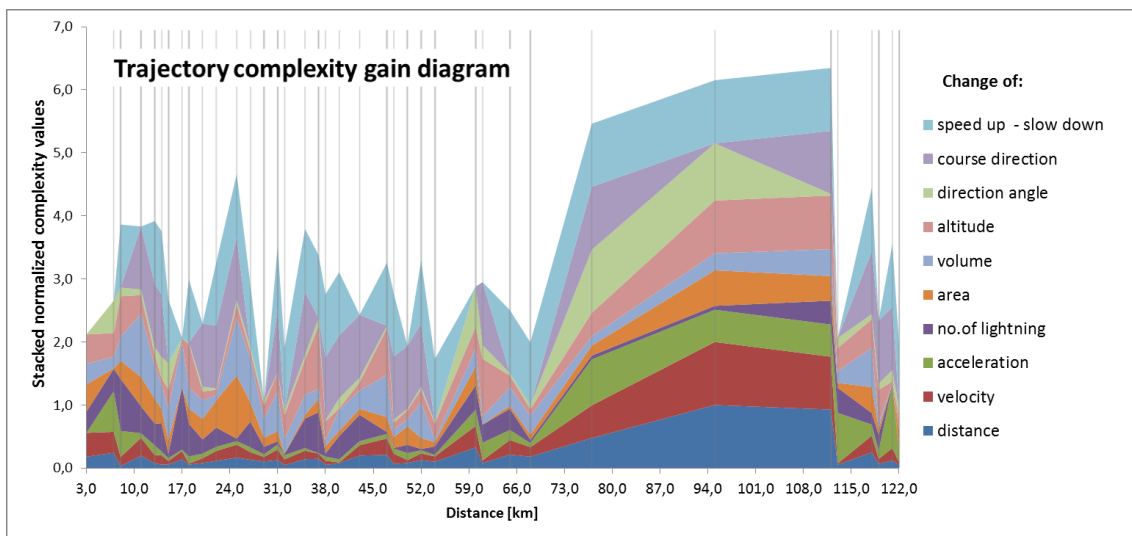


Figure 4-39: TCG - by travelled distance.

Similar to the trajectory wall (Tominski et al. 2012), the stacked complexity values can also be visualized in a 3D visualization, using a geographic map as 2D surface and stacking complexity values in the 3rd dimension (z-axis) along the travelled distance. Thus, spatial information can be presented together with trajectory complexity information. Figure 4-40 illustrates an implementation of that idea: Thereby the stacked normalized complexity values, visualized as bar chart like in Figure 4-37, are used as z-axis and thus form the 3rd dimension on top of 2D map with track points in orange on cluster centroids in black. Cluster attribute changes are stacked in different colors over and between two successive cluster centroids (black dots on the 2D map). In order to improve visual investigation, an offset along z-axis is used. Thus, while interactively exploring the trajectory complexity using a bird view as shown in the screenshot, the stacked values do not

start directly from the 2D surface. Furthermore, a geo-referenced open-street-map is used to improve spatial orientation and bar chart complexity colors are slightly transparent.

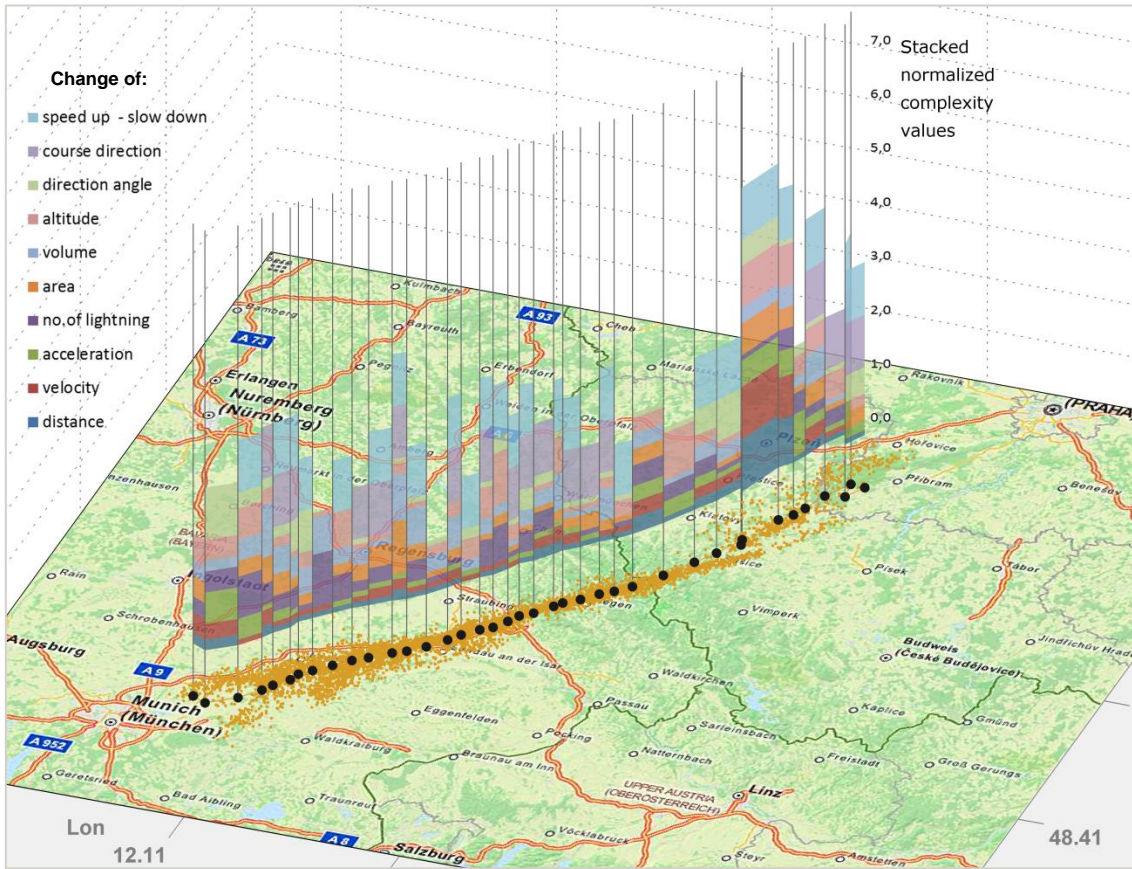


Figure 4-40: TCG bar chart on top of 2D map.

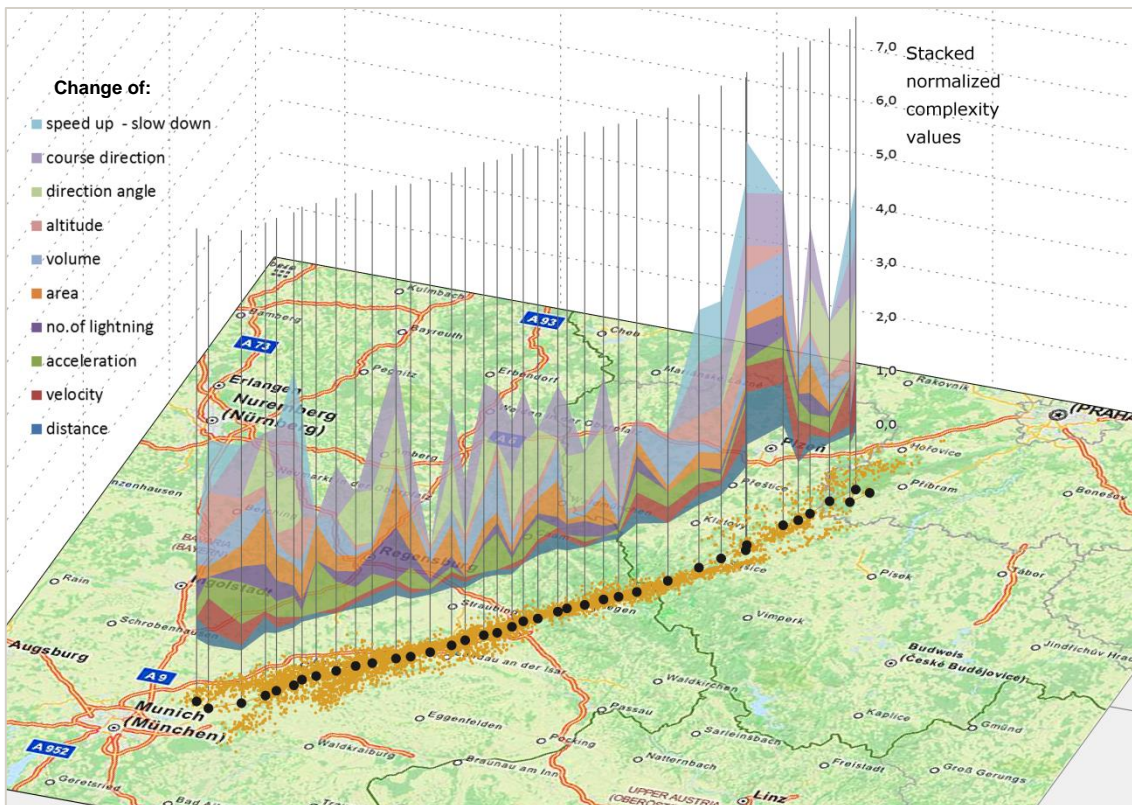


Figure 4-41: TCG diagram on top of 2D map.

The same settings are used in Figure 4-41, but instead of a bar chart, stacked complexity values are connected as in the diagram in Figure 4-39 for a better comparison. Instead of attribute changes between successive clusters, the same visualization can be applied to the actual attribute values. Figure 4-42 demonstrates this option applied to attributes instead of attribute changes as used in the TCG diagram. On the left, attribute values are shown in a connective diagram, while on the right a bar chart is used. Thus attribute values can be visually compared and peaks as well as outliers can be detected. Beside the cluster attributes (distance to previous cluster, velocity, acceleration, lightning point quantity, area, volume, altitude and direction angle), cluster events (course direction, shift from speed up to slow down) are treated as ‘attributes’ – set to ‘1’ if an event occurs, otherwise set to ‘0’. The 2D map including track points in orange and cluster centroids in black provide additional trajectory information.

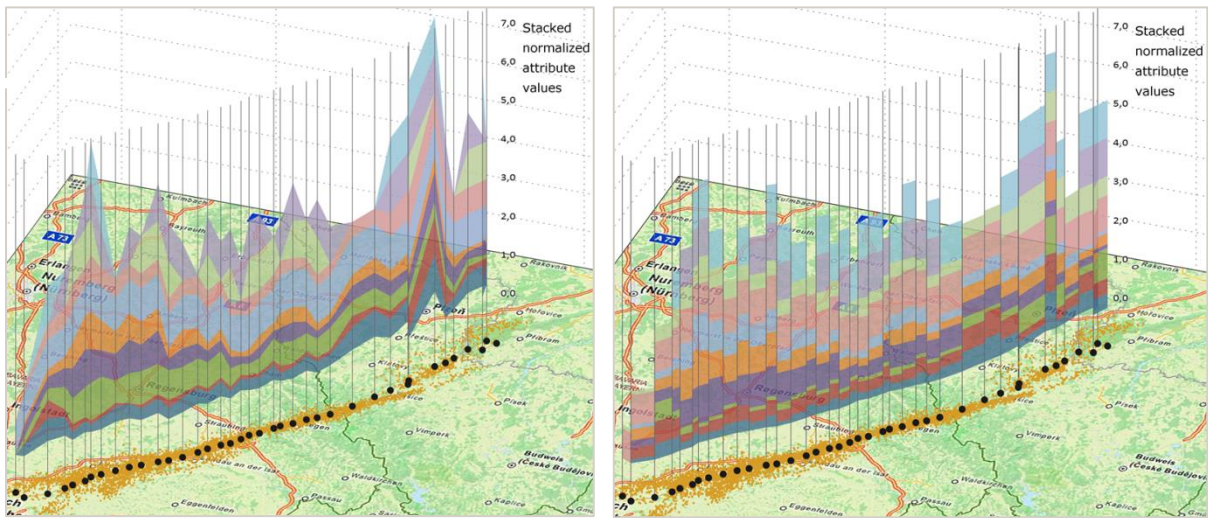


Figure 4-42: Connected stacked normalized cluster attribute value (left) and bar chart (right) on top of 2D map with 2D track points in orange and cluster centroids in black.

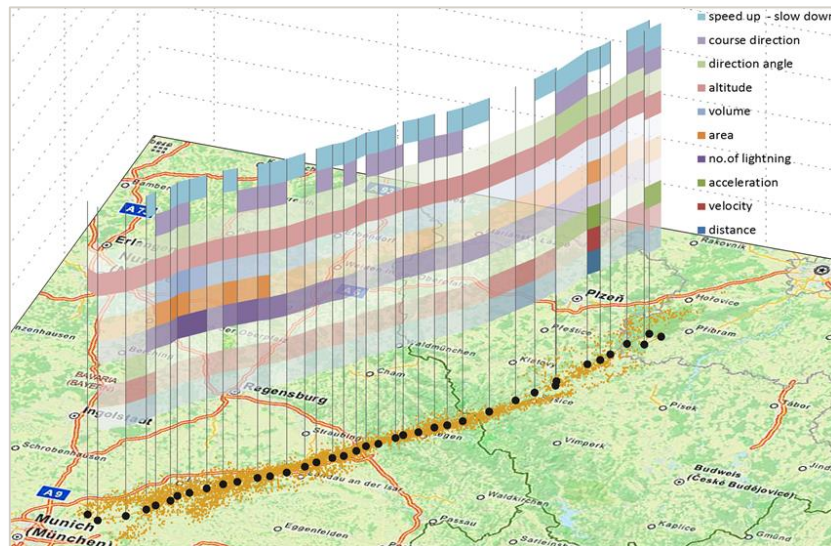


Figure 4-43: Trajectory wall with stacked complexity attribute bands on top of 2D map.

Figure 4-43 illustrates the lightning complexity attributes implemented into a trajectory wall based on (Tominski et al. 2012). Each complexity attribute is represented by its own band. Attribute values are represented by degree of brightness while a large brightness refers to low attribute value and thus to a low complexity. In comparison with the TCG diagram or bar chart, the trajectory wall has the advantage that temporal differences of each attribute are easier to explore along

each band. On the other hand, complexity changes and peaks are easier to detect using the TCG approach (highest z-value) while using the trajectory wall the user need to visually add brightness values of each temporal step, which is a difficult task with doubtful estimated results.

Another option we suggest is an integration of stacked attribute or attribute-change values inside a STC. The STC approach for spatially extended dynamic lightning clusters was already introduced in Section 4.2.4 and shown in Figure 4-16. A selection of complexity values (change of distance, velocity, acceleration, number of lightning points, area) was then integrated into each respective trajectory step of the largest track in the STC as shown in Figure 4-44. Along the z-dimension the sum of stacked complexity attributes was transformed for each time interval (10 minutes). In other words, stacked complexity attributes were normalized to the range from 0 to 10 minutes for each time interval on the z-axis. For the time step with the maximum complexity attribute sum (see Figure 4-37: time step '33'), complexity attributes shown in different colors, fully cover the entire according time interval. Consequently, in all other time steps, the remaining space is shown in light beige color and labeled as 'no attribute'. For this solution a strong user interaction with zooming operation is needed when stacking various attributes.

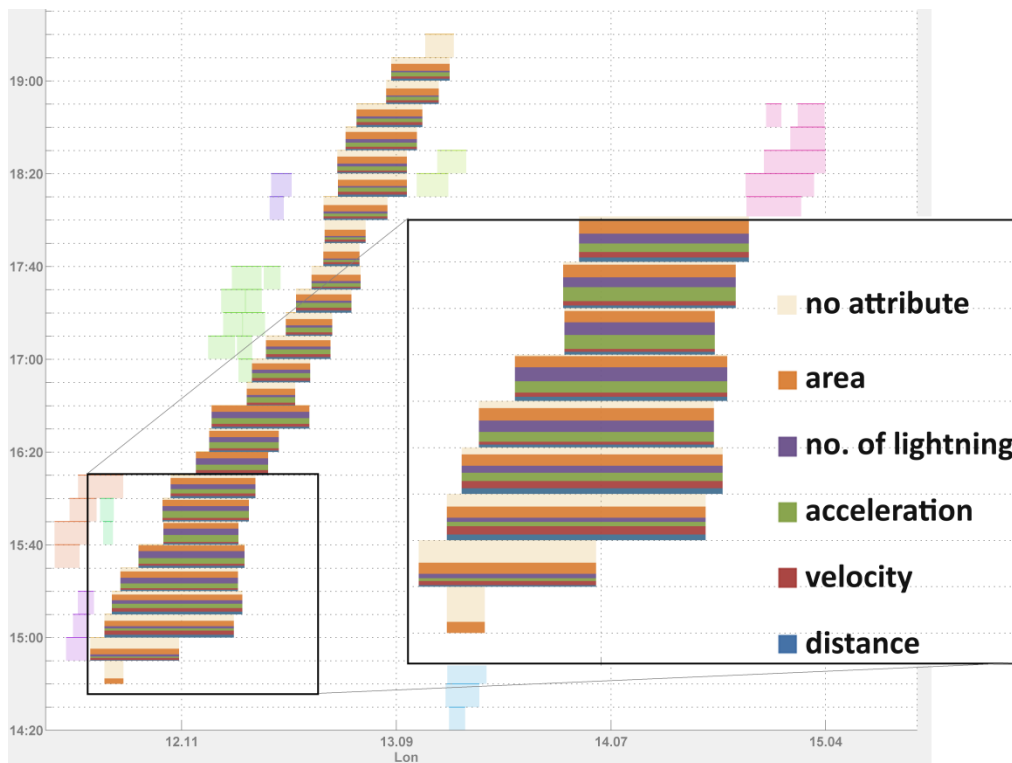


Figure 4-44: STC with stacked attributes values (complexity) applied to one track.

The visual complexity analysis helps to identify unusual trajectory movements and provides quantitative information about the grade or complexity of the dynamics for each time interval. Another option would be to establish complexity analysis for different spatial and temporal scales as well as for aggregated trajectories. In particular information about cluster volumes and altitude supports complexity investigation of the trajectory in 3D. Nevertheless, an additional interactive 3D view would help to understand temporal cluster changes in 3D. If we investigate lightning trajectories as SEOs (2D/3D lanes/polygons), there is not much to find in literature. If we focus on lightning trajectory lines (connected cluster centroids) we could analyze them using approaches presented in Section 2.6, in particular for trajectory comparison on similarity. An approach for lightning trajectory similarities applied to our test dataset is introduced in the following section.

4.4.2. Trajectory similarity

The existing approaches for similarity measurements and visualization for trajectory mainly apply to trajectories of individual moving points and are mostly based on spatial or/and temporal proximity (see Section 2.6).

Comparing lightning tracks is a relevant analysis task for the exploration of lightning data. Geometrical and semantic attributes and their changes of selected tracks can be tested for similarities. In order to compare various cluster attributes of two tracks, which change with time, we suggest a similarity matrix in combination with a similarity bar chart as shown in Figure 4-45. Our similarity matrix is based on trajectories of constant sample rates (in our case of 10 minutes).

Track 4 and 6 occur at the same time (around midnight on 26th of April, 2013) and both tracks are about 80 km away of each other. Comparison is made after 3 hours and 10 minutes, i.e. with 19 time intervals, whereby each row represents one time interval. Altogether 9 cluster attributes are compared: extension (dX, dY, dZ), number of points (No), cluster area (A), volume (Vol), velocity (v), distance to the previous cluster centroid (d) and moving direction angle (α). The attribute values of the first three time intervals are shown in Table 4-12. As can be clearly seen in the map (Figure 4-45), both trajectories nearly move towards the same direction of north-east, have a similar length and follow a similar route. But are they really that much alike as it seems to be?

Table 4-12: Attributes of two different tracks.

| | track 4 | | | | | | | | | track 6 | | | | | | | | |
|------|---------|------|-----|-----|-----|-----|-----|-----|------|---------|-----|-----|-----|-----|-----|-----|-----|-----|
| time | dX | dY | dZ | No | A | Vol | v | d | α | dX | dY | dZ | No | A | Vol | v | d | α |
| 1 | 5 | 5,9 | 2,9 | 22 | 19 | 21 | 0 | 0 | 0 | 9,1 | 6,3 | 6,2 | 19 | 35 | 103 | 0 | 0 | 0 |
| 2 | 11 | 5,4 | 3,4 | 15 | 40 | 56 | 6,5 | 4,8 | 126 | 10 | 10 | 3,3 | 18 | 59 | 92 | 7,4 | 5,2 | 111 |
| 3 | 12 | 7 | 2,8 | 50 | 57 | 88 | 2,4 | 1 | 93 | 6,3 | 7,2 | 8,3 | 21 | 29 | 88 | 5,4 | 3,3 | 106 |
| ... | ... | ... | ... | ... | ... | ... | ... | ... | ... | ... | ... | ... | ... | ... | ... | ... | ... | ... |
| 6 | 15,7 | 11,8 | 4,6 | 111 | 121 | 266 | 6,3 | 2 | 88,3 | 16 | 8,2 | 6,5 | 30 | 80 | 212 | 9,9 | 5,4 | 101 |

We can investigate the similarity of individual attributes, of the entire trajectory or of all attributes at a certain moment of time. In the similarity matrix, the attribute values of each time interval are compared with a maximum similarity of 100 %. We deduct the similarity between two tracks - for each time step and for each attribute as follows:

Equation 6:

$$\text{sim}(ak_{ti}) = (1 - |ak1_{ti} - ak2_{ti}| / \max\{|ak1_{t1} - ak2_{t1}|, \dots, |ak1_{tn} - ak2_{tn}|\}) * 100\%$$

Whereby $\text{sim}(ak_{ti})$ is the similarity of attribute 'ak' of two trajectories at the time 'ti'; it depends on the difference between the two attribute values and the maximum value difference of all attribute value pairs during the entire common lifetime. We can take the number of points (No) as an example while considering only the first three time intervals as listed in Table 4-12. The largest difference in number of points between track 4 and 6 is detected at time step 6, amounts to '81' (111-30) and refers to the lowest similarity which is hence set to 0 %.

Thus, for each of the first three time intervals, the similarity percentages are:

- Time interval 1: $(1 - |22 - 19| / 81) * 100\% = 96,3\%$
- Time interval 2: $(1 - |15 - 18| / 81) * 100\% = 96,3\%$
- Time interval 3: $(1 - |50 - 21| / 81) * 100\% = 64,2\%$

This percentage reflects attribute similarity, shown in the table/matrix middle.

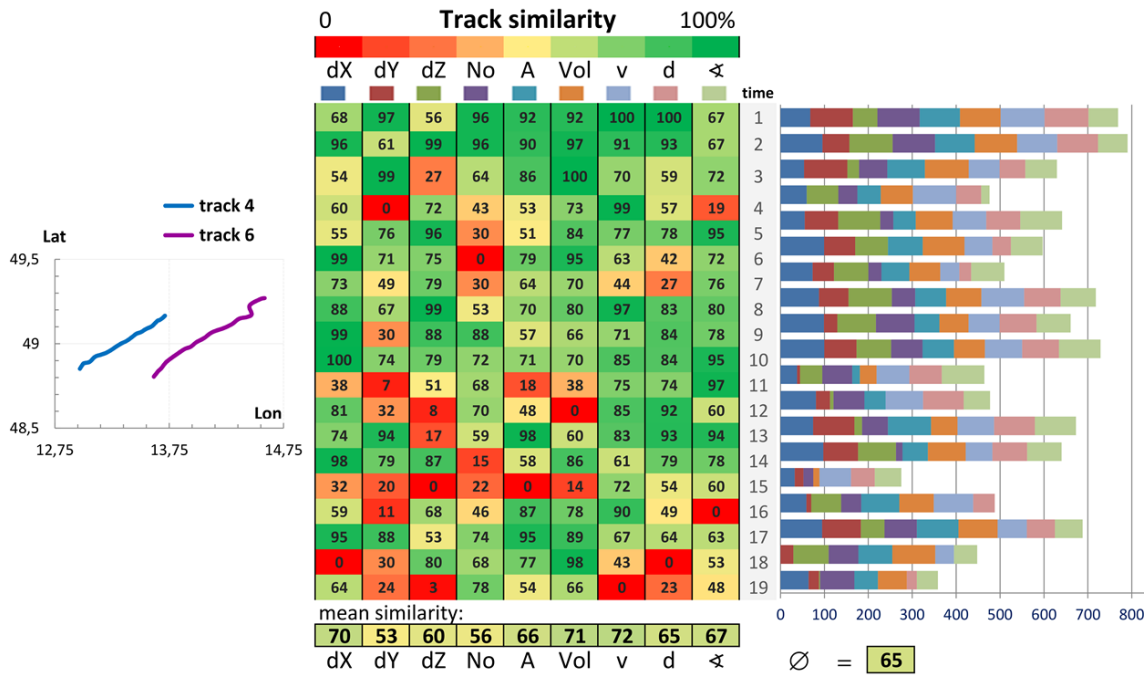


Figure 4-45: Similarity matrix and bar chart of two lightning tracks.

Using a color transition from red (no similarity) to green (identical value) the user can easily identify similarity information in the matrix, identify outliers, similarity changes in a time series and compare similarities of different attributes. The average similarity of each attribute time series is summarized in the table. For example cluster velocity attributes are most similar with an average of 72%. Moreover, the average of all attribute mean similarities is calculated, in our case 65%. For each time interval the bar chart on the left of the similarity matrix provides a quantitative overview about track similarity by adding up all determined attribute similarities. To summarize, track 4 and 6 look quite similar. Using our similarity matrix in combination with the similarity bar chart, we can get an insight into their detailed attribute value differences over time.

The comparison of trajectory dynamics is difficult when they differ in time and it requires the time transformation of trajectories. If two tracks which should be compared do not start at the same moment of time, trajectories can be shifted in time to a common start time or a common end time in order to enable parallel track periods for comparison. However, this approach is limited to trajectories of equal duration. Nevertheless, for tracks of disparate durations, track parts of equal durations can be compared using similarity matrix.

Besides comparing all cluster steps, similarity statements of two trajectories can also be based on statistical/summarized trajectory values, such as average speed, average direction, trajectory lifetime and TCG values. However, the above mentioned cluster-wise comparison supplies more detailed similarity results. Furthermore, the similarity search can be done by comparing cluster- or trajectory shape in 2D or 3D. For that comparison, shape attributes such as shape size, orientation, number of border edges can be considered. In literature a number of techniques for polygon shape matching exists, an overview is provided by Veltkamp & Hagedoorn (2001). Clustering or aggregation based on similarity measures for trajectories can be applied to lightning trajectories. In case that the test dataset is not large enough, spatio-temporal similar trajectories, which are also similar in speed and movement direction, could be grouped using the distance function approach suggested by Pelekis et al. (2007).

4.4.3. Temporal radar plots

Radar plots, also known as Kiviat chart, has been used for years as important visual and descriptive tools for multivariate data (Saary 2008). The principles of radar plots were introduced by Kolence & Kiviat (1973) and specified by Morris (1974). Radar plots are circular graphs consisting of a series of spikes or rays projected from a central point. Each spike represents a different variable label. The ray lengths are related to the values of the variables and the ray positions are connected with the neighboring variable values to form an radar figure (Saary 2008). Significant perceptual properties are size and shape of the resulting enclosed radar figure. Using a series of variable values, the resulting overlapping radar figures may indicate certain value distribution, correlation, outliers, peaks and thus common data patterns. However, the use of too many entries inside a radar plot may result in overplotting and difficult visual interpretation. An interactive use (e.g. radar figure selection, enabling and disabling) of the radar plot can overcome this drawback. Furthermore, radar plot interpretation requires a trained eye and data background understanding.

Being aware of the characteristics of radar plots, we raised the question if this graphic form can contribute to the visual analysis of dynamic SEOs. In the case of moving lightning clusters we included the following variables in a radar plot: latitude, longitude, cluster point quantity, cluster area and volume, velocity and distance to the previous cluster. All these variables change in time. Furthermore, we included the time itself as a variable. The results are drawn in Figure 4-46 where the lightning cluster variables of April 26th 2014 were used with 102 values for each of the 8 variables. All were normalized to the range from 0 to 1. Thus, the radar plot is less overloaded with axes information. However, spike axes labeling or legend is needed to communicate the exact geometrical attribute value and value range.

Spikes are displayed in different grays. The radar plot contains spatio-temporal information and reveals on the one hand information about similar clusters and on the other hand information about unique clusters and clusters attributes. An interactive use provides more insight into the radar plot. In Figure 4-46 two lightning clusters are selected and highlighted: cluster number 86 (spike in blue) and 27 (spike in red). The radar plot reveals that the blue one is the fastest cluster on April 26th and the red one the largest containing the most points inside a cluster. The visual analysis of the radar plot could be improved by changing it into an interactive explorable “temporal radar plot”. For our case we suggest to use the time as z-axis as illustrated in Figure 4-47.

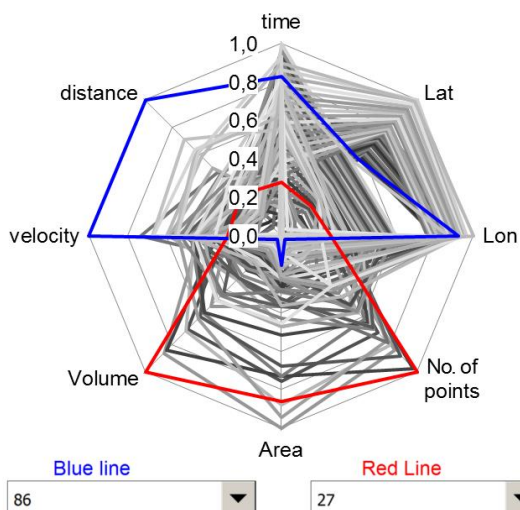


Figure 4-46: Radar plot with interactive cluster selection.

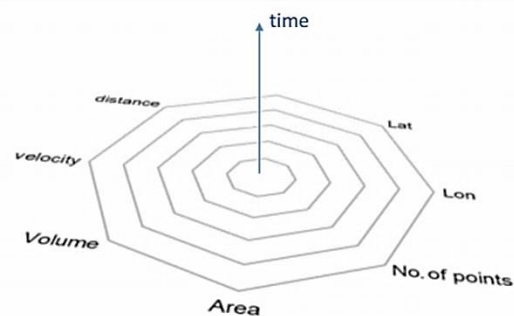


Figure 4-47: A “temporal radar plot”.

A “temporal radar plot” takes the form of an extruded polyeder. All k attributes except the time are included in a normal radar plot which varies along the time axis. In this way, the varying attribute values and locations with the time is embraced within a polyeder which is a sequentially layered radar plot along the the time axis. This polyeder allows the user a better insight into the attribute changes without overlapping and occlusion which used to be a major problem in traditional 2D radar plot consisting of a large dataset. A high level of interactive use is essential for the user to extract interesting information from the temporal radar plot. Figure 4-48 presents a temporal radar plot of the lightning test dataset on April 26th.

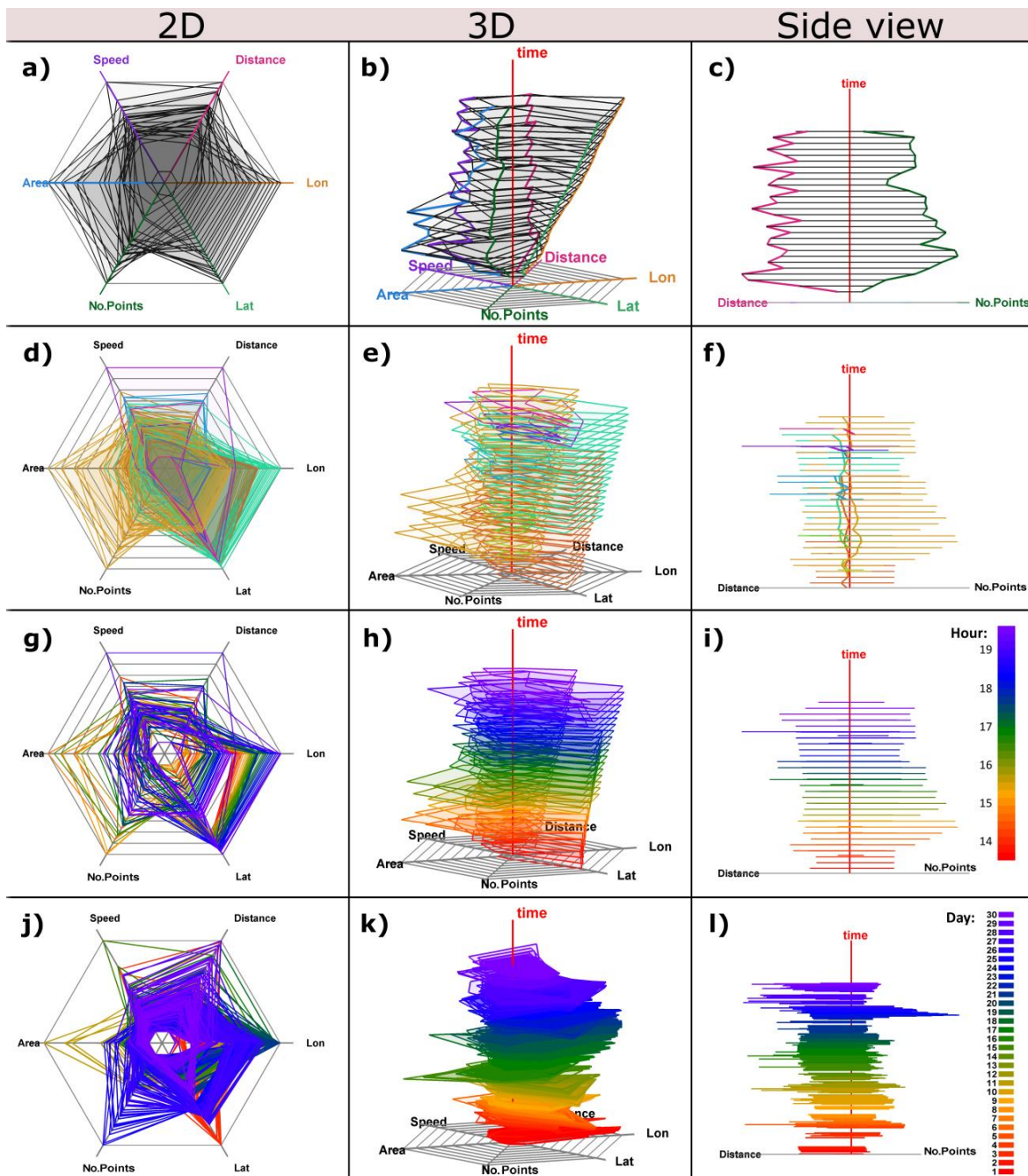


Figure 4-48: A temporal radar plot of the lightning data: from above (2D), 3D and side perspective a-c) show 1 single track while attributes are drawn in different colors; d-f) display 11 tracks colored by track affiliation on April 26th; g-i) show 11 tracks on April 26th with a time-based rainbow color scheme; j-l) contain all tracks during April with rainbow-time-color scheme.

The illustration is composed of three columns and four rows. In the left column 2D radar plots are shown. In the middle the corresponding temporal radar plots are presented and side views are

chosen in the right column showing the temporal development of two attributes (in this case 'distance of the lightning cluster centroid towards the previous one' and 'number of lightning points within one cluster').

Different rows in Figure 4-48 contain different test datasets: In the first row (a-c) a single lightning track is shown, consisting of 27 successively occurring clusters (duration of altogether 4 hours during April 26th 2013). The spikes representing the cluster attributes are displayed in gray. Cluster attributes (cluster centroid longitude and latitude, number of points, area, velocity and distance to previous cluster) are distinguished by colors and temporally connected values in 3D are expressed using the same color. With the help of side views two attribute courses can be compared (e.g. as in Figure 4-48-c 'distance to previous cluster' with 'number of cluster points'). A change of the side view angle or an adaption of the attribute/spike order allows the comparison of different pairs of attribute courses. In the second row (d-f) all lightning trajectories of April 26th 2013 (from 2pm to 7pm) are included in the polyeder. Spikes are drawn in different colors. 11 distinguishable colors refer to different track affiliations. Furthermore, the radar figure centroids are computed and connected through lines in the same track colors. Thus the changes in time are visually presented. In the third row (g-i) the same lightning cluster data of the 11 tracks are shown, but the spike colors are differentiated by a rainbow color scheme indicating different times when the corresponding lightning cluster occurred. The rainbow spectrum (as described in Section 4.3) can be divided into a certain number of intervals or smoothly transitions between the neighboring colors. The same color concept is applied to the lightning cluster data of the entire month of April 2013 shown in the last row (Figure 4-48-j,k,l). The applied rainbow color spectrum is illustrated in the legend of Figure 4-48-i,l. The use of time-dependent rainbow color scheme within the original 2D radar plot (as shown in Figure 4-48-g,j) provide temporal information and thus changes of the spikes in time can be visually analyzed much better than using time as an additional variable axis. However, facing large datasets, overlapping and occlusion are inevitable, making the visual exploration within the 2D plot difficult. The temporal radar plot along with its interactive use (zoom, pan, rotate, highlight by click, etc.) may overcome this drawback.

4.4.4. Temporal PCP

Inselberg was one of the first authors who introduced a visual approach called parallel coordinate plot, abbreviated as 'PCP' (Inselberg 1985), although the idea already existed. As early as 1880 Veltkamp & Hagedoorn (2001) illustrated different statistics of US states in a PCP like graph. PCP illustrates a k-dimensional data entry as a polyline on a plane plot by using k equidistant vertical axes parallel to each other. Each polyline intersects each axis at the location corresponding to the data value for that respective dimension. Each axis includes all data values of the corresponding dimension from the minimum to the maximum and axes are linearly scaled.

Similar to radar plots in the previous section, we included the same attributes of lightning cluster which represent the data dynamics in a PCP. Figure 4-49 shows the resulting PCP with lightning cluster attributes of April 26th. The altogether 102 polylines are colored in different gray tones. Two individual polylines can be interactively highlighted and thus compared (red and blue line). The plot visually provides spatio-temporal information. Time is used for the 1st axis. Temporal changes of geometrical attributes can be identified. However, a dataset of 102 entries has already made the change detection of temporal attribute an endeavor. The PCP interpretation also demands trained eyes. Large datasets may make the PCP difficult to read and require necessary simplification (line clustering) to improve the clarity.

In visual analytics of multivariate data, PCPs are often used together with several synchronized map- and graphic displays. The interactive change of a display triggers the synchronized change to all other displays, which can enable a direct visual comparison. An example for such visualiza-

tion system is provided by Guo et al. (2006), who combined PCP with *self-organized maps*, an attribute matrix and *small multiple maps*.

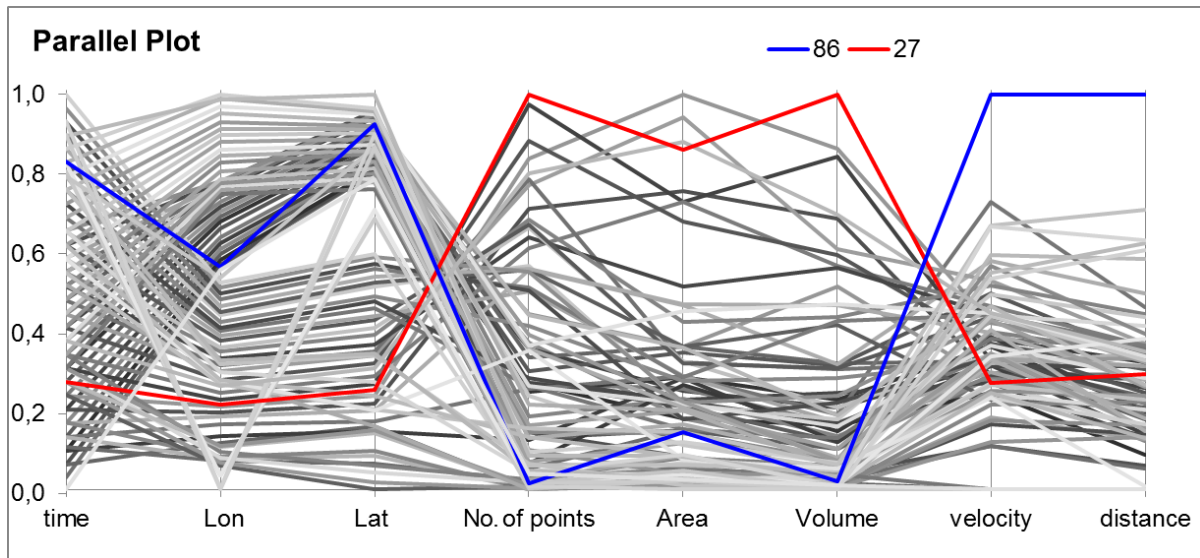


Figure 4-49: Parallel plot with the interactive highlighting of two clusters.

The idea of an extension of the PCP towards 3D was mentioned in various papers (Edsall 2003; Guo et al. 2011; Wegenkittl et al. 1997). Tominski et al. (2004) introduced a radial arrangement of PCP axes in 2D and 3D space called “Multi Comb” in combination with interactive axes. Streit et al. (2006) clustered polylines of a PCP using image processing tools after rasterization (Figure 4-50 left). In a second step (Figure 4-50 right) a third dimension was introduced whereby pixel density values (z-axis) were visualized.

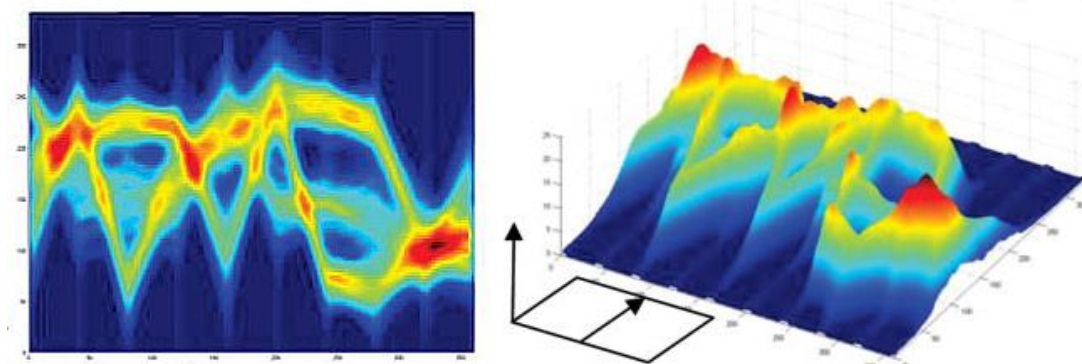


Figure 4-50: Clustered PCP lines (left), resulting 3D PCP (right), source: Streit et al. (2006).

Rübel et al. (2006) suggested a 3D PCP approach for gene data analysis which basically projects the PCP polylines on the x-z plane and extend the display with a third dimension in order to compare the attribute values of different genes, see Figure 4-51.

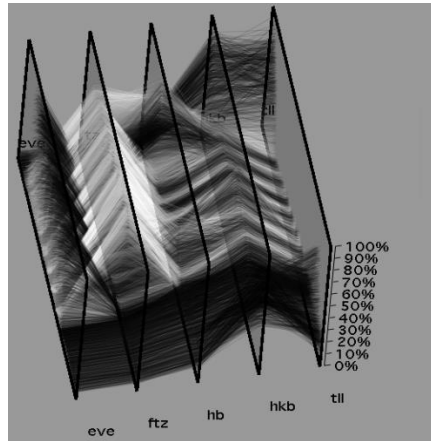


Figure 4-51: 3D PCP, source: Rübel et al. (2006).

Similar to the idea of Rübel et al., we suggest another extension of the PCP towards the temporal 3D PCP. We take the original plane view (x-y) of the PCP as basis and add – vertical to it – time as a new dimension.

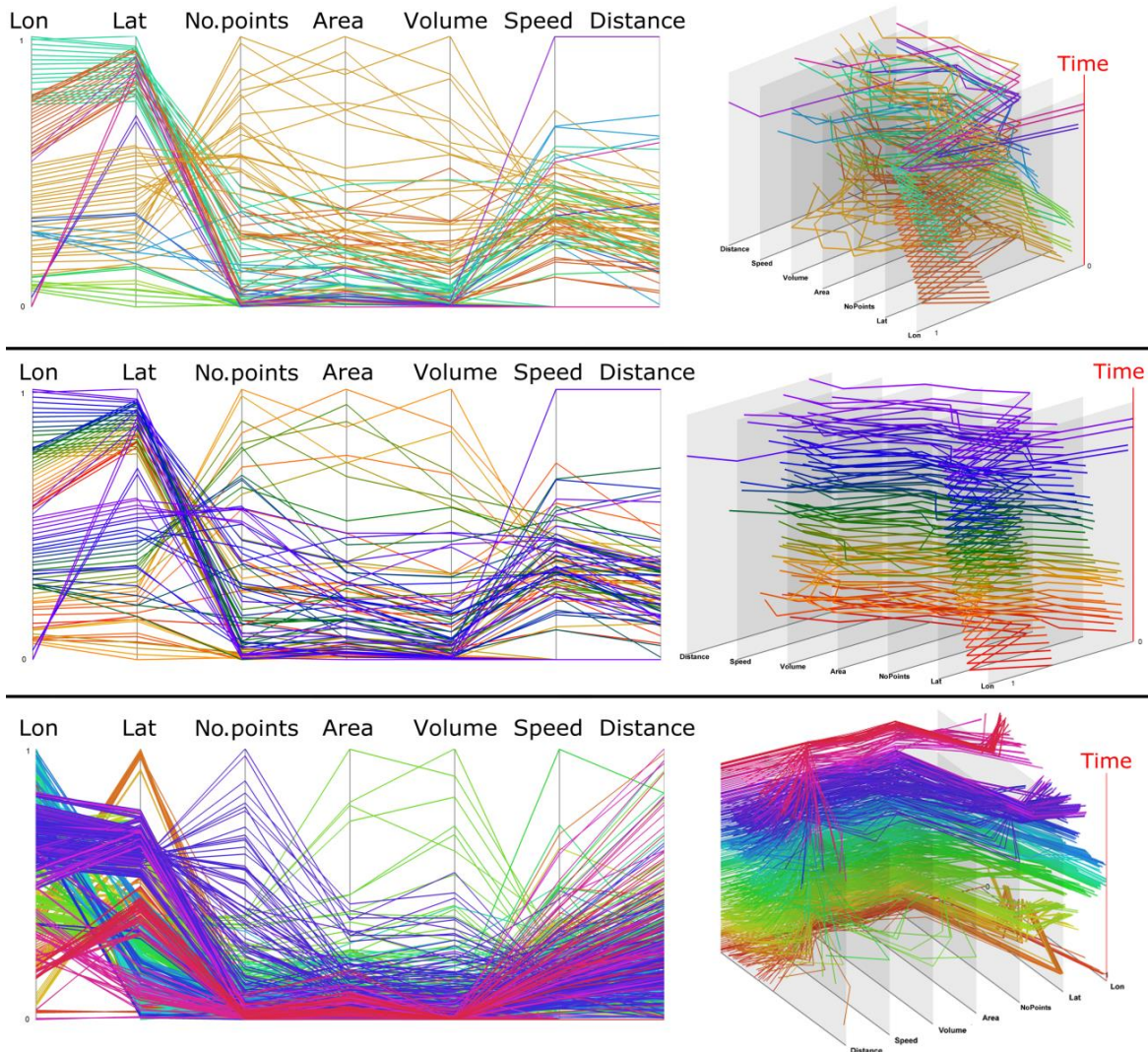


Figure 4-52: PCP (left) vs. temporal PCP (right) for lightning test dataset
 above: track-based polyline colors (April 26th 2013, 2-7pm)
 middle: time-based rainbow-colored polylines (April 26th 2013, 2-7pm)
 below: time-based rainbow-colored polylines (entire April 2013).

The results are presented in Figure 4-52. Three examples consist of the original PCP (left) and the extended approach of temporal PCP (right). On the top of Figure 4-52 lightning cluster and their attributes of April 26th are used. Polylines are distinguished by different track colors. The second example also includes all 11 tracks and their allocated clusters, but the polylines are distinguished by time-depending colors using the rainbow color scheme as explained in Section 4.3. The third example presented in Figure 4-52 (below) contains all clusters of April 2013. The polylines again are distinguished by colors referring to the respective lightning cluster time interval while using the rainbow color scheme. In comparison with the PCP, the interactive exploration of temporal PCP provides the additional insight into the temporal data patterns.

The visual exploration of PCP and temporal PCP might suffer from overlapping polylines of large datasets. Based on a classification solution for PCP introduced by Edsall (2003), polylines of the temporal PCP belonging to certain time intervals could be aggregated to polygons in order to improve pattern identification.

4.4.5. Table lens

To combine the overview and detailed information in one display is not an easy task, neither for visualization designers nor for users. One common information visualization method which can be used to solve this problem is table lenses introduced by Rao & Card (1994). Table lenses help to explore large amounts of tabular data, following the spreadsheet principle. In a table lens, attribute values are illustrated in columns and rows. The table cells are filled with colored and scaled horizontal bars. Each column represents a specific attribute and each row corresponds to all attributes of a single data object. Thus each column can be seen as a histogram. Table lenses contribute to visually identifying correlations among pairs of numerical attributes (Rao & Card 1994).

We adapted the table lens concept in order to visually analyze the lightning tracks during April 2013 within our test area. The results are illustrated in Figure 4-53. Six lightning tracks are shown, each track ID is displayed in the first column. The track data are arranged in rows. Each row represents one of 152 clusters. The ID of each cluster is shown in the third column. We extended the table lens in order to represent spatio-temporal data information. In the first column labeled as "lat-lon", the bar lengths differentiate only in colors, not in lengths. Above the table lens a spatial mosaic provides basic information where the respective lightning cluster is spatially located. The time is shown in the second column, whereas tracks and clusters are temporally sorted from bottom to top. Further cluster attributes included in the table lens are point quantity (in blue), cluster extension (in purple), cluster area and volume (in red) and cluster velocity and distance to the previous cluster (in green).

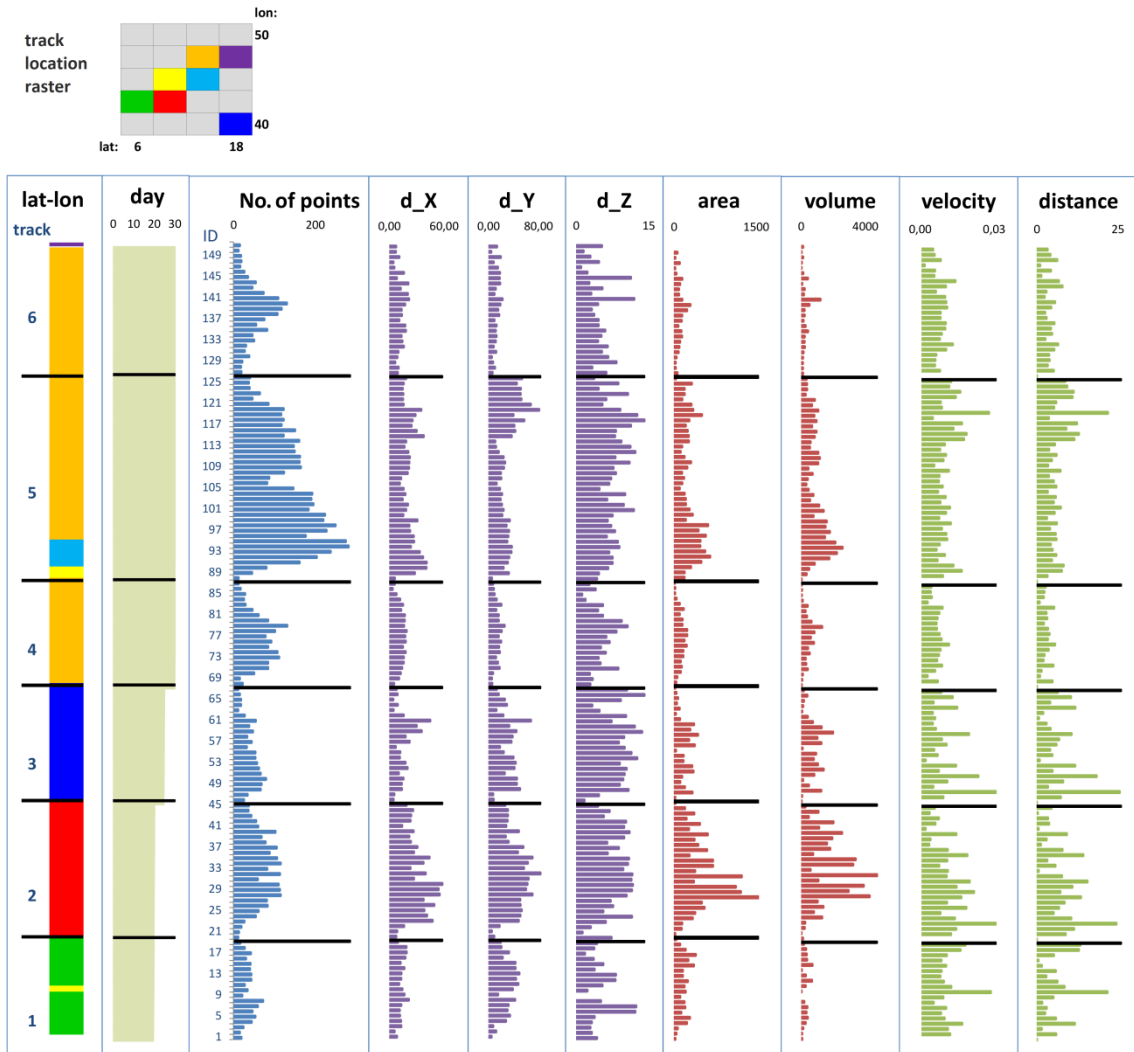


Figure 4-53: The table lens representing attributes and their values of six different lightning tracks.

An advantage of the table lens is that it enables visual exploration of large datasets: it provides information about data distribution and correlations among attributes. Another benefit is that it is easy to read since the spreadsheet display is a generally known visualization. Through an interactive use, scaling (zoom in and out), accessibility of numeric information (via click) or individual adaption of the table organization (re-organization of rows and columns) are possible.

4.4.6. Multivariate visual analytics of lightning data

In the previous section we introduced various visualization techniques which supports space time analysis of dynamic geodata and their attributes, in particular for SEOs. Visual analytics is a comprehensive approach for the visualization-supported analysis of dynamic geodata and their attributes. Often a visual analytics approach doesn't consist of a single graphic method, but of several synchronized complementary methods. We implemented a multivariate visual analytical toolbox for the lightning test dataset as illustrated in Figure 4-54.

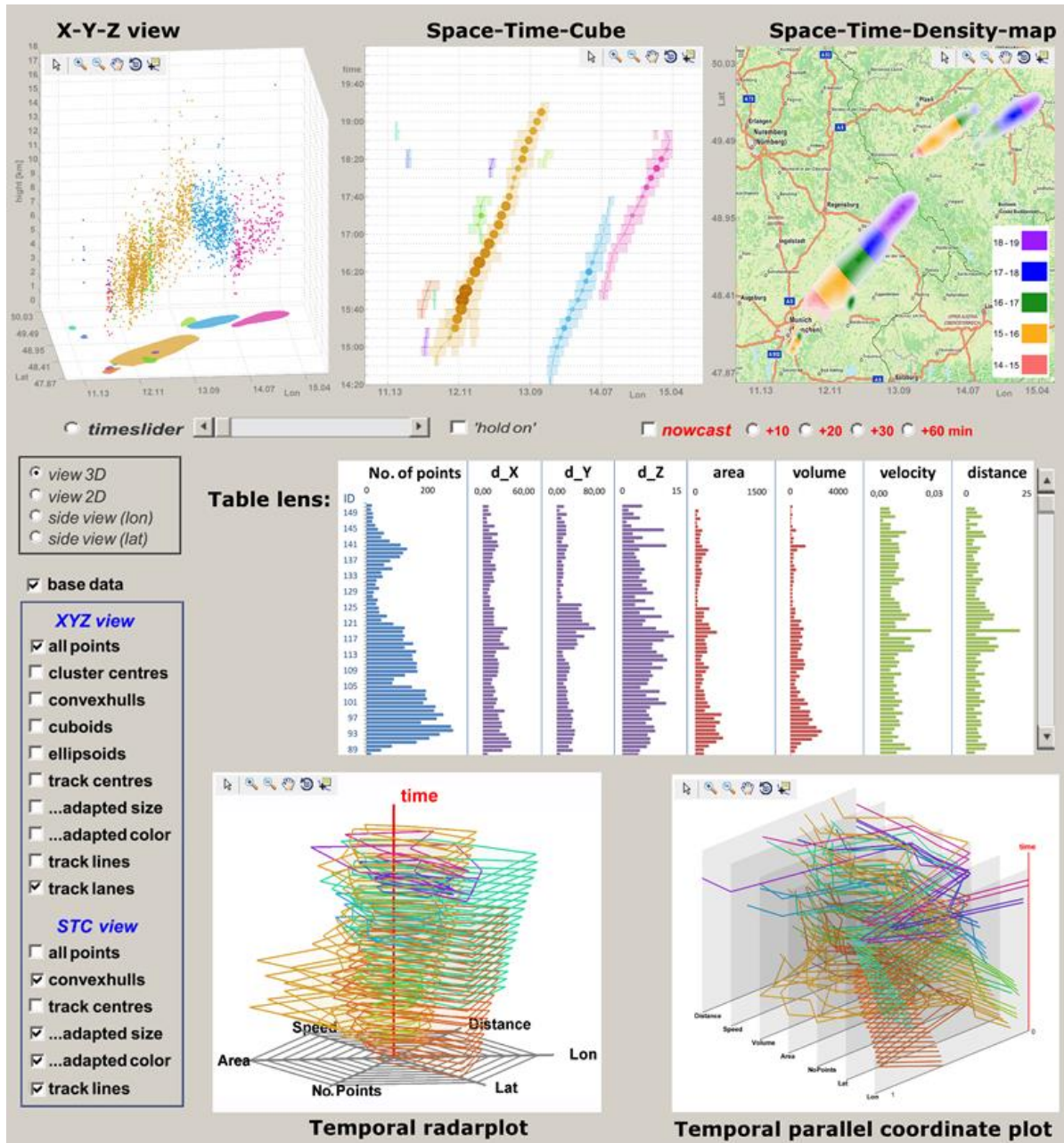


Figure 4-54: Multivariate visual analytics for lightning data (April 26th).

The toolbox consists of 2D/3D display for geographic track- and cluster visualization, STC, STDmap, table lens, temporal radar plot and temporal PCP. All displays are synchronized. Thus, when an object in one display is highlighted (e.g. one particular lightning cluster of interest), the object will be highlighted in all other displays. The same applies to enabling/disabling of objects, zooming and panning or using the time slider tool.

It has to be noted that the proposed visual analytical approaches for lightning cluster attribute investigations along a trajectory use cluster attributes in different units. That might not be suitable for direct comparison. To overcome this drawback, different attribute weights could be introduced. Using Matlab software on a computer with a CPU of 2,13 GHz and 4 GB RAM, the estimated runtime for processing lightning clusters and trajectories including different visualization options out of the entire test dataset (April 2013) including 70007 initial lightning points, is about 6 hours.

4.5. Discussion of the proposed visual explorative approaches for lightning movements

The visual analysis of dynamic lightning data can be focused not only on one or several lightning clusters, but also on one or several trajectories. Particular clusters/trajectories of interest can be selected while the selection could be based on certain spatial or/and temporal extension or on certain attribute information, such as cluster speed or moving direction. Table 4-13 provides a matrix overview of the proposed visual analytical approaches in relation to lightning cluster attributes and movement events. The table columns indicate and specify which cluster attributes and movement events can be addressed by which visual analytical approaches.

Table 4-13: The relative suitability of proposed visual analytical approaches for lightning cluster attributes and movement events

| | | TCG diagram ^I | Similarity matrix and bar chart ^{II} | Temporal Radar plot | Temporal PCP | Table lens | Time plot | |
|------------------------------|--|--------------------------|---|---------------------|--------------|------------|-----------|--------|
| Lightning cluster attributes | Time info (step no.) | Green | Green | Green | Green | Green | Green | |
| | Centroid | Lat | Yellow | Yellow | Green | Green | Yellow | Yellow |
| | | Lon | Yellow | Yellow | Green | Green | Yellow | Yellow |
| | | Alt | Green | Yellow | Yellow | Yellow | Yellow | Yellow |
| | Extension | dx | Yellow | Green | Yellow | Yellow | Green | Green |
| | | dy | Yellow | Green | Yellow | Yellow | Green | Green |
| | | dz | Yellow | Green | Yellow | Yellow | Green | Green |
| | | Area | Green | Green | Green | Green | Green | Green |
| | | Volume | Green | Green | Green | Green | Green | Yellow |
| | Internal structure | No. points | Green | Green | Green | Green | Yellow | Green |
| | | No. IC | Yellow | Yellow | Yellow | Yellow | Yellow | Yellow |
| | | No. GC | Yellow | Yellow | Yellow | Yellow | Yellow | Yellow |
| | | Density | Yellow | Yellow | Yellow | Yellow | Yellow | Yellow |
| | Movement information | Velocity | Green | Yellow | Green | Green | Green | Yellow |
| | | Acceleration | Green | Yellow | Yellow | Yellow | Yellow | Yellow |
| | | Direction | Green | Green | Yellow | Yellow | Yellow | Yellow |
| Distance | | Green | Green | Green | Green | Green | Green | |
| Cluster movement events | Returns, stops | Yellow | Red | Red | Red | Yellow | Yellow | |
| | Cluster splitting or merging | Yellow | Red | Red | Red | Yellow | Yellow | |
| | Cluster shape change (grow shrink deform) | Yellow | Red | Red | Red | Yellow | Yellow | |
| | Interactions with other objects or locations | Yellow | Red | Red | Red | Yellow | Yellow | |
| | Particular attribute values (maximum altitude) | Yellow | Red | Red | Red | Yellow | Yellow | |
| | Speed up - slow down shift | Green | Red | Red | Red | Yellow | Yellow | |
| | Major course change | Green | Red | Red | Red | Yellow | Yellow | |

colors: red = restrictively usable method, yellow = possible, green: implemented

^I attribute change of consecutive clusters

^{II} attribute change of two clusters belonging to two different trajectories

We distinguished between three categories: red indicates that the approach is only restrictively usable; yellow refers to that the approach is appropriate to use and green states that the approach is appropriate and was also implemented for lightning data in this thesis. Events are treated as attributes by using for example the value '1' and '0' if the event takes place or not. In TCG diagrams the attribute value changes of consecutive trajectory clusters are presented. The same applies to the similarity matrix of two selected trajectories. Two movement events 'cluster births' and 'disappearances' are not explicitly included in the table, because for our application case each approach starts with trajectory birth and ends with its disappearance.

An integration/combination of the TCG diagram on top of a 2D map display or inside the STC is illustrated in Figure 4-40 - Figure 4-44, where attributive cluster information is visually connected with the respective spatial location and thus allows an additionally insight into the trajectory complexity. Furthermore, the following trajectory attributes can be considered in the TCG diagram as well as in the similarity matrix: trajectory lifetime, length, sum of cluster attribute values, number of predefined cluster hotspots, average moving direction/speed, number of and distance to/from close trajectories, number of stops/returns/splits/merges, overall course description (linear, irregular), number of interactions with other objects/locations as well as number and distance of close trajectories. For radar plot, PCP, table lens and similarity matrix approach, additional lightning cluster attributes to be investigated could be cluster altitude and trajectory curveting at any cluster location. Furthermore, the change values rather than the absolute values of all attributes regarding the previous cluster step could be used.

Specific movement analysis tasks were already defined in Section 3.3.3. We now discuss how to relate the suggested novel visual analytical approaches (4.4.1 - 4.4.5) to these movement analysis tasks. The spatio-temporal information on interactive multidimensional map displays and the synchronized attributive information of dynamic objects on graphs or diagrams offer a much better visual impression than using just a single illustration, thus can strongly support the user to conduct the movement analysis. Table 4-14 gives an overview of how specific movement tasks are supported by the different visual analytical approaches. The number in the first table column refers to the movement analysis task holding the same number as in Table 3-4 provided in Section 3.3.3. The approaches are grouped in those targeted to attributive information and those for geospatial information. Green means that the approach is appropriate, while red indicates a restrictively use and blank cells means irrelevant.

For example, task '2' (see Table 3-4) aims to retrieve information about cluster speed, acceleration and moving direction angle. The appropriate methods for the direct retrieval of attribute values include temporal radar plot, temporal PCP, table lens and time plot. STC and XYZ-map can be restrictively used to indirectly provide information about cluster speed and acceleration, for instance, e.g. with color tones referring to speeds). Additionally, the user can visually explore an approximation of the moving direction angle through plotted cluster polygons and trajectories.

As mentioned in Section 4.4.1, lightning movement behavior could be separated into normal and unusual behavior. Based on predefined thresholds such as a certain maximum change of speed and/or moving direction, lightning clusters with unusual movements could be computationally identified and visually emphasized.

Table 4-14: Use of approaches for task specific movement analysis.

| Movement analysis tasks (see Section 3.3.3) Investigation of... | | Attributive information | | | | | | Geospatial information | | |
|---|---------------------------------------|-------------------------|---------------------------------|---------------------|--------------|------------|-----------|------------------------|-------|---------|
| | | TCG diagram | Similarity matrix and bar chart | Temporal Radar plot | Temporal PCP | Table lens | Time plot | STD map | STC | XYZ map |
| 1 | Moving objects | | | | | | | | Green | Green |
| 2 | Cluster movement attributes | | | Green | Green | Green | Green | | Red | Red |
| 3 | Special cluster events | | | Red | Red | Green | Green | Red | Green | Green |
| 4 | Special cluster hot spots | | | Red | Red | Green | Green | Red | Green | Green |
| 5 | Momentary cluster attribute changes | | | Green | Green | Green | Green | | | |
| 6 | Cluster interactions | Green | | Red | Red | Red | Red | | Red | Red |
| 7 | Compare clusters | | Red | | | | | | Green | Green |
| 8 | Predict clusters | | Green | Red | Red | Red | Red | | Red | Red |
| 9 | Internal cluster structure | | | | | | | | Green | Green |
| 10 | Trajectory movement attributes | | | | | | Green | | Red | Red |
| 11 | Trajectory events | Red | | | | Red | Green | | | |
| 12 | Trajectory course | Green | | | | | | | Green | Green |
| 13 | Trajectory interactions/relations | Green | | Red | Red | Red | Red | | Green | Green |
| 14 | Compare trajectories (similarities) | | Green | | | | | | Red | Red |
| 15 | Trajectory attribute data | | Green | Red | Red | Red | Red | | Red | Red |
| 16 | Temporal dependence of attribute data | Green | | Green | Green | Green | Green | | | |
| 17 | Uncertainty of movement path | Red | | Green | Green | Green | Green | | | |
| 18 | Movement anomalies | | | | | | | | Green | Green |
| 19 | Trajectory changes along its course | Green | Red | Green | Green | Green | Green | | | Green |
| 20 | Predict trajectory course | | | | | | | | Green | Green |
| 21 | Cluster changes along trajectories | Green | | Green | Green | Green | Green | | Green | Red |
| 22 | Trajectory movement complexity | Green | | Red | Red | Red | Red | Red | Red | Red |

green = appropriate method, red = restrictively suitable method

4.6. Users and usability issues

The target users of our approaches are domain specialists and geodata analysts who interact with the visualized dynamic phenomena. Furthermore, selected approaches, such as the 2D and 3D representation of lightning track lane on top of a base map, could be useful for interested lay public, in particular for demonstration purposes. To answer the question of how our visual analytical approaches influence a viewer's perception of lightning data, we need comprehensive tests of user interactions. Such usability tests aim to evaluate and improve usability and user friendly performance. They require knowledge about the user, the user's task as well as involved technology (Haklay 2010). Possible user tasks for movement analysis are listed Table 3-4 in Section 3.3.3. Various tests and evaluations of visual tools for the exploration of moving objects were reported in literature. However, tools and user tasks are mostly data and application specific. For instance, Demissie (2008) investigated the use of single static maps, multiple static maps, STC and animations within the visual analysis of moving people at three different levels of detail (complexity). The author concluded that animations are most suitable to retrieve stops, returns and speed change, while STC is most appropriate to present the moving paths.

"The anticipated user tests aim to investigate how the visualized information is perceived and understood. The usability of alternative approaches can be compared or iteratively improved. The iteration bears a two-fold meaning. On the one hand, the approach designers benefit from user's behavior. On the other hand, an improved approach will better empower the users. In the latter case, the users get trained to get along with the approach. Since the interactive and explorative use of dynamic SEPs requires some vocational adjustment, the corresponding usability tests should be conceptualized as a long-term endeavor involving repeating test sessions with the same target users" (Peters & Meng 2014a). User tests for explorative tools are demanding and need a long period of testing time beyond the scope of this thesis in order to extract statistically convincing and meaningful results for the visual movement analysis of dynamic SEOs, in particular for the application case of moving lightning clusters. An appropriate user tests is not part of this thesis but considered as relevant future work.

4.7. Chapter conclusion

This chapter was focused on the visual analysis of lightning data as a real case of dynamic SEO for the purpose of identifying and interpreting the spatial-temporal patterns embedded in lightning data and their dynamics. Concepts for lightning cluster and trajectory visualization were introduced and implemented along with a GUI which supports the investigation of lightning tracks and predicted lightning clusters including their prediction certainty within a 2D view, a 3D view or within a STC. These approaches provide insight into the dynamics of past and predicted 3D lightning clusters and cluster attributes over time. The novel density mapping approach "STDmapping" and other non-cartographic visual analytical approaches are synchronized to explore the movement of lightning test dataset. We showed how the movement complexity of a trajectory can be expressed and visualized and suggested a TCG diagram which aims to reveal movement diversity as well as unusual movement behaviors along a lightning trajectory. Furthermore, we discussed trajectory similarities and introduced a similarity matrix as one visual solution. With regards to the change of attribute values of dynamic objects in time (on the case of lightning data), we exposed the drawbacks of radar plot and PCP and introduced an extension of these methods, addressing temporal changes towards the third dimension, named as "temporal radar plot" and "temporal PCP". Additionally, we adapted table lens and a time plot for analyzing lightning trajectory attributes. Finally, we provided two overviews showing the relative suitability of visual analytical methods to various lightning data attributes and analysis tasks.

5. Final discussion

In this chapter we summarize the answers to the initially defined raised questions. The novelties and limitations of the methods proposed in the thesis are pointed out. Table 5-1 provides an overview about all proposed concepts and approaches and their applicability on different map displays. It should be noted that approaches developed and implemented for lightning data can be applied to other SEO/SEP. The last column reveals the applicability for dynamic SEOs and at the same time for line trajectories based on individual moving points.

Table 5-1: Approaches in the thesis and their innovations.

| | Novel concepts (blue), new methods (red), applied methods (grey) | On map display | On other displays* | 2D / 3D** | Adaptable for line trajectories |
|---|--|----------------------|--------------------------|--------------|---------------------------------------|
| for SEOs: | Generic concepts for visual exploration of dynamic SEOs | ✓ | ✓ | 2D & 3D | |
| for lightning data: | Lightning cluster and trajectory map presentation concept | ✓ | | 2D & 3D | |
| | STC concept for lightning data | | ✓ | 3D | |
| | Prediction and uncertainty visualization of lightning clusters | | | 2D & 3D | |
| in particular for lightning trajectories: | STDmapping | ✓ | | 2D | |
| | TCG diagram/bar chart | | ✓ | 2D | ✓ |
| | TCG diagram/bar chart on top of xyz-plot | ✓ | | 3D | ✓ |
| | TCG integrated in the STC | | ✓ | 3D | ✓ |
| | Similarity matrix and bar chart | | ✓ | 2D | ✓ |
| | Temporal radar plot | | ✓ | 3D | ✓ |
| | Temporal PCP | | ✓ | 3D | ✓ |
| | Table lens | | ✓ | 2D | ✓ |

* information visualization techniques (displays, graphs, etc.)

** requires interactive use

5.1. Approaches and results in relation to the research questions

In the following, we relate the contributions of this thesis with the five initially raised research questions.

1) *How can we describe and visually present dynamic SEOs/SEPs – in particular dynamic lightning clusters?*

We have identified three types of dynamic SEOs/SEPs: moving point groups (swarms), clustered point events and moving natural polygons (see Section 3.1). For dynamic SEP based on points, we argue for the necessary pre-processing in order to derive spatio-temporal polygons allocated to trajectories (see Section 3.2). For the sake of describing, presenting and analyzing the dynamics of SEOs, we distinguish between a spatio-temporal cluster reflecting a certain moment of time or the smallest time interval of interest of a moving SEO and the entire trajectory reflecting the

movement during the whole lifetime of a SEO. Spatial, temporal, spatio-temporal and further attributive information of SEOs are considered for SEO's clusters, trajectories and specific movement events. Non-visual and visual representations for the defined attributive information are provided. Further representation tools are STC, 3D map displays and non-cartographic displays, in which the geometry or/and semantic attributes of dynamic SEOs are illustrated. These representations aim to support the exploration of SEOs and their dynamics, and are appropriate for lightning data as an application case. As for dynamic SEO, lightning point events, which represent the moving lightning phenomena, the focus is on individual lightning clusters (spatio-temporal clusters) and lightning trajectories. The thesis has provided specific visualization concepts for lightning data on 2D and 3D map displays as well as for STC and non-cartographic displays. Visualization concepts distinguish between past, present and predicted lightning clusters and related semantic attributes. Furthermore, graphic variables of cluster and track representations are suggested (see 4.2).

2) *How can we visually analyze the movement of dynamic SEOs, in particular lightning clusters, using maps and other displays?*

The movement behavior of dynamic SEOs is comprehensively described (in Section 3.3.2) and specific movement analysis tasks are defined along with respective visual analytical approaches to solve these tasks (see Section 3.3.3). All movement analysis tasks and their specific visual solutions for SEOs are applicable for moving lightning clusters. For specific tasks analyzing the movement of lightning clusters, some novel approaches have been suggested. For the comparison of similarity of two lightning trajectories a similarity matrix is introduced (see Section 4.4.2). In order to evaluate the movement complexity within a lightning trajectory, the TCG diagram or TCG bar chart is suggested, which can be stacked also along z-dimension on top of a trajectory line projected on the 2D map surface. Several synchronized displays with interactive exploration functions can support the investigation of lightning cluster dynamics. User can extract movement information of SEOs directly on map displays. Further knowledge about the dynamics of SEOs can be gained through interaction with synchronized multidimensional, multivariate, cartographic and non-cartographic display tools.

3) *How can we incorporate temporal information in two-dimensional density contour maps for dynamic SEPs that are characterized by moving points or events?*

We introduced the STDmapping approach (in Section 4.3), which generates a 2D density surface based on contour intervals for spatially and temporally evolving points. Our method is characterized by a rainbow color scheme, which enables the user to visually extract spatio-temporal changes of point density and distribution. The STDmapping approach has been applied to the lightning test dataset and resulting density surfaces clearly reflect the dynamics of the lightning data. On the one hand, the map reader can extract local point density and point distribution information and the respective time. On the other hand, the map output reflects information about speed, speed changes, movement direction and direction changes of the dynamic SEP. The STDmapping method is conceptualized for point events representing a moving SEP. However, it can also be applied to dynamic swarm data. The thresholds dividing the successive surface sections can be adjusted depending on the underlying data, application case and the analysis purpose.

4) *How can existing geovisual-analytics approaches for spatial data be refined to address the visual exploration of dynamic data, in particular dynamic SEOs/SEPs?*

Radar plot as well as PCP can be used to visualize geometrical and semantic attributes of a moving polygon. However, to compare temporal changes of the cluster attribute, time information should be integrated. We choose to project a long time series of attribute records onto the third-

dimension (z-axis) thus facilitate the visual comparison without the disadvantage of overplotting. Furthermore, we suggest an interactive use of our temporal radar plot and temporal PCP in order to explore events, trends and patterns (see Section 4.4.3 and 4.4.4).

5) *Which information can be derived using geovisual analysis and geovisual analytics methods for dynamic SEOs?*

Information about dynamic SEOs that is visualized in 2D map as explained in Section 3.3.1 includes geometrical and semantic attributes and can be derived from spatio-temporal clusters, trajectories or specific situations/events of a SEO. Specific movement information of dynamic SEOs and its supporting visual analytical approaches is addressed in Section 3.3.2 and 3.3.3. The use of STC for SEOs enables exploration of temporal changes of geometrical and semantic information. A 3D map display provides additional insight into the spatial extension in height. Furthermore, non-cartographic displays can make specific trajectory information such as complexity, similarity or uncertainty visible. Moreover, non-cartographic displays are also appropriate to emphasize geometrical and semantic changes of moving SEOs.

5.2. Limitations of the proposed methods and comparison with related research

This thesis has made a number of contributions to support visual exploration of SEOs in particular for the lightning data as an application case. Nevertheless, some limitations remain, which we want to specify in the following in comparison with existing approaches:

➤ *Generic concept for visual exploration of dynamic SEPs*

Spatio-temporal data representation and visual analysis of dynamic data in a 3D space is still a widely untouched research field. Although, there are various mapping approaches for evolving polygons (e.g. thunderstorm visualization), no generic concept of visual movement analysis for SEOs/SEPs exists yet. Spatio-temporal relationships of moving polygons in a 2D space have been proposed. Concepts for visual investigation of dynamic data exist mostly for dynamic points (e.g. cars, vessels, people and airplanes). Our proposed concept has a generic nature, but its implementation is restricted to selected applications. Further adaptations to various scenarios are necessary.

➤ *Visual exploration of dynamic lightning data*

Specific investigations for the visualization or visual exploration of lightning data are very rarely reported in the literature. Mostly only the source data of lightning points are represented as individual points or temporally aggregated on a cell-grid. Based on the existing approaches such as 3D flash-like photo-realistic visualization of lightning points, time slider and the STC dealing with similar data, this thesis provides a comprehensive platform for the visual exploration of lightning data and their movement characteristics. However, the usability of the platform needs to be assessed by means of extensive user test.

➤ *STDmapping approach*

Existing density mapping approaches are able to consider either two moments of time or a series of time intervals within density information visualization in a STC. However, the targeted visual communication of point density changes necessitates user interactions, especially when a cluster of interest is bounded by other clusters, it can be hardly explored without interaction. Our STDmapping approach provides density and temporal information of moving point groups (or point events representing a dynamic SEP) on a static 2D map. Thus, it overcomes the drawbacks of existing approaches. Spatial and temporal clustering parameters/thresholds can be adapted in order to improve the resulting STDmap. The approach creates appropriate segmented density

surfaces. In other words, the approach is suitable if a movement and a main movement direction of the phenomena (polygon) are given and thus a tendency line together with temporal borderlines can be automatically identified. However, several movement cases may cause difficulties to identify the segments: (1) if the SEP is simultaneously expanding in several directions the tendency line needs to be split, which is no trivial task in the practice. (2) If the SEP is moving and returning after a circular track back to a previously passed location/area; or if the SEP is moving for and backwards. In these cases spatio-temporal polygons would overlap significantly and the resulting STDmap may become illegible.

➤ *Temporal radar plot and temporal PCP*

Existing radar plot and PCP approaches have been discussed in Section 4.4.3 and 4.4.4. Until now, temporal information could be included into radar plots and PCP only as an additional axis in the 2D plot. Consequently, visual exploration of temporal attribute changes is not easy, especially in the large datasets. Besides, the overlapping spikes are difficult to interpret. This thesis has extended the 2D radar plot as well as the 2D PCP to a 3D approach with the time as z-axis in order to compare temporal attribute changes in a PCP or radar plot. We implemented the temporal radar plot and temporal PCP to a test dataset. In comparison to the 2D approach, the overplotting can be avoided; the approach is suitable for relatively large datasets and the temporal attribute changes can be visually discovered. Nonetheless, both of our approaches suffer from the same limitation: Too large datasets may lead to a plot with either a very large z-axis or very narrow z-distances between successive entries. Data could be generalized as suggested in Section 4.4.3 and 4.4.4. This can make the big global temporal attribute changes visually recognizable, but local changes would be difficult to discern.

➤ *TCG diagram and bar chart*

Our proposed complexity diagram aims to investigate the track complexity based on temporally changing lightning track attributes (see Section 4.4.1). It can also be adapted to other scenarios of moving SEOs and line-trajectories based on moving points. The suggested complexity diagram - displayed (as the third dimension) on top of an 2D map as in Figure 4-40 and Figure 4-41 – is similar to the trajectory wall approach (Andrienko et al. 2014). In the trajectory wall, values of one attribute of all (or of a certain amount of selected) individual point objects (moving along a trajectory) are visually stacked for comparison – consequently the trajectory wall contains a constant height (z).

Our approach visually stacks several attributes of an SEO moving along a trajectory – thus TCG plot heights differ along/above trajectory positions (spatio-temporal cluster centroids). Moreover, complexity values are based on pre-processed clusters, thus the TCG plot displays aggregated attributes for each spatio-temporal interval. We can conclude that only the basic idea of both approaches is similar, but each of these two trajectory-stacking approaches provides different information. We provide several solutions to visualize stacked complexity attributes inside the proposed TCG: (a) via bar chart, (b) through curves or (c) curves by travelled distance, (d) via bar chart on top of 2D map or (e) stacked curves on top of 2D map. The options (d) and (e) have the drawback that if the SEO's movement is highly irregular with longer stops and various self-intersecting parts, its interactive exploration will become difficult and strong user interaction is needed. This concern could be alleviated by displaying only segments of interest and disabling the rest of the complexity diagram gain. Furthermore, we also integrated our TCG approach in the STC, which provides additional information about temporal changes of the trajectory complexity. However, its main limitation is that it requires strong user interaction with zooming operation when stacking various attributes.

➤ *Similarity matrix*

Existing visual approaches for trajectory similarities – also known as distance functions - have been discussed in Section 2.6. They focus on geographic similarity of line-trajectories. The spatially close tracks (track parts) are aggregated and/or displayed in the same color. Only very few methods offer a distance function approach based on primary (space and time) as well as derived motion parameters of trajectories (speed and direction). Our similarity matrix approach with bar chart can support a specific movement analysis of dynamic lightning clusters, namely, to compare the similarity of two trajectories (see Section 4.4.2). It can also be adapted to other lane- or line trajectory cases. A disadvantage of our similarity matrix approach is that only two trajectories can be compared and only a simultaneous trajectory part of both tracks can be considered. If the two trajectories do not start at the same moment of time, a shift/transformation has to be applied to provide a common start time.

6. Conclusion and outlook

For the investigation of the movement of spatially extended dynamic objects, the interactive visual tools, in particular the interactive use of several complementary and synchronized multidimensional and multivariate cartographic as well as non-cartographic displays, are very powerful. Depending on the complexity and the cartographic design of these tools, potential users could be decision makers with background knowledge about the investigated real case scenario, analysts who mostly have advanced skills in using and interpreting visual analytical tools or lay public for whom such tools serve for demonstration purposes.

The main goal of this dissertation has been to visually investigate the dynamics of SEPs, taking lightning data as a real case. The main contributions of this thesis include a generic concept for visual movement analysis of SEPs as well as a number of novel visualization and visual analytical techniques, which provide an insight into the dynamics of SEPs, in particular, the moving lightning clusters.

6.1. Terminology refinement of SEOs and pre-processing

A spatially extended and dynamic object or phenomena can be based on a moving point group or swarm. Another possible source is clustered point events, which are close in space and time and thus belonging to the same moving SEO. A third division of SEOs are natural polygons such as landslides, which are not based on captured point data. Depending on the data structure of SEOs, a corresponding pre-processing is required in order to determine the initial spatio-temporal polygons. Pre-processing involves temporal and spatial clustering with appropriate clustering thresholds and aggregation of derived clusters. This thesis provides a conceptual workflow to process spatio-temporal clusters of a SEO, the track-line as well as track-lane each cluster forms during its lifetime and relevant movement attributes of all clusters and trajectories describing the dynamics of the SEP.

6.2. Visual exploration of moving SEOs

Following the generic concept for the visual representation (mapping) and non-visual description of dynamic SEPs and their movement features, it is possible to choose an appropriate representation for the past and the predicted spatio-temporal cluster(s), trajectories or trajectory parts, particular SEO's movement events/situation etc. If a suggested visualization involves the third dimension, user interactions are required in order to support the data exploration. The aspects describing the movement behavior of SEOs help to understand and to structure the movement diversity of a dynamic SEP. Depending on the type of data and on the application case, specific movement analysis tasks are defined and associated visual explorative methods developed to supporting data analysts and decision makers to perform those tasks.

6.3. Representation and visual analysis of lightning data

This work provides an encompassing conceptual set of visual presentations and visual analysis methods and tools for dynamic lightning data. Visual concepts are distinguished for (1) lightning clusters and their 'momentary' movement attributes and (2) lightning trajectories (lines and lanes) and their 'continuous' movement attributes. Thus, various mapping options of lightning points, spatial-temporal lightning clusters or aggregated clusters towards tracks can be applied. Among others, a workflow for 3D point selection with symbol size adaption based on local point densities allows a representative and legible representation of the 3D lightning point cloud with minimum information loss. A broad set of visual investigative methods (e.g. 3D view, STC, time slider tool, nowcast-tool) as well as an interactive graphic user interface support the investigation of the

dynamics of lightning cluster and trajectory attributes. Moreover, a concept of determining and visualizing nowcasted lightning clusters and their prediction uncertainty helps to gain a visual insight into the near future movement of dynamic lightning data.

Our proposed visualization techniques and interactive analytical tools are developed for analysts and decision makers dealing with lightning data or other dynamic SEOs. The visualization of nowcasted lightning clusters in combination with prediction uncertainty buffer, for instance, can help decision makers at an airport to define safety corridors for flying and landing airplanes.

6.4. Density maps for dynamic lightning data

One of the key issues for the understanding of spatio-temporal phenomena is the representation of density and distribution information. The STDmapping approach can reveal general pattern and concise generalization of temporal and density information, and has thus reached the goal of incorporating temporal information in 2D density maps with layered tints corresponding to different temporal segments. The temporal borders are visualized as lines perpendicular to the moving tendency lines. Tendency lines are either straight or curved. Moreover, abrupt or smooth color gradients between neighboring temporal segments can be applied. The resulted STDmaps comprise spatio-temporal information about density, distribution, movement pattern such as moving direction and speed of dynamic point clusters. Thus, our approach supports the pattern detection/extraction of spatio-temporal phenomena without having to activate interactive tools. Furthermore, our approach can be adapted to dynamic phenomena represented by point events as well as to moving point groups.

6.5. Visual analytical approaches for lightning clusters

Interactive visual analytical tools can provide new knowledge within lightning exploration and, hence, support decision-making in thunderstorm forecast, flight scheduling or lightning damage prevention. With this thesis we provide a set of visual analytical approaches to enable interactive visual exploration of lightning data and in particular their dynamics. It allows users to investigate lightning point data, derived spatio-temporal lightning clusters and trajectories, their movement attributes as well as their evolution.

We offer a visual analytical solution for exploring the movement complexity of lightning trajectories. Our TCG approach can be stacked along the trajectory on top of a 2D base map. It also provides an insight into unusual movement behaviors along the trajectory. The similarity matrix assists analysts to compare the similarity of two lightning trajectories. Furthermore, the interactive use of the temporal radar plot and temporal PCP may facilitate the visual investigation of geometrical and semantic attribute changes in time. Our approaches demonstrated the capability of interactive visual exploration using a lightning test dataset. Besides, we investigated the feasibility of existing visual analytical approaches (time plot and time lens) for the lightning data scenario and their integration in a user-friendly interactive system. We suggested a multivariate interactive GUI, wherein various proposed visual approaches/displays are integrated and synchronized in order to gain an insight into lightning dynamics as well as to explore events, patterns and trends. This thesis provides two kinds of added values: scientific/methodological findings within visual exploration of dynamic SEPs which are generally valid, and empirical findings which are valid primary for lightning data, but potentially adaptable to other application cases.

6.6. Outlook

The investigation of dynamic phenomena is an ongoing research field. This thesis is among the first to make some contributions to the visual exploration of SEOs by providing a generic concept for visual movement analysis of SEP along with some specific approaches for evolving lightning

clusters. Further studies may involve three parts: (1) general improvements, (2) improvements of specific approaches and (3) verifications of proposed approaches through usability studies/tests.

6.6.1. General improvements

As mentioned already in (Peters & Meng 2013), for meteorological investigations, the proposed approaches could be extended towards two modules: (1) visual thunderstorm analysis and (2) thunderstorm nowcasting. Thereby, synchronized real-time information from satellite images, radar and lightning records have to be integrated. Using such data would also be the basis for a reliable nowcasting of lightning cells. Knowledge discovery can be performed in real-time or posteriori. A thunderstorm warning system requires (nearly) real-time processing (incremental updating). Therefore, the visualizations and interactive visual tools representing nowcasted lightning and other thunderstorm data need to perform fast and reliably. Visual investigations of recorded lightning tracks can be performed using posteriori-processing. Moreover, it is worthwhile to develop the dynamic mapping technologies for geo-sensory systems which, for example, demand the dynamic derivation of density layers, contour lines or discrete classes from the values regularly sent by various sensors.

Claramunt and Jiang's spatio-temporal relationship model (2000) could be adapted and thus improved for moving SEP in the way that the model also considers clusters (polygons), cluster centroids (points), trajectory lines (polylines formed by connected centroids) and trajectory lanes (polygons) in 2D and in 3D space. The adaptation would allow to describe, for instance, the spatio-temporal relationship of two trajectory lines, or to define whether the trajectory of one SEO temporally overlaps and spatially touches the trajectory line of the other SEO. Further relevant investigations could focus on visual explorative tools for moving lightning clusters, for example, for the understanding of the relationship between lightning movements and other meteorological information (e.g. wind, temperature). Another extension would be the incorporation of photo-realistic visualization of lightning events in the proposed visual representation tools.

Furthermore, the proposed approaches could be adapted for different spatial and temporal scales. In order to avoid occlusion and overplotting, for smaller scales trajectories as well as their attributes could be aggregated towards trajectory groups.

6.6.2. Improvements of specific approaches

Regarding the STDmapping approach, the method could be extended towards 3D space, taking also altitude information into account. Besides point events, possible applications for STDmapping could be also swarm dataset, containing moving swarm objects. As mentioned in (Peters & Meng 2014b), we also consider investigating the relation between the characteristics of initial data (spatio-temporal change of point coordinates, density, distribution) and their modeling parameters (time interval, movement tendency, boundary lines) with the purpose of describing the dynamic phenomena with minimum information loss or distortion for the subsequent visualization and use of STDmaps. Not only the STDmapping approach, but also TCG-diagram, temporal PCP and temporal radar plot could be tested with larger (longer) lightning datasets or data from other SEP applications.

6.6.3. Verifications of proposed approaches

"A conceptual shift in expected user profile requires an appropriate response in studies that evaluate user responses to the tools and techniques being developed. Analyzing tool effectiveness and efficiency through traditional empirical success metrics such as, error rate and task completion time via repeated trials on large numbers of users is unlikely to be appropriate in the context of a tool intended to enable a small number of professionals to analyze complex data"

(Andrienko et al. 2008a). Research in the area of interactive visual analysis draws on expertise in visual analytics, exploratory data analysis, interface design and cognitive ergonomics. The theories of cognitive ergonomics can support the identification of constraints for visualizations and their interpretations (Keim et al. 2008). From these constraints and viewers' roles and characteristics, parameters for the visualization design can be derived. If the visualization is embedded in an interactive system, it will possess a two-fold added value – empower users and learn from user's behavior (Peters & Meng 2013).

As mentioned before, to evaluate our proposed methods, a comprehensive user test is necessary. It is our responsibility to verify the proposed approaches. That will on the one hand refine and thus improve our approaches, and on the other hand it will define which method is the best for which movement analysis task regarding its usefulness and effectiveness. Using possibly a crowd-sourcing environment, lightning experts and interested lay people could be involved in order to verify the usability of our lightning GUI prototype. A central challenge will be to provide a user friendly performance for the visual lightning movement analysis functions. The usability test of STDmap for lightning data requires the participation of users who are domain specialists and should make decisions based on their understanding of visualized lightning data. Specific user tasks related to the extraction of certain spatio-temporal density information or dynamic patterns should be repeatedly conducted and evaluated. Various interactive functions should be made available to allow these users to manipulate the visualization for the purpose of a more efficient exploration, for instance, by adapting the color scheme, changing the time interval etc.

7. References

1. Allen JF (1983) Maintaining knowledge about temporal intervals. *Communications of the ACM* 26:832-843.
2. Álvarez G, Gilberto M (2013) Representing uncertainty of moving objects datasets introduced by density - based aggregation of trajectories. In: Enschede, University of Twente Faculty of Geo-Information and Earth Observation (ITC).
3. Andrienko G, Andrienko G (2009) Building a Visual Summary of Multiple Trajectories, Paper presented at the GeoViz Hamburg 2009 Workshop, Hamburg, Mar, 2009.
4. Andrienko G, Andrienko N (2010) A general framework for using aggregation in visual exploration of movement data. *The Cartographic Journal* 47(1):22-40.
5. Andrienko G, Andrienko N, Bak P, Keim D, Kisilevich S, Wrobel S (2011a) A conceptual framework and taxonomy of techniques for analyzing movement. *Journal of Visual Languages & Computing* 22:213-232.
6. Andrienko G, Andrienko N, Demsar U, Dransch D, Dykes J, Fabrikant SI, Jern M, Kraak M-J, Schumann H, Tominski C (2010) Space, time and visual analytics. *International Journal of Geographical Information Science* 24:1577-1600.
7. Andrienko G, Andrienko N, Dykes J, Fabrikant SI, Wachowicz M (2008a) Geovisualization of dynamics, movement and change: key issues and developing approaches in visualization research. *Information Visualization* 7:173-180.
8. Andrienko G, Andrienko N, Hurter C, S R, Wrobel S (2011b) From movement tracks through events to places: extracting and characterizing significant places from mobility data, Paper presented at the IEEE Conference on Visual Analytics Science and Technology (VAST), 2011b.
9. Andrienko G, Andrienko N, Jankowski P, Keim D, Kraak M-J, MacEachren A, Wrobel S (2007a) Geovisual Analytics for Spatial Decision Support: Setting the Research Agenda. *International Journal of Geographical Information Science* 21:839-857.
10. Andrienko G, Andrienko N, Keim D, MacEachren AM, Wrobel S (2011c) Challenging problems of geospatial visual analytics. *Journal of Visual Languages and Computing* 22:251.
11. Andrienko G, Andrienko N, Schumann H, Tominski C (2014) Visualization of Trajectory Attributes in Space–Time Cube and Trajectory Wall. In: *Cartography from Pole to Pole*. Springer:157-163.
12. Andrienko G, Andrienko N, Wrobel S (2007b) Visual analytics tools for analysis of movement data. *ACM SIGKDD Explorations Newsletter* 9(2):38-46.
13. Andrienko N, Andrienko G (2006) *Exploratory analysis of spatial and temporal data*. Springer Berlin, Germany.
14. Andrienko N, Andrienko G (2007) Designing visual analytics methods for massive collections of movement data. *Cartographica: The International Journal for Geographic Information and Geovisualization* 42(2):117-138.
15. Andrienko N, Andrienko G (2012) A visual analytics framework for spatio-temporal analysis and modelling. *Data Mining and Knowledge Discovery*:1-29.
16. Andrienko N, Andrienko G (2013) Visual analytics of movement: An overview of methods, tools and procedures. *Information Visualization* 12:3-24.
17. Andrienko N, Andrienko G, Gatalsky P (2003) Exploratory spatio-temporal visualization: an analytical review. *Journal of Visual Languages & Computing* 14:503-541.
18. Andrienko N, Andrienko G, Pelekis N, Spaccapietra S (2008b) Basic concepts of movement data. In: *Mobility, Data Mining and Privacy*. Springer:15-38.

19. Andrienko N, Andrienko G, Stange H, Liebig T, Hecker D (2012) Visual analytics for understanding spatial situations from episodic movement data. *KI-Künstliche Intelligenz* 26(3):241-251.
20. Assent I, Krieger R, Müller E, Seidl T (2007) VISA: visual subspace clustering analysis. *ACM SIGKDD Explorations Newsletter* 9(2):5-12.
21. Bertin J (1983) *Semiology of graphics: diagrams, networks, maps*. The University of Wisconsin Press, Madison, WI, USA.
22. Betz HD, Schmidt K, Oettinger WP (2009) LINET – An International VLF/LF Lightning Detection Network in Europe. In: Betz HD, Schumann U, Laroche P (eds) *Lightning: Principles, Instruments and Applications*. Springer Netherlands, Dordrecht:115-140.
23. Betz HD, Schmidt K, Oettinger WP, Montag B (2008) Cell-tracking with lightning data from LINET. *Adv. Geosci.* 17:55-61.
24. Blok C (2000) Monitoring change: characteristics of dynamic geo-spatial phenomena for visual exploration. In: *Spatial cognition II*. Springer:16-30.
25. Bolliger M, Binder P, Rossa A (2002) Tracking cloud patterns by rapid scan imagery in the Alpine region. In: *Proc. 10th AMS conference on Mountain Meteorology*,. Park City, UT, USA:73-80.
26. Bonelli P, Marcacci P (2008) Thunderstorm nowcasting by means of lightning and radar data: algorithms and applications in northern Italy. *Nat. Hazards Earth Syst. Sci* 8:1187-1198.
27. Borland D, Taylor II RM (2007) Rainbow color map (still) considered harmful. *IEEE computer graphics and applications* 27(2):14-17.
28. Bowers KJ, Johnson SD (2004) Who Commits Near Repeats? A Test of the Boost Explanation. *Western Criminology Review* 5(3).
29. Boyandin I, Bertini E, Bak P, Lalanne D (2011) Flowstrates: An Approach for Visual Exploration of Temporal Origin - Destination Data, Paper presented at the Computer Graphics Forum, 2011.
30. Brewer C, Harrower M [http://http://www.colorbrewer2.org/](http://www.colorbrewer2.org/), accessed last: 10/2014.
31. Burrough P, Karssenberg D, Van Deursen W (2005) Environmental modeling with PCRaster. *GIS, Spatial Analysis and Modeling*:333-356.
32. Buziek G, Dransch D, Rase W-D (2000) *Dynamische Visualisierung: Grundlagen und Anwendungsbeispiele für kartographische Animationen*. Springer,
33. Casati R, Varzi AC (2008) Event concepts. *Understanding events: From perception to action*:31-53.
34. Čerba O, Brašnová K (2012) Cartographic Visualization of Temporal Aspect of Spatial Data, Paper presented at the AutoCarto 2012, Columbus, Ohio, USA, September 16-18 2012.
35. Chen L, Özsu MT, Oria V (2005) Robust and fast similarity search for moving object trajectories, Paper presented at the Proceedings of the 2005 ACM SIGMOD international conference on Management of data, 2005.
36. Claramunt C, Jiang B (2000) A representation of relationships in temporal spaces. *Innovations in GIS VII: GeoComputation* 7:41-53.
37. Cook K, Grinstein G, Whiting M, Cooper M, Havig P, Liggett K, Nebesh B, Paul CL (2012) VAST Challenge 2012: Visual analytics for big data, Paper presented at the Visual Analytics Science and Technology (VAST), 2012 IEEE Conference on, 2012.
38. Cressie N (1992) *Statistics for spatial data*. Terra Nova 4(5):613-617.
39. De Boor C (1978) *A practical guide to splines*. Springer-Verlag New York.
40. Demissie B (2008) Moving Objects in Static Maps, Animation, and the Space-Time Cube. In: *ITC, The Netherlands (Master's thesis)*.

41. Demšar U, Verrantaus K (2010) Space–time density of trajectories: exploring spatio-temporal patterns in movement data. *International Journal of Geographical Information Science* 24(10):1527-1542.
42. Dixon M, Wiener G (1993) TITAN: Thunderstorm identification, tracking, analysis, and nowcasting-A radar-based methodology. *Journal of Atmospheric and Oceanic Technology* 10:785-797.
43. Dukaczewski D (2007) Method of choice of variables and cartographic presentation methods for complex cartographic animations, Paper presented at the Proceedings of the XXIII International Cartographic Conference ACI/ICA, 2007.
44. Dykes J, MacEachren AM, Kraak M-J (2005) Exploring geovisualization. Elsevier,
45. Dykes JA, Mountain D (2003) Seeking structure in records of spatio-temporal behaviour: visualization issues, efforts and applications. *Computational Statistics & Data Analysis* 43(4):581-603.
46. Eccles R, Kapler T, Harper R, Wright W (2008) Stories in geotime. *Information Visualization* 7(1):3-17.
47. Edsall RM (2003) The parallel coordinate plot in action: design and use for geographic visualization. *Computational Statistics & Data Analysis* 43:605-619.
48. Forer P, Huisman O (2000) Space, time and sequencing: Substitution at the physical/virtual interface. *Information, Place, and Cyberspace: Issues in Accessibility*:73-90.
49. Galton A (2003) Desiderata for a spatio-temporal geo-ontology. In: *Spatial Information Theory. Foundations of Geographic Information Science*. Springer:1-12.
50. Galton A (2004) Fields and objects in space, time, and space-time. *Spatial cognition and computation* 4:39-68.
51. Galton A (2005) Dynamic collectives and their collective dynamics. *Spatial Information Theory*:300-315.
52. Gatalsky P, Andrienko N, Andrienko G (2004) Interactive analysis of event data using space-time cube, Paper presented at the Information Visualisation, 2004. IV 2004. Proceedings. Eighth International Conference on, 2004.
53. Gershon N (1998) Visualization of an imperfect world. *Computer Graphics and Applications, IEEE* 18(4):43-45.
54. Goodchild MF (1988) Stepping over the line: technological constraints and the new cartography. *The American Cartographer* 15:311-319.
55. Goodchild MF (2010) Twenty years of progress: GIScience in 2010. *Journal of Spatial Information Science* (1):3-20.
56. Goodchild MF, Glennon A (2008) Representation and computation of geographic dynamics. *Understanding dynamics of geographic domains*:13-30.
57. Goodchild MF, Yuan M, Cova TJ (2007) Towards a general theory of geographic representation in GIS. *International journal of geographical information science* 21(3):239-260.
58. Griethe H, Schumann H (2006) The Visualization of Uncertain Data: Methods and Problems, Paper presented at the SimVis, 2006.
59. Guo D, Chen J, MacEachren AM, Liao K (2006) A visualization system for space-time and multivariate patterns (vis-stamp). *Visualization and Computer Graphics, IEEE Transactions on* 12(6):1461-1474.
60. Guo H, Wang Z, Yu B, Zhao H, Yuan X (2011) TripVista: Triple perspective visual trajectory analytics and its application on microscopic traffic data at a road intersection, Paper presented at the Pacific Visualization Symposium (PacificVis), 2011 IEEE, 2011.

61. Güting RH, Böhlen MH, Erwig M, Jensen CS, Lorentzos NA, Schneider M, Vazirgiannis M (2000) A foundation for representing and querying moving objects. *ACM Transactions on Database Systems (TODS)* 25(1):1-42.
62. Haggett P (1990) *The geographer's art*, Oxford:
63. Haklay M (2010) *Interacting with geospatial technologies*. Wiley Online Library.
64. Han J, Kamber M (2006) *Data mining: concepts and techniques*. Morgan Kaufmann, San Francisco, CA, USA.
65. Handwerker J (2002) Cell tracking with TRACE3D—a new algorithm. *Atmospheric Research* 61:15-34.
66. Hao MC, Dayal U, Sharma RK, Keim DA, Janetzko H (2010) Variable binned scatter plots. *Information Visualization* 9(3):194-203.
67. Harrower M (2003) Representing uncertainty: Does it help people make better decisions, Paper presented at the UCGIS Workshop: Geospatial Visualization and Knowledge Discovery Workshop, 2003.
68. Hengl T (2003) Visualisation of uncertainty using the HSI colour model: computations with colours, Paper presented at the Proceedings of the 7th International Conference on GeoComputation, 2003.
69. Hering AM, Morel C, Galli G, Sényesi S, Ambrosetti P, Boscacci M (2004) Nowcasting thunderstorms in the Alpine region using a radar based adaptive thresholding scheme, Paper presented at the Proceedings of the third ERAD Conference, Visby, Sweden, 6 - 10 September 2004.
70. Holtt T, Magdy A, Chen G, Gopalakrishnan G, Hoteit I, Hansen CD, Hadwiger M (2013) Visual analysis of uncertainties in ocean forecasts for planning and operation of off-shore structures, Paper presented at the Visualization Symposium (PacificVis), 2013 IEEE Pacific, 2013.
71. Holtt T, Magdy A, Zhan P, Chen G, Gopalakrishnan G, Hoteit I, Hansen CD, Hadwiger M (2014) Ovis: A Framework for Visual Analysis of Ocean Forecast Ensembles.
72. Holten D, Van Wijk JJ (2009) Force - Directed Edge Bundling for Graph Visualization, Paper presented at the Computer Graphics Forum, 2009.
73. Huang Y, Chen C, Dong P (2008) Modeling herds and their evolvments from trajectory data. In: *Geographic Information Science*. Springer:90-105.
74. Huang Z, Feng X, Xuan W, Chen X (2007) Causal relations among events and states in dynamic geographical phenomena, Paper presented at the Geoinformatics 2007, 2007.
75. Hurter C, Ersoy O, Telea A (2012) Graph bundling by kernel density estimation, Paper presented at the Computer Graphics Forum, 2012.
76. Hurter C, Tissoires B, Conversy S (2009) Fromdady: Spreading aircraft trajectories across views to support iterative queries. *Visualization and Computer Graphics, IEEE Transactions on* 15(6):1017-1024.
77. Hwang J-R, Kang H-Y, Li K-J (2005) Spatio-temporal similarity analysis between trajectories on road networks. Springer,
78. Inselberg A (1985) The plane with parallel coordinates. *The Visual Computer* 1(2):69-91.
79. Isard W (1970) On notions and models of time. *Papers in Regional Science* 25(1):7-31.
80. Jain AK, Dubes RC (1988) *Algorithms for clustering data*. Prentice-Hall, Inc., Upper Saddle River, NJ, USA.
81. Jansenberger EM, Stauer-Steinnocher P (2004) Dual Kernel density estimation as a method for describing spatio-temporal changes in the upper austrian food retailing

- market, Paper presented at the 7th AGILE Conference on Geographic Information Science, 2004.
82. Johnson B, Shneiderman B (1991) Tree-maps: A space-filling approach to the visualization of hierarchical information structures, Paper presented at the Visualization, 1991. Visualization'91, Proceedings., IEEE Conference on, 1991.
 83. Johnson JT, MacKeen PL, Witt A, Mitchell EDW, Stumpf GJ, Eilts MD, Thomas KW (1998) The storm cell identification and tracking algorithm: An enhanced WSR-88D algorithm. *Weather and Forecasting* 13:263-276.
 84. Johnson SD, Bernasco W, Bowers KJ, Elffers H, Ratcliffe J, Rengert G, Townsley M (2007) Space-time patterns of risk: a cross national assessment of residential burglary victimization. *Journal of Quantitative Criminology* 23(3):201-219.
 85. Keim D, Andrienko G, Fekete J-D, Görg C, Kohlhammer J, Melançon G (2008) Visual analytics: Definition, process, and challenges. In: *Information Visualization - Human-Centered Issues and Perspectives*. Springer, Berlin, Germany:154-175.
 86. Kitagawa N, Brook M, Workman EJ (1962) Continuing currents in cloud-to-ground lightning discharges. *Journal of Geophysical Research* 67:637-647.
 87. Köbben B, Yaman M (1996) Evaluating dynamic visual variables, Paper presented at the Proceedings of the seminar on teaching animated cartography, ACI/ICA, Madrid, 1996.
 88. Kolence KW, Kiviat PJ (1973) Software unit profiles & Kiviat figures. *ACM SIGMETRICS performance evaluation review* 2(3):2-12.
 89. Kraak M-J, MacEachren AM (1994) Visualization of spatial data's temporal component. *Proceedings, Spatial Data Handling, Advances in GIS Research*. Edinburgh, Scotland:391-409.
 90. Kraak M-J, Ormeling F (2011) *Cartography: visualization of spatial data*. Guilford Press.
 91. Kreiß J-P, Neuhaus G (2006) *Einführung in die Zeitreihenanalyse*. Springer Berlin,
 92. Krisp JM, Peters S (2011) Directed kernel density estimation (DKDE) for time series visualization. *Annals of GIS* 17(3):155-162.
 93. Krisp JM, Peters S, Burkert F (2013) Visualizing Crowd Movement Patterns Using a Directed Kernel Density Estimation, Paper presented at the Earth Observation of Global Changes (EOGC), Munich, Germany, 2010/08/26/28 2013.
 94. Krisp JM, Peters S, Murphy CE, Fan H (2009) Visual Bandwidth Selection for Kernel Density Maps. *Photogrammetrie - Fernerkundung - Geoinformation* 2009(5):445-454.
 95. Krisp JM, Peters S, Mustafa M (2011) Application of an Adaptive and Directed Kernel Density Estimation (AD-KDE) for the Visual Analysis of Traffic Data, Paper presented at the GeoViz2011, Hamburg, Germany, March 10-11, 2011 2011.
 96. Krisp JM, Peters S, Polous K, Fan H, Meng L (2012) Getting in and out of a taxi: spatio-temporal hotspot analysis for floating taxi data in Shanghai, Paper presented at the Networks for Mobility 2012, Stuttgart, 2012.
 97. Krisp JM, Špatenková O (2010) Kernel density estimations for visual analysis of emergency response data. In: *Geographic Information and Cartography for Risk and Crisis Management*. Springer:395-408.
 98. Kwan M-P (2003) Geovisualisation of activity-travel patterns using 3D geographical information systems, Paper presented at the 10th international conference on travel behaviour research (pp. pages pending), Lucerne, 2003.
 99. Laboratory DS <http://genie.sis.pitt.edu/>, accessed last: 09/2014.
 100. Lakshmanan V, Hondl K, MacGorman D, Stumpf GJ (2004) The use of Lightning Mapping Array data in WDSS-II, Paper presented at the 22nd Conference on Severe Local Storms, 2004.

101. Lampe OD, Hauser H (2011) Interactive visualization of streaming data with kernel density estimation, Paper presented at the Pacific Visualization Symposium (PacificVis), 2011 IEEE, 2011.
102. Langford M, Unwin DJ (1994) Generating and mapping population density surfaces within a geographical information system. *Cartographic Journal*, The 31:21-26.
103. Li L, Schmid W, Joss J (1995) Nowcasting of motion and growth of precipitation with radar over a complex orography. *Journal of applied meteorology* 34:1286-1300.
104. Liu H, Gao Y, Lu L, Liu S, Qu H, Ni LM (2011) Visual analysis of route diversity, Paper presented at the Visual Analytics Science and Technology (VAST), 2011 IEEE Conference on, 2011.
105. Longley P (2005) *Geographic information systems and science*. John Wiley & Sons,
106. MacEachren AM (1995) *How Maps Work: Representation, Visualization, and Design*. The Guilford Press.
107. MacEachren AM, Kraak MJ (2001) Research challenges in geovisualization. *Cartography and Geographic Information Science* 28:3-12.
108. MacEachren AM, Monmonier M (1992) Geographic visualization - introduction. *Cartography and Geographic Information Systems* IXX:97-200.
109. MacEachren AM, Robinson A, Hopper S, Gardner S, Murray R, Gahegan M, Hetzler E (2005) Visualizing geospatial information uncertainty: What we know and what we need to know. *Cartography and Geographic Information Science* 32(3):139-160.
110. MacEachren AM, Taylor DRF (1994) *Visualization in modern cartography*. Pergamon Press.
111. MacEachren AM, Wachowicz M, Edsall R, Haug D, Masters R (1999) Constructing knowledge from multivariate spatiotemporal data: integrating geographical visualization with knowledge discovery in database methods. *International Journal of Geographical Information Science* 13(4):311-334.
112. Maciejewski R, Rudolph S, Hafen R, Abusalah A, Yakout M, Ouzzani M, Cleveland WS, Grannis SJ, Ebert DS (2010) A visual analytics approach to understanding spatiotemporal hotspots. *Visualization and Computer Graphics, IEEE Transactions on* 16:205-220.
113. Mackaness WA, Ruas A, Sarjakoski LT (2007) *Generalisation of geographic information: cartographic modelling and applications*. Elsevier Science, Amsterdam, The Netherlands.
114. Martinez M, Levachkine S (2009) Dynamic Models of Geographic Environment using Ontological Relations. In: *Information Fusion and Geographic Information Systems*. Springer:165-176.
115. McCormick BH, DeFanti TA, Brown MD (1987) Visualization in scientific computing. *Computer graphics* 21(6).
116. Mennis JL, Peuquet DJ, Qian L (2000) A conceptual framework for incorporating cognitive principles into geographical database representation. *International Journal of Geographical Information Science* 14(6):501-520.
117. Meyer V (2010) Thunderstorm Tracking and Monitoring on the Basis of Three-dimensional Lightning Data and Conventional and Polarimetric Radar Data. In: *Faculty of Physics. Ludwig-Maximilians-Universität München, Munich, Germany*:128.
118. Mitas L, Brown WM, Mitasova H (1997) Role of dynamic cartography in simulations of landscape processes based on multivariate fields. *Computers & Geosciences* 23(4):437-446.
119. Monmonier M (1990) Strategies for the visualization of geographic time-series data. *Cartographica: The International Journal for Geographic Information and Geovisualization* 27(1):30-45.

120. Moreira J, Ribeiro C, Saglio J-M (1999) Representation and manipulation of moving points: an extended data model for location estimation. *Cartography and Geographic Information Science* 26(2):109-124.
121. Morris MF (1974) Kiviat graphs: conventions and figures of merit. *ACM SIGMETRICS Performance Evaluation Review* 3(3):2-8.
122. MOVE <http://www.move-cost.info/>, accessed last: 09/2014.
123. Nakaya T, Yano K (2010) Visualising Crime Clusters in a Space time Cube: An Exploratory Data analysis Approach Using Space time Kernel Density Estimation and Scan Statistics. *Transactions in GIS* 14:223-239.
124. Neuwirth C, Spitzer W, Prinz T (2012) Lightning density distribution and hazard in an alpine region. *Journal of Lightning Research* 4:166-172.
125. NVAC <http://vis.pnnl.gov/>, accessed last: 09/2014.
126. O'Sullivan D, Unwin DJ (2003) *Geographic information analysis*. John Wiley & Sons.
127. Pang A (2001) Visualizing uncertainty in geo-spatial data, Paper presented at the Proceedings of the Workshop on the Intersections between Geospatial Information and Information Technology, 2001.
128. Pelekis N, Kopanakis I, Marketos G, Ntoutsis I, Andrienko G, Theodoridis Y (2007) Similarity search in trajectory databases, Paper presented at the Temporal Representation and Reasoning, 14th International Symposium on, 2007.
129. Peters S (2011) Interactive Scale-dependent multidimensional Point Data Selection using enhanced Polarization Transformation, Paper presented at the Advances in Cartography and GIScience. Volume 1, 2011.
130. Peters S (2013) Quadtree-and octree-based approach for point data selection in 2D or 3D. *Annals of GIS* 19(1):37-44.
131. Peters S, Betz H-D, Meng L (2014) Visual Analysis of Lightning Data Using Space-Time-Cube. In: *Cartography from Pole to Pole*. Springer:165-176.
132. Peters S, Krisp JM (2010) Density calculation for moving points, Paper presented at the 13th AGILE International Conference on Geographic Information Science, Guimaraes, Portugal, 2010/05/10/14.
133. Peters S, Meng L (2013) Visual Analysis for Nowcasting of Multidimensional Lightning Data. *ISPRS International Journal of Geo-Information* 2:817-836.
134. Peters S, Meng L (2014a) Spatio-Temporal Density Mapping for Spatially Extended Dynamic Phenomena - a Novel Approach to Incorporate Movements in Density Maps (submitted). *International Journal On Advances in Intelligent Systems* 7(3&4).
135. Peters S, Meng L (2014b) Spatio Temporal Density Mapping of a Dynamic Phenomenon, Paper presented at the GEOprocessing 2014 - The Sixth International Conference on Advanced Geographic Information Systems, Applications, and Services, Barcelona, Spain, 23. - 28.03.2014 2014b.
136. Peuquet DJ (1994a) It's about time: A conceptual framework for the representation of temporal dynamics in geographic information systems. *Annals of the Association of American Geographers* 84:441-461.
137. Peuquet DJ (1994b) It's about time: A conceptual framework for the representation of temporal dynamics in geographic information systems. *Annals of the Association of American Geographers* 84(3):441-461.
138. Peuquet DJ (2002) *Representations of space and time*. Guilford Press.
139. Pfoser D, Jensen CS (1999) Capturing the uncertainty of moving-object representations, Paper presented at the Advances in Spatial Databases, 1999.
140. Porter MD, Reich BJ (2012) Evaluating temporally weighted kernel density methods for predicting the next event location in a series. *Annals of GIS* 18(3):225-240.

141. Rao R, Card SK (1994) The table lens: merging graphical and symbolic representations in an interactive focus+ context visualization for tabular information, Paper presented at the Proceedings of the SIGCHI conference on Human factors in computing systems, 1994.
142. Ratti C, Wang Y, Ishii H, Piper B, Frenchman D (2004) Tangible User Interfaces (TUIs): a novel paradigm for GIS. *Transactions in GIS* 8(4):407-421.
143. Resch B, Hillen F, Reimer A, Spitzer W (2013) Towards 4D Cartography-Four-dimensional Dynamic Maps for Understanding Spatio-temporal Correlations in Lightning Events. *The Cartographic Journal* 50(3):266-275.
144. Rinehart RE, Garvey ET (1978) Three-dimensional storm motion detection by conventional weather radar.
145. Rinzivillo S, Pedreschi D, Nanni M, Giannotti F, Andrienko N, Andrienko G (2008) Visually driven analysis of movement data by progressive clustering. *Information Visualization* 7(3-4):225-239.
146. Robertson C, Nelson TA, Boots B, Wulder MA (2007) STAMP: spatial-temporal analysis of moving polygons. *Journal of Geographical Systems* 9(3):207-227.
147. Romanenko K, Xiao D, Balcom BJ (2012) Velocity field measurements in sedimentary rock cores by magnetization prepared 3D SPRITE. *Journal of Magnetic Resonance*:120-128.
148. Rübél O, Weber GH, Keränen SV, Fowlkes CC, Hendriks CL, Simirenko L, Shah N, Eisen MB, Biggin MD, Hagen H (2006) PointCloudXplore: Visual analysis of 3D gene expression data using physical views and parallel coordinates, Paper presented at the Proceedings of the Eighth Joint Eurographics/IEEE VGTC conference on Visualization, 2006.
149. Saary MJ (2008) Radar plots: a useful way for presenting multivariate health care data. *Journal of clinical epidemiology* 61(4):311-317.
150. Sakr M, Andrienko G, Behr T, Andrienko N, Güting RH, Hurter C (2011) Exploring spatiotemporal patterns by integrating visual analytics with a moving objects database system, Paper presented at the Proceedings of the 19th ACM SIGSPATIAL International Conference on Advances in Geographic Information Systems, 2011.
151. Scheepens R, van de Wetering H, van Wijk JJ (2014) Contour based visualization of vessel movement predictions. *International Journal of Geographical Information Science* 28(5):891-909.
152. Scheepens R, Willems N, van de Wetering H, Andrienko G, Andrienko N, van Wijk JJ (2011a) Composite density maps for multivariate trajectories. *Visualization and Computer Graphics, IEEE Transactions on* 17(12):2518-2527.
153. Scheepens R, Willems N, van de Wetering H, van Wijk JJ (2011b) Interactive visualization of multivariate trajectory data with density maps, Paper presented at the Pacific Visualization Symposium (PacificVis), 2011 IEEE, 2011b.
154. Schiewe J (2013) Geovisualization and Geovisual Analytics: The Interdisciplinary Perspective on Cartography. *Kartographische Nachrichten (Special Issue 2013)*:122-126.
155. Schmid CF, MacCannell EH (1955) Basic Problems, Techniques, and Theory of Isopleth Mapping*. *Journal of the American Statistical Association* 50(269):220-239.
156. Scott DW (2009) *Multivariate density estimation: theory, practice, and visualization*. Wiley.com.
157. Shipley TF (2008) An invitation to an event. *Understanding Events: From Perception to Action: From Perception to Action*.
158. Shipley TF, Fabrikant SI, Lautenschütz A-K (2013) Creating Perceptually Salient Animated Displays of Spatiotemporal Coordination in Events.259-270.

159. Short M, D'Orsogna M, Brantingham P, Tita G (2009) Measuring and modeling repeat and near-repeat burglary effects. *Journal of Quantitative Criminology* 25(3):325-339.
160. Silverman BW (1986) *Density estimation for statistics and data analysis*. CRC press,
161. Slocum TA, McMaster RB, Kessler FC, Howard HH (2009) *Thematic cartography and geovisualization*. Pearson Prentice Hall Upper Saddle River, NJ.
162. Soul K, Archibald E, Hardaker P, Hounsell A (2002) Using the GANDOLF system as a tool to aid the forecasting of lightning strikes. *Meteorological Applications* 9(2):229-238.
163. Steinacker R, Doringner M, Wölfelmaier F, Krennert T (2000) Automatic tracking of convective cells and cell complexes from lightning and radar data. *Meteorology and Atmospheric Physics* 72:101-110.
164. Stoilova-McPhie S, Villoutreix BO, Mertens K, Kemball-Cook G, Holzenburg A (2002) 3-Dimensional structure of membrane-bound coagulation factor VIII: modeling of the factor VIII heterodimer within a 3-dimensional density map derived by electron crystallography. *Blood* 99(4):1215-1223.
165. Streit M, Ecker RC, Österreicher K, Steiner GE, Bischof H, Bangert C, Kopp T, Rogojanu R (2006) 3D parallel coordinate systems—A new data visualization method in the context of microscopy - based multicolor tissue cytometry. *Cytometry Part A* 69(7):601-611.
166. Thomas JJ, Cook KA (2005) *Illuminating the path: The research and development agenda for visual analytics*. IEEE Computer Society Press.
167. Tiakas E, Papadopoulos AN, Nanopoulos A, Manolopoulos Y, Stojanovic D, Djordjevic-Kajan S (2006) Trajectory similarity search in spatial networks, Paper presented at the Database Engineering and Applications Symposium, 2006. IDEAS'06. 10th International, 2006.
168. Tominski C, Abello J, Schumann H (2004) Axes-based visualizations with radial layouts, Paper presented at the Proceedings of the 2004 ACM symposium on Applied computing, 2004.
169. Tominski C, Schumann H, Andrienko G, Andrienko N (2012) Stacking-based visualization of trajectory attribute data. *Visualization and Computer Graphics, IEEE Transactions on* 18:2565-2574.
170. Tukey JW (1977) *Exploratory data analysis*. Addison-Wesley.
171. Turdukulov UD, Kraak M-J, Blok CA (2007) Designing a visual environment for exploration of time series of remote sensing data: In search for convective clouds. *Computers & Graphics* 31(3):370-379.
172. Tversky B, Zacks JM, Hard BM (2008) The structure of experience. *Understanding events: How humans see, represent, and act on events*:436-464.
173. Vasiliev IR (1997) Mapping time. *Cartographica: The international journal for geographic information and geovisualization* 34(2):1-51.
174. Veltkamp RC, Hagedoorn M (2001) *State of the art in shape matching*. Springer,
175. Virrantaus K, Fairbairn D, Kraak M-J (2009) ICA Research Agenda on Cartography and GI Science. *Cartographic Journal, The* 46:63-75.
176. VisMaster <http://www.vismaster.eu/>, accessed last: 09/2014.
177. Vlachos M, Kollios G, Gunopoulos D (2002) Discovering similar multidimensional trajectories, Paper presented at the Data Engineering, 2002. Proceedings. 18th International Conference on, 2002.
178. Ware C (2012) *Information visualization: perception for design*. Elsevier.
179. Wegenkittl R, Loffelmann H, Groller E (1997) Visualizing the behaviour of higher dimensional dynamical systems, Paper presented at the Visualization'97., Proceedings, 1997.

180. Wicklin R <http://blogs.sas.com/content/iml/2014/10/01/colors-for-heat-maps/>, accessed last: 10/2014.
181. Wilcox DJ, Harwell MC, Orth RJ (2000) Modeling dynamic polygon objects in space and time: a new graph-based technique. *Cartography and geographic information science* 27(2):153-164.
182. Wiley D, Ware C, Bocconcelli A, Cholewiak D, Friedlaender A, Thompson M, Weinrich M (2011) Underwater components of humpback whale bubble-net feeding behaviour. *Behaviour* 148(5-6):5-6.
183. Willems N, Van De Wetering H, Van Wijk JJ (2009) Visualization of vessel movements, Paper presented at the Computer Graphics Forum, 2009.
184. WMO <http://www.wmo.int/pages/prog/amp/pwsp/Nowcasting.htm>, accessed last: 09/2014.
185. Wood CH, Keller CP (1996) *Cartographic design: Theoretical and practical perspectives*. Wiley.
186. Wood J, Dykes J, Slingsby A (2010) Visualisation of origins, destinations and flows with OD maps. *The Cartographic Journal* 47(2):117-129.
187. Yang P, Tang X, Wang S (2008) Dynamic Cartographic Representation of Spatio-Temporal Data. *The International Archives of the Photogrammetry, Remote Sensing and Spatial Information Sciences* 37.
188. Yeung LH, Lai ES, Chiu SK (2007) Lightning Initiation and Intensity Nowcasting Based on Isothermal Radar Reflectivity-A Conceptual Model, Paper presented at the The 33rd International Conference on Radar Meteorology, 2007.
189. Yuan M (1996) Temporal GIS and spatio-temporal modeling, Paper presented at the Proceedings of Third International Conference Workshop on Integrating GIS and Environment Modeling, Santa Fe, NM, 1996.
190. Yuan M, Hornsby KS (2007) *Computation and visualization for understanding dynamics in geographic domains: a research agenda*. CRC Press.
191. Zinner T, Betz H-D (2009) Validation of Meteosat storm detection and nowcasting based on lightning network data, Paper presented at the EUMETSAT Meteorological Satellite Conference, 2009/09/21/25 2009.
192. Zinner T, Mannstein H, Tafferner A (2008) Cb-TRAM: Tracking and monitoring severe convection from onset over rapid development to mature phase using multi-channel Meteosat-8 SEVIRI data. *Meteorology and Atmospheric Physics* 101:191-210.

8. Acknowledgments

With the completion of this thesis I would like to express my special gratitude and appreciation to all who have accompanied and supported me during the last years.

First of all, I would like to express my honest gratitude to my supervisor Prof. Liqiu Meng for all her warm-hearted help and professional as well as fruitful supervision. It is my honor and fortunate to be her student.

Furthermore, my gratitude also goes to my co-supervisors, Prof. Gennady Andrienko and Prof. H.-D. Betz, for reviewing my work and giving me valuable advises and comments. Special thanks I want to give to my family, in particular my wife, my parents, and my parents-in-law for their enormous support. I would also like to thank Nowcast Company for the significant support on providing the test data. Moreover, I am very grateful to all of my department colleagues for the warm-hearted atmosphere, a pleasant working relationship, and their help during the last years.